European Commission

COST
European cooperation
in the field of scientific
and technical research

COST 507

Definition of thermochemical and thermophysical properties to provide a database for the development of new light alloys

Proceedings of the final workshop
Vaals, the Netherlands
9 to 12 March 1997

Volume 1

EUR 18171 EN

EUROPEAN COMMISSION

Édith CRESSON, Member of the Commission
responsible for research, innovation, education, training and youth

DG XII/B.1 — RTD actions: Cooperation with non-member countries and international organisations — European Economic Area, COST, Eureka and international organisations

Contact: Mr Peter Lobotka
Address: European Commission, rue de la Loi 200 (SDME 1/44), B-1049 Brussels — Tel. (32-2) 29-65512; fax (32-2) 29-65925

European Commission

COST
European cooperation
in the field of scientific
and technical research

COST 507

Definition of thermochemical and thermophysical properties to provide a database for the development of new light alloys

Proceedings of the final workshop
Vaals, the Netherlands
9 to 12 March 1997

Volume 1

COST Secretariat, Brussels, June 1998

1998

EUR 18171 EN

A great deal of additional information on the European Union is available on the Internet. It can be accessed through the Europa server (http://europa.eu.int).

Cataloguing data can be found at the end of this publication.

Luxembourg: Office for Official Publications of the European Communities, 1998

Volume 1: ISBN 92-828-3901-X
Volumes 1 to 3: ISBN 92-828-3900-1

Printed in Belgium

Preface

The Final Workshop of the COST 507 Action was planned to enable the participating scientists in each project to report, either in an oral or poster presentation, on the work carried out during the 3 years of Round 2. At the same time it provided an opportunity for discussion and coordination of the final content and form for presentation of the experimental results and thermodynamic evaluations from the different participating laboratories. These Proceedings of the Workshop constitute one of 2 volumes (the other presenting evaluated data), which together summarise the results and information assembled during the entire COST 507 Action. The compiled data are presented in tabulated and graphical form such that they can be used for calculation or retrieval of information of direct relevance to alloy design and development.

The Workshop was well attended by some 50 participants from all but one of the 14 signatory countries to the Action. The organisation of both the oral and poster presentations according to the 'Key System' structure used to coordinate the work of Round 2 allowed logical and self-consistent discussion of the problems associated with specific alloy categories and of the way these had been dealt with by the 'Key System' partners.
A coordination plan for the COST 507 Action is presented below.

As Key Speakers, Dr.Christophe Sigli (Péchiney), Mr.Colin Small (Rolls-Royce), Prof.Lazar Rokhlin (Baikov Institute) and Prof.Günter Petzow (MPI für Metallforschung) provided stimulating reviews of the determination of phase constitution for different alloy categories and on the relevance of the results for technological applications and quality of life. Examples of the implementation of results from the COST 507 Action in new alloy development work at Péchiney and Rolls-Royce were presented.

The oral and poster presentations produced many lively discussions and the informal surroundings of the Workshop venue encouraged many scientific exchanges outside the meeting rooms themselves.

This was a very productive and successful final meeting for all participants in the COST 507 Action and demonstrated very clearly the highly effective interaction which has been established between the project partners in the course of the closely integrated experimental and evaluation work required to produce the final database. The scientific contacts formed in this Action will undoubtedly be of great benefit to future European research projects

Last, but by no means least, I should like to acknowledge the considerable efforts made by many members of LTH, in particular Iñaki Hurtado and Tanja Jantzen, in assembling abstracts, organising posters and poster-boards, manning the information desk, compiling these Proceedings and carrying out many other time-consuming jobs associated with the organisation of meetings of this kind.

The programme for the Workshop is attached.

Philip Spencer (Workshop organiser)
Aachen, March 1998

Programme

Sunday March 9

14.00 Registration opens
18.00 Welcoming reception
19.30 Dinner

Monday March 10

08.30 Welcoming remarks
08.40 Invited speaker 1
Dr. Christophe Sigli (Péchiney)
09.15 Invited speaker 2
Mr. Colin Small (Rolls Royce)
09.50 Coffee break and posters
10.20 Invited speaker 3
Prof. Lazar Rokhlin (Baikov Inst. of Met.)
11.00 Ternary phase diagram assessments
11.45 Thermophysical properties and database
12.30 Lunch
14.00 Lead System 1 (Al-Fe-Mg-Mn-Si) report
16.00 Coffee break and posters
16.30 Lead System 1 report continued
18.30 End of session
19.30 Dinner

Tuesday March 11

08.30 Lead System 2 (Al-Cu-Mg-Si) report
09.45 Lead System 3 (Al-Cu-Mg-Zn) report
10.15 Coffee break and posters
10.45 Lead system 3 continued
11.30 Lead system 4 (Al-Li-Cu-Mg-Zr) report
12.30 Lunch
14.00 Lead systems 5 and 6 (Al-Ti-Me-X) report
16.00 Coffee break and posters
16.30 Lead systems 5 and 6 continued
18.30 End of session
19.30 Conference Dinner

Wednesday March 12

09.15 Invited speaker 4
Prof. Günter Petzow (MPI, Stuttgart)
09.45 Database Manager's report
Dr. Ibrahim Ansara (LTPCM, Grenoble)
10.15 Coffee break and posters
10.45 Summary and selected examples of practical application of the COST 507 database
Dr. Tim G.Chart (Chairman COST 507)
11.30 End of session
12.30 Lunch

COST 507 STRUCTURE

Measurement and Evaluation of Thermochemical and Thermophysical Properties to Provide a Database for the Development of New Light Alloys

Signatory Countries: Austria
Belgium
Finland
France
Germany
Greece
Italy
Netherlands
Norway
Portugal
Spain
Sweden
Switzerland
United Kingdom

Participating with : Baikov Institute of Metallurgy, Russia

Coordination Groups

A Experimental measurements

B Critical phase diagram assessment

C Thermochemical evaluation & calculation

D Thermophysical properties

Key Systems

1. Al-Mg-Mn-Fe-Si (Cu, Cr, Ti, C)
2. Al-Mg-Si-Cu (Fe, Ni)
3. Al-Zn-Cu-Mg (Zr, Cr, Si)
4. Al-Li-Cu-Mg-Zr (H)
5. Ti-alloys (with metals and non-metals)

Institutes and scientists participating in COST 507 Round 2

A1: Inst. für Physikalische Chemie der Universität Wien
Prof.P.Rogl

A2: Inst. für Anorganische Chemie der Universität Wien
Prof.H.Ipser

A4: Inst. für Physikalische Chemie der Universität Wien
Prof.P.Rogl, Dr.J.Schuster

B1: Dept. Metaalkunde en Toegepaste Materiaalkunde, Katholieke Universiteit Leuven
Prof.L.Delaey, Prof.P.Wollants

CH1: Laboratoire de Métallurgie Physique, Ecole Polytechnique Fédérale de Lausanne
Prof.W.Kurz

D2: Max-Planck-Inst. für Metallforschung, Inst. für Werkstoffwissenschaft, Stuttgart
Prof.F.Sommer

D3: Lehrstuhl für Theoretische Hüttenkunde, RWTH Aachen
Dr.P.J.Spencer

D4: AG Elektronische Materialien, TU Clausthal
Prof.R.Schmid-Fetzer

D8: Lehr- und Forschungsgebiet Werkstoffwissenschaften, RWTH Aachen
Prof.E.Lugscheider

D9: Inst. für Kerntechnik und Energiewandlung eV, Univ.Stuttgart
Dr.G.Neuer

D11: Max-Planck-Inst.für Metallforschung, Inst.für Werkstoffwissenschaft, PML, Stuttgart
Dr.H.L.Lukas

D12: Materials Science International Services GmbH, Stuttgart
Dr.G.Effenberg

F1: Centre de Thermodynamique et de Microcalorimetrie (CTM), CNRS, Marseille
Dr.A.Zahra, Dr.R.Castanet

F3: Pechiney Centre de Recherches de Voreppe, Voreppe
Dr.C.Sigli

F4: Laboratoire de Thermodynamique et Physico-Chimie Métallurgiques, INPG, Grenoble
Dr.I.Ansara

GR1: Mirtec S.A., Volos
Mr.P.Polatidis

GR2: Laboratory of Materials, Dept. of Engineering, University of Thessaly
Dr.G.Haidemenopoulos

I1: Instituto di Chimica Generale, Universita di Genova
Prof.R.Ferro

N1: SINTEF SI; Hydro Aluminium A/S; Elkem Aluminium ANS, Oslo
Dr.P.Kolby

P1: Universidade do Minho, Guimares
Dr.F.Castro

RU1: Baikov Inst. of Metallurgy of the Russian Academy of Sciences, Moscow
Prof.O.Bannykh

S1: Dept. of Materials Processing, Royal Inst. of Technology, Stockholm
Prof.I.L.Svensson

S2: Dept. of Materials Technology, Royal Inst. of Technology, Stockholm
Prof.R.Sandstrom

S3: Dept. of Physical Metallurgy, Royal Inst. of Technology, Stockholm
Prof.B.Sundman

SF1: Lab. of Materials Processing and Powder Metallurgy, Helsinki Univ. of Technology
Dr.M.Hämäläinen

SF2: Physical Metallurgy and Materials Science, Helsinki Univ. of Technology
Prof.J.Kivilahti

SF3: Dept. of Materials Science and Rock Engineering, Helsinki Univ. of Technology
Prof.L.Holappa

UK1: Centre for Materials Metrology and Technology, CMMT, National Physical Laboratory, Teddington
Dr.T.G.Chart

Index

"A Summary of the COST 507 Action and Examples of practical Applications of the Database"
T.G. Chart

Plenary lecture "Materials, technology and quality of life"
G. Petzow

A1 "Phase relations in the Al-rich part of the system Al-Fe-Mn"
F. Weitzer, P. Rogl and M. Bohn

A2 "Thermodynamical properties and phase diagram of Cu-Mg-Si and Cu-Mg-Y alloys"
H. Ipser, V. Ganesan and F. Sommer

A4 "Experimental investigations and thermodynamic modeling of the constitution of quaternary Al-Ti-Metal-Nonmetal systems"
J. Schuster and P. Rogl

CH1 "Directional solidification and phase equilibria in Al-Ni system"
O. Hunziker and W. Kurz

D2 "Thermodynamic investigations of Cu-Mg-Si, Cu-Mg-Y, Al-Mg-Zn, Al-Cu-Mg, Al-Mg-Si and Al-Cu-Zr alloys"
Y.B. Kim, H. Feufel, U. Stolz and F. Sommer

D3 "Thermodynamic evaluations for high-strength, hot-strength and wrought aluminium alloys"
T. Jantzen, S.G. Fries, I. Hurtado, M.H.G. Jacobs and P.J. Spencer

D4 "Thermodynamic assessments, experiments ans applications related to the Ti-Al-V(Ni)-N system"
K. Zeng and R. Schmid-Fetzer

D8 "Experimental investigations in ternary and quaternary Ti-Al-Metal systems"
E. Lugscheider, K. Schlimbach, M. Koschlig and I. Reinkensmeier

D9 "Thermophysical properties of light metal alloys"
G. Jaroma-Weiland, R. Brandt, P. Reipert and G. Neuer

D11 "Thermodynamic assessment in the Al-Cu-Mg-Zn system"
P. Liang, H.L. Lukas, H.J. Seifert and F. Aldinger

F1 "Heat capacity data on some Al-based alloys"
C.Y. Zahra and A.-M. Zahra

GR2 "Differential scanning calorimetry and thermodynamic calculations aimed at the development of Al-Mg-Si cast alloys with Cu, Ag and Sm additions"
G.N. Haidemenopoulos and A.N. Vasilakos

I1 "Thermodynamic optimization and evaluation of phase equilibria in Rare Earth alloys"
R. Ferro, G. Borzone, A. Saccone, G. Cacciamani, S. Delfino, M. Giovannini, D. Macciò and N. Parodi

N1 "Evaluation of the Al-Mg-Mn-Fe-Si system"
P. Kolby, C.J. Simensen and M.E. Seiersten
"A Thermochemical Assessment of Data for the Al-rich Corner of the Al-Mn-Si System" *you may find this article under UK1*
M.H. Rand, P. Kolby and T.G. Chart

S3 "Extrapolations based on Ti-C-N"
B. Sundman and L.F.S. Dumitrescu
"A Thermochemical Assessment of Data for the Al-rich Corner of the Al-Fe-Mn System, and a Revision of Data for the Al-Mn System" *you may find this article under UK1*
Å. Jansson and T.G. Chart

SF1 "An experimetal investigation of the Cu-Li-Mg phase diagram"
L. Rokhlin, M. Hämäläinen and T. Dobatkina
"An experimental investigation of the Cu-Mg-Zr phase diagram"
N. Bochvar, M. Hämäläinen, L. Rokhlin and E. Lysova
"Experimental investigation of the Cu-Mg-Zr system"
"Thermodynamic evaluations of the Al-Li-Cu-Mg-Zr systems"
M. Hämäläinen, H. Braga, N. Bochvar, T. Dobatkina, E. Lysova and L.L. Rokhlin

UK1 "Smith thermal analysis studies of Al-rich regions of the Al-Mn, Al-Mn-Fe and Al-Mn-Si systems"
J.A.J. Robinson, F.H. Hayes, A. Serneels, F. Weitzer and P. Rogl
"A thermodynamic assessment of the Ti-Al-V system"
F.H. Hayes and J.A.J. Robinson
"A Thermochemical Assessment of Data for the Al-rich Corner of the Al-Mn-Si System"
M.H. Rand, P. Kolby and T.G. Chart
"A Thermochemical Assessment of Data for the Al-rich Corner of the Al-Fe-Mn System, and a Revision of Data for the Al-Mn System"
Å. Jansson and T.G. Chart

A Summary of the COST 507 Action and Examples of Practical Applications of the Database

Tim G Chart

Chairman, COST 507 Management Committee

Chart Associates, Ashford, Middlesex, UK

Abstract

At the Vaals Workshop this presentation was made primarily using a series of colour OHP's summarising work progress during the course of the Action on a fairly personal basis, as a tribute to the scientists (mainly present at the meeting) who have contributed to the work over the years. A written summary of this is not possible. Here, a brief history of COST 507 is presented, together with a summary of the results achieved. For those not wishing to read the details, please refer to the Concluding Remarks - "the proof of the pudding is in the eating".

Origins of COST 507

It is more than appropriate that this Final Workshop for the COST 507 project should take place in Vaals, a few kilometres from the Rheinisch Westfälische Technische Hochschule Aachen. The Action began, in its infancy, as a BRITE-EURAM Project Proposal, submitted by Philip Spencer, RWTH, on behalf of SGTE (Scientific Group Thermodata Europe) in 1986, Philip at the time living in Vaals. This proposal, at the suggestion of the COST Secretariat, led to COST 507 Round I, the original Memorandum of Understanding signed 8th December 1988 on behalf of Germany, Greece, France, Norway and United Kingdom. The project initially involved 14 signatory countries: A, B, CH, D, E, F, GR, I, N, NL, P, S, SF, and UK, indeed, most of the signatory countries at the time, and the Baikov Institute of Metallurgy, Moscow, joined during Round I.

The project was given the formal, rather cumbersome, title "Measurement and Evaluation of Thermochemical and Thermophysical Properties to Provide a Database for the Development of New Light Alloys", normally abbreviated to "A Database for Light Alloys".

Summary of Objectives:

The principle objective of this project has been to provide a computerised thermodynamic database to permit the calculation of multicomponent phase equilibria for light alloys based on aluminium, magnesium and titanium, to aid materials scientists and engineers in the development and successful utilisation of a wide range of commercial light alloys. Experimental studies, required to provide missing information, critical assessment of ternary alloy phase diagrams and the acquisition of thermophysical properties have been included.

The database has been geared to deal with a broad range of applications, from conventional wrought and casting alloys for transport, aerospace and packaging, through to high-tech materials including titanium aluminides for gas turbine blades, aluminium-lithium based alloys, metal-matrix composites and high-strength low-density alloys. Environmental applications including recycling have been involved. The project as a whole has been targeted to provide the requirements of European industry and commerce in this field, based on discussions with representatives from industry.

Organisation, Management

The organisation and management of the project, commencing at RWTH Aachen, has centred around the Max-Planck-Institut für Metallforschung, Stuttgart, with Prof Dr multi Günter Petzow (known by his friends as "Petz") as the original Chairman of the 507 Management Committee, together with the National Physical Laboratory, Teddington and Günter Effenberg, Materials Services International GmbH, with immense help and support from the COST Secretariat in Brussels. Philip Spencer, RWTH, has always been a key player, as originator of the Action and Coordinator Group C (see below), and now, the Final Workshop, after some 10 years, returns in 1997 to Aachen:

COST 507 1986-1997

RWTH Aachen 1986

↘

MPI Stuttgart
NPL Teddington
MSI Stuttgart

COST Secretariat
Brussels

↘

RWTH Aachen 1997
(Vaals)

Round I led to a computerised working database for 63 binary systems, provided by Himo Ansara, LTPCM Grenoble, our Database Manager [94Ans], together with constitutional data for some 35 ternary systems.

In order to deal with industrial requirements within existing resource limitations, six "leading systems" were defined before the commencement of Round II during the Leuven Workshop 1991 (see Appendix) in collaboration with industry, and the work load prioritised:

Aluminium-based systems		Titanium-based systems	
1	Al-Mg-Mn-Fe-Si	5	Ti-Al-metal
2	Al-Si-Cu-Mg	6	Ti-Al-non metal
3	Al-Zn-Cu-Mg		
4	Al-Li-Cu-Mg-Zr		

The prime purpose of Round II was to move to multi-component systems of the real industrial world, as required by European industry and commerce.

In addition to the continuation of the four Coordination Groups established during Round I to manage the Action:

Group A	Experimental phase diagram and thermodynamic investigations	Peter Rogl
Group B	Phase diagram assessments	Günter Effenberg
Group C	Thermodynamic database	Philip Spencer
Group D	Thermophysical properties	Greg Haidemenopoulos

System Managers "volunteered" to manage, in conjunction with the Coordinators the division and timing of the workload, according to the matrix shown in Table 1.

The strategy was to:

1 Compile and critically assess constitutional data prior to calculation;
2 Generate missing data by experiments;
3 Critically assess and optimise thermodynamic data;
4 Generate and compile thermo-physical data.

Meetings

A considerable number of formally structured meetings, progress meetings, working groups and quite informal get-togethers have taken place over the years. Some of the more important are given in the Appendix. Please note that this Appendix is not meant to suggest that COST 507 has been governed by bureaucracy. Quite the opposite. All meetings, including those of the Management Committee, consisted of people doing real work for the overall project.

It is very nice to report that during the entire course of the Action, all Management Committee meeting decisions were unanimous, which for a group involving representatives from some 14 European countries, is an indication of the calibre of those involved, and the measure of success.

Of note for future COST Actions, the mechanism of "Working Group" meetings, and "Short Term Scientific Missions", supported by DG XII, whereby relatively large groups of scientists or a few individuals respectively, could meet for short periods to work and exchange ideas, was particularly profitable.

Table 1

COST 507 Round II

Project Management, December 1996

Classification by Group and System and System Managers

System	Group A	Group B	Group C	Group D
1 Al-Mg-Mn-Fe-Si N1 P Kolby	A1, B1, F3, D2, N1, UK1	A1, B1, D12	B1, F3, D11, N1, S3, UK1	D9, GR2, S2
2 Al-Si-Cu-Mg D3 P J Spencer	A2, B1, D2, I1, UK1	B1, D12, I1, RU1	D3, D11, I1, S3, UK1	D9, F1, GR2 S2
3 Al-Zn-Cu-Mg D11 H J Seifert	A2, D2, I1, UK1	B1, D12, I1	B1, D3, D11, D12, I1, S3, UK1	F1, GR1, S2
4 Al-Li-Cu-Mg-Zr SF1 M Hamalainen	CH1, D2, P1, RU1	D12	SF1,	
5 Ti-Al-Me S3 B Sundman	A4, B1, D1, D4, D8, UK1	A4, B1, D4, D12, RU1	B1, D3, D4, D12, F4, S3, SF3, UK1	D9, GR1
6 Ti-Al-NMe UK1 T G Chart	A4, B1, D4, UK1	A4, B1, D4, D12	A4, B1, D4, D11, S3, SF2, SF3, UK1	

Group A **Experimental measurement**
Group B **Critical assessment**
Group C **Thermodynamic evaluation**
Group D **Thermophysical properties**

An Example using the COST 507 Database

Here an example using data from "Leading System 1 is given. The quinary system Al-Fe-Mg-Mn-Si is important to the aluminium industry since it encompasses the 1000, 3000 and 5000 series wrought alloys. These cover, eg, major products including lithographic sheet, UBC's (universal beverage cans) body and can end material, and material for automotive applications (body panels, space frames etc). Figs 1-3 show calculated proportions of the phases present as a function of temperature for an "idealised" 5000 series alloy, and demonstrate the power of the existing database. To determine such information by experiment, whilst crucial in specific test cases, would be prohibitively expensive and time-consuming. Such information is not only of relevance to the development and improvement of the above products, but also to their recycling.

Thus the database, still under continuing development and improvement, and currently including 78 binary and some 25 ternary datasets (in addition to the ternary assessments from Coordination Group B) is "up and running".

Concluding Remarks

During the Vaals Workshop quotations in relation to the use of the thermodynamic database were kindly provided on behalf of Alcan International Ltd and Rolls-Royce plc. The former is reproduced here, together with an update of the latter:

Please refer to Figs 4 and 5.

"The COST 507 database for aluminium alloys has been widely used in model alloy work: knowledge of equilibrium conditions is a prerequisite for kinetic analyses of solidification, homogenisation and annealing. The final quinary database will be an invaluable tool for the European aluminium industry, applicable to alloy design and optimisation, process modelling and efforts to improve recyclability through increasing iron and silicon tolerance."

Dr P V Evans
Alcan International Ltd, Banbury Laboratory

Please refer to Fig 6.

"Titanium aluminides based on the TiAl phase are a relatively new class of lightweight high temperature materials that will find application in the gas turbine in the near future. The 1st generation alloys were based on Ti - 48 at% Al with additions of 2 - 4 at% transition metals. However the alloy chemistry was not optimised for gas turbine applications and the chemistry microstructure relationships were poorly understood. The titanium aluminide data from COST 507 has been used and extended by Rolls-Royce to assist in solving and understanding these problems. This has enabled a viable production process for small components to be identified and initial production for testing in advanced engine demonstrators is underway".

Rolls-royce plc

Thanks

Especial thanks are due to the sponsoring organisations, without which COST 507 could not have taken place. It is a pleasure to thank sponsors' representatives, many of whom took a very active part in the work planning and execution, for example, Colin Small of Rolls-Royce plc, Paul Evans of Alcan International Ltd (Banbury Laboratory) and Christophe Sigli of Pechiney.

Thanks are due to the many scientists involved, also those concerned with organisational aspects over the years - particularly Prof Petzow and his staff at the Max-Planck-Institute für Metallforschung and Monsieur Pithan and his staff of DG XII, including especially our various Scientific Secretaries, particularly Martin Kedro and Peter Lobotka.

On behalf of everyone I take pleasure in thanking our four Coordinators - Peter Rogl, Günter Effenberg, Phil Spencer and Greg Haidemenopoulos, and our Database Manager, Himo Ansara. Also Dr Alan Prince and Prof Björn Uhrenius who accepted invitations to act as external evaluators for the Action. Günter Effenberg needs a special mention, since he not only coordinated Group B but throughout the years took a major leading role in the overall management of the project. I hope to be forgiven for not mentioning many other names, all having made important contributions.

Acknowledgements

Figs 4, 5 and 6 are reproduced here with kind permission of Alcan International Ltd (Banbury Laboratory) and Rolls-Royce plc.

Reference

94Ans I Ansara, *Thermochemical Database for Light Metal Alloys*, COST 507, Concerted Action on Materials Sciences, European Commission, DG XII, Luxembourg, 1995

Appendix

COST 507: Some Key Meetings

RWTH Aachen	Sep '86	Completion of Brite-Euram Proposal
Irsee	May '87	Framework for an Al-Project
RWTH Aachen	Nov '87	Initial plans for 507
Brussels	Dec '87	COST New Projects Group
Brussels	Feb '89	First Management Committee Meeting
MPI Stuttgart	May '89	Coordination Framework Established
Brussels	Sep '89	Management Committee
MPI Stuttgart	Oct '89	Coordination Meeting
Brussels	Sep '90	Management Committee
NPL Teddington	Dec '90	Coordination Meeting
RWTH Aachen	Jun '91	Coordination Meeting
Hofburg Vienna	Nov '91	COST Ministerial Conference
Leuven	Dec '91	Leuven Workshop
Haldensee Tirol	May '92	Coordination Meeting
Stockholm	Jun '92	COST Senior Officials, Round II
Schloβ Ringberg	Nov '92	Seminar and MC Coordination Meeting
Paris	Jun '93	EUROMAT'93
Brussels	Dec '93	Management Committee
MPI Stuttgart	Jan '94	Coordination Meeting
NPL Teddington	Mar '94	Coordination and Modelling Meeting
St Margherita Ligure	Apr '94	Workshop and Management Committee
NPL Teddington	May '94	Coordination Meeting
Skiathos	Sep '94	Coordination Meeting
Brussels	Dec '94	Management Committee
RWTH Aachen	Jan '95	Coordination Meeting
Schloβ Ringberg	Feb '95	Coordination Meeting
Schloβ Ringberg	Mar '95	Coordination Meeting
MPI Stuttgart	Nov '95	Management Committee and Working Group
CA Ashford	Jul '96	Budget and Workshop Planning
NPL Teddington	Sep '96	Working Group Meeting
Brussels	Dec '96	Management Committee and Working Group
Brussels	Jan '97	Working Group (Final Workshop)
Vaals	Mar '97	Final Workshop and Management Committee

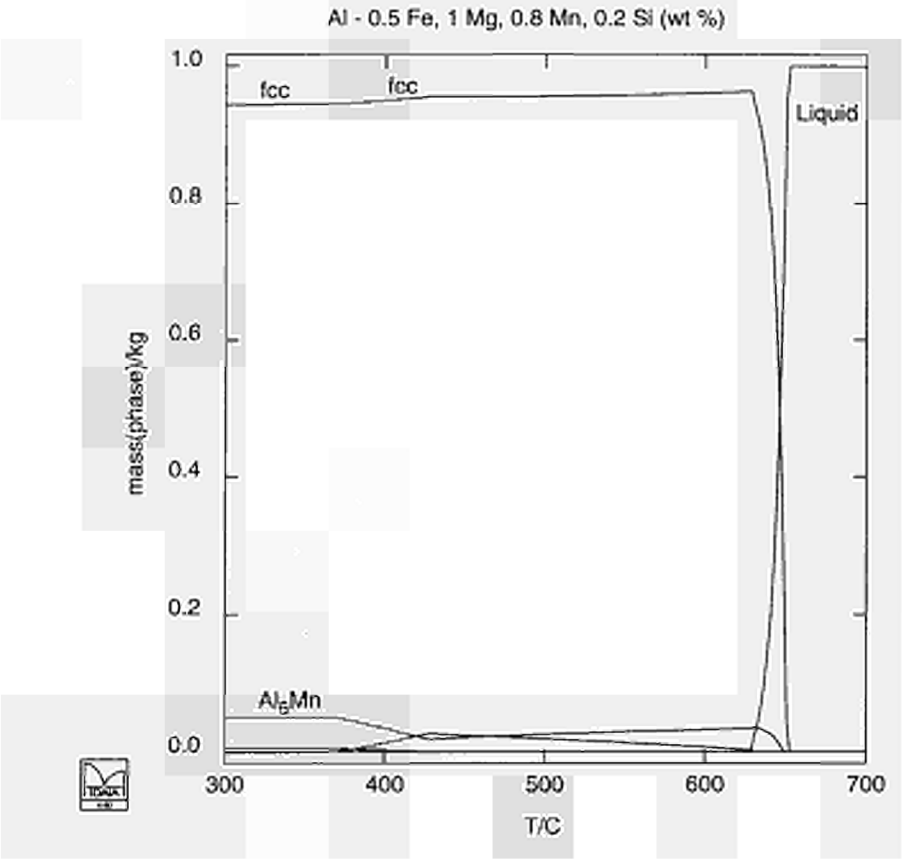

Fig 1 Calculated mass fraction plot for an "idealised" 5 component 5000 series type alloy, showing the proportions of the phases present as a function of temperature.

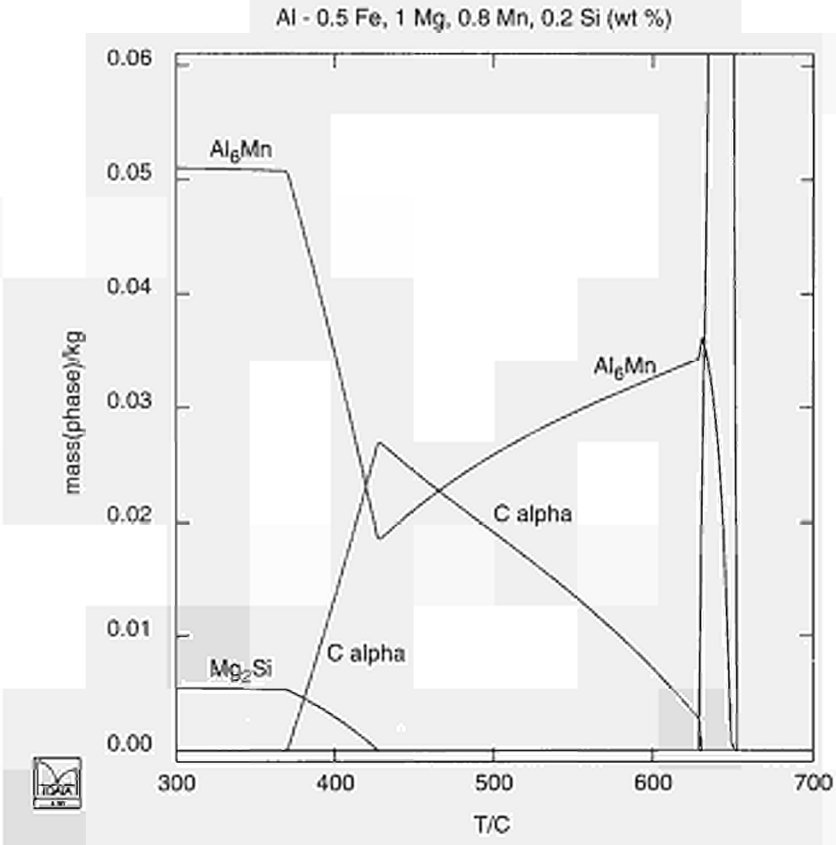

Fig 2 Calculated mass fraction plot for an "idealised" 5 component 5000 series type alloy, showing the proportions of the phases present as a function of temperature. The plot is expanded to show more clearly the phases present.

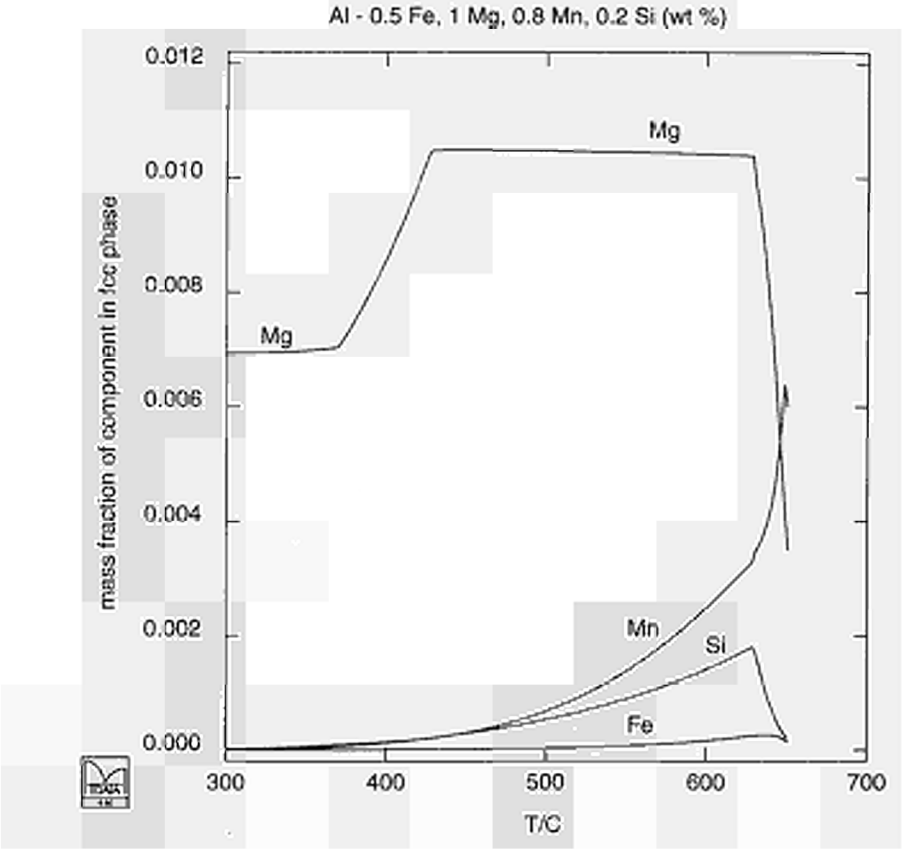

Fig 3 Calculated mass fraction plot for an "idealised" 5 component 5000 series type alloy, showing the distribution of the components in the fcc phase.

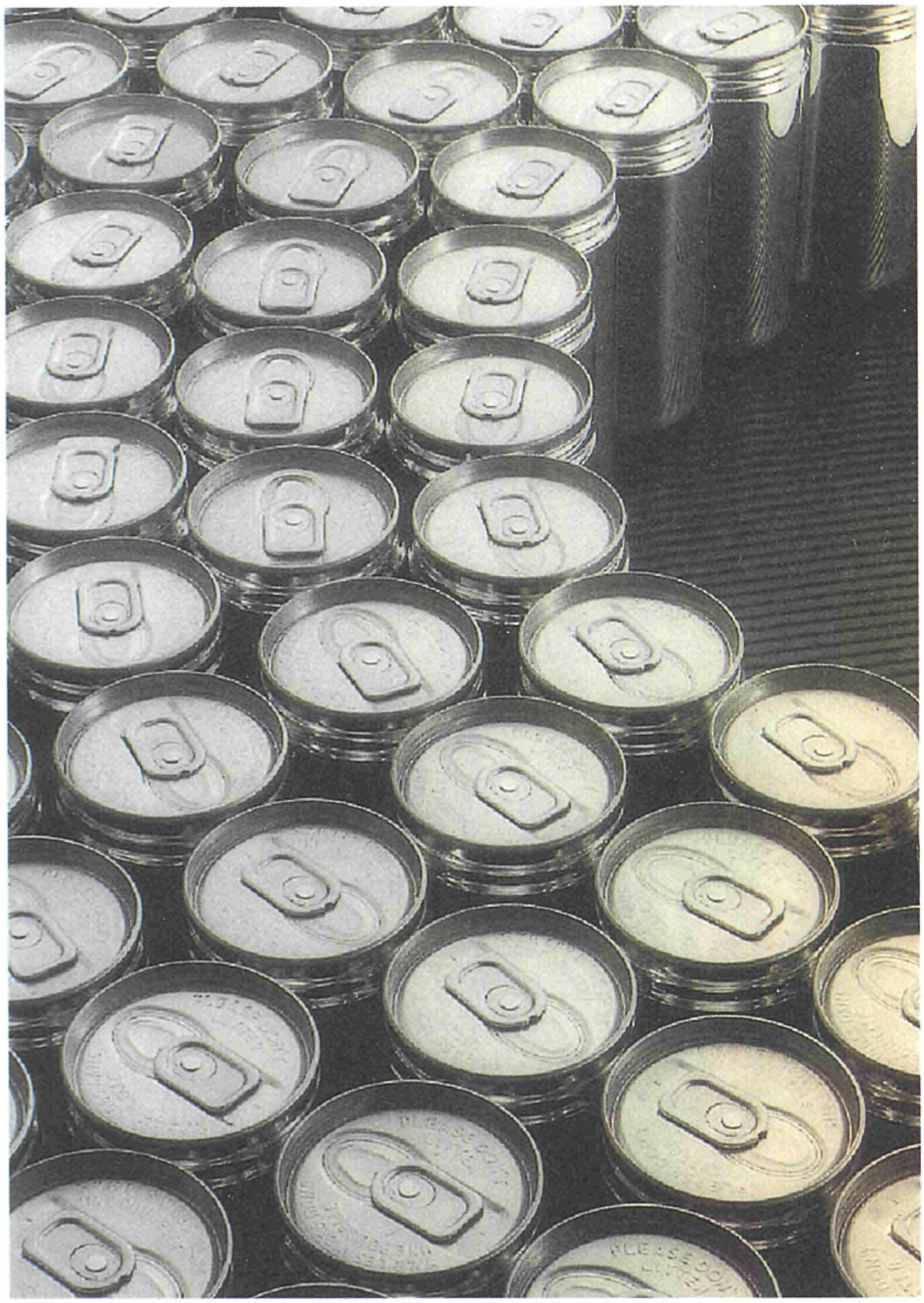

Fig 4 Aluminium beverage cans. The COST 507 database is applicable to alloy design and optimisation, and in this example, efforts to improve recyclability of scrap.

Fig 5 The Aluminium Intensive Vehicle (AIV) built by Ford using Alcan's weld bond technology results in a final on-the-road vehicle weight reduction of approximately 21%

Fig 6 High pressure compressor vane from an advanced gas turbine core design manufactured in a titanium aluminide.

MATERIALS, TECHNOLOGY AND QUALITY OF LIFE

G. Petzow

Max-Planck-Institut für Metallforschung, Stuttgart (D)

ABSTRACT

Technological progress is closely linked with the evolution of materials. An assessment of the availability of materials for future developments shows a huge potential of unrealized materials compared with those already available. Today's tailor-made materials are the consequence of a gradually improving understanding of the architecture of matter.

Materials science which explores the structure, properties, preparation and processing of materials is supported in many cases by models and concepts of physics, chemistry and crystallography. The great significance of materials science in technological progress is that it can lead to a basic understanding of internal structure, so that new materials can be developed consequently for specific applications. In this connection computational phase studies and thermochemical data play an important role.

The topic chosen reflects an attempt to illustrate the interplay between many materials and technologies. With less resources, less energy and smaller environmental impact, and based on more innovative materials and technologies the today's standard living must be kept constant and made accessible to all people.

INTRODUCTION

All of us are aware of the rapid changes in our world caused by scientific discoveries and technological developments. Scientists and technologists contribute decisively to our modern society and have to master not only the advantages but also the disadvantages of present and future discoveries and technologies. This is in full accordance with the words of Albert Einstein: *"Awareness of the human being and his fate should always be the ultimate concern in specialized scientific endeavors. One should never lose sight of this among al diagrams and equations".*

Since all of us are more or less concerned with materials in some way, I would like to focus in my presentation especially the role of materials in the socio-econonic-context of technology, especially in view of the increasing meaning of the ecological situation. The topic chosen reflects an attempt to illustrate one of the many facets of materials science.

HISTORICAL DEVELOPMENT

The implementation of technological ideas and concepts relies on the existence of suitable materials which in turn are constantly being improved by the demands of these new technologies. This reciprocal relation has always had a decisive effect on human progress. Between man, materials and technology is a steady interaction ongoing for millions of years. The base of progress is an unalterable interconnected three-way relationship as simplified shown schematically in Fig. 1 [1].

The earth's population has been continuously multiplying since early man first appeared about two million years BC. E.g. the population grew by a factor of 100 in about 100 000 years, from estimated 100 000 to 10 million, and this was reached about 4000 BC. Despite natural catastrophes, plagues and decimating wars, by 1820 the population had grown again by a factor of 100 to 1 billion people, this time in less than 6000 years.

Today there are about 6 billion people and the doubling rate is only about 33 years. Accordingly, it could be possible that in not quite 200 years time there will already be 100 billion (10^{11}) people on earth. The period for the factor 100 in population increase is less than 400 years. Compared to 6000 and 100 000 years the population increase becomes alarming fast. All of us are aware, those extrapolations often are not reasonable. But no matter whether the steep increase will continue or come into a final state mankind is faced with drastic increase of population during the upcoming decades. Overpopulation will more and more influence our life and our thinking.

The conditions for the flourishing of the species *Homo Sapiens* have improved over time such that man has made the earth his subject. Through his materials and their use in technical devices and processes, man has made favorable living conditions which he modifies continually and to which he in turn continuously adapts.

Materials are one of our oldest cultural assets. Historical eras are named after the materials that dominated at that time: the Stone Age, the Copper and the Bronze Age and the Iron Age possibly the end of which we are living through at this time. New materials such as polymers, semiconductors and superconductors, advanced alloys and ceramics. the amorphous metals, and increasingly the composite materials, are appearing on the scene and providing an impetus for technological developments, often with far-reaching consequences. One can expect the discovery of more materials in the future. Every chemical compound and every alloy is a material that could potentially revolutionize our lives to the extent that the first stone tools revolutionized the life of early man.

Materials are turned into tools, devices, machines, houses and streets. Revolutionary technological developments have, as in the case of materials, followed in quick succession in modern times. Thus important developments such as printing, radar, radio, telephone, satellites, rockets etc. that enhance man's favorable living conditions, are not shown in Fig. 1 for reasons of clarity. In Fig. 1, the rise of the evolutionary curves for materials and technology includes the number of discoveries and technological events.

In the interaction with materials and technology man is the decisive partner, of course. Materials and Technologies are ambivalent. They are, a priori, neither good nor bad. Only man decides about their applications.

Considering the importance of materials for the evolution of mankind it is necessary to have an idea on the availability of materials.

AVAILABILITY OF MATERIALS

Today there is a broad spectrum of materials available, as schematically expressed in Fig. 2. Just counting the materials which have been stored in databanks, over ten million different materials are already in application. This may seem to be a large number, but the number of unrecorded materials is by far greater, as will be shown later.

Materials are prerequisite for technology and human life. But even today materials are mostly taken for granted - they are self evident to most people. Without materials men immediately would fall in great trouble and the statement by Georgius Agricola [2], given more than 500 years ago, would become true. He wrote:

"... If mankind ceased to use metals, all the possibilities to guard and preserve health, as well as to lead a life corresponding to our cultural values would be taken away. People would lead the most detestable and most miserable life among wild animals ..."

Everything said about metals can be generalized to all materials. Agricola addressed the social aspects of materials: problems of public health and culture as well as general questions of standards of living. He made the connection between materials technology and society in context of his time.

In our days the increasing needs for materials are obvious from Fig. 3 showing the trends in application of materials in the U.S. [3]. The steep increase in materials consumption caused not only by the fast growing of population but also by higher demands of people.

The expected increase in the consumption according to Fig. 3 would be very good to improve our economies but at the same time with a heavy burden on our anyhow limited resources. And indeed the growing demand of materials imply the "looting" of our planet on nonrenewable sources, which becomes directly evident by Fig. 4 [3].

It has taken a long time for developments to reach their current rate (Fig. 1). But today the question arises, whether the steeply increasing population curve and the pace of technological innovations really present true progress! Our earth, often compared with a spaceship, has limited resources and as a consequence its loading capacity is limited. The "spaceship" earth with limited resources and increasing population is confronted with serious problems.

In this universal consideration, the planet earth is a part that may give up energy to its surroundings, but can replace it again from outside, from the sun. The energy losses can be balanced, as shown schematically in Fig. 5 [4]. But it is another matter for material converted by the economy under application of energy. Out of raw products arise commodities and foodstuffs. If the consumption of materials out of the order of the concentrated storage places into scattering by mass production and to refuse dumps is regarded as an increase in the entropy (measure of irreversibility), then this fits with the generalization of the thermodynamic laws. The material entropy in the global ecosystem of the world causes an increase in the disorder, or rather in the uniform intermixture [5, 6].

This economic occurrence, which increases on dramatic by population growth, has a direction. It goes from the concentration of the material towards distribution and scattering. The potential of materials decreases as they are used technically. They go from a certain concentration, that one can also call order, over to an even distribution called disorder of chaos. Entropy is also therefore defined as a measure of disorder or a measure of probability of a state. Disorder is always more probable than order. It should be noted here that Albert Einstein described the entropy law as the most important law of science.

There was a first warning more than twenty years ago by a report to the Club of Rome [7]. Its authors predicted a catastrophic situation early in the next millennium. In case the conditions of that time would remain, the increase of population would cause a need for more food, more industrial production, more energy and raw materials and as a consequence an increase of pollution, as schematically expressed in Fig. 6. All that would have yield to an unbalanced situation on earth in the next century creating the catastrophe. But fortunately today, about 20 years after the first report to the Club of Rome, a new prediction with updated information has been given [8]. It is realized that the situation has changed to a more positive side:

- Population rate is decreased since 1971 from 2.1 % to 1.7 % per annum.
- The energy and materials consumption became more reasonable; recycling.
- Better materials and technologies are available.

Therefore, the catastrophe is shifted further to the future and there is even hope for avoidance by achieving a steady state on our planet by further improving of the mentioned three general points of view.

This new prediction expresses the first success of ecological renewal, which will more and more influence our life and our thinking. A similar situation to present times has happened in history already twice: around 4.000 BC when early man settled from a nomadic behavior as hunters and began with agriculture. And then around the middle of the 18th century: the industrial revolution. In both cases a change in the habits of living was essential because of the population growth and in both cases materials and technologies have reached a standard which allows such drastic changes in human being. We are now obviously in the beginning of a third renovation: the ecological renewal. And again, there is no alternative to technology. Ecology cannot be realized besides technology and not against technology. But there is only one choice for industry and that is to adapt ecologically [9]. New materials and innovative technologies offer a means just for that. There does not seem to exist another solution of our ecological problems than a broadly distributed development of technologies and materials. So far materials concerned, three directions are important for approaching the steady state on earth:

Recycling - Optimizing of materials - New materials.

RECYCLING OF MATERIALS

Fortunately, consumption of materials does not have to be a synonymous with an irrecoverable loss, such as is the case with energy use, but - at least in the most favorable case - must be considered as a stage within the cycle of materials shown schematically in Fig. 7 [10]. The path taken by the substances leads from the resources and raw materials to the materials themselves, which become waste after their use in products of various technological areas. At best the waste products can be recycled; in less favorable cases they have to be stored in refuse dumps. But even those waste products not suitable for reuse are not lost from this cycle, unless they cannot be decomposed by chemical processes or micro-organisms and thus cannot be fed back as resources. Even waste must be considered as a products that cannot simply be thrown away but must be utilized to stretch the available resources. Many successful examples support this point. This might be underlined by Fig. 8 showing the recycling rates for some important classes of materials [3].

The values achieved are a beginning and will certainly be improved in the near future. Much material can be won back through recycling. Recycling is therefore correct as a concept and as a responsibility absolutely necessary. Non-renewable resources must be recycled if the industrial society wants to retain its standard of living at roughly the same level. However, a complete recovery cannot be achieved as the second law of thermodynamics demands a tribute in the form of entropy. A more or less large remainder disappears from exploitability and provides storage and environmental problems, as it doesn't disappear as a substance.

OPTIMIZING OF MATERIALS

As shown in Fig. 2 there are many classes of available engineered materials, metals, ceramics, polymers etc. with manifold, very different properties, which are intensively studied, initially strictly separated in the classes. Since about 40-50 years, however, the overlap between these classes has become apparent. Materials science as a scientific discipline began to grow. Materials science is supported in many cases by concepts of chemistry, physics and crystallography.

Some time ago, the well-known physicist John M. Ziman said that the coming decades belong to materials science. The considerable success of materials science was its explanation of empirical findings accumulated in large numbers and the resultant improvements and extensions. The great significance of materials science in technological progress is that it can lead to a basic understanding of internal structure, so that new materials can be invented and tailor-made for specific applications, literally by microstructural and molecular design.

As can be seen from Fig. 9 the structure and properties of materials are determined by a whole range of characteristics which extend across a very wide range, from atomic dimensions in the tenth of a nanometre range to the dimensions of structures in the centimeter or meter range [11]. All of the characteristics in this range of scale of several magnitudes contribute, in their own particular way, to the characteristic profile of a given material. In addition to the structure, determined by the interaction of the various types of atomic bonding, the microstructure of a material also plays a significant role in determining its characteristic properties, from nano- to macrostructures. The microstructure is an important domain within the science of materials. More and more often it bridges the gaps in communication between scientists, who seldom enough venture outside their atomic field of interest, and engineers, who show little interest in leaving their safe macroscopic ground of their continuum conception.

It is surely immediately apparent that the enormous range within which microstructures occur, also encompasses an extensive and fascinating world which even today cannot as yet be continuously observed to modeled because the effective parameters are too numerous. There are, however, many rules which permit such microstructures to be generated precisely and reproducibly.

Even though materials are an ancient cultural inheritance of man, their scientific exploitation began only at the beginning of this century. Today we know that the internal architecture of a material is determined by the type of atoms it contains and their three dimensional arrangement in accordance with certain degrees of order: from strictly ordered arrangements, such as in crystals, to extremely disordered or chaotic arrangements such as occur in some solidified melts.

As an example of a material of the highest order, Fig. 10 shows a section from a copper single crystal. The copper atoms are strongly arranged in the cubic face centered structure. Each light colored fleck is produced by a whole column of atoms. The image was produced by transmission

of a nanometre thick single crystal copper-foil in a high resolution high voltage electron microscope. The direct resolution of this instruments is 0.105 nm, which is less than the distance between the adjacent copper atoms and can thus be resolved [12]. The enormous power of this microscope is best demonstrated by comparison with the human eye. Were our own eyes to have the same ability, we would be able to see a tennis ball on the surface of the moon.

In Fig. 11, a direct lattice image of a silicon nitride alloy, areas of higher order are clearly visible from the periodic contrast [13]. Between these areas there exists only a thin amorphous film 0.1 nm thick, ,which markedly differs in its composition from the crystalline areas, as can be seen from the electron energy loss spectrum inserted in the upper right of Fig. 11. The Yb_2O_3 sintering aid has become concentrated in the glass phase. Two ordered atomic arrangements of differing orientation are apparent, separated by an amorphous phase. The symmetry of the atomic arrangement, in contrast to Fig. 10 exists in various different areas separated by a disordered phase. A microstructure has thus to some extent been formed from both the elements of order and chaos.

Whilst symmetry, as the building plan of the structure of a material, plays an important role, it is the deviations from it which make the reality. The type, amount, arrangement, size, shape and orientation of the various phases in their respective ordered conditions all go to form the actual microstructure of the material which thus results from the combination of each of all phases and the defects they each contain. Such defects can be from nil to three dimensional, and in size from vacancies and dislocations to grain boundaries, pores and shrinkage cracks. The various different combinations of these factors result in the fascinating multiplicity of possibilities.

The microstructural parameters strongly influence many of the properties of a material. Because of this, a great deal of attention is paid to the microstructure in science, development and testing of materials. As a rule, each material contains many million microstructural features in each cubic centimeter. Even a single crystal, in which such an important feature as the grain boundaries is missing, still contains various different ordered conditions and thus has a microstructure. These microstructural features can exist in sizes spanning more than ten orders of magnitude (Fig. 9).

Today there is a whole range of instruments with which nearly all of the features across this range can be made visible. In this sense one may use the term **continuous materialography** [14].

The higher the requirements of a material, the more stringent are the requirements on its microstructure, i.e. the more accurately must its microstructure be established. The aim is to be able to create a microstructure specifically designed to produce a given property profile. The terms "microstructural engineering" and "microstructural design" are the keywords used to describe this process. Only in this way can the strictyl defined materials needed for stringent operating conditions and close property tolerances be realized.

Typical contemporary examples are the oxides, nitrides, carbides and borides. These chemical compounds have been known for a long time, but it is only recently that they have been turned into advanced ceramic materials exhibiting useful properties. The prerequisite for this was a procedure to design a well-defined, fine-grained microstructure. How marked this detailed characterization of the morphology of a microstructure can be, can be seen in Fig. 12 as an example. Scanning electron micrographs are shown of the microstructure of an alumina-zirconia alloy. , as well-known cutting tool material. Both samples have the same composition. The light particles are zirconia inclusions in the alumina matrix, which appears gray. Both samples were prepared by densification of the same starting material. However, different densification processes were used. Although the treatments applied did not differ greatly, a large difference in strength resulted - nearly a factor of two The reason for this is a minute variation in the microstructure. The treatment of the sample shown on the left resulted in a more pronounced grain growth, and as a direct consequence of the microstructural coarsening, the strength decreased markedly.

The advanced ceramic materials. chosen as an example to convey a feeling and understanding of the significance of microstructures, have experienced a fascinating boom in the last few years and more breakthroughs can be expected in the future. The possibility of optimizing new materials by microstructural leads us to thoughts on the realization of novel materials and their availability.

NEW MATERIALS

After all recent developments of new materials, the question as to the potential of further materials arises. Can we hope for significant new contributions, especially if we consider the great multitude of materials already available? **The answer is straight-forward: yes!**

In fact, potential materials are in abundance and the possibilities of combining and varying elements are almost unlimited even though there are just over 100 elements. The following considerations may help to clarify this: Elements can be mixes or alloyed respectively and combined to systems, for instance the well-known iron-carbon system, which involves many carbon steels and cast irons. Let us consider 86 of the 100 or so elements we know, and ignore inert gases and the transuranic elements. If we combine these 86 elements to binary, ternary, quaternary systems and so on, up to the 86-element system, the total number of possible systems comes to as many as 7.7×10^{25}!

In Fig. 3 the number of possible systems is plotted as a function of the number of elements N. This can be drawn only on a logarithmic scale, otherwise the ordinate would extend to the Milky Way. We have only 86 unary systems (the elements), 3.655 binary systems, more than 100.000 ternary systems and so on and the maximum of 6.6×10^{24} systems is reached with 43 elements. Beyond this maximum the number of possible systems decreases and finally only 1 system with all 86 elements exists (which contains all other systems as subsystems).

On the other hand, the number of systems investigated decreases steeply as the number of components increases. Altogether about 10.000 systems are known to date, most of them only partially. This is marked by the hatched area in Fig. 3. This area represents all known materials. The ratio of known to possible systems is as small as 10^{-22}.

This "mountain" of materials shown in Fig. 3 is hardly accessible in reality and represents a huge reservoir of materials. Despite the numerous combinations of elements used in today's materials, a much larger multitude of unknown possibilities remains. Among these could be numerous technological material combinations, which some day could play a role similar in importance to today's steels, superalloys, advanced ceramics and so on.

The dimension of this reservoir increases if one considers that one phase diagram containing many technical alloys is counted only once in this plot. Further multiplication results from the fact that neither modifications (e.g. graphite, diamond and carbon) nor metastable states, e.g. glasses, are included. And even more possibilities arise by variation of the molecular arrangements as in the case of polymer materials. Thus, an incredible abundance of possible materials is a formidable task and nevertheless a great challenge for the materials science community. However, many of the possible element combinations will be without practical significance. But likewise, many element combinations will result in new engineering materials. In particular, combinations of light elements such as silicon, aluminum, carbon, oxygen and nitrogen, that are abundant in the earth's crust, are of special economic and ecological significance.

One prerequisite for the utilization of the "mountain" of materials is presented by the computer-aided study of multi-elemental material systems, a method which has already been developed to a high standard. At present, phase diagrams of up to 10 elements are being calculated. Relatively few experiments are then sufficient to verify these systems. The computer software employed is already widely in use and is an important tool for the understanding of multi-elemental materials and their complex phase equilibria [15].

Phase diagrams are concise plots of equilibria relationships in heterogeneous materials. By their nature they only represent thermodynamically equilibrium conditions which relate the physical state of a mixture with the number of substances of which it is composed and with the environmental conditions imposed on it. In other words phase diagrams are comprehensive descriptions of constitution of matter so far relations between different phases are concerned. The principles of phase equilibria are central to an understanding of many scientific and technological disciplines and are important guidelines in the production, processing and application of materials.

In recent years there have been many technological breakthroughs via new materials. Those materials have a key position since they enable new technologies, not possible before, because of the lack of proper materials. Only a few examples of recent breakthroughs are demonstrated by Figs. 14, 15 and 16. All these developments expressed by Figs. 14 to 16 are typical examples for real progress with striking influence on the ecological behavior.

Especially convincing to be seen is the ecological advantage in an actual industrial development which might come into mass production in the next few years, namely the ceramic valves for automotive engines made of silicon nitride alloys. Compared to metallic valves they are lighter (two third) and have a better wear behavior yielding to higher performance, lower fuel consumption and lower exhaust emission [16].

All these examples demonstrate quite clearly: materials science can help to ensure that the technological evaluation is on the right track: Not only the use of our resources and energies is enhanced, but also our environment is better protected. In short: With less resources, less energy and a smaller environmental impact we must attempt to make today's highest standard of living accessible to all people, based on more intelligent, innovative materials and technologies. In very short: **More with less** [17].

The challenges and general trends in the field of materials science are schematically shown in Fig. 17. In addition to the already known and well approved classes of materials, composite materials, so called intelligent materials, as well as anisotropic materials and those with cellular structure are investigated worldwide to find new materials for new demands in technology.

CONCLUSION

With less resources, less energy and a smaller environmental impact, based on more intelligent, innovative materials and technologies materials science can contribute significantly to the change in industrial culture. A change that will lead to a socio-economic and ecological future with man in harmony with his materials and his technology. Materials science is a truly interdisciplinary field, incorporating and interacting with most engineering and science disciplines. In materials science a collaborative work between scientists and institutions in the European countries can be established without any problems. Not a costly program is necessary to reach the goal, but just a coordination of special advantages of the partners and in addition some new thinking and adaptation. - Or expressed in the simple words of Linus Pauling:

"If man had as much sense as reason,
things would be a lot simpler!"

REFERENCES

[1] G. Petzow, "Man, Materials and Technology - Opportunities and Concerns" in High-Tech Ceramics, pp. 1-15, ed. G. Kostorz, Academic Press, London, 1989.

[2] G. Agricola, "De Re Metallica Libri XII", 1556 (revised ed. 1961), pp. 11-12, Deutscher Taschenbuch Verlag, München, 1977.

[3] H. Czichos, "Werkstoffe als Basis industrieller Produkte", Stahl und Eisen, 114 (1994) Nr. 12, pp. 63-70.

[4] A. Frisch, C. Kaniut, priv. information.

[5] Ch. Schütze, "Das Grundgesetz vom Niedergang", Carl Hanser Verlag, München, 1989.

[6] N. Georgescu-Roegen, "The Entropy Law and the Economic Process", Cambridge/Mass. 1971.

[7] D.H. Meadows, D.L. Meadows, J. Randers, W.W. Behrens III, "The Limits to Growth", Universe Books, New York, 1972.

[8] D.H. Meadows, D.L. Meadows, J. Randers, "Beyond the Limits", Chelsea Green Publ., Co., Post Mills, Vermont, 1992.

[9] J. Huber, "Die Regenbogengesellschaft", S. Fischer Verlag, Frankfurt, 1985.

[10] H. Czichos, in Atlas Bulletin 5, pp. 20-23, United Nations, New York, 1988.

[11] G. Petzow, F. Mücklich, "Microstructure - Fascinating Variety in Stringent Rules", J. Pract. Metallography, 33, 1996, pp. 64-82.

[12] F. Phillipp, R. Höschen, M. Osaki, G. Möbus, M. Rühle, "A New High-Voltage Atomic Resolution Microscope Approaching 1 Angstroem Point Resolution Installed in Stuttgart", Ultramicroscopy, 56, 1994, 1.

[13] H.J. Kleebe, M.J. Hoffmann, M. Rühle, "Influence of Secondary Phase Chemistry on Grain Boundary Film Thickness in Silicon Nitride", Z. Metallkde., 83, 1992, pp. 610-617.

[14] G. Petzow, "Metallographisches, Keramographisches, Plastographisches Ätzen", 6., überarbeitete Auflage, Gebrüder Borntträger Berlin, Stuttgart, 1994.

[15] G. Petzow, E.Th. Henig, U. Kattner, H.L. Lukas, "Der Beitrag thermodynamischer Rechnung zur Konstitutionsforschung", Z. Metallkde., 75, 1984, pp. 3-10.

[16] R. Hamminger, J. Heinrich, "Keramische Ventile für Automobilmotoren", Spektrum der Wissenschaften, Jan. 1993, pp. 114-116.

[17] D. Altenpohl, "Materials in World Perspective", Springer-Verlag, Berlin, Heidelberg, New York, 1980.

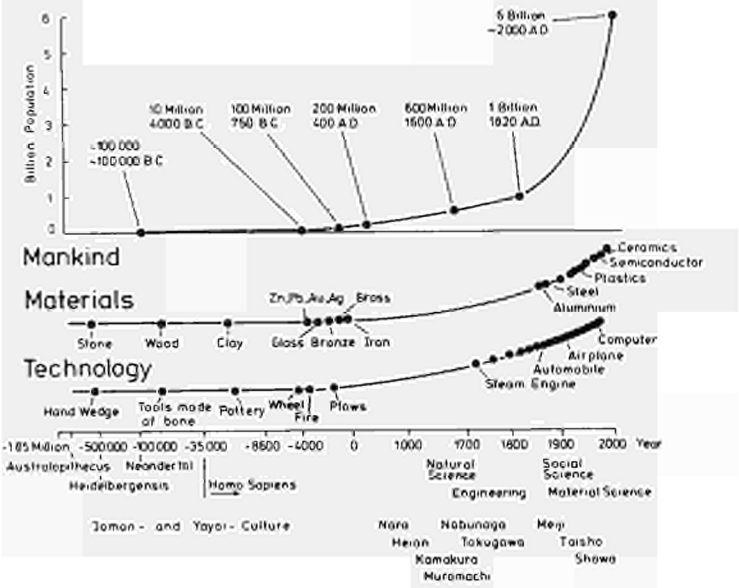

Fig. 1: Evaluation of man, materials and technology

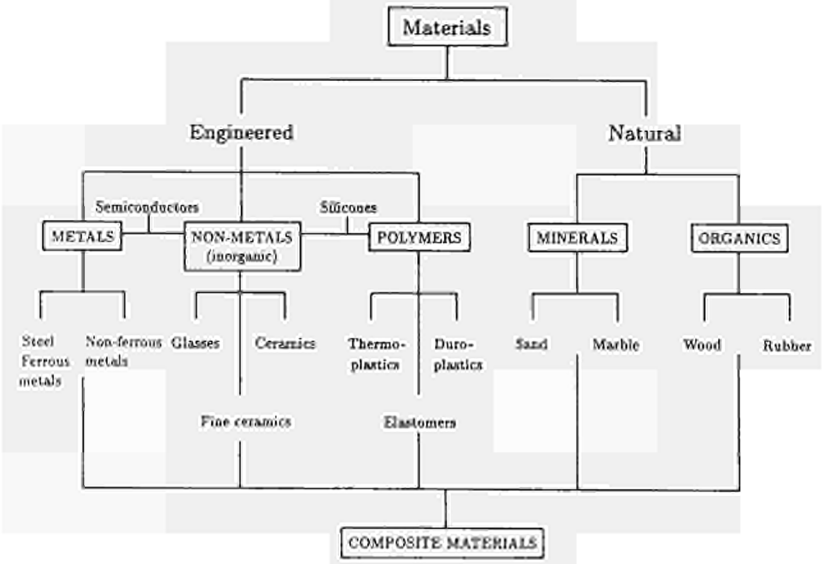

Fig. 2: Classifications of materials

Trends in Application of Materials in the U.S. (Turnover in Billions of US-$)

Materials	1970	1980	1990	2000
Metals	120 (49 %)	132 (46 %)	135 (41 %)	141 (38 %)
Polymers	36 (15 %)	53 (19 %)	76 (23 %)	96 (26 %)
Anorganic Materials (e.g. ceramic, glass)	38 (16 %)	45 (16 %)	53 (16 %)	63 (17 %)
Others (especially wood)	49 (20 %)	55 (19 %)	66 (20 %)	70 (19 %)
Total	243	285	330	370

Fig. 3: Trends for consumption of materials in the USA (Turnover in billions of US$)

Metal World Resources 1992/93, Production 1992 and Expected Lasting Period

Raw Material	Resources Mio. t	Production 1000 t	Lasting Period years
Iron	68 880	505 422	136
Bauxite	22 983	108 669	211
Copper	328	9 405	35
Zinc	149	7 245	21
Lead	70	2 991	23
Nickel	36	905	40
Tin	5	176	28

Source: Bundesanstalt für Geowissenschaften und Rohstoffe (BGR), Oct. 1994

Fig. 4: Metal world resources 1992/93, production 1992 and expected lasting period

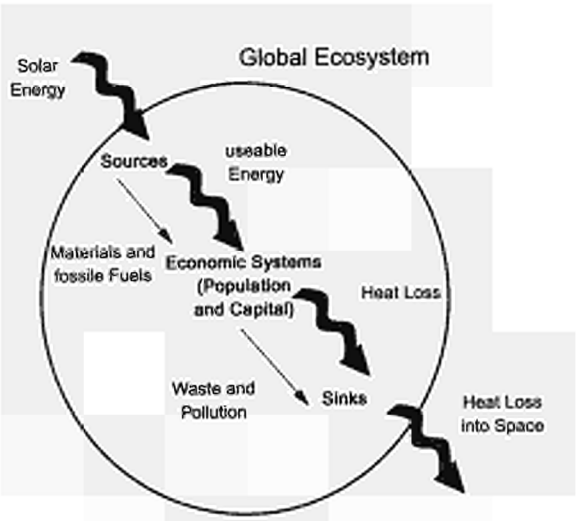

Fig. 5: Population and capital in a global system

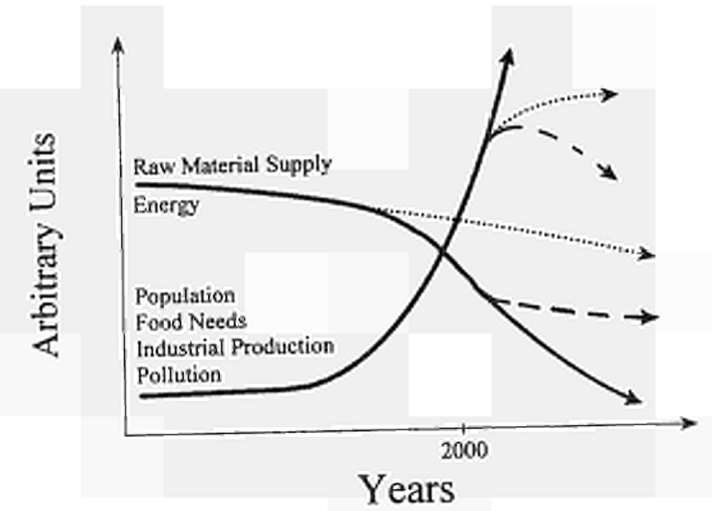

Fig. 6: Change of the situation in "spaceship" earth (schematically)

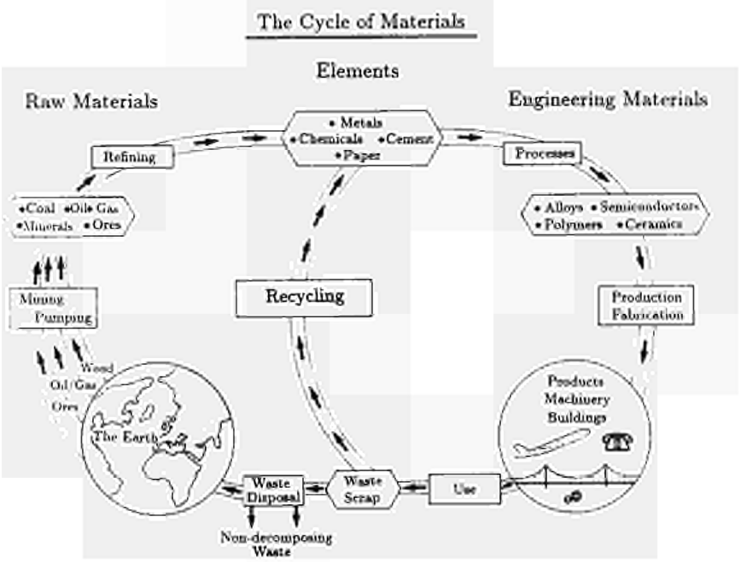

Fig. 7: Cycle of materials

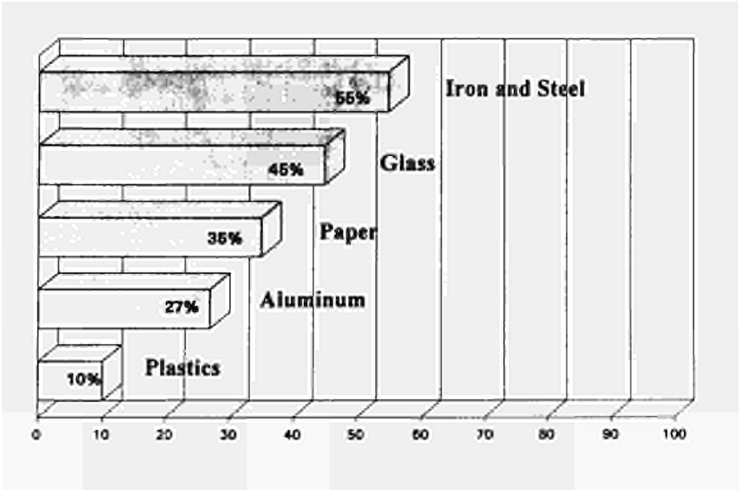

Fig. 8: Recycling rates of several materials

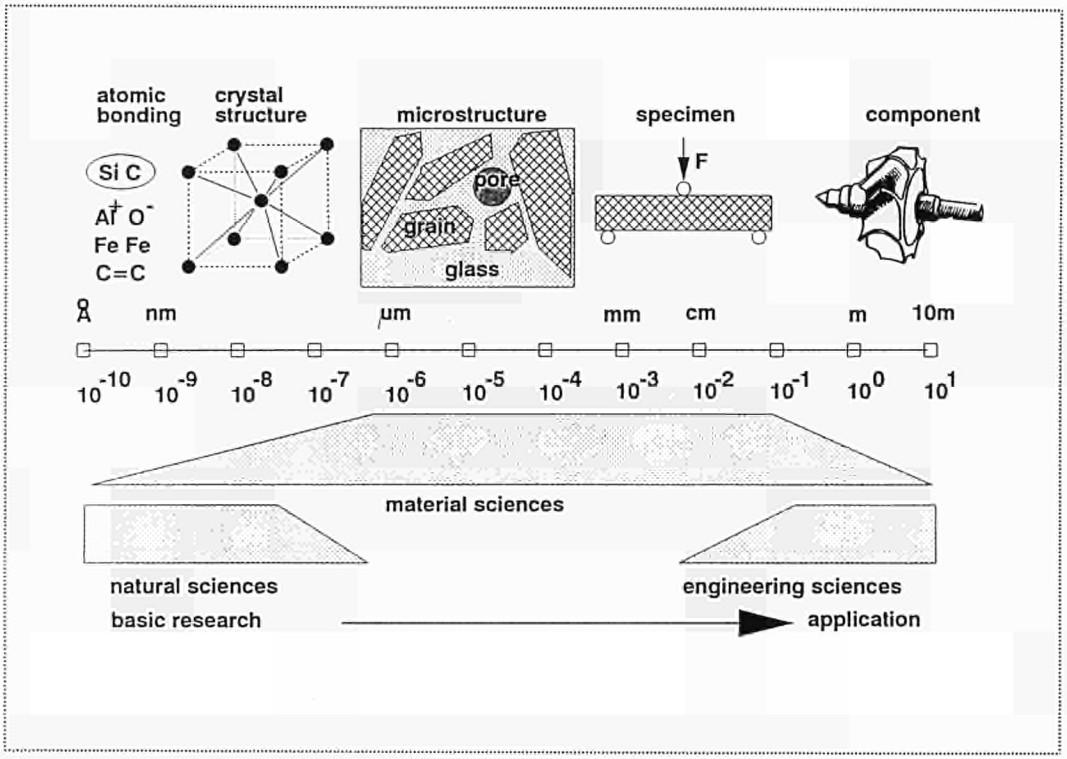

Fig. 9: Microstructural characteristics ranging from the atomic to component size

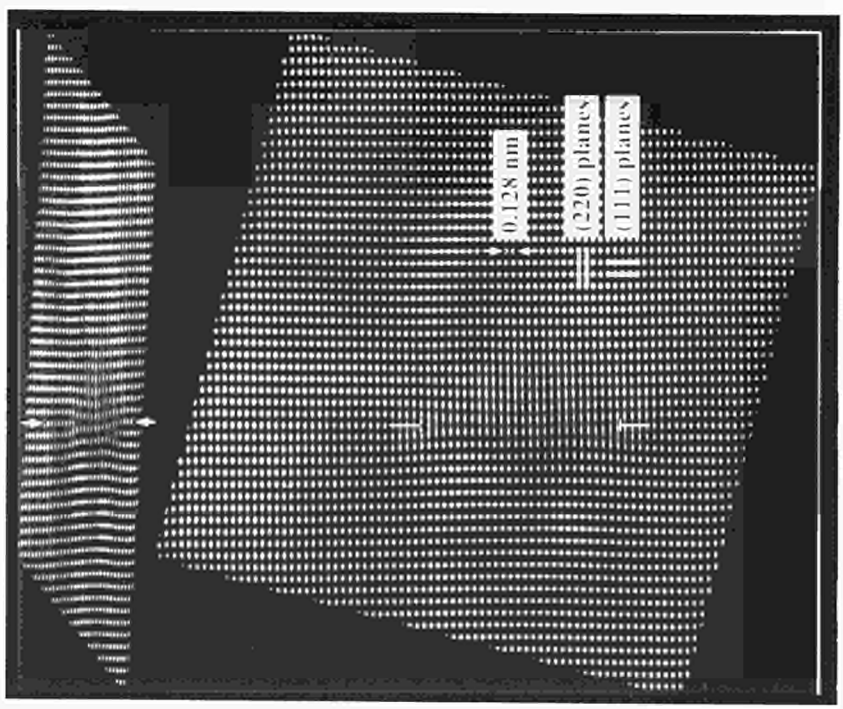

Fig. 10: Direct image of atomic arrangement in a copper single crystal

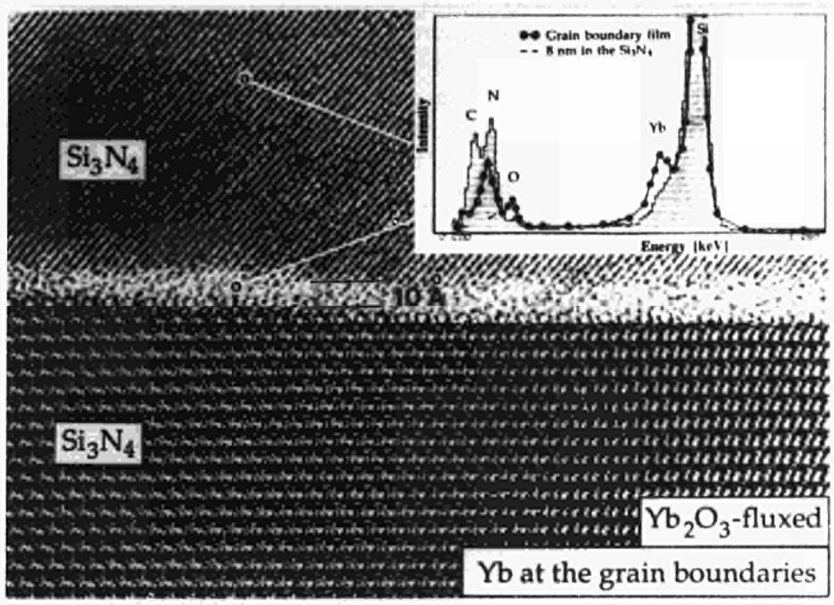

Fig. 11: High resolution electron microscopic image of a Silicon Nitride (Si_3N_4) alloy with and amorphous grain boundary phase in which the sintering additive Ytterbium Oxide (Yb_2O_3) has become concentrated (compare with electron energy loss spectrum in the insert)

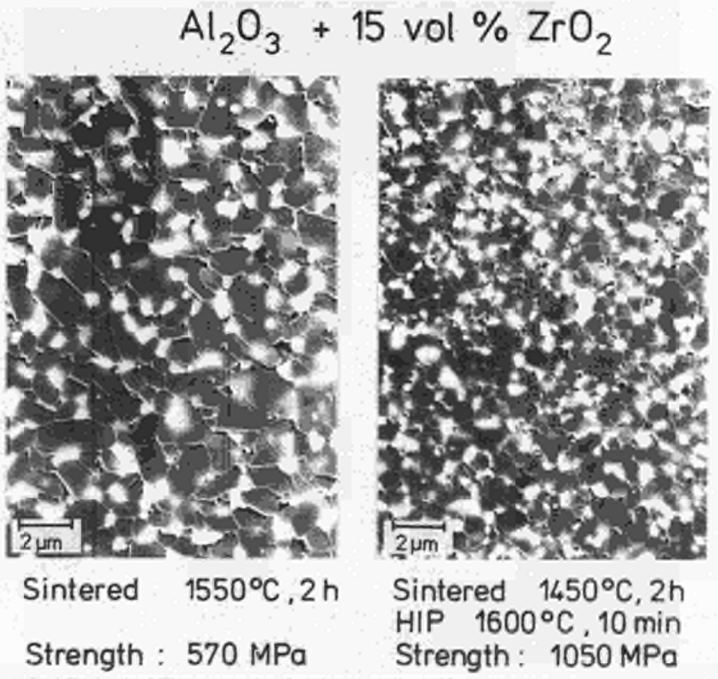

Fig. 12: Example of a microstructural optimization of a dispersion-strengthened alumina-zirconia (Al_2O_3-ZrO_2) ceramic

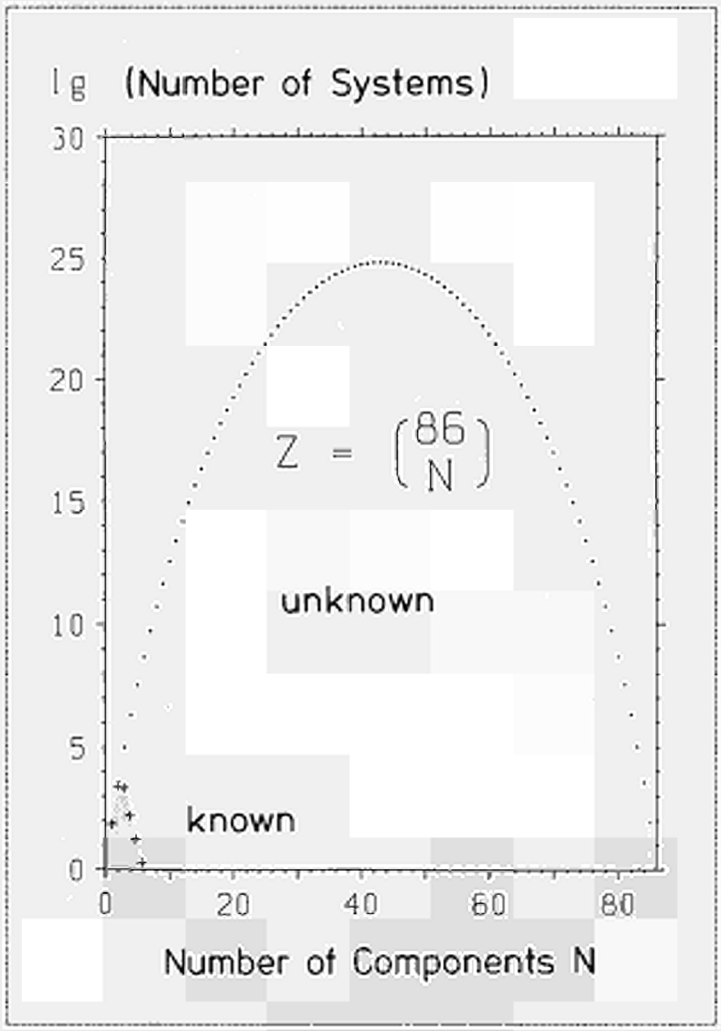

Fig. 13: The "mountains" of materials

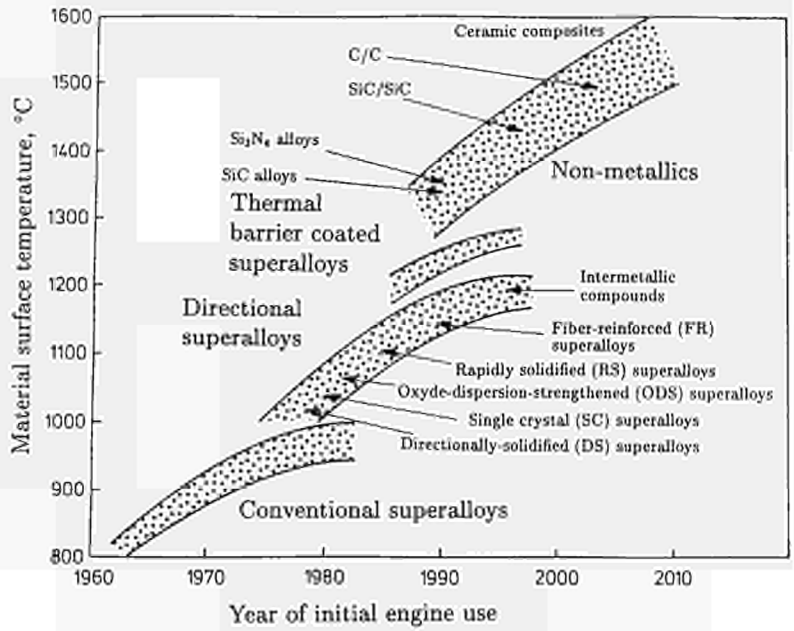

Fig. 14: Evolution of high-temperature materials

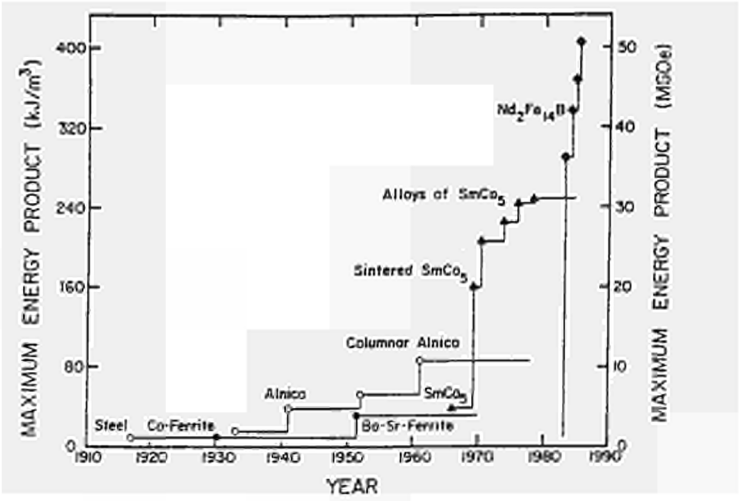

Fig. 15: Evolution of the maximum energy product of permanent magnets

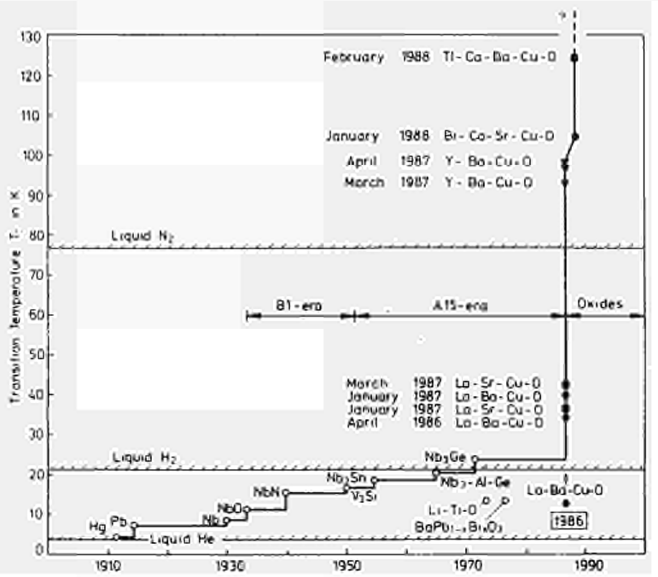

Fig. 16: Evolution of high Tc-Superconductors

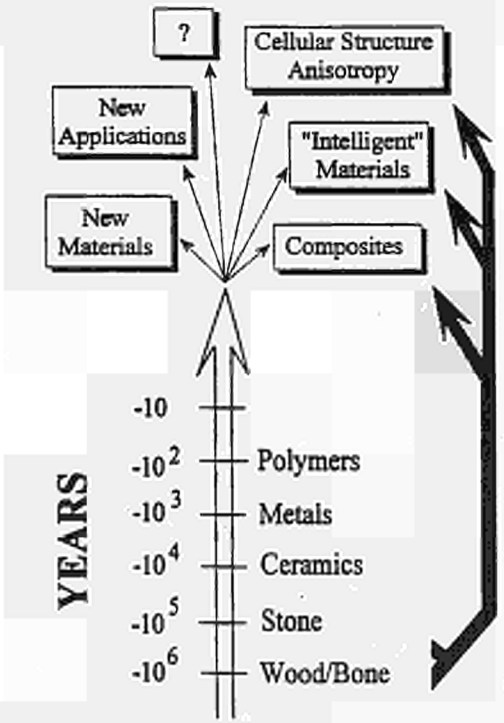

Fig. 17: Challenges and trends in materials development

Phase Relations in the Aluminium-rich Part of the System: Aluminium-Iron-Manganese

F. Weitzer*, P. Rogl* and M. Bohn**

*Institut für Physikalische Chemie, Universität Wien, A-1090 Wien, Währingerstraße 42, Austria
**CNRS-URA 1278, Centre de la Microsonde Electronique de l'ouest, IFREMER, F-29263 Plouzané, Brest, France

Abstract

Phase relations in the manganese-rich part of the ternary system Al-Fe-Mn have been established for an isothermal section at 550 °C for Al concentrations higher than 70 at.%. Experimental techniques employed were optical microscopy, EPMA and X-ray powder diffraction analysis of arc-melted alloys. The samples were subsequently annealed in Al_2O_3-crucibles sealed in evacuated quartz capsules for up to 1500 h and were finally quenched in cold water. Phase equilibria in the Al-Fe-Mn are characterized by the formation of extended solid solution ranges extending from the binary far into the ternary system. The homogeneity regions determined at 550 °C were: $(Fe_xMn_{1-x})Al_6$ with the $MnAl_6$-type for $0 \le x \le 0.6$; $(Fe_xMn_{1-x})Al_{4.15}$ (λ-$MnAl_{4+x}$-type) for $0 \le x \le 0.08$ and $(Fe_xMn_{1-x})Al_4$ (μ-$MnAl_4$-type) for a ternary compound τ_1 with a small range at 550 °C for $0.08 \le x \le 0.20$.

1 Introduction

The various degrees of beneficial influence of alloying elements on grain refinement and precipitation hardening in aluminium spurred an early interest in aluminium-iron-manganese alloys. Despite numerous investigations, which dealt with the constitution of the Al-Fe-Mn system, a complete phase diagram has not yet been established. A critical assessment of all the information available in literature up to 1990 was provided by [92Ran]. For a better understanding of alloy behaviour in technical applications as well as a basis for a proper thermodynamic description of the ternary diagram, work throughout COST 507-II attempted to determine the phase relations for the Al-rich region of the ternary system Al-Fe-Mn within a partial isothermal section at 550 °C including a reinvestigation of the isothermal reactions in the Al-Mn system by high resolution Smith thermal analysis.

2 Experimental

Samples, each of a total weight of about 1g, were prepared by arc melting 4N ingots of Al (Alfa Ventron, Karlsruhe, FRG), platelets of Mn (99.9% pure, South Africa) and lumps of Fe (claimed purity of 99.9%, supplied by J.Matthey & Sons, UK). To ensure maximum homogeneity the alloy buttons were remelted several times under as low an electric current as possible in order to keep the total weight losses below 0.5 mass%. A part of each button was annealed at 550 °C for up to 1500 h. Each specimen was contained in a small alumina crucible and sealed under vacuum in a quartz tube which

after heat treatment was submerged in cold water. Precise lattice parameters and standard deviations were obtained by a least squares refinement using Guinier Huber CrKα_1 or Fe-Kα_1 X-ray powder data at room temperature employing an internal standard of 99.9999% pure Ge (a_{Ge} = 0.5657906 nm). The microstructures of the alloys in the as-cast and annealed condition were studied by optical microscopy on surfaces prepared by SiC-grinding and polishing the resin mounted alloys with diamond pastes down to 1/4 μm grain size. A CAMEBAX SX50 wavelength dispersive spectrograph was used for proper identification of the phases and precipitates. Quantitative analyses were performed comparing the Al-Kα, Fe-Kα and MnKα emissions of the three elements in the alloys with those from Al_2O_3 and/or elemental Al, Fe, Mn as reference materials and applying the PAP correction procedure [85Pou]. An annealed alloy with composition $Al_{71.3}Fe_{28.7(4)}$ (in at.%) defined by wet chemical analysis served as internal standard. The experimental parameters employed were 20 kV acceleration voltage, 15 to 20 nA sample current and spectrometer crystals such as TAP for the AlKα and LiF for the FeKα and MnKα radiation.

3 Results and Discussion

3.1 Binary Systems

The binary systems are accepted from [90Mas]. Some controversy concerns the true melting behaviour of Fe_4Al_{13} (earlier 'FeAl$_3$') for which [86Len] claimed congruent melting. A recent critical assessment of the Al-Mn binary system is due to [87McA]. Isothermal reactions, solidus and liquidus values have been reanalysed by means of precise Smith thermal analysis for a series of seven selected Al-Mn alloys including also the metastable reactions on cooling (for further details on this joint research see the COST-507 report by the research group of F. Hayes in Manchester-UMIST). The crystallographic data and ranges of existence for all of the binary equilibrium phases pertinent to the phase diagram are listed in Table 1.

3.2 Solid Phases

Phase relations in the Al-Fe-Mn ternary are characterizsed by the formation of extended solid solutions, which at 550 °C tend to extend from the binary transition metal aluminides far into the ternary system at a constant aluminium content thus reflecting considerable Fe/Mn atom exchange. Whereas the large solid solubility in $(Fe_xMn_{1-x})Al_6$ and its temperature dependence (increasing iron content with decreasing temperature) have been corroborated by various research teams (see i.e. [92Ran]), there is little known on the ternary mutual solubility of the various iron and manganese aluminides.

We determined the concentration dependence of the unit cell dimensions at 550 °C for $(Fe_xMn_{1-x})Al_6$, $(Fe_{1-x}Mn_x)_4Al_{13}$, $(Fe_{1-x}Mn_x)_2Al_5$ and for $(Fe_xMn_{1-x})_4Al_{11}$ as a function of the Fe/Mn atom exchange. Compositions richer in iron generally show smaller unit cell volumes suggesting a ratio of the atom radii $R_{Fe}/R_{Mn} < 1$. The solubility limits derived from X-ray analyses are in good accordance with those obtained from quantitative EPMA evaluation for two- or three-phase alloys. The results of the EPM analysis determine the vertices of the various three-phase equilibria as well as the solid phase

boundaries of the single phase regions at 550 °C. Whereas earlier data (see e.g. [92Ran]) agree on a large solid solubility of Fe in $MnAl_6$ (continuous solid solution in rapidly quenched alloys [94Ser], but $(Fe_xMn_{1-x})Al_6$, $0 \le x \le 0.6$ at 550 °C derived in this work), earlier investigations claimed very low Mn-solubilities in Fe_4Al_{13} (earlier '$FeAl_3$'), and in Fe_2Al_5 and negligible Fe-solubility in $MnAl_{4.15}$ (earlier '$MnAl_5$'), as well as in $MnAl_4$. As seen from our data, the homogeneity region at 550 °C $(Fe_{1-x}Mn_x)_4Al_{13-y}$ extends to a rather broad field in the ternary, ranging from 72 to 76.5 at.% Al at $x = 0.2$ ($0 \le y \le 2.72$) and up to $(Fe_{1-x}Mn_x)_4Al_{13}$, $0 \le x \le 0.22$ at 550 °C. Maxium solubility of 9.5 at.% Mn is observed at 550 °C for $(Fe_{0.65}Mn_{0.23})_4Al_{13-y}$, $y = 2.46$. Solid solubility limits were determined at 550 °C for Fe_2Al_5 $(Fe_{1-x}Mn_x)_2Al_{5-y}$, $0 \le x \le 0.14$ at $y = 0$ and $0 \le x \le 0.23$ at $y = 0.3$. For $(Fe_xMn_{1-x})Al_{4.15}$ we obtained, $0 \le x \le 0.08$, for $(Fe_xMn_{1-x})Al_4$, $0 \le x \le 0.01$ and for $(Fe_xMn_{1-x})_4Al_{11}$, $0 \le x \le 0.13$.
In the present investigation at least four ternary compounds τ_1 to τ_4 have been identified. Whereas τ_2 to τ_4 seem to form at a fixed composition, a small homogeneous range at 550 °C was determined for τ_1 with an aluminium content of 80 at.% Al : $(Fe_xMn_{1-x})Al_4$, $0.08 \le x \le 0.20$. Results of the X-ray phase analysis on a series of ternary alloys annealed at 550 °C are presented in Table 1.

3.3 Isothermal Section at 550 °C

Fig. 1 presents the phase equilibria derived from X-ray powder data, metallographic and electron microprobe analysis on alloys annealed at 550 °C.

4 Acknowledgements.

Part of the research reported herein has been supported by the Austrian FFF under Zl.5/681/2823 which is gratefully acknowledged.

5 References

80Kon A. Kontio, E.D. Stevens, P. Coppens, R.D. Brown, A.E. Dwight and J.M. Williams, "New Invetigation of the Structure of Mn_4Al_{11}", Acta Crystallogr., **B36**, 435-436 (1980).

85Pou L. Pouchon and F. Pichoir, "Electron Probe Microanalysis applied to Thin Surface Films and Deposits", J.Microsc.Spectrosc.Electron., **10**, 279 (1985).

86Len A. Lendvai, "Phase Diagram of the Al-Fe System up to 45 mass% Iron", J. Mater. Sci., **5**, 1219-1220 (1986).

87McA A.J. McAllister and J.M. Murray, "The Al-Mn (Aluminium-Manganese) System", Bull. Alloy Phase Diagrams, **8**, 438-447 (1987).

89Sho C.B. Shoemaker, D.A. Keszler and D.P. Shoemaker, Acta Crystallogr., **B45**, 13-20 (1989).

90Mas T.B. Massalski, "Binary Alloy Phase Diagrams", ASM International, Materials Park, Oh, 2nd edn., (1990).

91Vil P. Villars and L.D. Calvert, "Pearson's Handbook of Crystallographic Data for Intermetallic Phases", 2nd edn., ASM Internat., Materials Park, (1991).

92Ran Q. Ran, "Aluminium-Iron Manganese", in Ternary Alloys, Eds. G. Effenberg and G. Petzow, Vol **5**, 250-264 (1992).

93Fra H.F. Franzen and G. Kreiner, J. Alloys Compounds., **202,** L21-L23 (1993).

94Ser A. Serneels, G. Davignon, X. Niu, P. Lebrun L. Froyen, B. Verlinden and L. Delaey, "MTM-COST 507II-Report", June 1994, p. 1-10.

94Bur U. Burkhardt, Y. Grin and M. Ellner, "Structure Refinement of the Iron-Aluminium Phase with the Approximate Composition Fe_2Al_5", Acta Crystallogr., **B50**, 313-316 (1994).

94Shi N. Shi, X. Li, Z. Ma and K. Kuo, Acta Crystallogr., **B50**, 22 (1994).

95Ell M. Ellner, "Polymorphic Phase Transf. of Fe_4Al_{13} Causing Multiple Twinning with Decagonal Pseudo-Symmetry", Acta Crystallogr., **B51**, 31 (1995).

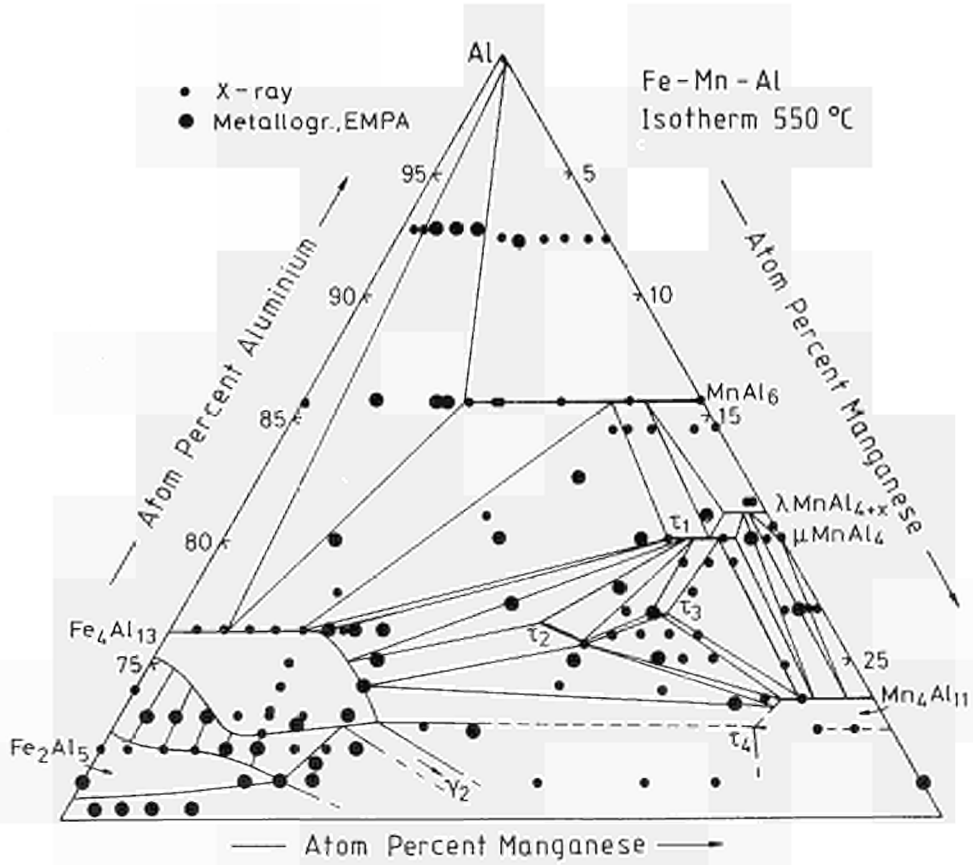

Fig. 1: Fe-Mn-Al system, partial isothermal section for the Al-rich region > 70 at.% Al at 550 °C; location of alloy samples and techniques of investigation.

Table 1: Crystallographic Data of the Binary and Ternary Phases Pertinent to the Isothermal Section in the System Al - Fe - Mn at 550 °C

Phase	Space group	Proto-type	Lattice parameters in nm a	b	c	α (°)	ß(°)	γ(°)	Comment	Reference
(Al)	$Fm\bar{3}m$	Cu	0.40496	-	-	-	-	-	<660.452 °C	[90Mas]
Fe_4Al_{13}	C2/m	Fe_4Al_{13}	1.5492	0.80783	1.2471	-	107.69	-	<1152 °C, 74.5 to 76.6 at.% Al	[90Mas]
			1.56615	0.79949	1.24561	-	107.60	-	$Al_{72.5}Mn_{9.5}Fe_{18}$, EPMA	this work
HT-Fe_4Al_{13}	Bmmm	HT-Fe_4Al_{13}	0.77510	0.40336	2.3771	-	-	-	splat cooling	[95Ell]
Fe_2Al_5	Cmcm	Fe_2Al_5	0.76559	0.64154	0.42184	-	-	-	<1169 °C, 71.0 to 73.0 at.% Al	[94Bur]
			0.76903	0.64207	0.42161	-	-	-	$Al_{70.5}Mn_{5.9}Fe_{23.6}$, EPMA	this work
$FeAl_2$	$P\bar{1}$	$FeAl_2$	0.4787	0.6461	0.8800	91.75	73.29	96.89	<1171 °C, 66.0 to 66.9 at.% Al	[90Mas,91Vil]
$MnAl_{12}$	$Im\bar{3}$	$MnAl_{12}$	0.7507	-	-	-	-	-	<512 °C	[90Mas,91Vil]
$MnAl_6$	Cmcm	$MnAl_6$	0.75551	0.64994	0.88724	-	-	-	<705 °C	[90Mas,91Vil]
			0.74960	0.64937	0.88359	-	-	-	$Al_{85.8}Mn_{5.4}Fe_{8.8}$, EPMA	this work
λ,$MnAl_{4+x}$	$P6_3/m$	λ,$MnAl_4$	2.8382	-	1.2389	-	-	-	<960 °C, 81.0 to 83.2 at.% Al	[93Fra,87McA]
			2.84249	-	1.24161	-	-	-	$Al_{80.4}Mn_{18}Fe_{1.6}$, EPMA	this work
μ,$MnAl_4$	$P6_3/mmc$	μ,$MnAl_4$	1.998	-	2.4673	-	-	-	<923 °C, 79.2 to 81.0 at.% Al	[89Sho,87McA]
φ,Mn_3Al_{10}	$P6_3/mmc$	Co_2Al_5	0.7543	-	0.7898	-	-	-	metastable	[91Vil]
h,Mn_4Al_{11}	$Pna2_1$	HT-$MnAl_3$	1.4837	1.2505	1.2457	-	-	-	1002 to 895 °C, 71.3 to 75.0 at.% Al	[94Shi,87McA]
δ,Mn_4Al_{11}	P1	LT-Mn_4Al_{11}	0.5095	0.8879	0.5051	89.35	100.47	105.08	<916 °C, 73 at.% Al	[80Kon]
			0.50711	0.88251	0.50594	89.89	100.52	105.26	$Al_{73.3}Mn_{26.7}Fe_4$, EPMA	this work
γ_2,Mn_5Al_8	$R\bar{3}m$	Cr_5Al_8	1.2671	-	0.7936	-	-	-	<988 °C, at 63 at.% Al	[92Ran]
									53.0 to 68.6 at.% Al	[87McA]
			1.2611	-	0.7927	-	-	-	at 55 at.% Al	[92Ran]
			1.2599	-	0.7911	-	-	-	at 52 at.% Al	[92Ran]
			1.25973		0.79023				$Al_{64.5}Mn_{28}Fe_{7.5}$, EPMA	this work
τ_1,$Mn_{1-x}Fe_xAl_4$	unknown								2.0 to 4.0 at.% Fe	this work
τ_2,$(Fe_{1-x}Mn_x)_4Al_{13}$	Bmmm	HT-Fe_4Al_{13}	0.7843	0.3992	2.3765	-	-	-	9.0 to 10.0 at.% Fe	this work
τ_3,$(Mn_{1-x}Fe_x)_3Al_{10}$	$P6_3/mcm$	φ,Mn_3Al_{10}	0.75521		0.78698	-	-	-	single phase at 5 at.% Fe	this work
			0.75463		0.78633	-	-	-	multiphase at 5.3at.% Fe	this work
τ_4,$(Mn_{1-x}Fe_x)Al_{3-x}$	$Pna2_1$	HT-$MnAl_3$	1.4721(9)	1.2339(8)	1.2432(8)	-	-	-	$Al_{72}Mn_{23}Fe_5$, EMPA	this work

Thermochemical Properties and Phase Diagram of Cu-Mg-Si and Cu-Mg-Y Alloys

Herbert Ipser[a], V. Ganesan[a], and Ferdinand Sommer[b]

[a] Institut für Anorganische Chemie der Universität Wien, Austria
[b] Max-Planck-Institut für Metallforschung, Stuttgart, F.R.G.

Abstract

This research forms part of the COST 507 program on the two leading systems Al-Mg-Si-Cu and Al-Zn-Cu-Mg (with the additional/substitutional elements Zr, Cr, Rare Earths). It includes magnesium vapor pressure measurements in the binary Mg-Y system as well as in the two ternary systems Cu-Mg-Y and Cu-Mg-Si in Vienna. Additionally, enthalpies of formation for liquid ternary alloys were determined by a calorimetric method in Stuttgart. All thermodynamic data were combined to provide a full thermodynamic description for liquid ternary Cu-Mg-Y and Cu-Mg-Si alloys.

1 Introduction

Light alloys based on aluminum, magnesium, and titanium are of still increasing importance for a wide range of technological applications. A knowledge of the thermodynamic properties and of the phase relationships in the corresponding multicomponent systems is essential in designing such light alloys for particular industrial purposes. Many of these materials are based on aluminum containing several other alloying elements like Cu, Mg, Si, Mn, rare earth elements, etc. For example, it was found that some of the ternary silicides formed in the Cu-Mg-Si system, such as Cu_3Mg_2Si or $Cu_{16}Mg_6Si_7$, may serve as precipitation hardeners in such alloys [73Roc].

On the other hand, small additions of rare earth metals increase the corrosion resistance of rapidly solidified magnesium alloys by improving microstructural and chemical homogeneity together with an enhanced solid solubility limit [90Heh]. In order to understand the solidification behavior of the metastable phases and their transformation characteristics, a thorough knowledge of the thermodynamic properties together with the corresponding phase diagram is necessary. Although yttrium is strictly speaking not a rare earth metal by itself, its properties are very similar to those of the heavier rare earth elements, and therefor its influence on magnesium alloys should be very much alike.

Since virtually nothing is known about the thermochemistry of the corresponding ternary systems it was decided to extend the series of investigations of ternary magnesium alloys (see for example [94Feu, 94Gna, 95Feu]) with a study of the thermodynamic properties of ternary liquid Cu-Mg-Si and Cu-Mg-Y alloys. Furthermore, no Gibbs energy data are available for binary liquid Mg-Y alloys. In

order to facilitate the evaluation of the data in the ternary Cu-Mg-Y system, an investigation of the partial thermodynamic properties of binary liquid Mg-Y alloys was added.

In all cases, magnesium vapor pressures were measured by an isopiesic method which had been developed during Round I of the COST 507 Action [94Gna]. From these, thermodynamic activities of magnesium were derived in the usual way [89Ips]. A calorimetric method [80Som, 82SomI] was employed to determine enthalpies of mixing for liquid alloys. The results were combined to provide a complete description of the thermodynamic mixing behavior for the liquid alloy systems.

2 The Binary Mg-Y System

For the isopiestic vapor pressure measurements in the binary Mg-Y system, tantalum crucibles were originally used, since graphite had been ruled out due to the high stability of the respective yttrium carbides. However, it was found that liquid magnesium-yttrium alloys had a strong tendency to creep out of these crucibles and to react with the graphite crucible holders. Therefore it was attempted to use alumina as container material, which created a new problem since gaseous magnesium reacts rather rapidly with aluminum oxide. Finally, magnesia crucibles were used to contain the samples which prevented any side reactions, but which still did not completely prevent creeeping of the liquid alloys.

Activites of magnesium were determined at 1173 K for liquid alloys with magnesium contents beyond 50 at%. A complete description of the experiments and the corresponding results can be found in **Appendix 1**; they have been published as [97GanI].

3 The Ternary Cu-Mg-Y System

Magnesium vapor pressures were determined using the described isopiestic method [93Gna] along an isopleth with a constant concentration ratio of $x_{Cu}/x_Y = 1/2$. This composition was selected because of the eutectic around 65 at% Y in the Cu-Y binary system [92Oka] which was to guarantee a maximum stability range of the liquid phase in the corresponding ternary section. As in the Mg-Y binary system we had to use magnesia crucibles to contain the samples due to the reactivity of yttrium with graphite. Although some of the liquid alloys showed some creeping tendency it was a much less severe problem than in the binary Mg-Y system. From the magnesium vapor pressures thermodynamic activities of magnesium were derived and converted to a common temperature of 1173 K using partial enthalpy data from the calorimetric measurements. The integral Gibbs energy of mixing for liquid alloys in this section was calculated by means of a Gibbs-Duhem integration following the method outlined by Pelton and Flengas [69Pel].

The entalpy of mixing for ternary liquid alloys was measured along five different isopleths, starting in all cases with liquid binary alloys: one section starting from a binary liquid Cu-Y alloy with 67 at% Y (as in the isopiestic experiments, see above),

three different sections starting from binary liquid Cu-Mg alloys (50, 75, and 90 at% Mg), and one section starting from a binary liquid Mg-Y alloy (8 at% Y).

The obtained experimental results for ternary liquid alloys were interpreted using an association model [82Som2, 90Som]. It was found that a good description was possible with the assumption of three binary associates (Cu_2Mg, CuY, Mg_2Y). With the model parameters obtained from the three limiting binary systems it was possible to calculate thermodynamic properties for ternary liquid alloys. Although there are some indications for ternary interactions, the existing experimental data are still not extensive enough to warrant a corresponding evaluation. All experimental details and the final results are summarized in **Appendix 2** and are published as [97Gan2].

4 The Ternary Cu-Mg-Si System

4.1 Thermodynamic Properties

Magnesium vapor pressures were determined along an isopleth with a constant concentration ratio of $x_{Cu}/x_{Si} = 7/3$ using again the described isopiestic method [93Gna]. This particular composition was selected because of a minimum melting temperature of 802°C at the eutectic point (30 at% Si) in the Cu-Si binary system [86Ole]. It was supposed to guarantee a maximum stability range of the liquid phase in the corresponding ternary section which, however, was reduced considerably by the appearance of a melting point maximum of about 950°C around 33 at% Mg and 13 at% Si [39Wit, 60Asc]. From the vapor pressure measurements, partial thermodynamic properties of magnesium were derived; they are presented for a temperature of 1173 K. A Gibbs-Duhem integration was performed based on the method of Pelton and Flengas [69Pel], using the obtained magnesium activities to calculate integral Gibbs energies of mixing for liquid alloys in the investigated isopleth.

The enthalpy of mixing in this isopleth with $x_{Cu}/x_{Si} = 7/3$ was determined by solution calorimetry [80Som]. Measurements were performed starting both from liquid binary $Cu_{0.7}Si_{0.3}$-alloys (and adding solid magnesium) and from liquid magnesium (adding solid $Cu_{0.7}Si_{0.3}$-samples). Partial enthalpies of mixing of magnesium were derived from the obtained data and were found to be in very good agreement with those derived from the temperature dependence of the magnesium activities.

The obtained thermodynamic results are again interpreted by the described association model [82Som2, 90Som]. All experimental details as well as the final results can be found in **Appendix 3** and will be published soon [97Gan3].

4.2 Phase Diagram

The Cu-Mg-Si phase diagram along the isopleth with $x_{Cu}/x_{Si} = 7/3$ was studied by means of differential thermal analyses (DTA) and X-ray powder diffraction methods. With these it was possible to derive the shape of the liquidus curve. The phase relationships at lower temperatures are very complicated (see also [60Asc]), and it was found that additional measurements will be necessary outside the investigated section

(especially around 33 at% Mg) in order to be able to interpret all experimental observations unequivocally and to construct a correct and consistent phase diagram. These experiments are still in progress.

5 Acknowledgement

The financial support of this study by the Austrian „Bundesministerium für Wissenschaft, Verkehr und Kunst" (contract No. GZ 49.888) and the German „Bundesministerium für Wissenschaft, Forschung und Technologie" (contract No. 03K72025) within the framework of the COST 507 project is gratefully acknowledged.

6 References

39Wit H Witte, Metallwirtschaft, 1939, **18**, 459-463.

60Asc L J Aschan, Acta Polytechn Scand, Chem Includ Metall Ser No 11, 1960, 1-63

69Pel A D Pelton, S N Flengas, Can J Chem, 1969, **47**, 2283-2292.

73Roc E G Rochow: *Comprehensive Inorganic Chemistry, vol. 1*, J C Bailor, Jr, H J Emeleus, R Nyholm, and A F Trotman-Dickenson, eds, Pergamon Press, Oxford, 1973, p. 1361.

80Som F Sommer, J J Lee, B Predel, Z Metallkd, 1980, **71**, 818-821.

82 Som1 F Sommer, Materials and Physical Chemistry in Liquid Metal Systems, H M Borgstedt, ed, Plenum Press, New York, 1982, 387-393.

82 Som2 f Sommer, Z Metallkd, 1982, **73**, 72-76; 77-86.

86Ole R W Olesinski, G J Abbaschian, Bull Alloy Phase Diag, 1986, 7, 170-178.

89 Ips H Ipser, R Krachler, K L Komarek, *Thermochemistry of Alloys*, H Brodowsky and H-J Schaller, eds, Kluwer Academic Publishers, Dordrecht, 1989, pp. 293-306.

90Heh F Hehmann, F Sommer, B Predel, Mater. Sci. Eng., 1990, **A125**, 249.

90Som F Sommer, J Non-Cryst Solids, 1990, **117/118**, 505-512.

92Oka H Okamoto, J Phase Equil, 1992, **13**, 102-103.

94Feu H Feufel, M Krishnaiah, F Sommer, B Predel, J Phase Equil, 1994, **15**, 303-309.

94Gna T Gnanasekaran, H Ipser, Met Mater Trans B, 1994, **25B**, 63-72.

95Feu H Feufel, F. Sommer, J Alloys Comp, 1995, **224**, 42-54.

97Gan1 V Ganesan, H Ipser, J Chim Physique, 1997, in print.

97Gan2 V Ganesan, F Schuller, H Feufel, F Sommer, H Ipser, Z Metallkd, 1997, submitted for publication.

97Gan3 V Ganesan, H Feufel, F Sommer, H Ipser, Met Mater Trans, 1997, publication in preparation.

Summary of Final Report: Project: A4

Experimental Investigations and Thermodynamic Modelling of the Constitution of Quaternary Al-Ti-Metal-Nonmetal Systems

Julius Schuster and Peter Rogl

Institut für Physikalische Chemie Univ. Wien, Währingerstr. 42,
A-1090 Wien, Austria

The results achieved have been presented in form of several manuscripts and publications. Active research cooperation existed throughout the project with groups D4, D11, I1, and UK1.

1.System Ti-Al-C-N. Thermodynamic calculations of the boundary systems Ti-Al-C and Ti-Al-N revealed consistency of the observed phase equilibria with the experimental results obtained in COST 507-round I. For completion of the investigations started in Cost507-I phase equilibria were investigated experimentally at 1375°C. For alloys up to 50 at.%Ti 16 four-phase equilibria were observed or are likely to exist. A scheme of the existing three- and four-phase was established. The two N-phases showed no solubility for the corresponding nonmetal. Although the two H-phases form a complete solid solution at 1480°C, there is a miscibility gap in the nitrogen-rich region. For the region with more than 50 at% Ti a vertical section $Ti_3AlC_xN_{1-x}$ was investigated revealing a novel quaternary perovskite phase P(t) with tetragonal lattice distortion. At temperatures below 1200°C a Re_3B type phase Ti_3AlN was discovered which proved to be isotypic with Zr_3AlN. These results were discussed in detail in publications 1,2.

2.System Ti-Cu-Al-N. As there were no data available on the Ti-Cu-N boundary system a reinvestigation was necesssary in terms of an isothermal section at 850°C revealing a novel phase Ti_3CuN with hitherto unknown crystal structure (Ref. 3). Based on these results as well as on new critical assessments of the Ti-Cu-Al (Ref. 4) and Ti-Al-N (Ref. 5) ternaries, the major part of the Ti-Al-Cu-N quaternary was investigated experimentally at 850°C employing XRD, SEM-EDX and LOM (Ref. 6). The composition of the quaternary eta phase was characterized with respect to its metal ratio by SEM-EDX. A slight deficiency in N is likely (Ref. 7), From the thermodynamic data of the binary boundary systems as well as from the evaluated phase equilibria in the ternary boundary systems thermodynamic data could be extracted for the ternary boundary phases and the quaternary eta-phase (Refs. 8, 9). Employing these data we could prove and amend consistency in the entire quaternary system Ti-Al-Cu-N.

3.System Ti-Sn-Al-N. The investigation of the phase equilibria of the boundary system Ti-Al-Sn in terms of an isothermal section at 900°C was extended into the melting range. The existence of the ternary phase Ti5AlSn2 was also observed in as cast alloys and isotypic phases were also synthesized for the combinations (Ti,Zr,Hf)-(Sn,Pb)-Al (Ref. 10). The ternary boundary system Ti-Sn-N was studied at 900°C employing XRD, SEM-EDX and LOM. No ternary phase was found. Similarly no quaternary phase was encountered in the experimental investigations of the Ti-Al-Sn-N quaternary. The final results are presented in two papers, (Ref.11) and (Ref.12).

4.System Ti-Ni-Al-N. Detailed investigations concerned the ternary phase equilibria Ti-Ni-N at 900°C, as only limited information existed for the join TiN-Ni. No ternary compound exists, however, a large N-uptake up to 11 at%N has been observed from quantitative EPMA for Ti_2NiN_{1-x} ($x \leq 0.5$) (Ref.13). Based on the thermodynamic calculation of the quaternary system in cooperation with group D4 (TU-Clausthal), specific regions of interest have been investigated in detail: (a) precise solid solubility limits of Ni in α_2Ti_3Al and γTiAl and (b) isothermal reactions and solidus/liquidus for selected ternary alloys employing Smith calorimetry. Phase Equilibria in the Ti-Al-Ni isothermal section at 900°C and 1000°C have shown several discrepancies to earlier data in the literature. A compound Ti_3NiAl_2N has been identified and characterized by XRD (Ref. 14).

5.System Ti-Al-Mn-N. The investigation of the phase equilibria in the Ti-Mn-N ternary at 900°C revealed the existence of hitherto unknown new compounds in the Ti-Mn binary. A reinvestigation of the binary system in cooperation with group I1 (Genua) has been performed with XPD, LOM, EMPA and DTA. A complete constitutional diagram x vs. T from 600°C to melting was presented (Ref.15). Three incongruently melting compounds exist in the region $Ti_{45}Mn_{55}$ to $Ti_{55}Mn_{45}$, and four peritectic phases have been identified in the region between $TiMn_2$ and Mn. The ternary phase equilibria studies were also extended up to 1 bar of N_2 at 900°C (Ref.16 and Ref. 17). No ternary compound exists.

6.System Ti-Al-B-C. With respect to the inconsistencies in literature data concerning the calculation of the quaternary system, the section Ti-Al-B was reinvestigated at 1000°C. Quantitative EMPA proved the coecistence of TiB, Ti3B4 and TiB2 with a2 Ti3-xAl1+x (35.5 at.%Al). Based on this new experimental results a thermodynamic calculation of the System Ti-Al-B was attempted by our partner group D11 (MPI-Stuttgart). Results are summarized in Ref. 18.

7. Further contributions to COST 507-II. Within the regularly held meetings among the partner groups in Cost 507-II, latest results were reported and ad hoc cooperations were carried out with Cost 507-II partners in further systems of interest.

(Ti,V,Ta)-Al-N with COST507-II partner D4 (TU-Clausthal): Logistical assistence was given regarding the description of these three ternary systems.

W-B, W-B-C with COST507 Partner D11 (MPI Stuttgart): As part of the quinary system the subsystems W-B and W-B-C have been assessed and modelled by

thermodynamic optimization. A full set of thermodynamic data has been published for W-B (Ref.19) and is provided for W-B-C (Ref. 20).

Hf-C, Zr(Hf)-B-C with group UK1 (NPL-London): The subsystems Hf-C Ti-Zr-B, Ti-Hf-B, Zr-B-C, and Hf-B-C have been assessed and calculated by thermodynamic optimization (Ref.21 to 25). A full set of thermodynamic data has been provided. Difficulties in the binary boride evaluation have forced a calculation and optimization of the data sets on the basis of ternary boride systems (26, 27).

Duration of project: 3 years

Total amount of funding received (in ECU): 147.500.-

Total manpower involved (in man years) 3.5

Number of publications from COST 507-II: 27

(a) number of contributions to scientific journals: 7
(b) number of contriubutions to conferences: 9
(c) other: 11

Publications

(Manuscripts or copies of References Nr.1-6, 13,16,17,19 and 20 have already been submitted as part of the annual reports 1994 and 1995. Manuscripts of the remaining publications and contributions covering the period following the last annual report are enclosed below).

1) M.Pietzka and J.C.Schuster "Das Perowskitsystem Ti_3AlC_{1-x}-Ti_3AlN_{1-x}", in "Nichtmetalle in Metallen '94", D.Hirschferld ed., (DGM Informationsges. Verl., Oberursel, FRG, 1995) 227-2136

2) M.Pietzka and J.C.Schuster "Phase Equilibria in the Quaternary System Ti-Al-C-N" J.Amer.Ceram.Soc., 79 (1996) 2321-2330

3) N.Durlu and J.C.Schuster "The Ternary System Titanium-Copper-Nitrogen" 8th Int.Conf. on High Temp.Mater.Chemistry, Wien, Austria, 1994.

4) J.C.Schuster "The System Ti-Cu-Al", manuscript submitted to COST507-II, Group B (June 1995)

5) J.C.Schuster "The System Ti-Al-N", manuscript submitted to COST507-II, Group B (June 1995)

6) N.Durlu, U.Gruber, M.Pietzka, H.Schmid and J.C.Schuster "Phases and Phase Equilibria in the Quaternary System Ti-Cu-Al-N" Z.Metallk., accepted

7) J.C.Schuster "Quaternary Nitrides Having η-Type Crystal Structures", paper presented at "Journee de Etudes sur les Nitrures" (St.Malo,France,1996)

8) M.A.Pietzka and J.C.Schuster "A Simple Method to Estimate the Stability of Ternary and Quaternary Phases" paper presented at "CALPHAD XXV" (Erice,Italy,1996)

9) M.A.Pietzka and J.C.Schuster "Estimation of the Thermochemical Stability of Ternary and Quaternary Phases Within the System Ti-Cu-Al-N at 850°C" manuscript in preparation

10) M.A.Pietzka and J.C.Schuster "New Ternary Aluminides T_5M_2Al Having W_5Si_3-Type Crystal Structure" J.Alloys and Compounds, 230 (1995) L10-L12

11) J.C.Schuster and M.A.Pietzka "On the Constitution of the System Ti-Al-Sn-N", paper presented at "Thermodynamics of Alloys" (Marseille, France, 1996)

12) M.A.Pietzka and J.C.Schuster "Phase Equilibria of the Quaternary System Ti-Al-Sn- N", J.Alloys and Compounds, in print

13) Y.LeFrieck, J.Bauer, P.Rogl and M.Bohn "The N-Ni-Ti System", J.Phase Equilibria, to be submitted

14) B.Huneau "Etude du Systeme Ternaire Al-Ni-Ti" INSA Rennes, Diploma Thesis (1996)

15) R.Krendelsberger, P.Rogl, J.Bauer, A.Saccone and R.Ferro "The Titanium-Manganese System", paper presented at the Hauptversammlung DGM (Stuttgart, FRG, 1996)

16) J.Bauer, R.Krendelsberger, P.Rogl and D.Antoine "The Mn-Ti-N System" Met.Trans,Ser.A., in preparation

17) P.Rogl, D.Antoine and J.Bauer "The Manganese-Titanium-Nitrogen System", paper presented at Hauptversammlung DGM (Bochum, FRG, 1995)

18) C.Bätzner, G.Effenberg, P.Rogl, J.Bauer and M.Bohn "Experimental Investigation and Thermodynamic Modelling of the System Al-B-Ti", paper presented at "12th Intl.Symp.Boron, Borides and Rel.Compounds" (Baden, Austria, 1996)

19) H.Duschanek and P.Rogl "Critical Assesment and Thermodynamic Calculation of the Binary System Boron-Tungsten", J.Phase Equilibria 16 (1995) 150-161

20) H.Duschanek and P.Rogl "Critical Assessment and Thermodynamic Calculation of the Ternary System Boron-Carbon-Tungsten", to be published in "Ternary Alloys. Special Issue"

*21) H.Bittermann and P.Rogl "The System Hafnium-Carbon" J.Phase Equilibria, to be submitted

*22) H.Duschanek and P.Rogl "Critical Assessment and Thermodynamic Modelling of the Ternary System Zirconium-Boron-Carbon" manuscript submitted to COST-II Groups B,C (Nov.1996)

*23) H.Bittermann and P.Rogl "A Thermodynamic Modelling of the Ternary System Hf-B- C", paper presented at "12th Intl.Symp.Boron, Borides and Rel.Compounds" (Baden, Austria, 1996)

*24) H.Bittermann and P.Rogl "Critical Assessment and Thermodynamic Calculation of the Hf-B-C System", manuscript submitted to COST-II Group ... (Dec. 1996)

25) C.Bätzner, G.Effenberg and P.Rogl "Metal BoroCarbides in the Electronic Materials Science International Workplace", paper presented at "12th Intl. Symp.Boron,Borides and Rel.Compounds" (Baden,Austria, 1996)

26) H.Bittermann, H.Duschanek and P.Rogl "A Thermodynamic Modelling of the Ternary System Ti-Zr-B and Ti-Hf-B", paper presented at CALPHAD XXV (Erice,Italy,1996)

27) H.Bittermann and P.Rogl "Critical Assessment and Thermodynamic Calculation of the Ternary System Boron-Hafnium-Titanium", J.Phase Equilibria, in print

Summary of final report

Directional solidification and phase equilibria in Al-Ni system

O. Hunziker and W. Kurz

Laser surface resolidification and Bridgman directional solidification experiments have been performed in order to determine the microstructure selection map for Ni-rich Ni-Al alloys and Ni-Al-Ti alloys.

It has been shown that taking into account disorder trapping is necessary in order to explain why does γ'-Ni_3Al only grow as primary phase from the liquid at low velocity (below 100 μm/s). The effect of disorder trapping in γ' has been evaluated by laser experiments on $Ni_3(Al,Ti)$, where growth of γ' is thermodynamically favoured by the presence of Ti.

An interactive program calculating the microstructure map has been developed on the basis of models for dendritic, eutectic and plane front growth. This program is an efficient tool in order to optimise the phase diagram by fitting the calculated microstructure map to the experimental map.

The phase diagram determined by this optimisation method displays the following characteristics, necessary to fit the solidification results:

- A very small temperature difference between the stable β-γ' and the metastable β-γ eutectics (<0.05K). This temperature interval is probably overestimated in all recent versions of Ni-Al phase diagram.
- Similar liquidus slopes for γ-Ni and γ'-Ni_3Al near the eutectic temperature.
- Solid composition of γ'-Ni_3Al close to 76 at% Ni.
- Solidification interval for γ'-Ni_3Al between 1 and 4 K, determined at 2.3 K in the optimised version.

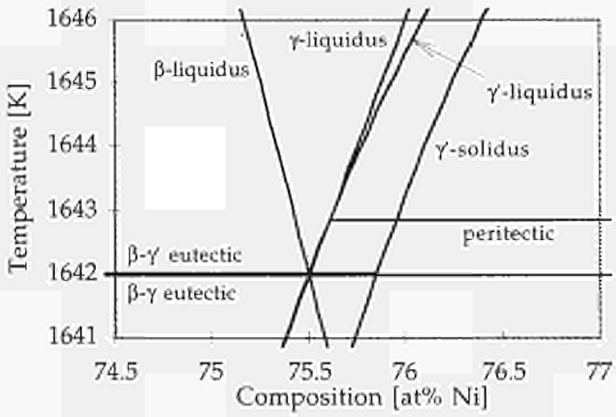

Optimised phase diagram with metastable extensions near the melting point of γ'-Ni_3Al.

Duration of project: 2 years
Total amount of funding received (in ECU): 53'000.- (79'000.- SFr)
Total manpower involved (in man-years) : 2
Number of publications from action COST 507-II : 3
(a) Number of contributions to scientific journals : 1 (accepted)
(b) Number of contributions (posters, present at conf.) : 2 (1 accepted)

Thermodynamic Investigations of Cu-Mg-Si, Cu-Mg-Y, Al-Mg-Zn, Al-Cu-Mg, Al-Mg-Si, Al-Cu-Li and Al-Cu-Zr Alloys

Y.B. Kim, H. Feufel, U. Stolz and F. Sommer

Max-Planck-Institut für Metallforschung
Seestr. 75, D-70174 Stuttgart, Germany

Abstract

The enthalpy of mixing of liquid ternary aluminium and magnesium alloys has been determined to understand the thermodynamics and the phase equilibria of these light alloys. The experiments were performed using a high-temperature isoperibolic type of solution calorimeter.

Results for four sections with constant composition ratios of two components are obtained for liquid Al-Cu-Mg alloys at 986 K. Within the range of experimental accuracy, the measured enthalpies of mixing of a single series and of the points of intersection are self-consistent. An association model is used to calculate the thermodynamic mixing functions of ternary liquid alloys based on model parameters which are determined from thermodynamic results of the base binary systems. The calculated enthalpy of mixing shows systematically less negative values than the measured values. The existence of ternary phases and the possibility to obtain metastable quasicrystals by rapid solidification show that these deviations are caused by additional ternary interactions in the liquid state. These ternary interactions are correlated with a value of 1.8 of the mean number of conduction electrons per atom.

The enthalpy of mixing of liquid Al-Mg-Zn ternary liquid alloys was determined in the temperature range between 883 K and 933 K. An association model is used to

calculate the thermodynamic mixing functions of the ternary alloys based on the thermodynamic properties of the binary bordering systems. The calculated values of the enthalpy of mixing show a good agreement with measured values within the range of experimental accuracy. The presence of additional ternary interactions or ternary associates in the liquid state could not be observed.

Enthalpies of mixing of ternary liquid Cu-Mg-Y alloys were determined along five different sections. For one of these sections ($x_{Cu}/x_Y = 0.5$), magnesium vapor pressures were measured by means of an isopiestic method (A2), and the corresponding values of the magnesium activity at 1173 K were derived as a function of composition. The Gibbs energy of mixing was computed by a Gibbs-Duhem integration. An association model was applied to calculate the thermodynamic functions of mixing for ternary liquid alloys using the model parameters of the base binary systems.

Thermodynamic properties of ternary liquid Cu-Mg-Si alloys with a constant composition ratio $x_{Cu}/x_{Si} = 7/3$ were determined using a combination of different experimental methods: Enthalpies of mixing were measured by isoperibolic calorimetry and magnesium vapor pressures were obtained by an isopiestic method (A2). Partial thermodynamic properties of magnesium were derived from the vapor pressure data, and the composition dependence of the magnesium activities is given for 1173 K. Gibbs energies of mixing for liquid alloys were calculated by a Gibbs-Duhem integration. Finally, an association model was applied to provide the thermodynamic functions of mixing for ternary liquid alloys using the model parameters of the three limiting binary systems.

The enthalpy of mixing of liquid Al-Cu-Zr alloys were determined along eigth different sections at 1480 ± 5 K using two different measurement procedures. The enthalpy of mixing exhibit very negative values with a minimum of about -53 kJ mol^{-1} at the composition $Al_{50}Cu_{20}Zr_{30}$.

The enthalpy of mixing of liquid Al-Cu-Li alloys were obtained for two sections with constant composition ratios ($Al_{0.80}Li_{0.20}$-Cu, $Al_{0.84}Cu_{0.16}$-Li) at 945 K and 986 K, respectively.

The enthalpy of formation of the congruently melting ternary phases τ_5-$Fe_2Al_{7.4}Si$ and τ_6-$Fe_2Al_9Si_2$ was measured using an isoperibolic high temperature solution calorimeter by solution in a liquid aluminium bath at 1343 K. The values for the enthalpies of formation at 298 K are $\Delta_{form}H(Fe_2Al_{7.4}Si) = -34.3 \pm 2$ kJ mol^{-1} and $\Delta_{form}H(Fe_2Al_9Si) = -24.5 \pm 2$ kJ mol^{-1}.

The enthalpies of formation and fusion as well as the heat capacity of Mg_2Si were measured calorimetrically. The Al corner of the Al-Mg-Si ternary system was investigated by DTA and optical micrography. A few points of the solvus of the Al(fcc) solid solution were determined by dilatometry. The results of these experiments together with literature data were used to redetermine a complete set of analytical descriptions of the Gibbs energies of all stable phases of the Al-Mg-Si system by (D11).

Introduction

It is the aim of this study to determine experimentally thermodynamic properties of liquid and solid ternary aluminium and magnesium alloys. The results contribute to understand their thermodynamics and make it feasible with available literature data to evaluate or reevaluate the corresponding phase equilibria. The enthalpy of mixing of liquid Al-Cu-Mg, Al-Mg-Zn, Cu-Mg-Y, Cu-Mg-Si, Al-Cu-Zr and Al-Cu-Li alloys has been determined calorimetrically. The enthalpy of formation at room temperature of ternary intermetallic compounds in the system Al-Fe-Si have been determined calorimetrically. All investigations are performed in collaboration with other partners within COST 507-2 [Al-Cu-Mg, Effenberg (D12), Spencer (D3); Al-Mg-Zn, Effenberg (D12), Lukas (D4); Cu-Mg-Y, Ipser (A2), Spencer (D3); Cu-Mg-Si, Ipser (A2), Spencer (D3); Al-Cu-Zr, Hämäläinen (SF1); Al-Cu-Li, Hämäläinen (SF1); Al-Mg-Si, Lukas (D4), Kolby (N1); Al-Fe-Si, Rogl (A1)]. The COST 507-2 action has given the opportunity to carry out this work in good collaboration and continous discussion with the european partners. The results of the different systems are presented in detail as publications.

Determination of the Enthalpy of Mixing of Liquid Aluminium-Copper-Magnesium Alloys
Y. B. Kim, F. Sommer and B. Predel
Z. Metallkd., 86 (1995) 9, 597-602.

Calorimetric Investigation of Liquid Aluminium-Magnesium-Zinc Alloys
Y.B. Kim, F.Sommer and B. Predel
J.Alloys and Comp., 247 (1997) 43-51

Thermodynamic Properties of Ternary Liquid Cu-Mg-Y Alloys
V. Ganesan, F. Schuller, H. Feufel, F. Sommer and H.Ipser
to be published in Z. Metallk., (1997)

Thermochemistry of Ternary Liquid Cu-Mg-Si Alloys
V. Ganesan, H. Feufel, F. Sommer and H. Ipser
to be published in Met.Trans. B (1997).

Enthalpy of Mixing of Liquid Al-Cu-Zr Alloys
to be published

Enthalpy of Mixing of Liquid Al-Cu-Li Alloys
to be published

On the Thermodynamic Stability and Solid Solution Behaviour of the Phases τ_5-$Fe_2Al_{7.4}Si$ and and τ_6-$Fe_2Al_9Si_2$
M. Vyboronov, P. Rogl and F. Sommer
J.Alloys and Comp.247 (1997) 154-157

Investigation of the Al-Mg-Si System by Experiments and Thermodynamic Calculations
H. Feufel, T. Gödecke, H. L. Lukas and F. Sommer
J.Alloys and Comp., 247 (1997) 31-42.

Thermodynamic evaluations for high-strength, hot-strength and wrought aluminium alloys

Tatjana Jantzen, Suzana G. Fries, Iñaki Hurtado, Michel H. G. Jacobs and Philip J. Spencer

Lehrstuhl für Theoretische Hüttenkunde, RWTH Aachen, Kopernukusstr.16, D-52074 Aachen, Germany

Abstract

In this work, thermodynamic evaluations of the binary system Cu-Si and the ternary systems Al-Cu-Mg, Al-Cu-Si, Al-Cu-Zn, Cu-Mg-Si, Cu-Mg-Y and Cu-Mg-Ni are presented. The results of the calculations are compared with published experimental data and with experimental data which have become available during the progress of the COST Action 507.

1 Introduction

High-strength, hot-strength and wrought aluminium alloys are of considerable technological importance. For their design and development a knowledge of the phase constitution, which influences the mechanical and physical properties of the alloys and thus their suitability for particular applications, is essential.
LTH has been concerned with the thermodynamic evaluation of systems based on Al-Cu-Mg-Si-Zn (Ni,Y),which is one of the key systems in COST 507 Round 2.
The binary sub-systems have already been evaluated in the first round of COST 507. The thermodynamic assessment of the ternary systems, on which calculations in more complex systems are based, has been the major aim of the work in the second round.
Particular attention has been given to the modelling of phases such as the Laves and the T phase, since it is essential that the models used are compatible for the description of the extensions of the phases into all the different subsystems in which they appear.

2 Data Assessment

A significant number of all the binary and ternary sub-systems of the Al-Cu-Mg-Si-Zn system, on which calculations in more complex systems are based, have already been evaluated in the first round of the COST-507 Project.

2.1 The Cu-Si system

In view of experimental data and the necessity to describe ternary systems into which several of the binary phases extend, the Cu-Si system was re-evaluated.

In the Cu-Si system there are six compounds ($Cu_{85}Si_{15}$-β, $Cu_{19}Si_6$-η, $Cu_{33}Si_7$-δ, Cu_4Si-ε, $Cu_{56}Si_{11}$-γ, $Cu_{87}Si_{13}$-κ), all of them were modelled as stoichiometric phases. The binary phase $Cu_{85}Si_{15}$-β which has the crystallographic structure bcc-A2, extends into the ternary Al-Cu-Si system, and the phase $Cu_{87}Si_{13}$-κ with the structure hcp-A3 exists in the Cu-Mg-Si system. Although there is a lack of experimental data necessary for a reliable definition of the ranges of stability of these binary phases, the phases were nevertheless now modelled as non-stoichiometric in order to describe the solution of other elements in them. Table 1 summarizes the invariants which were used for the optimisation of the bcc-A2 and hcp-A3 phases.

Table 1. Invariant equilibria used for the optimisation of the Cu-Si system

Phase equilbria	[40Smi]	present work
liquid + fcc-A1 = bcc-A2	1125	1125
liquid + bcc-A2 = $Cu_{33}Si_7$-δ	1097	1093
liquid + bcc-A2 = hcp-A3	1115	1116
fcc-A1 + $Cu_{56}Si_{11}$-γ = hcp-A3	825	826
$Cu_{33}Si_7$-δ + hcp-A3 = bcc-A2	1058	1059
$Cu_{33}Si_7$-δ + hcp-A3 = $Cu_{56}Si_{11}$-γ	1002	1008

The calculated phase diagram is presented in Fig. 1. Above 673 K it shows good agreement with the known experimental data [73Hul].

2.1 The Al-Cu-Mg system

The phase diagram of the Al-Cu-Mg system is very complicated and contains three ternary, near-stochiometric compounds Q ($Al_7Cu_3Mg_6$), V ($Al_{11}Cu_{11}Mg_4$) and S(Al_2CuMg), one non-stoichiometric phase T with the $Mg_{32}(Al,Cu)_{49}$ prototype structure, and three Laves phases. The Laves-C15 phase, extending from the Cu-Mg binary to higher Al concentrations, transforms first into the C-36 and then the C-14 Laves type structures, with slight deviation of stoichiometry from Cu and Mg ideal compositions. The phase diagram data [83Bel], [81Mel], [55Zam], [49Ura], [59Phi] and experimental thermodynamic data [86Rod], [72Pre], [86Not], [46Pet] provide basic information for the optimisation of this system. New investigations of Al-Cu-Mg alloys were carried out by [95Kim] and [95Soa] in the COST Action and used in the assessment.

Figure 2 presents the calculated isothermal section at 785 K and shows the solubility ranges of the Laves phases. The calculated solvus curves and solvus surface in the Al-corner are in satisfactory agreement with the experimental data (Figures 3-4).

The invariant reactions in the Al-corner, which are important for commercial Al alloys, are given in Table 2 and compared with experimental data.

Figure 5 presents the calculated liquidus surface of the Al-Cu-Mg system. The liquidus isotherms at 1100K, 1000 K, 900 K and 800 K are indicated by the dashed contours.
Figure 6 shows the calculated and experimental isopleth at 70 wt.% Al. The experimental liquidus is well reproduced by the calculations.

Table 2. Invariant equilibria with (Al)

Composition, mole fraction	present work, T (K)	[91Pri]	[59Phi]	[83Bel]
liquid + S = (Al)+ T	**741**	**741**	**740**	**743**
x(liquid,Al)	0.668	0.659	0.656	0.655
x(liquid,Cu)	0.049	0.044	0.047	0.047
x(liquid,Mg)	0.283	0.297	0.300	0.298
liquid =(Al) + θ + S	**775**	**779**	**780**	**775**
x(liquid,Al)	0.739	0.734	0.766	0.756
x(liquid,Cu)	0.155	0.171	0.153	0.153
x(liquid,Mg)	0.106		0.081	0.091
		0.095		
liquid = S + (Al)	**776**	**788**	**791**	**788**
x(liquid,Al)	0.726	0.726	0.750	0.719
x(liquid,Cu)	0.104	0.137	0.120	0.130
x(liquid,Mg)	0.170	0.137	0.130	0.151
liquid = T +(Al) + β	**717**	**716**	**724**	**724**
x(liquid,Al)	0.631	0.628	0.637	0.641
x(liquid,Cu)	0.012	0.012	0.011	0.011
x(liquid,Mg)	0.357	0.358	0.352	0.348

2.2 The Al-Cu-Si system

The liquidus surface of the ternary system has been calculated using the thermodynamic evaluations of the binary sub-systems. The calculations are in reasonable agreement with the experimental liquidus data of [36His], [34Mat] and [53Phi], which are located in the central part of the phase diagram (T=1073, 973 and 873 K in Figure 7). Isopleth sections at 4 wt.% Cu, 1 wt.% Si and 2 wt.% Cu are presented in Figures 8-10 and compared with the experimental data of [53Phi] and [90Kuz2].

2.3 The Al-Cu-Zn system

Only the Al-rich corner of the ternary system Al-Cu-Zn has been preliminarily assessed. This limitation is due to the problems in finding a suitable model for the so-called γ-phase. This phase extends between the γ-phase in the Al-Cu binary and the similarly named γ-phase in the Cu-Zn binary. The experimental results indicate complete solubility for the entire composition range between the phases. Nevertheless, the structures of the two binary phases are different

and have been independently described by different sublattice models in the first round of the COST-507 project, Table 3.
The presence of a non-first order transition from $D8_3$ to $D8_2$ seems necessary to make compatible both structures, although there is lack of experimental data to corroborate it. Thus, it may be essential to make systematic measurements of Cp along the γ-phase region in order to determine the possible order-order transition boundary.

Table 3. Structures of the binary γ-phases and sublattices used to describe them.

γ phase	in binary Al-Cu	in binary Cu-Zn
Structure	$D8_3$ (cP52), $P\bar{4}3m$	$D8_2$ (cI52), $I\bar{4}3m$
Sublattice model	$(Al)_{16}:(Al,Cu)_4:(Cu)_{32}$	$(Cu,Zn)_8:(Cu,Zn)_8:(Cu)_{12}:(Zn)_{24}$

From the point of view of the sublattice models, two alternatives are possible. Either to build an „hypothetical intermediate" sublattice to connect both structures or to modify the binary descriptions of the binary γ-phases. The first alternative has some advantages, such as its rapid implementation and the lack of necessity for a change in the binary descriptions already in use. Its main disadvantage is related to the complications it introduces in the phase description, which will increase for higher order systems. Thus, even if this „provisional" solution is first used, a modification of the binary descriptions seems to be inevitable in the long term. The new model should account for the experimentally observed structures and atomic occupancies for the whole range of the γ-phase.
Experimentally, eight crystallographically different positions are observed, which in a simplified model could be reduced to four. In this case a possible sublattice model for describing the γ-phase would be:

$$(Al,Cu,Zn)_8 : (Cu)_8 : (Cu,Zn)_{12} : (Al,Cu,Zn)_{24}$$

The ternary Al-Cu-Zn system also displays one ternary phase, τ, with a large range of solubility. This phase is present below 740°C at compositions close to $Cu_{40}Zn_{20}Al_{34}$. Its main feature is that at low temperatures its range of existence is split into two non-interconnected zones. In one of these regions, denoted as τ′, the experimental results show that a superstructure is created by the presence of structural vacancies, fig. 11. The vacancies produce a loss of symmetry in this τ′ phase (rombohedral) with respect to the high temperature τ phase (B2).
Crystallographically, both τ and τ′, could be described as a single phase using a two sublattice model containing vacancies: $(Al,Zn)_1 : (Cu,Va)_1$
However, such a model, although simple, would not be compatible either with the present descriptions of the B2 structures or with the description of the A2-B2 ordering transition. Thus, the actually compatible model should be

$$(\underline{Al},Cu,\underline{Zn},Va)_1 : (Al,\underline{Cu},Zn,\underline{Va})_1$$

There is a complete lack in the literature of thermodynamic data for the τ and τ′ phases. Thermodynamic measurements for this phase, such as enthalpies of formation and Cp, are badly needed.

2.4 The Cu-Mg-Si system

The Cu-Mg-Si system displays one Laves phase, C15 and two near-stoichiometric ternary phases σ ($Cu_{16}Mg_6Si_7$) and τ (Cu_3Mg_2Si). Published experimental information for the system is limited to the Cu-corner, where DTA and X-ray measurements have been reported in [60Asc]. For the thermodynamic assessment of the Cu-Mg-Si system, the partial and integral enthalpies of mixing, the activities of Mg in the liquid phase and DTA determinations of phase boundaries reported in [97Gan] were used. The calculations are compared with experimental data in Figures 12 and 13. The invariant reactions which were used for the optimisation of the system are presented in Table 4.

Table 4. Invariant reactions

Phase equilibria	Literature	present work, T (K)
liquid = (Si) + $Cu_{19}Si_6$-η + σ	1015 [97Gan] 1013 [60Asc]	1015
liquid = CuMg2 + Mg2Si + τ	797 [97Gan]	798
liquid = (Si) + Mg2Si + τ	1043 [39Wit]	1037
liquid = σ	1099 [97Gan]	1102
liquid = τ	1203 [97Gan]	1206

The measurements were carried out for the isopleth Cu_7Si_3 + Mg only. A complete assessment of the system requires additional experimental data.

2.5 The Cu-Mg-Y system

For the thermodynamic assessment of the system use has been made of available thermodynamic evaluations of the binary sub-systems.
The basis of the evaluation is provided by the thermodynamic measurements carried out by [97Gan]. Figures 14 and 15 show the calculated partial enthalpies of Y in the liquid phase compared with the experimental data.

2.6 The Cu-Mg-Ni system

In the system Cu-Mg-Ni experimental information concerning the solid phases is lacking. Therefore the evaluation of the system is restricted to the temperature and concentration range for which experimental data are available.
The activity data of Mg in the liquid phase as reported in [93Gna1] and [93Gna2] for several isopleths are reproduced well. In Fig. 16 the experimental activity data are plotted together with the result of the calculation for the

isopleth X_{Cu}/X_{Ni}=0.5. In Figure 17 the results of the calculation of this isopleth are compared with the experimental data.

Acknowledgement

The financial support of the German Bundesministerium für Bildung, Wissenschaft, Forschung und Technologie, project 03K7203 6, within the framework of COST Action 507, is gratefully acknowledged.

3 References

[34Mat] K.Matsuyama, Kizoki no Kenkyu, 1934, **11**, 461-190.
[36His] C.Hisatsune, Mem.Coll.Eng.Kyoto to Hagane, 1936, **22**, 597-622.
[39Wit] H. Witte, Metallwirtschaft, 1939, **18**, 459-463.
[40Smi] C.S.Smith, Trans. AIME, 1940, **137**, 313-329.
[46Pet] D.A.Petrow,G.S.Berg, Zhur. Fiz. Khim., 1946, **20**, 1475
[49Ura] G.G.Urazov, M.S.Mirgalovskaya, Izv. Sekt. Fiz. Khim. Anal., 1949, **19**, 514.
[53Phi] H.W.L.Philips, J. Inst. Metals, 1953, **82**, 9-15.
[55Zam] M.I.Zamotorin, Lenin. polit. instit., Trudy, 1955, **180**, 32.
[59Phi] H.W.Phillips, J. Inst. Metals, 1959, **25**, 27.
[60Asc] L.J.Aschan, Acta Polyt.Scan., Ch 11, 1960, **285**.
[72Pre] B.Predel, H.Ruge, Mater. Sci. Eng., 1972, **9**, 141.
[73Hul] R.Hultgren, D.D.Desai, D.T.Hawkins, M.Gleiser and K.K.Kelley, Selected Values of Thermodynamic Properties of Binary Alloys, American Society of Metals, 1973.
[81Mel] E.V.Mel'nik, V.V.Kinzhibalo, Russ.Metall., 1981, **3**, 154.
[83Bel] A.I.Beljaew, *Metalloved. alumin.*, Metallurgia, Moscow, 1983, 73.
[86Rod] E.K.Rodionova, N.M.Martynova, Zh.Fiz.Khim., 1986, **6**, 1382.
[86Not] M.Notin, M.Dirand, D.Bouaziz, C.R.Acad.Sci.Paris, 1986, **302**, 63
[90Kuz2] G.M.Kuznetsov, L.N.Kalkulova, O.B.Mamzurin, Izvest.Vyssh. Zaved., 1990, **2**, 94-100.
[91Pri] A.Prince, G.Effenberg, *"Aluminium-Copper-Magnesium", inTernary Alloys*, ed. G.Petzow, G.Effenberg, Vol.4, VCH Verlagsges., Weinheim, 1991, 547.
[93Gna1] T.Gnanasekaran, H.Ipser,J.Chim.Phys.,1993, **90**, 367-372.
[93Gna2] T.Gnanasekaran, H.Ipser,J.Non-Cryst.Solids,1993,**156-158**,384-387.
[95Kim] Y.B.Kim, F.Sommer, B.Predel, Z.Metallkd., 1995, **86**, 597.
[95Soa] D.Soares, L.F.Malheiros, M.Hämäläinen, F.Castro, J.Alloys and Compounds, 1995, **220**, 179.
[97Gan] V.Ganesan, F.Schuller, H.Feufel, F.Sommer, H.Ipser, 1997, to be published.

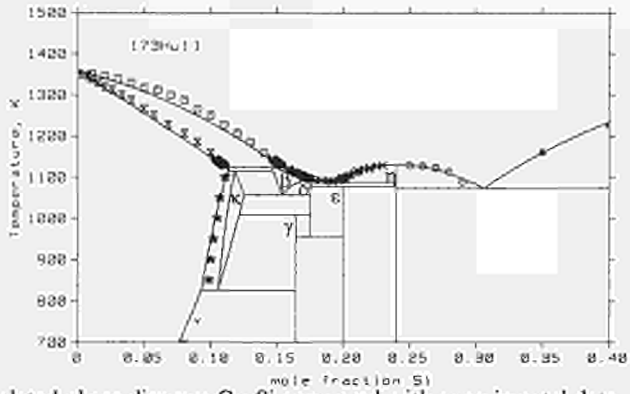

Fig. 1. The calculated phase diagram Cu-Si compared with experimental data.

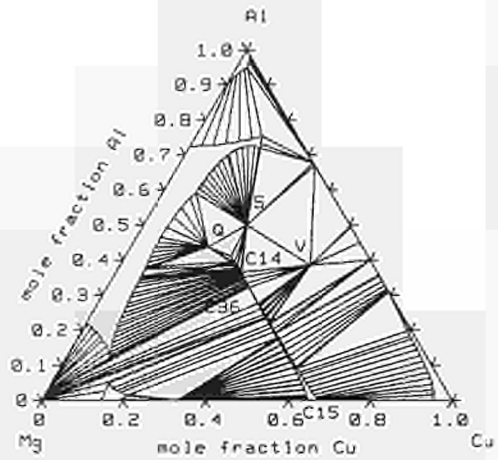

Fig.2.Isothermal section at 785 K in the Al-Cu-Mg system.

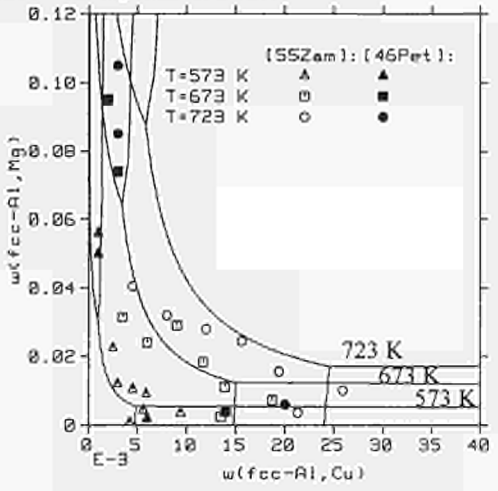

Fig.3.Solubility ranges of Cu and Mg in (Al) in the Al-Cu-Mg system.

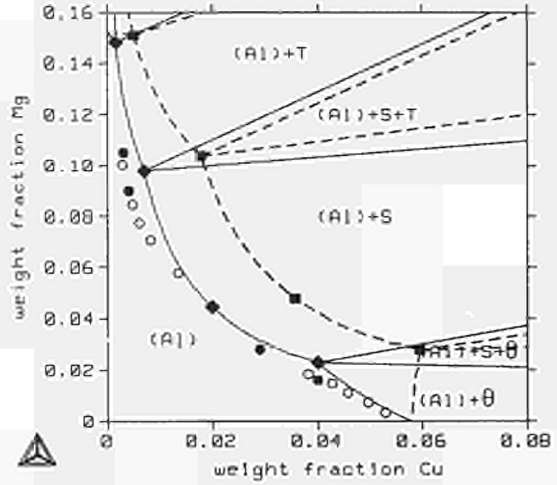

Calculation or experiment	solvus surface	Invari-ants
[59Phi]	○	●
ternary L(fcc) used	⌒	◆
no ternary L(fcc) used	⌒	■

Fig.4.Solvus surface in the Al-corner in the Al-Cu-Mg system.

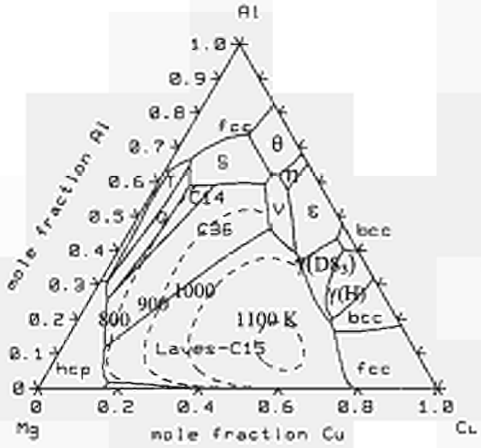

Fig.5.Liquidus surface in the Al-Cu-Mg system.

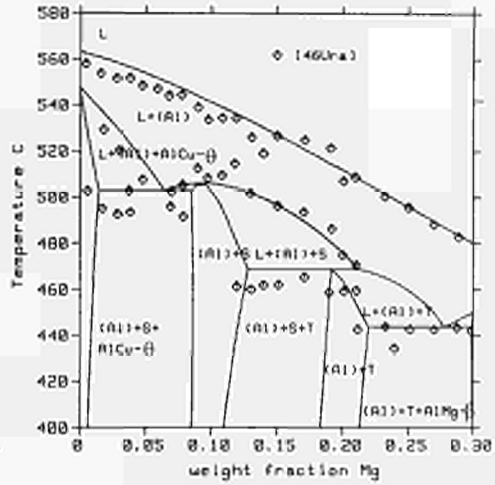

Fig.6.Isopleth at 70 wt.% Al in the Al-Cu-Mg system.

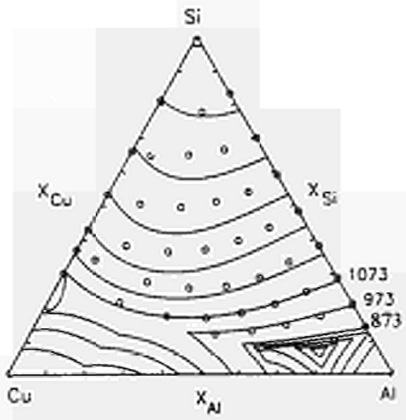

Fig.7.Liquidus surface in the Al-Cu-Si system.

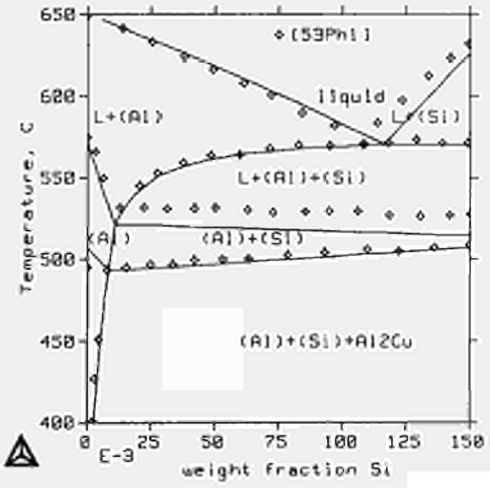

Fig.8.Isopleth at 4 wt.% Cu in the Al-Cu-Si system.

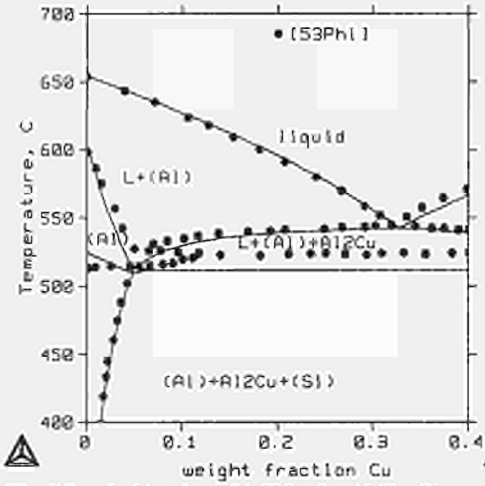

Fig.9. Isopleth at 1 wt.% Si in the Al-Cu-Si system.

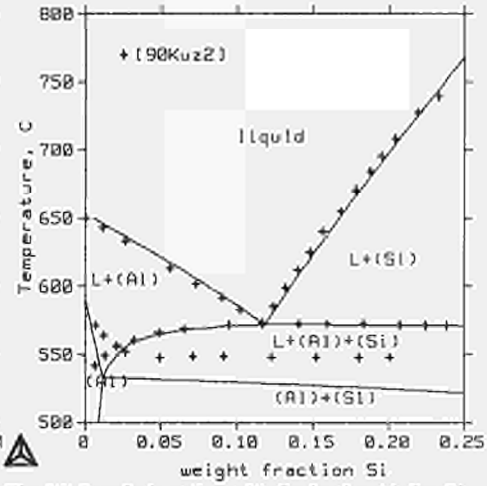

Fig.10. Isopleth at 2 wt.% Cu in the Al-Cu-Si system.

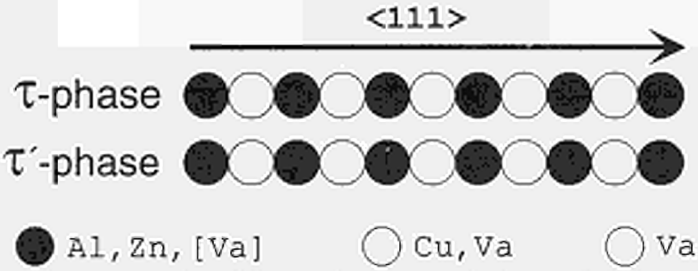

Fig.11. Schematic representation of the atomic occupancy in the τ and τ´ phases for the Al-Cu-Zn system. The direction <111> in the cubic lattice is considered.

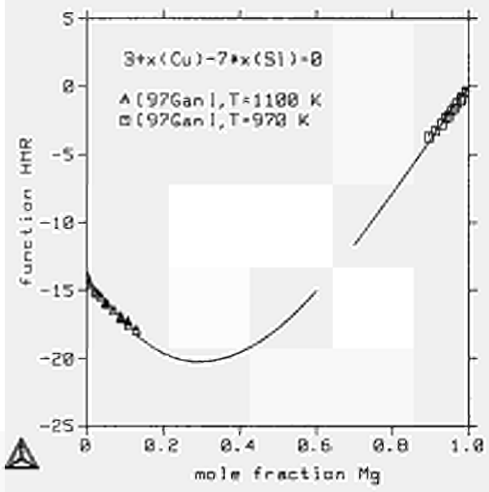

Fig.12. Integral enthalpy of mixing in the Cu-Mg-Si system.

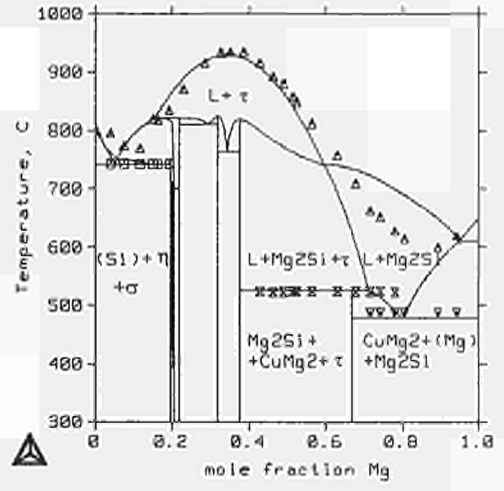

Fig.13. Isopleth Cu_7Si_3+Mg compared with experimental data [97Gan].

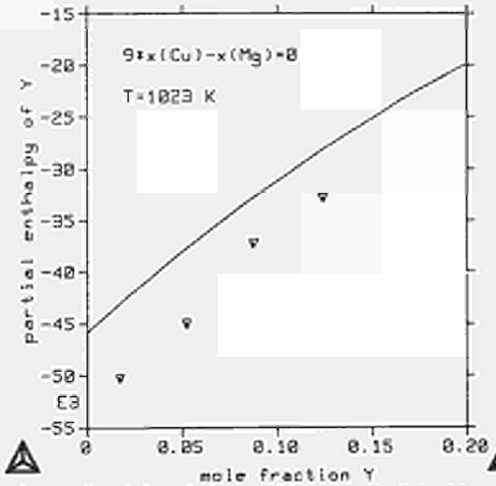

Fig.14. Partial enthalpy of Y in the Cu-Mg-Y system for a constant Cu/Mg ratio of 9/1.

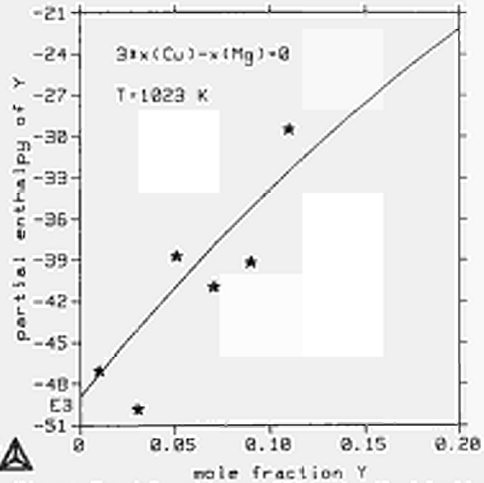

Fig.15. Partial enthlapy of Y in the Cu-Mg-Y system for a constant Cu/Mg ratio 3/1.

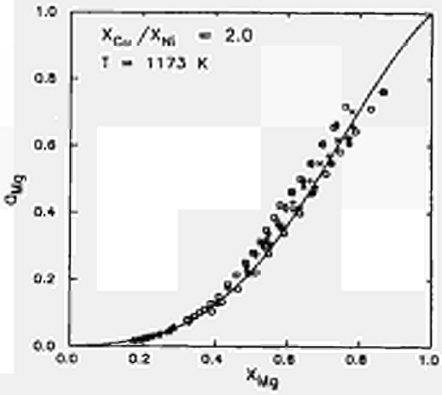

Fig.16. Calculated activity of Mg in the liquid state together with experimental data [93Gna1] and [93Gna2].

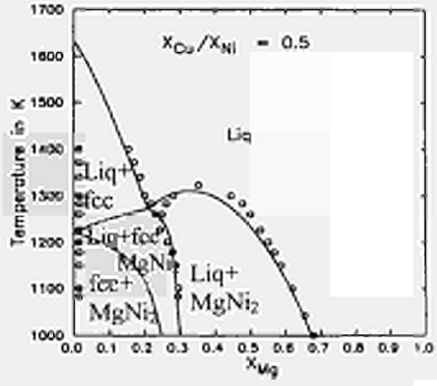

Fig.17. Calculated isopleth of the system Cu-Mg-Ni together with experimental data [93Gna1] and [93Gna2].

Thermodynamic Assessments, Experiments and Applications Related to the Ti-Al-V(Ni)-N System

Kejun Zeng and Rainer Schmid-Fetzer

AG Elektronische Materialien, Technische Universität Clausthal
Robert-Koch-Str. 42, D-38678 Clausthal-Zellerfeld, Germany

Abstract

This research forms part of the COST507-II programme on the Ti-Al-metal-nonmetal system (Leading systems 5 and 6). It includes assessments and thermodynamic modeling of the Ti-N, V-N, Ti-Al-N, Ti-V-N and Al-V-N systems. Missing or inconsistent experimental data on the ternary systems have been identified. These special experiments were performed partly in the own lab and partly by our COST partners at the *Universität Wien*. Substantial cooperation on assessment involved especially the *LTPCM-ENSEEG, Grenoble*, and the *University of Manchester/UMIST*. Our accomplishments are documented in seven publications, given as appendices to this report.

Further work on the Ti-Ni-N and Ti-Al-Ni systems is currently under way, involving thermodynamic modeling as well as the performance of key experiments, again in cooperation with the *Universität Wien*. This work is depicted here. It will be finalized and published with the termination of our project in May 1997.

The application of the generated thermodynamic datasets to a variety of technological problems in materials design and processing of materials is emphasized. Exciting applications are given, covering the span between metallic titanium alloys and the nitride ceramics.

1. Introduction

The overall system currently under study is the Ti-Al-metal-nonmetal system. This report addresses especially the quaternary Ti-Al-V-N, which is essentially described by its ternary edge systems. An extension into important subsystems of the quaternary Ti-Al-Ni-N is also given.

Most of our work has been finalized to a publication level. The second section provides a concise description of the specific systems which were part of our study. The third section emphasizes applications. Details are given in an appendix composed of the matching publications which emerged from this project. Work on the systems involving Ni is in progress and will be finalized at the end of our still ongoing project within COST507-II by May 1997.

2. Data Assessment and Experimental Work

2.1 Ti-N system [96Zen1]

A comprehensive critical assessment has been made of the experimental constitution data of the Ti-N system. The result differs from previous evaluation of the solid state equilibria [93Jon] and is supported also by recent experimental data. Based on the selected original experimental phase diagram and thermodynamic data from the literature, a set of thermodynamic functions for the Ti-N system has been chosen and the parameters were optimized by the least squares method. A stepwise optimization procedure is useful in this system and described in some detail. Four different analytical descriptions were used to model the four different types of stable phases in the Ti-N system: gas, liquid, solid solution phases αTi, βTi, and δ-TiN_{1-x}, and stoichiometric compounds: ε-Ti_2N, η-Ti_3N_2, and ζ-Ti_4N_3. Most of the experimental information is in accordance with the modeling, especially the invariant equilibria. The identification of reliable experimental data is demonstrated to be a point of distinction in this system. No derived values like the tabulated Gibbs energy of formation were used in optimization. The phenomenon of congruent vaporization or sublimation is found to be restricted to the liquid and δ phases. A phase diagram including also this information on the gas phase equilibria is presented and used to explain the discrepancies arising in experimental data due to the composition shift of samples during evaporation. Details are given in a publication [96Zen1] (see appendix I).

2.2 V-N system [97Du1]

A consistent thermodynamic data set for the V-N system is obtained by a computer-aided least squares method applied to all of the experimental phase diagram and thermodynamic data available from the literature. The sublattice model $V_1(N,Va)_a$ is used to model the phases: fcc (a=1), bcc (a=3), and hcp (a=0.5). The liquid phase is described by the Redlich-Kister formula, and the gas phase is treated as an ideal gas. Special attention is paid to the modeling of the fcc phase with its exceptional bulk of experimental data. This phase is first analyzed by an ideal solution, then by a regular, and finally by a subregular interaction in the nitrogen sublattice. The other solution phases are analyzed with similar modeling procedures. This step-by-step analysis procedure permits insight into reliable estimations for the parameters at each of the higher level models. Comparisons between the calculated and measured phase diagram and thermodynamic quantities show that most of the experimental information is satisfactorily accounted for by the thermodynamic calculation. Inconsistent experimental information is identified and ruled out. The thermodynamic properties of the fcc and hcp phases in the V-N system are compared with those in the Cr-N and Ti-N systems and related to Neumann-Kopp's rule. Details are given in a publication [97Du1] (see appendix II).

2.3 Ti-Al-N system [97Zen1, 96Zen2]

The Ti-Al-N phase diagram has been assessed and a consistent set of thermodynamic functions has been developed. Three ternary line compounds, τ_1-$Ti_3AlN_{0.56}$, τ_2-$Ti_2AlN_{0.82}$, τ_3-$Ti_3Al_2N_2$, and the ternary solubilities of αTi and βTi have been modeled. An estimated model for the metastable mutual solubilities of the nitrides

AlN and TiN_{1-x} is also given. Various combinations of different versions of the Ti-Al and Ti-N binary data have been tried. Finally, two versions of the present modeling are offered, based on two versions of the Ti-Al system. The experimental phase equilibria at 1300°C can be well reproduced. Inconsistencies are detected at lower temperatures, which are also related to the observed melting behavior of the ternary compounds. Additional key experiments have been performed by our COST partner (*Universität Wien*) and the results confirm that previous data refer to insufficient equilibration. These inconsistencies and the current approach to determine the Gibbs energies of the ternary phases in such a complex situation are discussed in detail. Applications of the developed thermodynamic modeling include: (1) the joining of AlN with Ti-braze, where also our own thin film experiments on the Ti/AlN interface reaction are reported, and an interpretation of the diffusion path is given; (2) diffusion barriers in semiconductor contacts, where an interpretation of the Al/TiN interface reaction is given; (3) the *in-situ* synthesis of Al-matrix composites, strengthened with ($TiAl_3$+AlN) reaction products during sintering of Al+TiN powder mixtures; (4) the formation of mixed AlN-TiN hard coatings and their stabilities with respect to the pure nitrides; and (5) the nitridation of Ti-Al alloys. Details are given in a publication [97Zen1] (see appendix IIIa). Preliminary data were published in [96Zen2] (see Appendix IIIb).

2.4 Ti-V-N system [97Zen2]

Experimental Ti-V-N phase diagram data have been thermodynamically assessed and a consistent set of thermodynamic functions has been developed. Calculations have been performed to reveal some important features of the system. Problem areas in experimental data are indicated. The thermodynamic calculation is linked with limiting cases for solid state diffusion kinetics. This is applied to a numerical simulation of ternary solidification processes of Ti-V-N alloys and to a discussion of nitriding behavior of Ti-V alloys. Details are given in a publication manuscript [97Zen2] (see appendix IV).

2.5 Al-V-N system [97Du2,3]

Thin film diffusion couples V/AlN have been used to investigate the phase relationships in the Al-V-N system. The couples were prepared by electron beam evaporation and annealed at 1000 and 1300°C for 144 and 69 hr., respectively. The phases were identified by X-ray diffraction. The Al-N-V ternary phase diagram is calculated from the thermodynamic parameters of the corresponding binary systems. It is shown that the direct extrapolation from the binary edges can describe the experimental isothermal section at 1300°C from the literature. For the isothermal section at 1000°C, however, the extrapolation does not reproduce the reported AlN+(V)+VN_X phase equilibrium. The calculated Al-N-V phase diagram is also compared with the phase assemblage data resulting from our own thin film diffusion couples V/AlN. It is plausible that these assemblage data are associated with intermediate states approaching true equilibrium states. Details are given in two publications [97Du2, 97Du3] (see appendices Va and Vb)

2.6 Ti-Al-V system

A preliminary assessment of various modeling approaches to the Ti-Al-V system has been performed in close cooperation with the *University of Manchester/UMIST*. The focused work on that alloy system is now carried out by that COST partner. This agreement has also strengthened our focused work on the N-containing ternary edge systems of the quaternary Ti-Al-V-N system.

2.7 Ti-Ni-N system

The Ti-Ni-N phase diagram has been thermodynamically assessed. The liquid and the recently found ternary compound Ti_2NiN_x by [95Fri] have been modeled. It is found that the discrepancies of the experimental data between [91Bin] and [79Fuk] are due to the different experimental conditions. They are essentially in good agreement. A number of missing key experiments are identified by the preliminary calculations. These experiments have been performed in close cooperation by the *Universität Wien*. This work is close to completion, and the publications are in preparation.

2.8 Ti-Al-Ni system

A thermodynamic assessment of the Ni-rich part of the Ti-Al-Ni system has recently been provided by our COST partner, the *LTPCM-ENSEEG , Grenoble* [95Dup]. The purpose of our work is to use this as a basis for the development of a thermodynamic dataset for the entire composition range. Experimental data on the Ti-Ni-Al system have been thermodynamically evaluated to plan new key experiments in order to obtain reliable data for optimization of the system in the composition region less than 50 at.% Ni. Part of the experimental work was carried out at our COST partner *Universität Wien*. Further experimental work is being carried out currently at TU Clausthal. All the experimental work is done in close cooperation with our partner at the *Universität Wien*, involving also the exchange of a graduate student for 3 months. The purposes are mainly to check the tielines Ti_3Al-H($TiNi_2Al$) and λ(TiNiAl)-Ti_2Ni, and determine the phase relationships of the π($Ti_5Ni_2Al_{13}$) phase and its stability. These key data will allow for a final thermodynamic modeling of the entire ternary system. Work is in progress and will be published in due course by the end of our project.

3. Applications

3.1 Ti-Al-N system

3.1.1 AlN/Ti interface reaction: Joining of AlN with Ti-braze [97Zen1]

Since AlN and Ti are not in equilibrium at high temperatures, interfacial reactions will occur when AlN is joined by titanium braze. Fig. 11 in Appendix III shows the calculated isothermal section of the Ti-Al-N system at 1200°C and the imposed reaction path of the AlN/Ti contact system in accordance with [95ElS]. This path has

satisfied the three requirements of an interfacial diffusion path. In the beginning of reaction, AlN is decomposed and the nitrogen atoms are released to react with Ti to form nitride TiN_{1-x} between AlN and Ti layers. The TiN_{1-x} layer serves as a trap for nitrogen between AlN and Ti because nitrogen has a rather high solubility in it. Hence, the formed (αTi) phase between TiN_{1-x} and (βTi) must be nitrogen-depleted. Consequently, other diffusion paths which start from the Ti terminal but first go to the nitrogen-enriched α(Ti,N) phase, such as $\beta Ti/\alpha(Ti,N)/\tau_1/\gamma/\tau_2/\delta/AlN$, are impossible.

3.1.2 TiN/Al interface reaction

TiN as diffusion barrier between Al/Si [96Zen2]

TiN_{1-x} has been widely investigated as diffusion barrier between Al and Si. The Al/TiN/Si system has been shown to be stable at temperatures between 500 and 600°C for around 30 min., but fail at longer annealing times. It has been suggested that the barrier failure be initiated at the Al/TiN_{1-x} interface [82Wit]. The thermodynamic description of the Ti-Al-N system in [97Zen1] has been used to establish overall phase relationships of the Ti-Al-N system at 600°C and, then, in conjunction with diffusion kinetics, provide a theoretical interpretation of experimental results on the interfacial reaction between Al and TiN_{1-x} films. It is suggested that the observed stable $TiAl_3$/TiN contact at 600 °C was in metastable state due to extremely rapid growth of $TiAl_3$, and hence the three-phase equilibrium TiN-AlN-$TiAl_3$ proposed by [84Bey] is not a stable equilibrium.

Sintering of Al+TiN powder mixture [97Zen1]

A promising Al-matrix composite, which is hardened by intermetallic compounds $TiAl_3$ and AlN, have been synthesized from powder mixture of Al+TiN by means of reaction sintering within temperature range of 550~650°C [92Koy]. From the experimental results, it seems that there exists interdiffusion of Al and Ti but the nitrogen atoms do not diffuse, and the reaction path is $Al/TiAl_3/AlN/TiN$. This is similar to the interfacial reaction between thin films Al and TiN mentioned above. Therefore the thermodynamic description of the Ti-Al-N system in [97Zen1] can also be applied to this case.

3.1.3 Metastable AlN-TiN films [97Zen1]

Discussion has been given on the thermodynamic description of the metastable solutions in AlN-TiN thin films. It was concluded that fcc-(Al) and fcc-TiN_x should not be treated as the same phase. Using the current datasets a calculation of the Gibbs energy surface of δ-$(Ti,Al)N_{1-x}$ in the ternary system is possible. This provides also data for the decomposition of N-deficient metastable films.

3.1.4 Nitridation of Ti-Al alloys [97Sch]

An application of the data to the nitridation of Ti-Al alloys is in preparation. A key point is that the stable and metastable "stability diagrams" can be calculated. using the nitrogen pressure as a variable [97Sch].

3.2 Ti-V-N system

3.2.1 Solidification of Ti-V-N alloys [97Zen2]

Solidification of the Ti-V-N alloys have been simulated under the equilibrium and Scheil conditions, respectively (Fig. 11 and 12 in Appendix IV). It has been shown that in the high temperature range, say above 2200°C, the solidification process of the alloys containing 5 at.% V is close to the equilibrium state, but it moved towards the Scheil mode in the temperature range below 2200°C. The calculated composition range of vanadium in the secondary α of the alloy 70Ti-5V-25N (at.%) by the Scheil model is very close to the experimental one. But that of the β phase by Scheil model is larger and higher than the measured one, which indicates that the diffusion of vanadium in β can still proceed down to at least 1600°C.

3.2.2 Nitridation of Ti-V alloys [97Zen2]

When a Ti-V alloy with higher than 50 at.% Ti is exposed to nitrogen at 1400°C, the nitrogen atoms are first dissolved in the β phase. After β is saturated with nitrogen, the α phase starts to form in the surface region. With the nitriding proceeding, the δ phase appears. This nitriding process is presented in Fig. 13 in Appendix IV as dashed line for the alloy of 80Ti-20V (at.%). Therefore, the outer layer on the samples nitrided for a long enough time is the Ti-rich fcc phase $(Ti,V)N_{1-x}$ with a few percent of vanadium. The morphology of the reaction zone depends on the vanadium content of the alloy. The α layer can be avoided by increasing the vanadium content or by increasing the nitriding temperature.

3.3 Ti-Ni-N system

The calculated phase diagrams are being used to analyze the denitrification and phase formation during the sintering process of TiN-Ni mixed powder compacts. It is found that the temperature at which the liquid phase appears strongly depends on the pressure. The thermodynamic dataset can be applied to design the sintering techniques for the TiN-Ni powder mixture. This work is in progress.

References

79Fuk M. Fukuhara and H. Mitani: *Nippon Kinzoku Gakkaishi* **43** (1979) 169-174.

82Wit M. Wittmer: *J. Appl. Phys.* **53** (1982) 1007-1012.

84Bey R. Beyers, R. Sinclair, and M. E. Thomas: *J. Vac. Sci. Technol. B* **2** (1984) 781-784.

91Bin S. Binder, W. Lengauer, and P. Ettmayer: *J. Alloys & Compounds*, **177** (1991) 119-127.

92Koy K. Koyama, M. Morishita, K. Suzuki, S. Yagi: *J. Jpn. Soc. Powder Powder Metall.* **39** (1992) 823-829.

93Jon S. Jonsson: "An assessment of the Ti-N system", in *"Phase relations in quaternary hard materials"*, Ph.D Thesis, KTH Stockholm (1993).

95Dup N. Dupin: "Thermodynamic evaluation of multicomponent nickel-base alloys", Ph.D Thesis, National Institute of Polytechnology of Grenoble, France (1995).

95Fri Y. L. Friec, J. Bauer, and P. Rogl: "The N-Ni-Ti system", *unpublished work* (1995).

95ElS M. H. El-Sayed, M. Naka, and J. C. Schuster: *Proc. 5th Europe-Japan Bilateral Colloq. on Composite Materials,* Corfu, Greece (1995) 329-333.

96Zen1* K. Zeng and R. Schmid-Fetzer: "A critical assessment and thermodynamic modeling of the Ti-N system", Z. Metallkde., **87** (1996) 540-554.

96Zen2* K. Zeng and R. Schmid-Fetzer: "Thermodynamic consideration of interfacial reaction between aluminum and titanium nitride", Proc. "Werkstoffwoche'96", DGM and DKG, (1996) in press.

97Du1* Y. Du, R. Schmid-Fetzer, H. Ohtani: "Thermodynamic assessment of the V-N system", Z. Metallkde. (1997) accepted.

97Du2* Y. Du, R. Wenzel and R. Schmid-Fetzer: "Calculation and measurement of the Al-V-N phase diagram", J. Chim. Phys. (1997), accepted.

97Du3* Y. Du, R. Wenzel and R. Schmid-Fetzer: "Thermodynamic analysis of reactions in the Al-N-Ta and Al-N-V systems", CALPHAD (1997) under review.

97Sch R. Schmid-Fetzer and K. Zeng: "Nitridation of Ti-Al Alloys: A Thermodynamic Analysis", in preparation (1997).

97Zen1* K. Zeng and R. Schmid-Fetzer: "Thermodynamic modeling and applications of the Ti-Al-N phase diagram", in "Thermodynamics of Alloy Formation", eds. Y. A. Chang and F. Sommer, The Minerals, Metals and Materials Society (TMS), Warrendale, PA, 275-294 (1997).

97Zen2* K. Zeng and R. Schmid-Fetzer: "The Ti-V-N system: Thermodynamic assessment and applications", manuscript to be submitted (1997).

Experimental Investigations in Ternary and Quaternary Ti-Al-Metal Systems

Erich Lugscheider, Klemens Schlimbach,
Lehr- und Forschungsgebiet Werkstoffwissenschaften, RWTH Aachen, Germany
Manfred Koschlig, Degussa AG, Hanau, Germany
and
Ingo Reinkensmeier, Eurobras GmbH, Menden, Germany

Abstract

This research forms part of the COST 507-II programme on the Ti-Al-Me-Me system (Key System 5). Within these work alloys of the system Ti-Al-Cu-Ni are investigated concerning its density, oxidation behaviour (825°C/15h), phase transition- and melting temperature for both conditions the molten and annealed state. Furthermore wetting - and joining tests were carried out on Ti_3Al- and TiAl-base material with alloys which have a good oxidation behaviour and a suitable melting temperature.

1 Introduction

The intermetallic α_2-Ti_3Al and γ-TiAl alloys possess particular mechanical and physical properties which make them of interest for use as structural materials in the aerospace and aircraft industries. In contrast to conventional Ti based alloys, the Titaniumaluminides have a higher resistance to oxidation and exhibit significantly less sensitivity to hydrogen embrittlement. These materials are able to exceed the application temperature of advanced Ti-alloys and also have the potential to replace nickel-based superalloys up to 800°C. Brazing seems to be the most successful joining method for this materials because of its less process temperature. Hence, the influence of the base material by a brazing process is much smaller than by a welding process. For the development of new filler metals for TiAl-based materials the knowledge of the metallurgical reactions between the filler metal and the base material is an important aspect; a further feature is a detailed investigation of the filler metals themselves. This includes the determination of the phases with X-ray diffraction, thermal analysis (ascertain the phase transition temperatures and melting ranges), determination of density and metallografic investigations (light- and electronmicroscopy).

2 Material and Methods

2.1 Fabrication of the alloys

The components of the alloys are weigh in with a precision of 0,01g (corresponding to ±0,1 wt.-%). The elements are molten in an arc-beam furnace by using a thoriated tungsten cathode and a water cooled copper crucible (anode). All alloys were molten four times in an argon atmosphere to guarantee a homogeneous distribution of the elements. As for the various investigations afterwards only, small parts of the fabricated alloys are necessary the samples are crushed mechanically.
Fig 1 gives an overview about the composition of the investigated alloys.

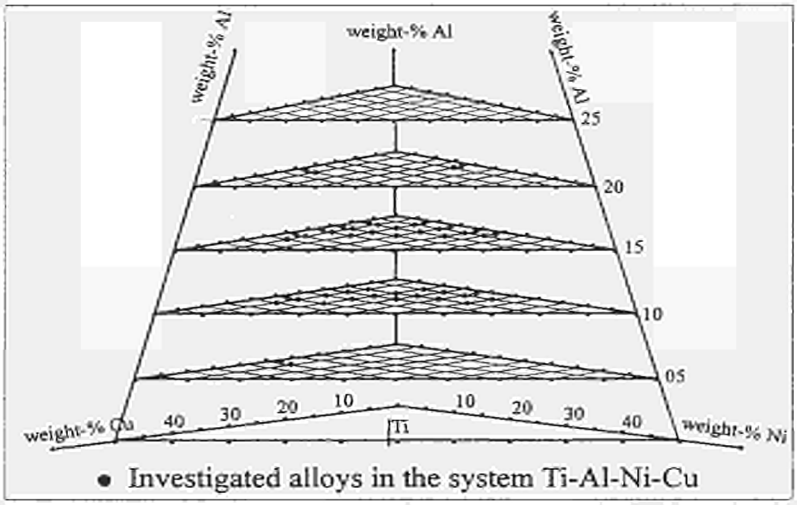

Fig. 1: Composition of the investigated alloys

2.2 Base material

The base material used for wetting- and joining tests is Ti48Al2Cr2Nb [at-%]. This material was produced by Plansee AG, Reutte, (Au), which has developed a special rolling process to produce sheets. The microstructure of this γ-TiAl material has the formation of a so-called „near gamma" microstructure. This microstructure consists of equiaxial γ-TiAl grains and small amounts of α_2-Ti_3Al at triple points and grain boundaries. The following table shows the characteristic temperatures.

	$T_{Liq.}$	T_{Braze}
Ti15AlNb	1050°C	900°C
Ti48Al2Cr2Nb	1500°C	1250°C

Fig. 2: Melting and brazing temperatures of the used base materials

3 Results and Discussion

3.1 Measurement of density

A pygnometer was used to determine the density of the fabricated alloys. The following tables show the various values in dependence on a constant Ti and Al proportion and a variable Cu and Ni content. The determined values of the alloys range roughly between 4 and 5 g/cm³ compared with 4,5 g/cm³ for CpTi.

The results show for all TixxAl-base systems a constant increasing of the density after increasing the Cu- and/ or the Ni-proportion. Furthermore there is no connection between density and phase transition evident. Because of its higher Al-amount the Ti20Al- and Ti25Al-based alloys have slightly smaller values than the Ti10Al- and Ti15Al-based alloys.

3.2 Measurement of characteristic temperatures

The problem is that especially the titanium will react with the Al_2O_3 crucible, if there is a liquid phase. Therefore it is possible to measure phase transitions in solid state, but no temperatures after the reaction with the crucible because the chemical reaction changes the composition of the alloys. The plots of cooling- and reheating-cycle demonstrate that the composition of the alloys have changed, hence the measurement of characteristic temperatures after the reaction with the crucible is impossible.
Table 5 shows the temperatures of phase transitions of the investigated alloys (heating rate: 20 K/min, atmosphere: Argon). Table 5 depicts the changing of characteristic temperatures determined for alloys in all base systems. Annealing the samples at 800°C -12 hours cause no evident changing of the characteristic temperature.

3.3 Oxidation behaviour

The investigation of the oxidation behaviour indicates no significant increasing of weight after a heat treatment at 600°C for 15 hours in atmosphere. Alloys with solidus temperatures above 900°C show no systematic behaviour after heat treatment at 825°C for 15h in atmosphere. Furthermore it is obvious, that a higher Al-portion causes a less increasing of oxidation weight. The value of the oxidation mass of the annealed samples reaches ca. 50% of those, which were casted. It is determined that a phase system in an equilibrium state has a much better oxidation behaviour than a system in the casted state. The absolute oxidation values are shown in Table 6.

3.4 Electronmicroscopy (SEM) and X-ray diffraction

The microstructure of nearly all investigated quaternary alloys consists of only three phases. In all investigated alloys the binary phase Ti_3Al was found. Furthermore complex binary and ternary phases like $Ti_xAl_yCu_z$ and $TiNi_3$ were determined. Phases containing all four system elements (Ti, Al, Cu, Ni) were also detected. The results of the X-ray diffraction are lines from binary and ternary compounds and some unidentified lines. The lack of data from possible quaternary phases prevents the assignment. The comparison of these two methods explain that there is no agreement between the results. The figures 3-6 in the appendix indicate the results for some selected alloys. The element distribution is originated from a SEM-analysis and the phase determination is based on the X-ray diffraction.

3.5 Wetting and Joining tests

The wetting and joining tests were carried out at 1100°C for the systems with a lower melting temperature e.g. Ti15Al-CuNi. Systems with a higher melting temperature e.g. Ti20Al-CuNi, are investigated at 1250°C. In general, there are three different cases of wetting behaviour obvious:

1. a complete melting and spreading with a small wetting angle (less than 30°)
2. no complete melting but some reactions between filler metal and substrate
3. no melting

The behaviour in cases two and three originate from a possible difference between melting- and brazing temperature of these systems mainly Ti20Al-based alloys. Due to high activity between Titanium and the ceramic crucible a thermodynamic reaction occurs, with the result that the melting temperature of some alloys could not be determined precisely. In comparison to the Ti25Al- and Ti20Al-systems the Ti15Al-based alloys show bigger wetting angles (Fig. 7) and a well-defined diffusion zone between the Ti_3Al-substrate and the filler matrix (Fig. 8) with a thickness of ca. 30µm. The SEM-analysis reveals that this zone consists of mainly TiAlCu- and TiNi-compounds. The Ti25Al-based systems show some erosion of the substrate (Fig.9) and a few pores within the filler matrix (Fig.10). It appears from the SEM analysis that there is a decrease of Cu- and Ni-diffusion within the interface. Furthermore there is a tendency for TiAl phase formation during the braze process.

4 Appendix

Tab. 1: Density of the Ti10Al-based alloys

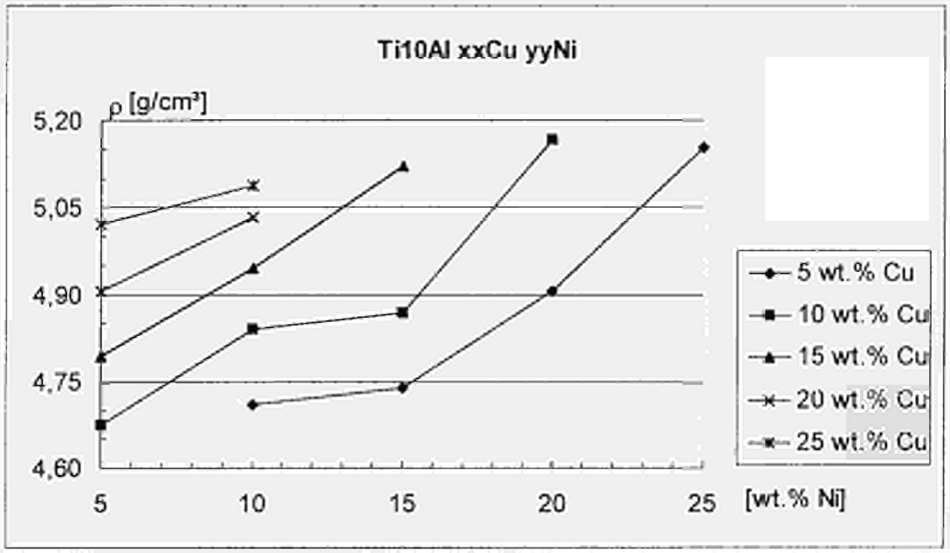

Tab. 2: Density of the Ti15Al-based alloys

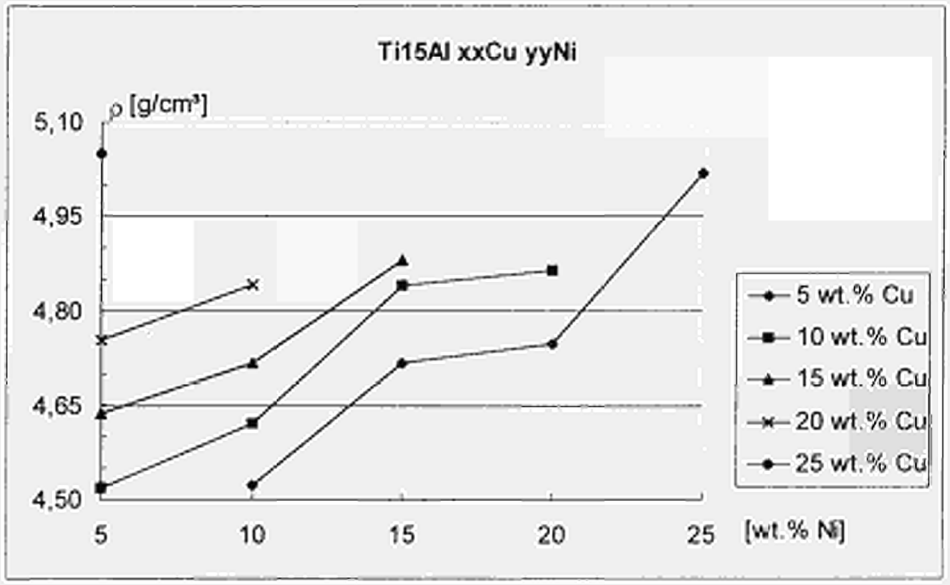

Tab. 3: Density of the Ti20Al-based alloys

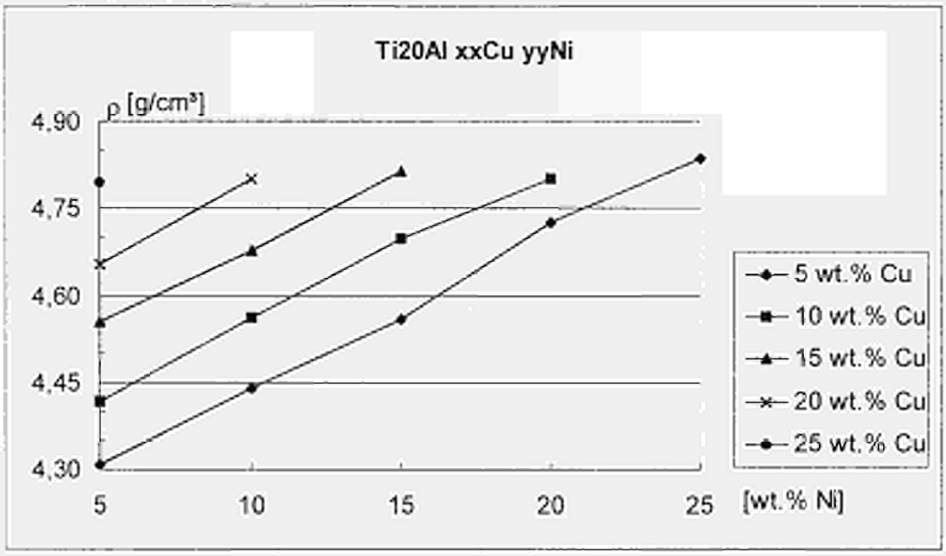

Tab. 4: Density of the Ti25Al-based alloys

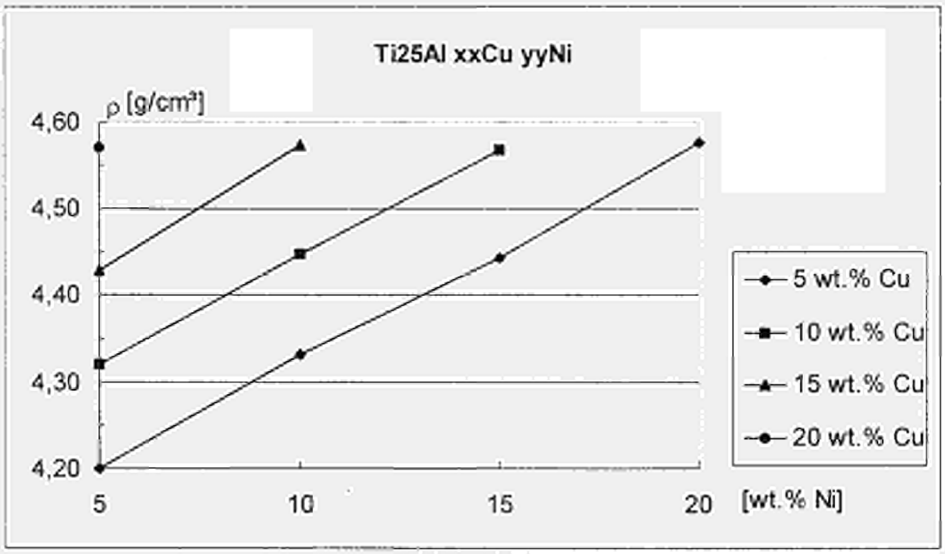

Tab.5: Characteristic temperatures of the investigated alloys

(*) reaction with the crucible

Alloy [wt.-%]	**characteristic temperatures [°C]**	* [°C]
Ti10Al 5Cu 5Ni	821, 972	
Ti10Al 5Cu 10Ni	835, 893, 1035	
Ti10Al 5Cu 15Ni	835, 890, 945	1174
Ti10Al 5Cu 20Ni	877, 911, 949	1192
Ti10Al 5Cu 25Ni	733, 910, 950	1017
Ti10Al 5Cu 30Ni	690, 888, 969	1029
Ti10Al 10Cu 5Ni	818	
Ti10Al 10Cu 10Ni	843, 927	944
Ti10Al 10Cu 15Ni	823, 936, 975	1104
Ti10Al 10Cu 20Ni	823, 940, 974, 1001	1175
Ti10Al 10Cu 25Ni	690, 850, 939	970
Ti10Al 15Cu 5Ni	861,976	996
Ti10Al 15Cu 10Ni	804, 826, 848, 917,946	
Ti10Al 15Cu 15Ni	824, 847, 921, 936	
Ti10Al 15Cu 20Ni	719, 804, 930	998
Ti10Al 20Cu 5Ni	725, 865, 955	1025
Ti10Al 20Cu 10Ni	859, 899, 947, 971	1060
Ti10Al 25Cu 5Ni	868, 976	
Ti10Al 25Cu 10Ni	860, 989	1146
Ti10Al 30Cu 5Ni	876, 976	1023
Ti15Al 5Cu10Ni	924, 975, 1071	1187
Ti15Al 5Cu15Ni	907, 975, 1057	1178
Ti15Al 5Cu20Ni	916, 969, 1054	1094
Ti15Al 5Cu25Ni	726, 908, 973, 1040	1118
Ti15Al 10Cu5Ni	843, 957, 1052	
Ti15Al 10Cu10Ni	973, 1016	1137
Ti15Al 10Cu15Ni	968, 1074	1133
Ti15Al 10Cu20Ni	956, 994, 1084	
Ti15Al 15Cu5Ni	863, 938	
Ti15Al 15Cu10Ni	842, 987, 1020	1148
Ti15Al 15Cu15Ni	974, 1078	1129
Ti15Al 20Cu5Ni	859, 954, 1048	1134
Ti15Al 25Cu5Ni	867, 945,1091	1124
Ti15Al 30Cu5Ni	865, 944, 1044	1139
Ti20Al 5Cu5Ni	750, 1033, 1059, 1188	

Tab.5. continued

Ti20Al 5Cu10Ni	1022, 1115, 1140	1269
Ti20Al 5Cu15Ni	1027, 1108,1153	1166
Ti20Al 5Cu20Ni	1032, 1150, 1173	1203
Ti20Al 5Cu25Ni	1033, 1162, 1207	1233
Ti20Al 10Cu5Ni	1023,1153	1338
Ti20Al 10Cu10Ni	1036, 1148, 1184	1266
Ti20Al 10Cu15Ni	1020, 1112, 1155	1188
Ti20Al 10Cu20Ni	1028, 1172, 1214	
Ti20Al 15Cu5Ni	989, 1020, 1157	1220
Ti20Al 15Cu10Ni	1017, 1133, 1175	1268
Ti20Al 15Cu15Ni	1019, 1110, 1162	1203
Ti20Al 20Cu5Ni	1025, 1184	1303
Ti20Al 20Cu10Ni	1018, 1124, 1174	1322
Ti20Al 25Cu5Ni	1015, 1169, 1198	
Ti25Al 5Cu5Ni	1087, 1218	1273
Ti25Al 5Cu10Ni	1217	
Ti25Al 5Cu15Ni	1102, 1230	
Ti25Al 5Cu20Ni	1086, 1203, 1229, 1250	1269
Ti25Al 10Cu5Ni	1234, 1245	1342
Ti25Al 10Cu10Ni	1223, 1238	
Ti25Al 10Cu15Ni	1222, 1267	
Ti25Al 15Cu5Ni	1075, 1226	1263
Ti25Al 15Cu10Ni	1089, 1222, 1234	1308
Ti25Al 20Cu5Ni	1229, 1243	1340

Tab. 6: Oxidation behaviour for selected alloys (molten- and annealed state)
*) commercial material

		Oxidation mass [mg/cm²]	
Alloy [wt.-%]	**Heat-treatment**	**molten-state**	**annealed-state**
Ti 99,9	600°C/15h	0,135*	
Ti 99,9	825°C/15h	10,48*	
Ti15Al	825°C/15h	2,82*	
Ti15Al 5Cu10Ni	825°C/15h	4,51	
Ti15Al 10Cu10Ni	825°C/15h	3,80	
Ti15Al 10Cu15Ni	825°C/15h	4,48	
Ti15Al 10Cu20Ni	825°C/15h	2,9	
Ti15Al 15Cu15Ni	825°C/15h	3,07	
Ti20Al 5Cu10Ni	825°C/15h	3,89	
Ti20Al 5Cu15Ni	825°C/15h	4,06	2,34
Ti20Al 5Cu20Ni	825°C/15h	1,01	
Ti20Al 5Cu25Ni	825°C/15h	4,18	3,48
Ti20Al 10Cu5Ni	825°C/15h	5,05	
Ti20Al 10Cu10Ni	825°C/15h	4,50	1,42
Ti20Al 10Cu15Ni	825°C/15h	5,05	
Ti20Al 10Cu20Ni	825°C/15h	3,61	
Ti20Al 15Cu5Ni	825°C/15h	3,90	2,68
Ti20Al 15Cu10Ni	825°C/15h	4,19	
Ti20Al 15Cu15Ni	825°C/15h	3,41	1,94
Ti20Al 20Cu5Ni	825°C/15h	5,80	
Ti20Al 20Cu10Ni	825°C/15h	3,64	
Ti20Al 25Cu5Ni	825°C/15h	3,28	1,67
Ti25Al 5Cu5Ni	825°C/15h	3,62	2,13
Ti25Al 5Cu10Ni	825°C/15h	1,77	
Ti25Al 5Cu15Ni	825°C/15h	1,42	
Ti25Al 5Cu20Ni	825°C/15h	1,37	1,67
Ti25Al 10Cu5Ni	825°C/15h	3,43	
Ti25Al 10Cu10Ni	825°C/15h	2,28	1,57
Ti25Al 10Cu15Ni	825°C/15h	3,03	
Ti25Al 15Cu5Ni	825°C/15h	3,97	
Ti25Al 15Cu10Ni	825°C/15h	3,46	
Ti25Al 20Cu5Ni	825°C/15h	3,60	3,47

Fig. 3: ESMA and X-ray diffraction of the alloy Ti 10Al 5Ni 5Cu

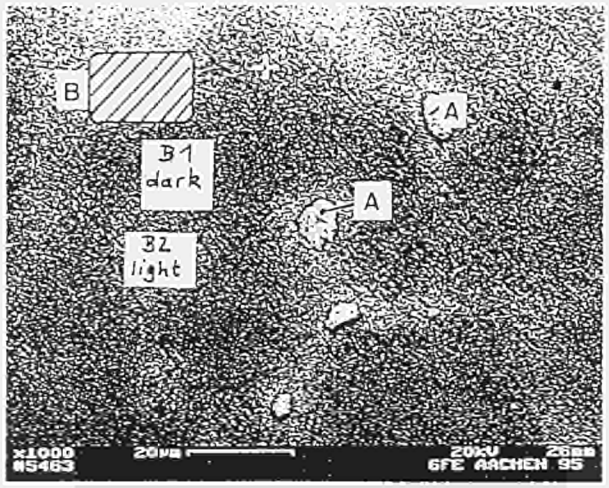

Ti 10Al 05Ni 05Cu
molten by arc

	Ti	Al	Ni	Cu
A	63,8	14,4	6,2	15,6
B1	74,5	18,6	3,9	3,0
B2	70,7	18,1	6.7	4.5

Composition of the phases [at%]

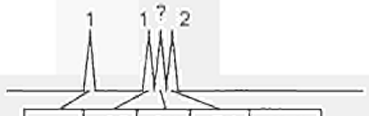

1-Ti
2-Ti3Al

41,5	45,7	47,2	47,9	2Θ [°]
2,53	2,31	2,24	2,21	d [A]

Fig. 4: ESMA and X-ray diffraction of the alloy Ti 15Al 20Ni 10Cu

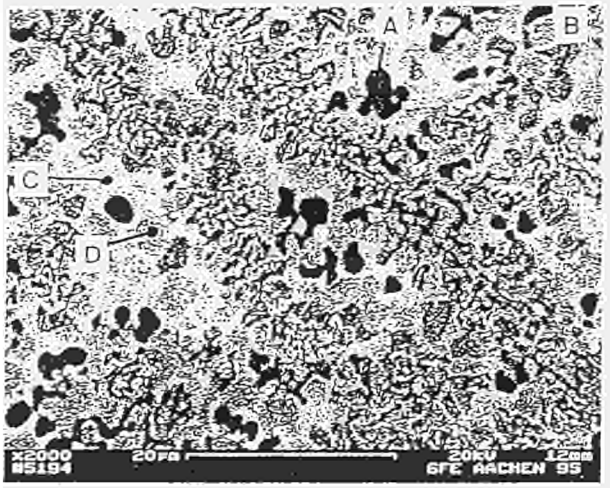

Ti 15Al 20Ni 10Cu
molten by arc

	Ti	Al	Ni	Cu
A	68,7	25,1	4,4	1,7
B	64,4	21,7	9,0	4,9
C	41,8	28,4	20,5	9,3
D	48,6	21,6	21,5	8,1

Composition of the phases [at%]

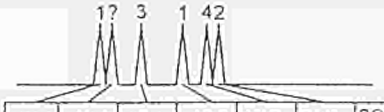

1-Ti3Al
2-TiAlCu/Ti4Al5Cu3
3-Ti/TiAl
4-TiAlCu/Ti4Al5Cu3/TiAlCu2

42,1	43,6	45,4	48,0	49,5	50,6	2Θ [°]
2,49	2,41	2,32	2,20	2,14	2,10	d [A]

Fig. 5: ESMA and X-ray diffraction of the alloy Ti 20Al 20Cu 10Ni

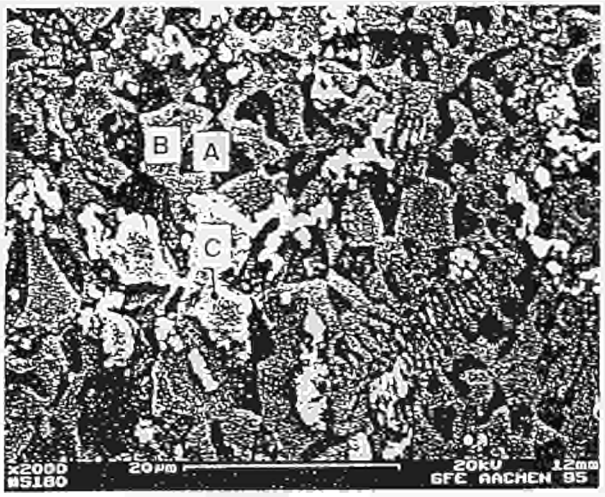

Ti 20Al 10Ni 20Cu
molten by arc

	Ti	Al	Ni	Cu
A	63,1	27,0	7,6	3,7
B	38,0	33,5	10,6	17,9
C	36,8	28,1	10,5	24,6

Composition of the phases [at%]

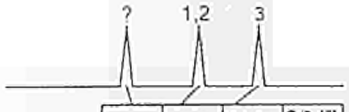

45,0	49,8	55,7	2Θ [°]
2,34	2,13	1,92	d [A]

1-TiAlCu/Ti4Al5Cu3/TiAlCu2
2-TiNi3
3-TiAlCu/Ti4Al5Cu3

Fig. 6: ESMA and X-ray diffraction of the alloy Ti 25Al 5Cu 10Ni

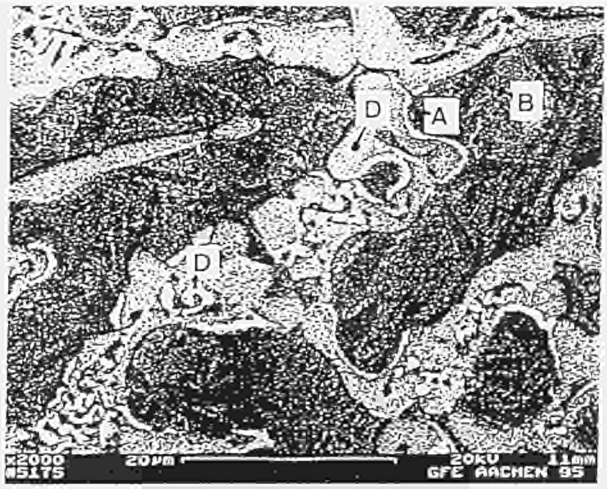

Ti 25Al 10Ni 05Cu
molten by arc

	Ti	Al	Ni	Cu
A	60,3	36,1	2,2	1,5
B	60,7	34,6	2,8	1,9
C	37,2	40,4	16,3	6,1
D	40,5	40,1	13,9	5,5

Composition of the phases [at%]

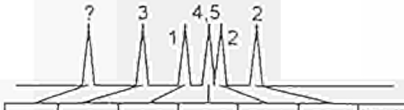

41,2	45,6	48,0	49,6	50,6	56,0	2Θ [°]
2,54	2,31	2,20	2,13	2,10	1,91	d [A]

1-Ti3Al
2-TiAlCu/Ti4Al5Cu3
3-Ti/TiAl
4-TiAlCu/Ti4Al5Cu3/TiAlCu2
5-TiNi3

Fig.7: Wetting angle of Ti 15Al 10Cu 20Ni on Ti_3Al-substrate

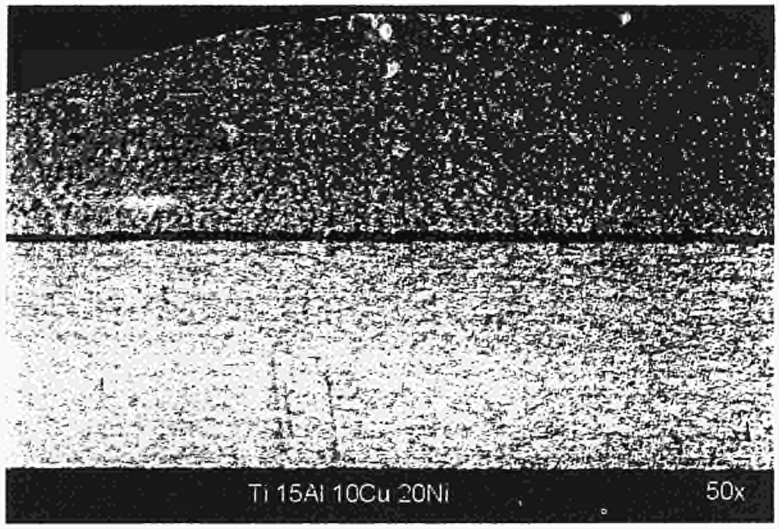

Fig.8: SEM-micrograph of the joining zone of the sample above

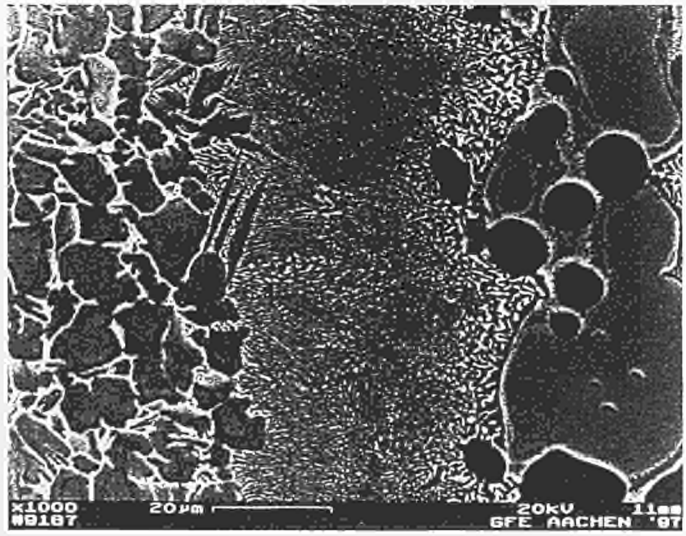

[at.-%]	Al	Ti	Nb	Cr	Cu	Ni
Pos.1	24,6	60	7	0,1	4,8	3,8
Pos.2	23,8	57	1,4	0,1	10,3	6,8

Fig.9: Wetting behaviour of Ti25Al10Cu10Ni on TiAl-substrate

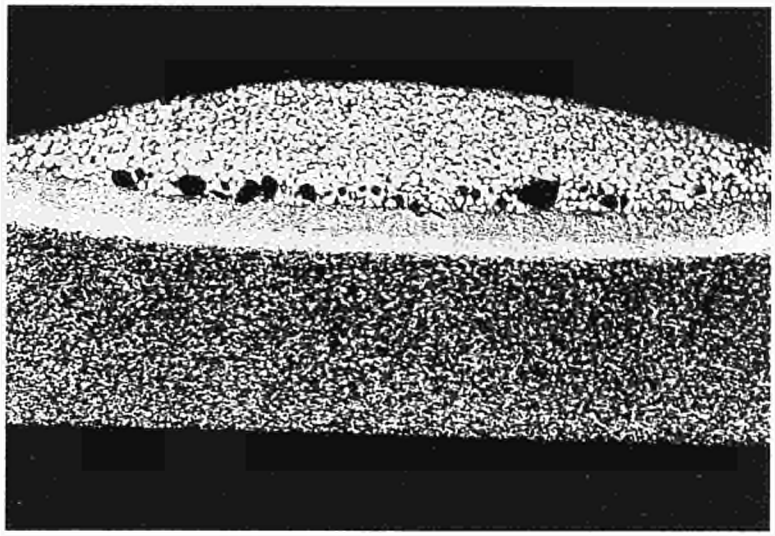

Fig.10: SEM-micrograph of the joining zone from the sample above

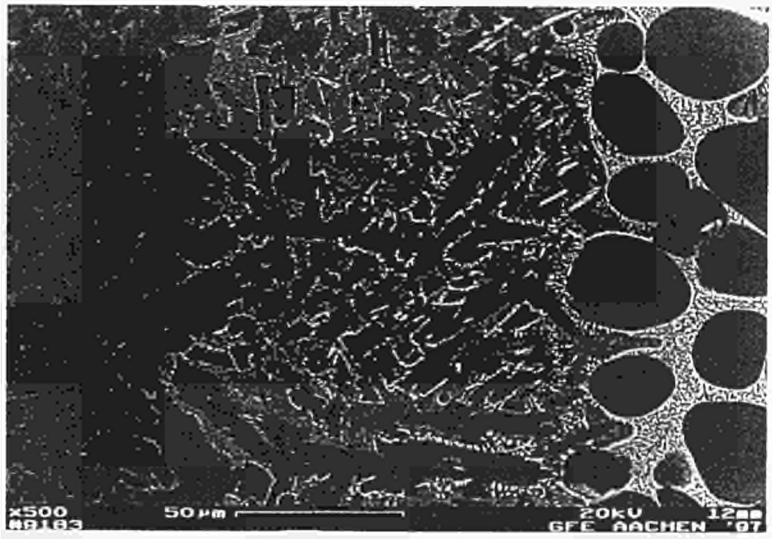

[at.-%]	Al	Ti	Nb	Cr	Cu	Ni
Pos.1	40,5	54	1,9	1,3	1,2	0,6
Pos.2	32	57	2	2,5	2,9	2,3
Pos.3	43	51	1,4	0,8	1,7	1
Pos4	37	40	1	1,5	8	12

Thermophysical Properties of Light Metal Alloys

G.Jaroma-Weiland[1], R.Brandt[1], P.Reipert[2], G.Neuer[1]

[1]Forschungsinstitut für Kerntechnik und Energiewandlung e.V., Stuttgart, Germany
[2]Kolbenschmidt AG, Neckarsulm, Germany

Abstract

In the factual data base THERSYST experimental data on thermophysical properties of Al-, Mg- and Ti-based alloys have been stored. Thermal conductivity and hardness of six industrial Al-Si-based alloys have been intensively investigated as a function of temperature and time. From these measurements the phenomenological correlation between thermal conductivity and hardness has been found. Electrical resistivity were determined on 11 ternary Al-Si-Zn alloys. For specimens with Zn-content greater than 20wt% a phase transition was observed around 290°C.

1 Introduction

Due to the low density of the light metal alloys they are gradually becoming more and more attractive. For optimum application the short and long term material properties of the alloys, such as strain and stress relation, fatigue strength, wear and corrosion resistance, etc. must be known. Data on thermophysical properties (thermal conductivity, thermal diffusivity, electrical resistivity, specific heat capacity and thermal expansion) of these alloys are of interest in two aspects:

- Many components are exposed to temperatures up to 400°C, resulting in generation of stationary and transient temperature fields. The knowledge of the temperature dependence of the thermal conductivity enables the calculation of the temperature distributions.
- Data for higher temperatures including the so called "mushy" zone and the melting range are necessary for numerical solidification models used in the casting industry.

Therefore it was one of the aims of the European research programme COST507 to study transport properties of light metal alloys to provide reliable experimental data and to characterize each alloy family. The experimental data on thermophysical properties available in the literature have been stored in the factual data base THERSYST [89Neu/Bra].

Experimental investigations have been performed at selected industrial Al-Si-based casts. Thermal conductivity and hardness have been measured as function of temperature and time. We attempted to find a correlation between these properties in order to reduce the expenses of thermal conductivity measurements in future.
Electrical resistivity was measured on temary Al-Si-Zn alloys. The thermodynamic evaluation of this system has been performed during 1st round of COST507-action

[96Jac/Spe]. Futhermore thermal conductivity and specific heat capacity measurements were carried out on quaternary Al-Ti-Cu-Ni alloys.

2 Storage of the thermophysical data in the data base THERSYST

Collection and evaluation of the publications dealing with thermophysical properties of light metal alloys, started in the 1st round of the COST507 project, have been continued. New data published in the literature were found by recherche in the literature data banks METADEX and INIS. Also data measured by partners of the Group D (GR2 -University of Tessaly, F1 - CNRS Marseille) were entered into THERSYST. The actual status of the data base: 1489 data-sets on 158 different alloys and metal matrix composites. 590 data-sets of this collection are referring to the properties describing the heat transport phenomena of 73 industrial alloys, i.e. their thermal conductivity, thermal diffusivity and electrical conductivity. Heat transport in alloys belongs to the most complex process and it is very difficult to predict thermal conductivity especially for highly alloyed materials. Analysis of experimental data of commercial wrought aluminium alloys made by Olafsson [96Ola] allowed him to present a model for calculating electrical resistivity at room temperature. This model based on Mathiessen's rule and on thermodynamical calculations gives good agreement with experimental data for AlCu- and AlMgSi-alloys, except for AlCu-alloys with higher Cu-content and no magnesium, and for AlMgSi-alloys with chromium. For highly alloyed materials especially cast alloys large discrepancies are expected. Therefore it is very important to collect reliable experimental data.

3 Experimental investigations

3.1 Materials

Aluminium-silicon-based alloys were supplied as casts by Kolbenschmidt AG. Their chemical compositions are given in Tab.1. All alloys were solution heat treated at 500°C, water-quenched and aged at different conditions to achieve defined metallurgical states.

Tab.1 Chemical composition (wt%) of Al-Si-based industrial alloys

Alloy	Si	Cu	Mg	Ni	Mn	Fe	others (Ti,Zn,Pb,Sn)
KS1275.1	10.76	1.00	0.97	0.91	0.18	0.42	0.07,0.07,0.02,0.02
KS270	9.49	2.64	0.86	0.01	0.03	0.19	0.05,0.01,0.01,0.01
KS226	8.44	3.09	0.49	0.05	0.39	0.60	0.09,0.46,0.08,0.02
KS1295	13.46	3.71	0.87	2.18	0.45	0.55	0.05,0.08,0.01,0.01
KS1275	13.04	1.01	0.89	0.79	0.11	0.60	0.06,0.12,0.03,0.03
KS281.1	18.56	0.99	0.98	0.79	0.10	0.59	0.06,0.10,0.02,0.02

Tab.2 Chemical composition of ternary Al-Si-Zn alloys

alloy	mole %			wt%		
	Al	Si	Zn	Al	Si	Zn
1	76.46	4.40	19.14	60.01	3.59	36.40
2	72.73	9.08	18.19	57.61	7.49	34.90
3	60.82	18.69	21.49	46.81	14.98	38.21
6	39.13	1.02	59.85	21.13	0.57	78.30
7	83.83	5.04	10.13	74.02	4.58	21.40
8	79.89	9.97	10.14	69.57	9.04	21.39
9	11.73	0.05	88.22	5.20	0.02	94.78
10	90.19	4.71	5.10	83.93	4.56	11.51
11	58.51	1.00	40.49	37.11	0.66	62.23
12	55.84	4.66	39.50	35.70	3.10	61.20
13	53.28	10.64	36.08	35.10	7.30	57.60

Ternary aluminium-silicon-zinc alloys were cast by Vereinigte Aluminium Werke Bonn. Their chemical compositions (in mole and weight%) are shown in Tab.2.

Quaternary Ti-Al-Cu-Ni alloys have been prepared by partner RU1 (Baikov Institute of Metallurgy, Russian Academy of Sciences, Moscow). The elements were molten three times in an arc-beam furnace under an argon atmosphere. The chemical composition of the alloys has been investigated by means of REM/EDX by partner D11 (MPI, Stuttgart,Germany)

Tab3. Chemical composition (wt%) of quaternary Ti-Al-Cu-Ni alloys

Alloy	Ti	Al	Cu	Ni
Ti-1	72.6	9.9	5.0	13.2
Ti-2	54.9	8.2	10.9	26.0
Ti-3	57.2	6.4	4.3	32.0
Ti-4	57.7	13.3	5.7	23.3
Ti-5	55.8	14.1	4.6	25.5

3.2 Determination of the physical properties

The thermal conductivity was measured by a comparative steady-state method using a commercial apparatus (TCFCM model of Holometrix Inc., Cambridge, USA). The cylindrical sample (25mm in diameter and 28mm long) was sandwiched between two identical reference samples from electrolytic iron. The measurements were carried out as function of temperature in air during heating and subsequent cooling cycle. Furthermore the thermal conductivity of two Al-Si-based alloys was measured at constant temperature (250°C and 300°C) as a function of time. Due to the high values of the thermal conductivity, the measurements on Al-based materials are very difficult and it is assumed that the experimental error exceeds the usual range of ±5%.

Hardness was determined at room temperature using the Brinell method. The measurements of hardness as a function of the aging time at constant temperature (250°C and 300°C) were carried out on KS1295 and KS281.1 specimens. Hardness was always measured on samples before and after measurements of their thermal conductivity.

The specific heat capacity was determined by means of a differential scanning calorimeter (DSC) using a "Perkin-Elmer-DSC-2" apparatus in the temperature range of 50-500°C. For these measurements discs of 6mm in diameter and 1mm thick were machined. The inaccuracy was below 3%.

Electrical resistivity measurements were carried out by means of the four point technique in the temperature range from 20°C to 400°C. The measurements were made on rods (1.5mm in diameter and 15mm long) during heating and subsequent cooling (0.5-2K/min) in vacuum of 2*E-5 Torr.

4 Results and Discussion

4.1 Thermodynamic analysis

Computional analysis was performed using the Thermo-Calc software package [85Sun/Jan] and the recently developed COST507 data base for light metal alloys [94Ans]. For two Al-Si-based alloys (KS1275.1 and KS1295) the following diagrams were prepared:

- isopleth section (with varying Si-content): Fig.1a and 1b, resp.,
- phase amount (in mole%) as a function of temperature: Fig.2a and 2b, resp.

The isopleth sections show relevant phase equilibria as a function of Si content. In both alloys four solid phases are present: (Al) solid solution, Mg_2Si and Al_2Cu (the Θ phase) precipitates as well as the Si diamond phase. From these diagrams it can be seen that an addition of Cu reduces the solidus temperature to 508°C for KS1295 compared to 543°C for KS1275.1. The Al_2Cu phase dissolves in KS1295 at 480°C while it dissolves at 360°C in KS1275.1.

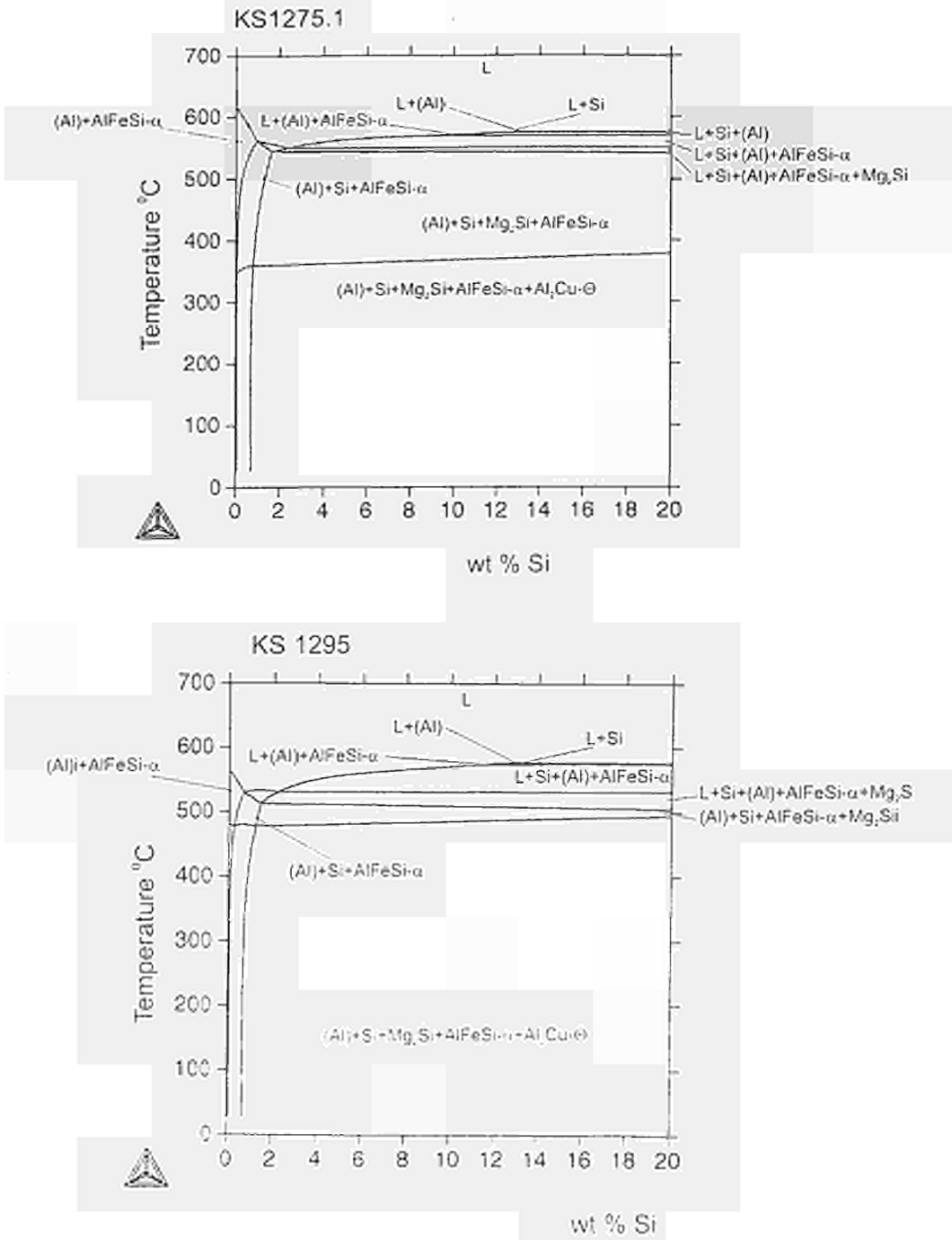

Fig. 1 Isopleth sections for alloys (a) KS1275.1 and (b) KS1295

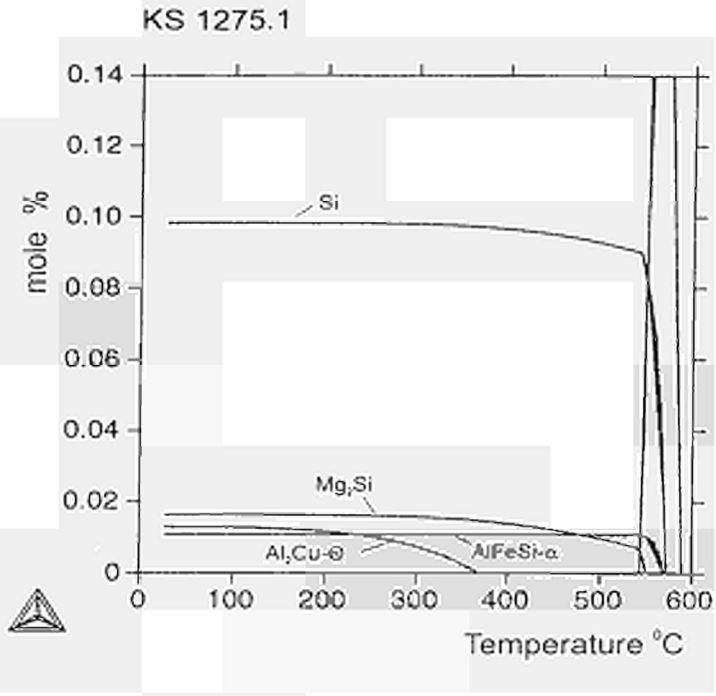

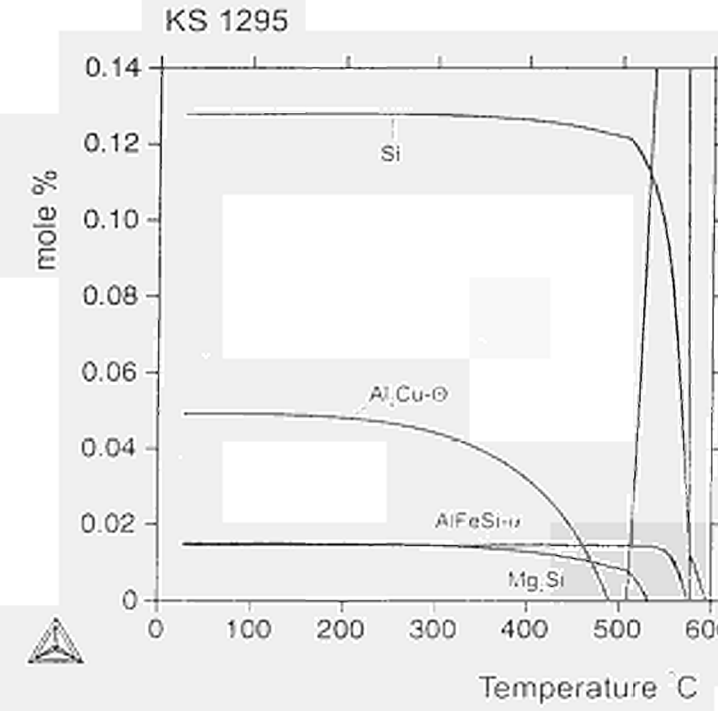

Fig.2 Phase amount (in mole%) as a function of a temperature for alloys (a) KS1275.1 and (b) KS1295

4.2 Thermal conductivity of industrial Al-Si-alloys

Thermal conductivity results of selected Al-Si-alloys are presented at Fig.3. For alloys with varying Si-content and constant amount of other elements the almost linear decreasing of thermal conductivity with increasing of Si has been observed (ca. 2 $Wm^{-1}K^{-1}$ per each weight % of Si). It is caused by the low solubility of Si in the Al-matrix and its precipitation as free silicon. Copper builds with aluminium the intermetallic compound Al_2Cu and its influence on thermal conductivity is more intensive: thermal conductivity of KS1295 (4%Cu) is 16% lower then KS1275 (1%Cu).

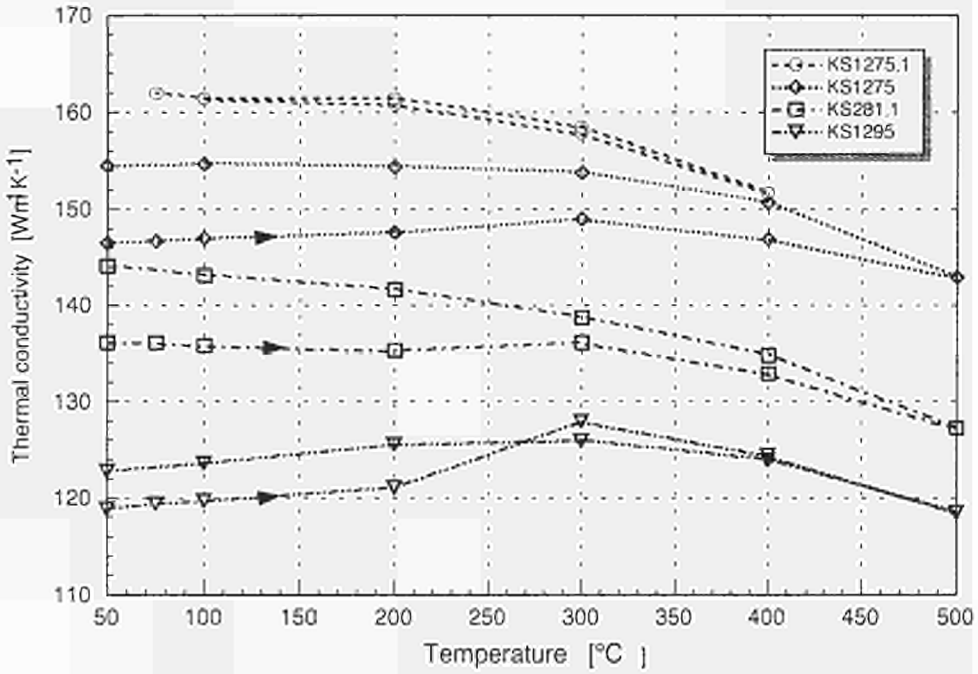

Fig.3 Thermal conductivity of Al-Si-based industrial alloys

The influence of the thermal treatment on the thermal conductivity can be observed in Fig.4. Specimens of alloy KS1295 were aged at different conditions (time and temperature) resulting in different hardness of the material. Investigations of thermal conductivity and hardness as a function of a temperature and time [96Jar/Rei] allowed us to find a correlation between the both properties for the examined alloys (Fig.5). Three curves obtained for KS1295 at 100, 250 and 300°C show approximately a linear correlation between thermal conductivity and hardness up to 150HB. The slope of the curves decreases with increasing temperature. At 100°C the curves for KS270 and KS1295 are nearly parallel in the almost whole range of the hardness.

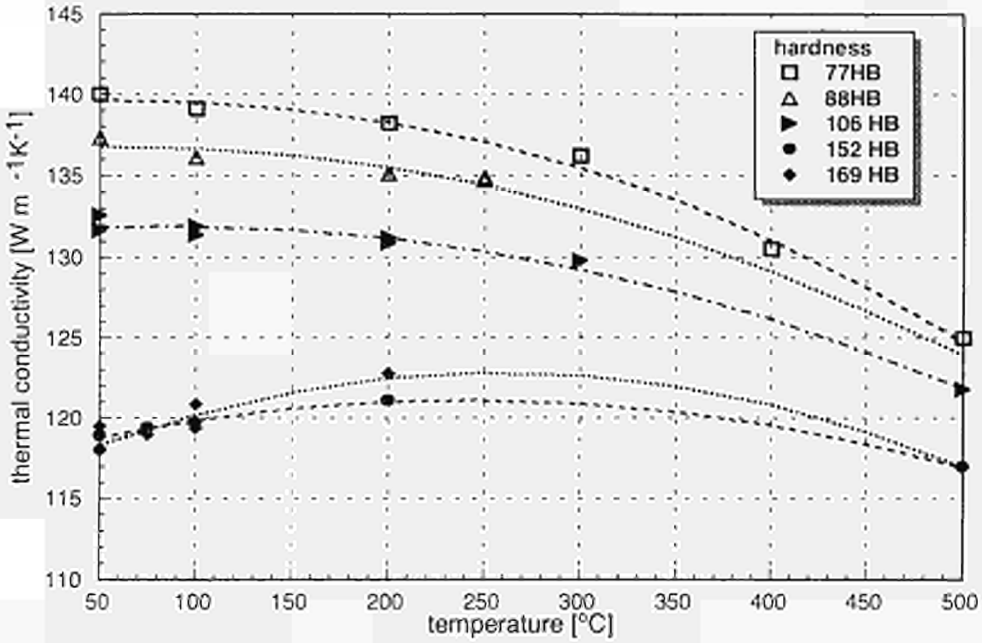

Fig.4 Thermal conductivity of alloy KS1295 with different hardness

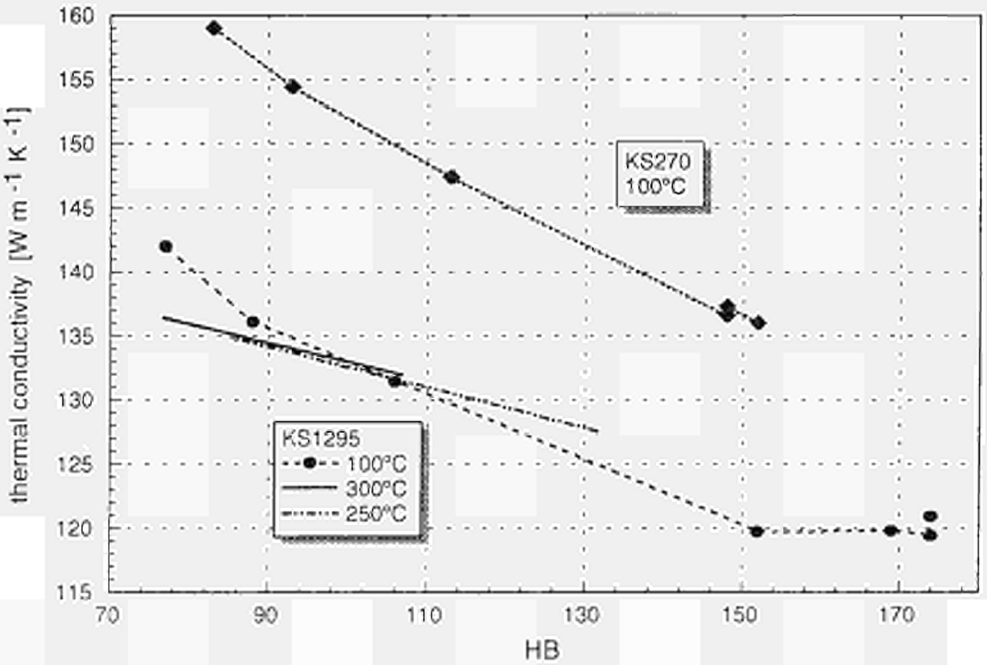

Fig.5 Correlation between thermal conductivity and hardness for KS270 and KS1295

4.3 Al-Si-Zn alloys

Electrical resistivity of Al-Si-Zn alloys was measured in as cast condition. Fig.6 represents the temperature dependence of three specimens: alloys 3 and 6 with high Zn concentrations undergo at around 290°C a phase transformation. On specimens with Zn content < 20wt% (e.g. alloy 7) this transformation was not observed. This behaviour confirms the DSC investigations of Zahra [96Zah]. The electrical resistivity values at room temperature are in good agreement with results obtained during 1st round [92Hol].

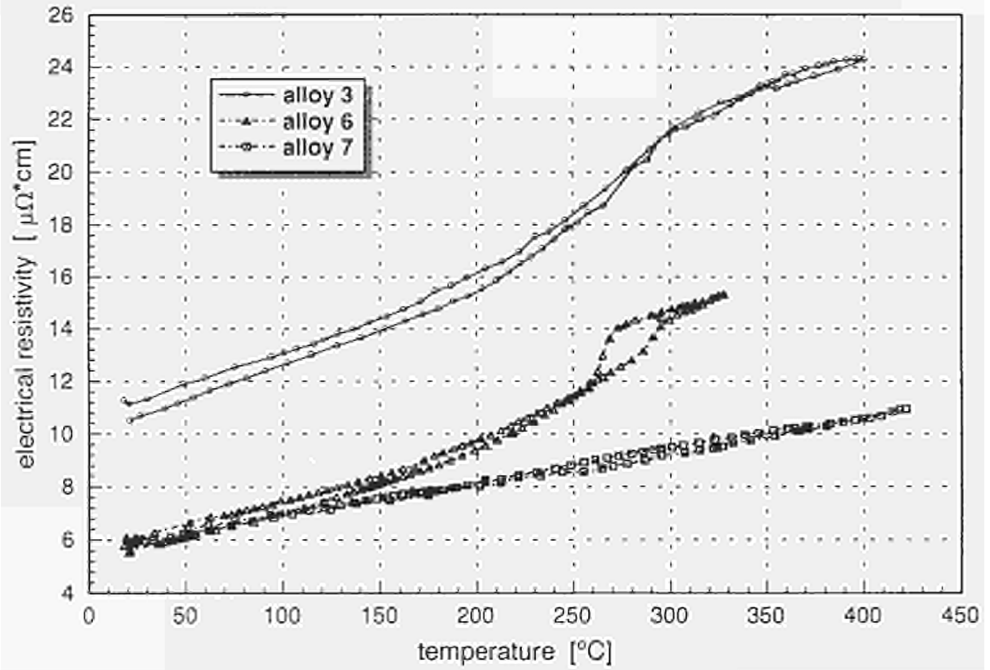

Fig. 6 Electrical resistivity of Al-Si-Zn alloys (specimens 3, 6, and 7)

4.4 Ti-Al-Cu-Ni alloys

Specific heat capacity measurements of quaternary Ti-based alloys were carried out under atmosphere of a flowing argon. Nevertheless it was not possible to protect the specimens against the oxidation. For alloys Ti-1 and Ti-4 the oxidation was observed already around 500 K. Therefore the specific heat capacity was measured after the samples were heated up to 1000K. Fig.7 presents the results of the measurements on alloys Ti-1, -4, and -5 as well as on the alloy TiAl10Cu5Ni25 prepared and investigated at RWTH, Aachen (project D8). DTA investigations made by D8 [95Lug/Köt] show that for alloys with Al-content lower than 15wt% the first phase transition occurs between 700 and 900°C, while for alloys with greater Al-content above 1000°C. From our DSC curves can be seen, that the first transition depends on Ni amount also. For alloys with Ni-content greater than 15wt% a rapid increasing of specific heat capacity above 500°C was observed.

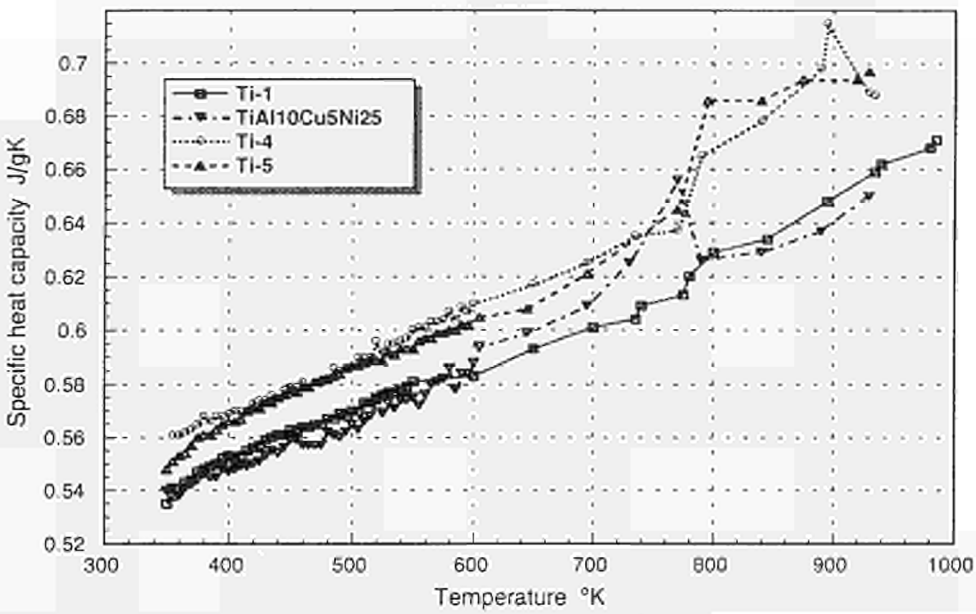

Fig. 7 Specific heat capacity of quaternary Ti-Al-Cu-Ni alloys

5 Conclusion

THERSYST data collection on thermophysical properties of light metal alloys comprises within about 1500 data-sets on 158 alloys and metal matrix composites. Data taken from publications were critically analyzed respecting to their reliability. Data base is installed as a standalone version at our institute and the data can be inquired of there.
Extensive investigations of thermal conductivity and hardness of industrial aluminium-silicon-based alloys have been performed in order to find the correlation between both properties. The hardness belongs to the important parameters describing the metallurgical state of the alloy. It can be quickly and readily determined. The measurements of the thermal conductivity are expensive and time consuming. The correlation obtained makes it possible to replace in some cases the thermal conductivity investigations by simpler hardness measurements.

References

85Sun/Jan B.Sundman, B.Janson, J.-O.Anderson, CALPHAD 1985, **9**, 153

89Neu/Bra G.Neuer, R.Brandt, G.Jaroma-Weiland, G.Pflugfelder, Int.J.Thermophys. 1989, **10**, 749-763

92Hol S.Holtz, Untersuchungen zur Thermodynamik und Konstitution des Legierungssystems AlSiZn; Diplomarbeit, Inst. für Metallkunde und Metallphysik der Universität Clausthal, 1992

94Ans I.Ansara, COST507 Data Base for Light Metal Alloys, Round 1, CEC, Brussels (1994)

94Jar/Bra G.Jaroma-Weiland, R.Brandt, G.Neuer, 1994, IKE-5-238, COST507 Thermophysical Properties of Light Metal Alloys (Institut für Kernenergetik und Energiesysteme der Universität Stuttgart)
96Jac/Spe M.H.G.Jacobs, P.J.Spencer, CALPHAD 1996, **20**, 307
96Jar/Rei G.Jaroma-Weiland, P.Reipert, R.Brandt, G.Neuer, 1996, 14th ECTP, Lyon, France, 16-19 Sept.
96Lug/Köt E.Lugscheider, B.Kötzing, L.Martinez, M.Koschlig, 4th Colloq.: Brazing, High Temperature Brazing and Diffusion Welding, 1995 Aachen, 27-29 July 1995
96Ola/San P.Olafsson, R.Sandström, A.Karlsson, Materials Sci.Forum 1996, **217-222**, 981
96Zah C.Y.Zahra, A.-M.Zahra, COST507/II, Final Report 1996, CNRS,Marseille

Thermodynamic Assessment in the Al-Cu-Mg-Zn System

P. Liang, H. L. Lukas, H. J. Seifert and F. Aldinger

Max-Planck-Institut für Metallforschung, Pulvermetallurgisches Laboratorium,
Heisenbergstr. 5, D-70569 Stuttgart, Germany

Abstract

The main part of this research is the assessment of the Al-Cu-Mg-Zn system, which is one of the key systems of the COST 507 project. Our contribution to it includes full optimization of the Cu-Mg-Zn and Al-Mg-Zn ternary systems and revision of the thermodynamic descriptions of the Al-Mg, Mg-Si, Mg-Zn and Al-Mg-Si systems, using experimental results planned after the assessments of round I and carried out by our partners of the COST 507 project. The optimization of the Al-Mg-Zn ternary system incorporates, in addition to the available published data, the results of experimental measurements carried out in a collaboration between CNRS at Vitry-sur-Seine, UMIST Manchester and MPI Stuttgart. The experiments on ternary Al-Mg-Zn alloys were specifically performed to provide missing data of the ternary solubilities of the Al-Mg and Mg-Zn phases as well as to improve the knowledge of the extensions of the homogeneity ranges of the ternary τ- and ϕ-phases.

In the Al-Mg-Si system the technically most important part, the solvus surface of the (Al) solid solution could be improved, on one hand due to a better description of the Gibbs energy of the Mg_2Si binary phase, derived from enthalpy of formation and melting as well as from heat capacity measurements, on the other hand by DTA, dilatometric and metallographic investigation of Al-rich alloys, which were carried out by F. Sommer's group at MPI Stuttgart.

1 Introduction

The phase relationships in the quaternary Al-Cu-Mg-Zn system are very complex and experimentally not well established. Only a partial phase diagram in the Al-rich corner was investigated [47Str]. No quaternary phase has been found. I. e. the phases encountered are the same as in the ternary sub-systems Al-Cu-Mg, Al-Cu-Zn, Al-Mg-Zn and Cu-Mg-Zn or quaternary extensions of them.

In the Al-Cu-Mg-Zn system, several non-stoichiometric phases with the same crystal structures exist in different ternary subsystems with quaternary ranges of homogeneity (T-Phase in the Al-Cu-Mg system and τ- Phase in the Al-Mg-Zn system, Mg_2Zn_{11} and $Mg_2Cu_5Al_6$, the Laves phases in the Cu-Mg-Zn and Al-Cu-Mg systems). In modelling these phases, the model descriptions have to be compatible with regard to possible mixing in the quaternary system. Therefore, the T-phase, Laves phases and $Mg_2Cu_5Al_6$ in the Al-Cu-Mg system have been modelled so as to allow combination with the τ-phase,

$MgZn_2$ (C14) and Mg_2Zn_{11} in the Al-Mg-Zn system and with the Laves phases in the Cu-Mg-Zn system.

2 Data Assessment

Due to the experimental measurements planned and carried out after round I of COST 507, revision of some already evaluated systems was desirable.

2.1 The Al-Mg System

The central part of the Al-Mg phase diagram was not yet well established until now. Therefore and because of interest in the formation of quasicrystals in rapidly quenched samples, the constitution between the β-(Al_3Mg_2-) and γ-($Al_{12}Mg_{17}$-) phases was re-investigated in a collaboration with CNRS at Vitry-sur-Seine [97Su]. The temperature range of stability of the ϵ-phase is shifted to lower temperatures than reported by Schürmann [81Sch]. The phase denoted as ζ by Schürmann seems to be only a modification of the γ-phase inside the γ homogeneity range. The γ-phase model in the compound energy formalism was changed to satisfy the suggestion made by I. Ansara et al. [97Ans].

A new optimization was made keeping for the phases fcc, liquid, hcp the description of N. Sauders [90Sau]. The calculated central part of the phase diagram after this description is shown in Fig. 1.

2.2 The Cu-Mg System

The parameters of the Laves phase $MgCu_2$ were modified to accept the lattice stabilities proposed to be used for all pure elements in the fictitious state of the Laves structure [92Sau, 93Cos, 94Coe, 94Zen].

$$G^{\text{Laves-C15}}_{\text{Cu:Cu}}(T) - 3{}^{\circ}G^{\text{SER}}_{\text{Cu}}(T) = 15000 \text{ J/mol.}$$

$$G^{\text{Laves-C15}}_{\text{Mg:Mg}}(T) - 3{}^{\circ}G^{\text{SER}}_{\text{Mg}}(T) = 15000 \text{ J/mol.}$$

Re-running the least squares program BINGSS with the set of experimental data used by [91Cou] yielded new parameters. These parameters virtually give the same phase diagram as those reported by [91Cou] with a maximal deviation of 0.02 mol% in the solubility limits of $MgCu_2$.

2.3 The Mg-Zn System

In the Mg-Zn system measurements of C_p^{liquid} at 28.1 mol% Zn in the temperature range 650 and 750 K were carried out [95Som], which confirm the magnitude of the positive

deviation from Kopp-Neumann's rule derived by [92Aga] from the temperature dependence of the enthalpy of mixing of the liquid, but the numerical value is refined to about 70% of that assessed by [92Aga].

Kowalski and Spencer [93Kow] in the Cu-Zn system assumed different lattice stabilities for pure Zn in its stable state (hcp with c/a = 1.856) and as hcp phase with axial ratio c/a = 1.556 (ϵ-Cu-Zn phase), which lies close to the ideal axial ratio c/a = 1.633. To get compatibility, in Mg-Zn the Mg(hcp) solid solution had to be reformulated to show the same lattice stability for the end member pure Zn as [93Kow] used for the ϵ-Cu-Zn phase.

Furthermore the $MgZn_2$ Laves phase should be modelled similarly as $MgCu_2$ with antistructure atom formation on both sublattices, although the only information for that is the vague statement: "The homogeneity range of $MgZn_2$ is about 1 at.%" [90Mas].

The Mg-Zn system was re-optimized using the experimental-data file of [92Aga] and the new C_p^{liquid} data of [95Som] (Fig.2). The Laves phase parameters ${}^0L^{MgZn_2}_{Mg:Zn,Mg}$ and ${}^0L^{MgZn_2}_{Mg,Zn:Zn}$ were estimated by trial and error to reproduce a maximum homogeneity range of 1 at.% for $MgZn_2$.

2.4 The Mg-Si System

The enthalpy of formation and melting as well as heat capacity of Mg_2Si were measured calorimetrically by [97Feu]. The Mg-Si system was re-optimized using the experimental-data file of [92Cha] together with the new data of Mg_2Si [97Feu].

2.5 The Al-Mg-Si System

New measurements on this system were carried out by F. Sommer's group at MPI Stuttgart. The Al corner of the Al-Mg-Si ternary system was investigated by DTA and optical micrography. A few points of the solvus of the (Al) solid solution were precisely determined by dilatometry. The results of these experiments and the updated Mg-Si system together with literature data were used to redetermine a complete set of analytical descriptions of the Gibbs energies of all stable phases of the Al-Mg-Si system. The technically most important part, the solvus surface of the (Al) solid solution could be improved (Fig. 3). A publication of this re-optimization is in press [97Feu] .

2.6 The Cu-Mg-Zn System

The assessment of the Cu-Mg-Zn system is mainly based on the critical review of experimental literature provided by COST 507, Coordination group B [94Gho]. The Cu-Mg-Zn phase diagram is characterised by the formation of three Laves phases $MgCu_2$, $MgZn_2$ and the $MgNi_2$-type phase Mg_2CuZn_3 (τ), which have large solubility ranges.

The three Laves phases were described by the "compound-energy-formalism" with Cu-Zn exchange, $Mg(Cu_{1-x}Zn_x)_2$ and slight antistructure atom formation (Cu and Zn on the Mg sublattices, Mg on the Cu-Zn sublattices). The Gibbs energy descriptions of the three quasibinary Laves phases were optimized using published liquidus, solidus and enthalpy of mixing data of the quasibinary system $MgCu_2$-$MgZn_2$ [48Koe, 52Lie, 64Kin, 79Pre]. The homogeneity ranges with respect to excess or deficient Mg were interpolated between the binary end members, since no reliable experimental data for the range of deviation from the stoichiometric MgX_2 are available in the ternary.

The solubilities of Mg in the binary Cu-Zn phases were interpolated from the binary Cu-Mg fcc and Zn-Mg hcp parameters respectively, as no experimental data for these solubilities were found in literature. To satisfy the Bragg-Williams description of ordering in the ternary range of the βCuZn phase, its formulation in the compound energy formalism was extended into ternary and quaternary systems.

The liquid phase was described as substitutional solid solution after the Redlich-Kister Muggianu formalism. No ternary parameters were introduced.

Using the optimized quasibinary parameters and the estimated ternary parameters, together with the parameters of the binary subsystems, the ternary Cu-Mg-Zn system was calculated. The results are shown in Fig. 4 to 9 and compared with the experimental values.

This optimization was presented at the conference " Thermodynamics of Alloys" at Marseille, Sep. 1996 and is in preparation for publication in Calphad.

2.7 The Al-Mg-Zn System

The Al-Mg-Zn ternary system is a relatively complex system which includes two ternary phases, τ and ϕ. The τ-phase has a large homogeneity region. Its ideal formula is $Mg_{32}(Zn,Al)_{49}$. It is cubic, space group Im3, 162 atoms to the unit cell [52Ber]. The ternary τ-phase was modelled according to its crystal structure with cubic symmetry as $(Mg)_{26}(Mg,Al)_6(Al,Zn,Mg)_{48}(Al)_1$ in the compound energy formalism. The unit cell of the ternary ϕ-phase was at first time determined in a collaboration between CNRS/ONERA in Châtillon, CNRS in Vitry-sur-Seine and MPI in Stuttgart using transmission electron microscopy [97Don]. The unit cell of the ϕ-phase is orthorhombic, space group Pbc2, or Pbcm with large lattice parameters (a=897.9, b=1698.8, c=1934 pm). The ϕ-phase was approximated by the sublattice formula $Mg_6(Al,Zn)_5$.

The optimization of the Al-Mg-Zn ternary system incorporates, in addition to the available published data, the results of experimental measurements carried out in a collaboration between CNRS at Vitry-sur-Seine, UMIST at Manchester and MPI at Stuttgart. The experiments on ternary Al-Mg-Zn alloys were specifically performed to provide missing data of the ternary solubilities of the Al-Mg and Mg-Zn phases as well as to improve the knowledge of the extensions of the homogeneity ranges of the ternary τ- and ϕ-phases. The alloys were investigated using X-ray diffraction, differential scanning calorimetry and DTA in the composition range around the τ- and ϕ-phases. The compositions of the constituent phases were determined by Electron Probe Micro Analysis (EPMA) and Energy Dispersive X-ray Spectroscopy (EDX).

The experimental results show that Zn substitutes Al in Al-Mg binary phases and Al substitutes Zn in Mg-Zn binary phases to several mol%, respectively. Therefore these binary phases with ternary solubilities were modelled as following:

β-AlMg: $Mg_{89}(\mathbf{Al},Zn)_{140}$

ϵ-AlMg: $Mg_{23}(\mathbf{Al},Zn)_{30}$

γ-AlMg: $Mg_{10}(\mathbf{Mg},Al,Zn)_{24}(\mathbf{Al},Mg,Zn)_{24}$

Mg_2Zn_{11}: $Mg_2(\mathbf{Zn},Al)_{11}$

$MgZn_2$: $(\mathbf{Mg},Al,Zn)(\mathbf{Zn},Al,Mg)_2$

Mg_2Zn_3: $Mg_2(\mathbf{Zn},Al)_3$

MgZn: $Mg_{12}(\mathbf{Zn},Al)_{13}$

The major constituents are denoted in boldface.

The ternary parameters of the τ- and ϕ-phases as well as the Al-Mg and Mg-Zn phases were adjusted using published data reviewed by Petrov [93Pet] and the new experimental results.

The liquid phase was described as substitutional solid solution after the Redlich-Kister Muggianu formalism. The measured partial enthalpies of the liquid [97Kim] do not exactly agree with this description, however, may be tolerated within the accuracy of the measurements. Therefore no ternary parameters were introduced for the Gibbs energy description of the liquid.

Using the optimized ternary parameters the ternary Al-Mg-Zn system was calculated. The results are shown in Fig. 10 to 15 and compared with the experimental values.

This optimization was presented at the conference " Thermodynamics of Alloys" at Marseille, Sep. 1996 and is in preparation for *thermochimica acta*.

2.8 The Al-Cu-Mg-Zn System

It was started to combine these ternary descriptions with the assessments of Al-Cu-Mg from Aachen and Al-Cu-Zn from Leuven to a full description of the quaternary Al-Cu-Mg-Zn system.

Acknowledgement

Financial support by the German "Bundesministerium für Bildung, Wissenschaft, Forschung und Technologie" (Contract 03K7208 0) is gratefully acknowledged.

References

[13Ege] G. Eger, Z. Metallkd., 1913, **4**, 28-127.

[26San] W. Sander, Z. Anorg. Chem., 1926, **154**, 144-151.

[33Sal] P. Saldau and M. Zamotorin, Z. Anorg. Chem., 1933, **213**, 377-382.

[40Kuz] V. G. Kuznetsov and E. S. Makarov, Izv. Sekt. Fiz.-Khim. Anal., 1940, **13**, 1177-1190.

[43Sie] G. Siebel, Z. Elektrochem., 1943, **49**, 218-221.

[47Str] D. J. Strawbridge, W. Hume-Rothery and A. T. Little, J. Inst. Met., 1947, **74**, 191-225.

[48Koe] W. Köster and F. Müller, Z. Metallkd., 1948, **39**, 352-359.

[50Mik] V. I. Mikheeva and O. N. Kryukova, Izv. Sekt. Fiz.-Khim. Anal., Akad. Nauk. SSSR., 1950, **20**, 76-93.

[50Nis] H. Nishimura and Y. Murakami, Mem. Fac. Eng. Kyoto Univ., 1950, **12**, 119-128.

[52Ber] G. Bergman, JL Waugh and L. Pauling Nature, 1952, **169**, 1057-1058.

[52Lie] K. H. Liester and H. Witte, Z. Metallkd., 1952, **43**, 396-401.

[64Kin] R. C. King and O. J. Kleppa, Acta Metall., 1964, **12**, 87-97.

[72Pre] B. Predel and H. Ruge, Mater. Sci. Eng., 1972, **9**, 141-151.

[79Pre] B. Predel, H. Bencker, W. Vogelbein and M. Ellner, J. Solid State Chem., 1979, **28**, 245-257.

[81Sch] E. Schürmann, E. Voss, Giessereiforschung, 1981, **33**, 43-46.

[90Mas] T.B. Massalski, (Ed.) *Binary Alloy Phase Diagrams*, ASM, Metals Park, Ohio, 1990.

[90Sau] N. Saunders Calphad, 1990, **14**, 61-70.

[91Cou] C. A. Coughanowr, I. Ansara, R. Luoma, M. Hämäläinen and H. L. Lukas, Z. Metallkd., 1991, **82**, 574-582.

[92Aga] R. Agarwal, S. G. Fries, H. L. Lukas, G. Petzow, F. Sommer, T. G. Chart and G. Effenberg, Z. Metallkd., 1992, **83**, 216-223.

[92Cha] N. Chakraborti and H. L. Lukas, Calphad, 1992, **16**, 79-86.

[92Sau] N. Saunders, private communication., 1992.

[93Cos] J. G. Costa Neto, S. G.-Fries, H. L. Lukas, CALPHAD, 1993, **17**, 219-228.

[93Kow] M. Kowalski and P. J. Spencer, J. Phase Equilibria, 1993, **14**, 432-438.

[93Pet] D. A. Petrov, in *Ternary Alloys*, Vol.7, G. Petzow G. Effenberg, ed., VCH Verlag, Weinheim, Germany, 1993.

[94Coe] G. C. Coelho, S. G.-Fries, H. L. Lukas, P. Majewski, J. M. Zelaya Bejarano, S. Gama, C. A. Ribeiro and G. Effenberg in: Klaus Schulze Symposium on Processing and Applications of High Purity Refractory Metals and Alloys, P. Kumar, H. A. Jehn and M. Uz eds., The Minerals, Metals and Materials Society, Warrendale, Pa. 15086, USA, 1994.

[94Zen] K. Zeng, M. Hämäläinen and I. Ansara, *Thermochemical database for light metal alloys*, COST 507, Concerned Action on Materials Sciences, European Commission, DG XII, Luxembourg, 1994.

[94Gho] G. Ghosh, H. L. Lukas and G. Effenberg, report to COST 507, Coordination Group B, 1994.

[95Som] T. Goedecke and F. Sommer, private communication.

[97Ans] I. Ansara, T. G. Chart, A. Fernández Guillermet, F. H. Hayes, U. R. Kattner, D. G. Pettifor, N. Saunders and K. Zeng, CALPHAD **21**, 1997, in press.

[97Don] P. Donnadieu, A. Quivy, T. Tarfa, P. Ochin, A. Dezellus, M. Harmelin, P. Liang, H. L. Lukas, H. J. Seifert, F. Aldinger and G. Effenberg, Z. Metallkd., 1997, in press.

[97Feu] H. Feufel, T. Gödecke, H. L. Lukas, and F. Sommer, J. Alloys Comp., 1997, in press.

[97Kim] Y. B. Kim, F. Sommer and B. Predel J. Alloys Comp., 1997, in press.

[97Su] H. L. Su, M. Harmelin, P. Donnadieu, C. Bätzner, H. J. Seifert, H. L. Lukas, G. Effenberg and F. Aldinger, J. Alloys Comp., 1997, in press.

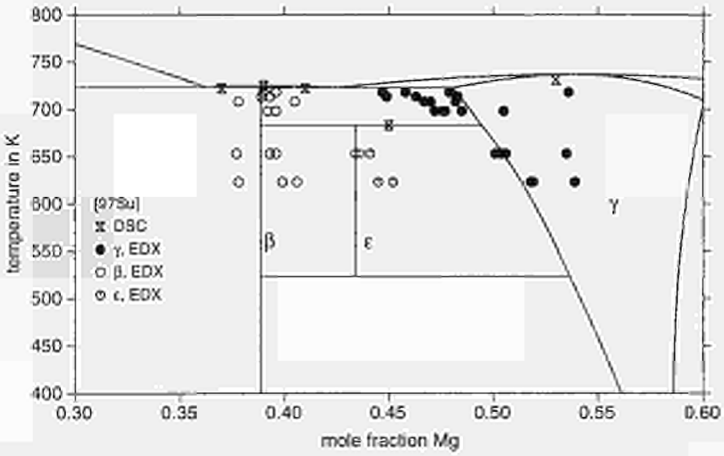

Fig. 1. Central part of the phase diagram of the Al-Mg system.

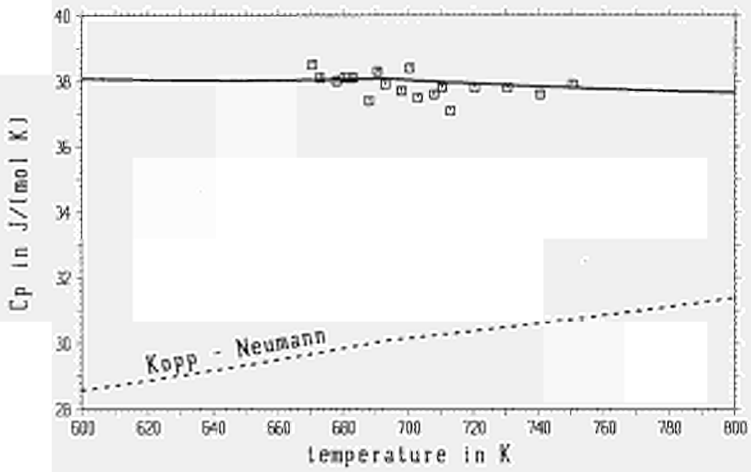

Fig. 2. C_p^{liquid} of a Mg-Zn alloy at 28.1 mol% Zn [95Som].

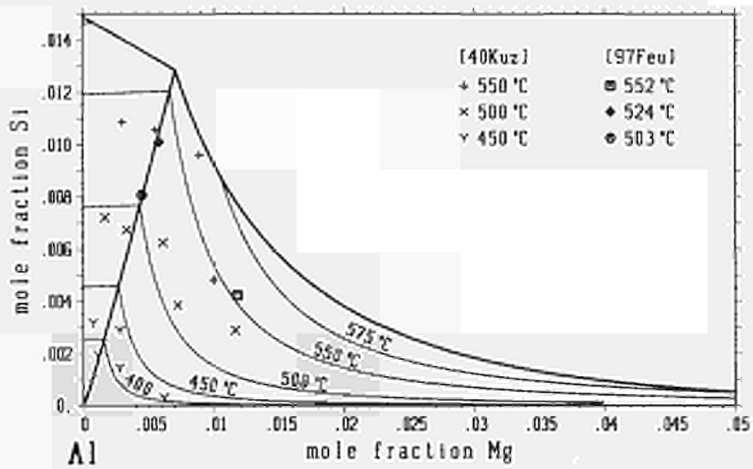

Fig. 3. Solvus of the (Al) solid solution of the Al-Mg-Si system.

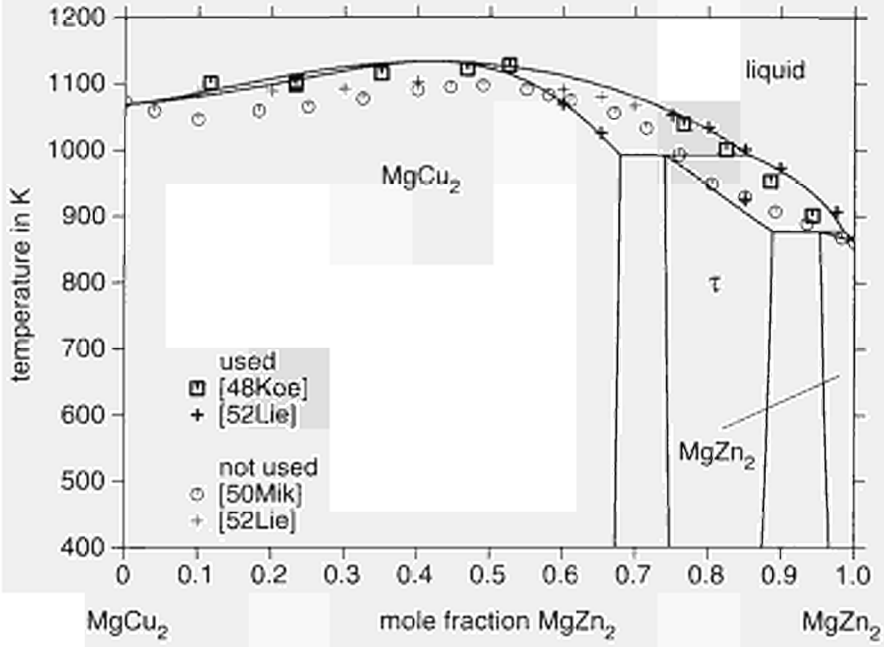

Fig. 4. The calculated $MgCu_2$-$MgZn_2$ quasibinary phase diagram.

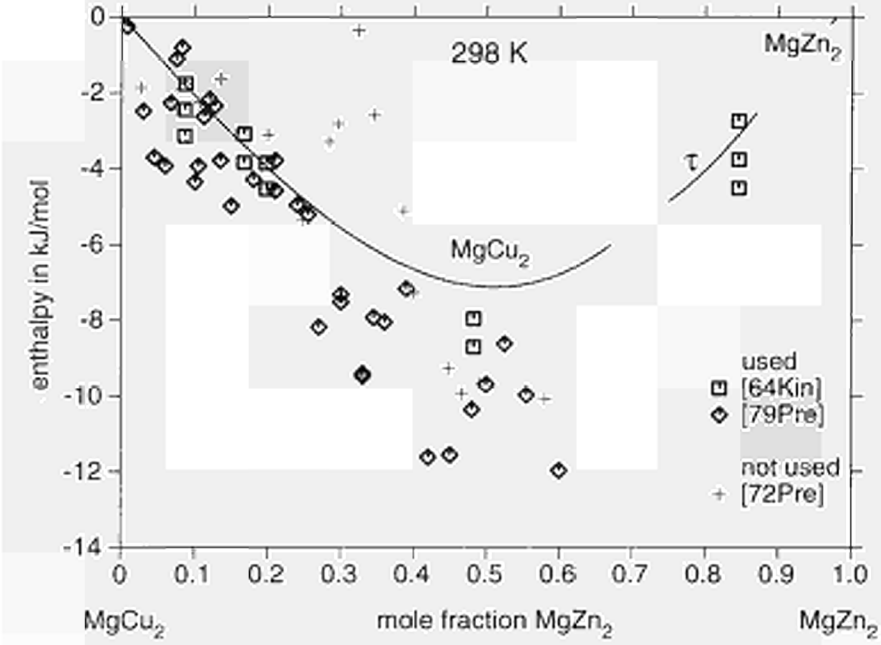

Fig. 5. Enthalpy of mixing of the Laves phases in the quasibinary $MgCu_2$-$MgZn_2$ system.

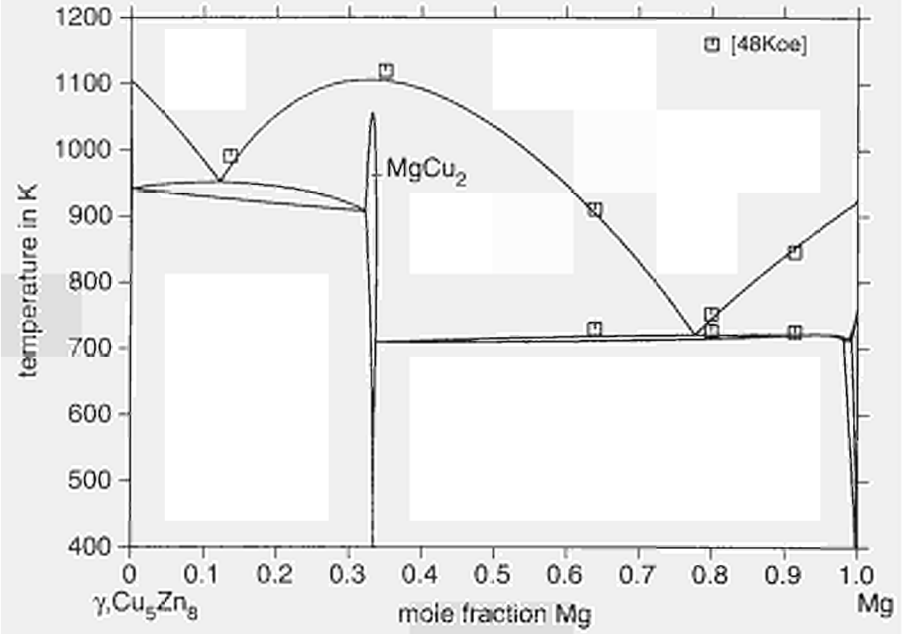

Fig. 6. Vertical section of the Cu-Mg-Zn system from γ to Mg.

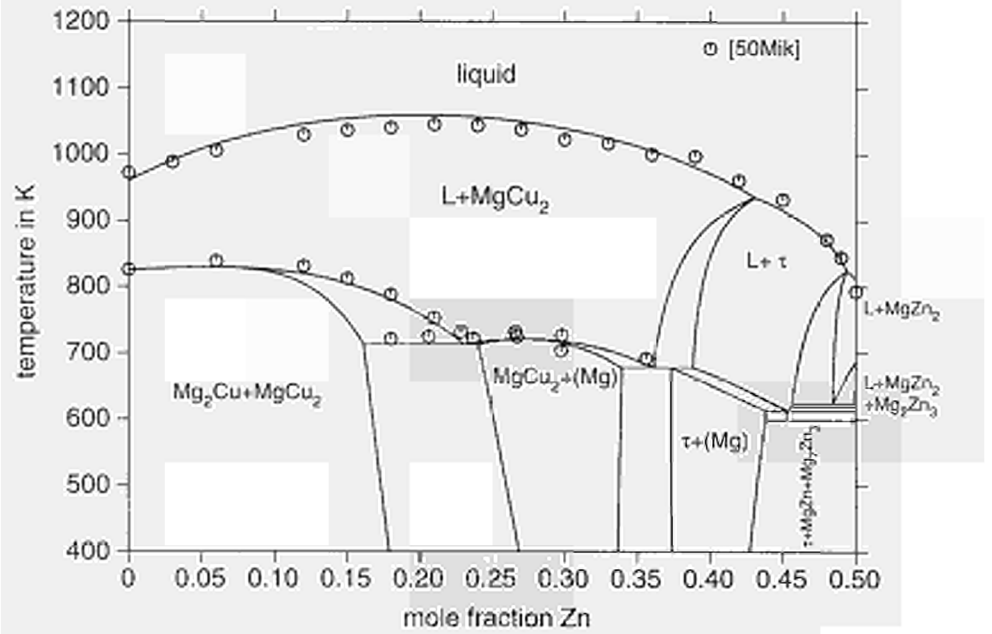

Fig. 7. Vertical section of the Cu-Mg-Zn system at 50 mol% Mg.

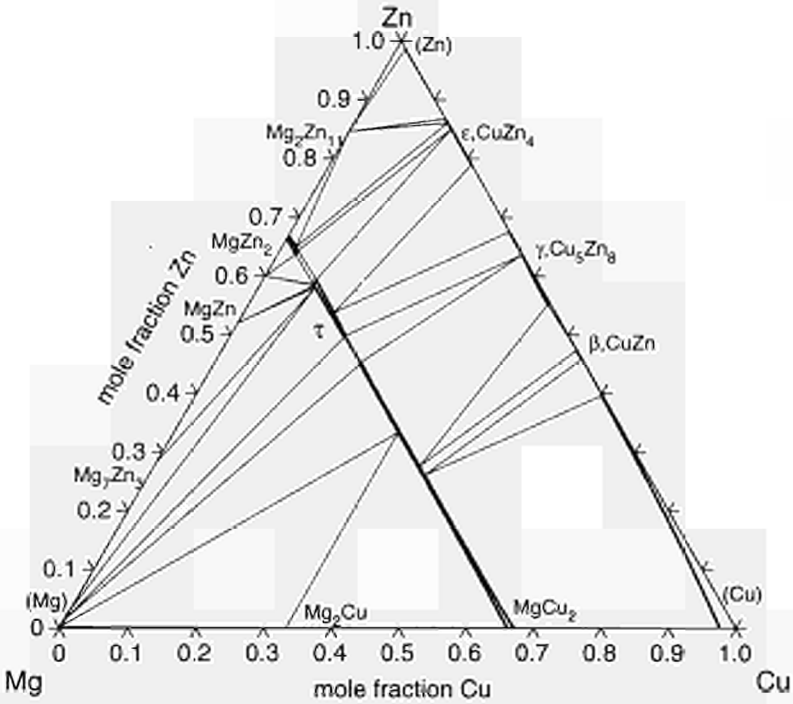

Fig. 8. Isothermal section at 600 K of the Cu-Mg-Zn ternary system.

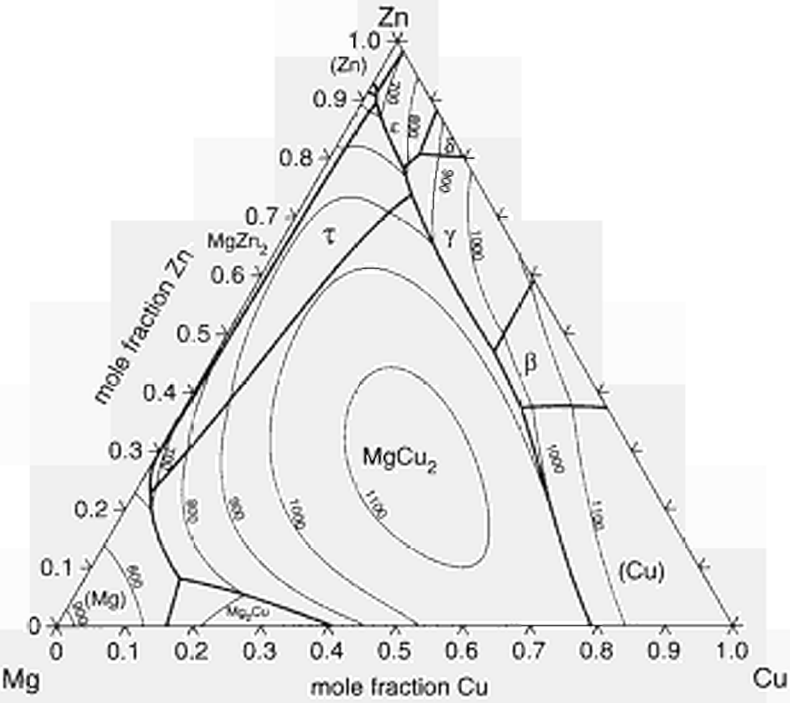

Fig. 9. Liquidus surface of the Cu-Mg-Zn ternary system.

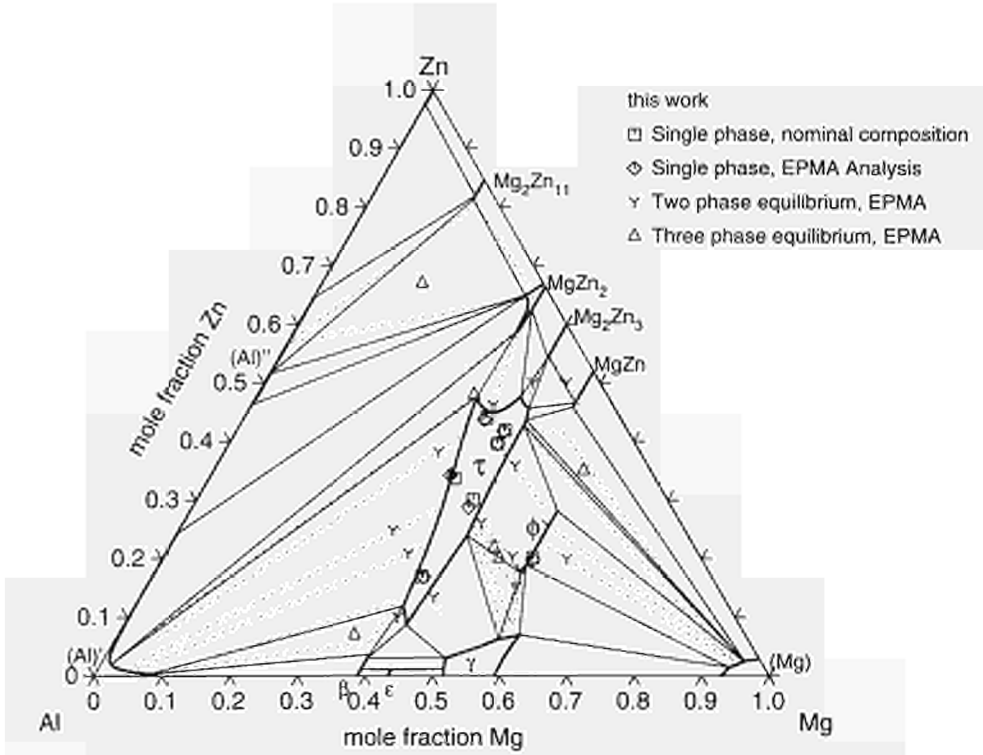

Fig. 10. Isothermal section at 608 K of the Al-Mg-Zn ternary system.

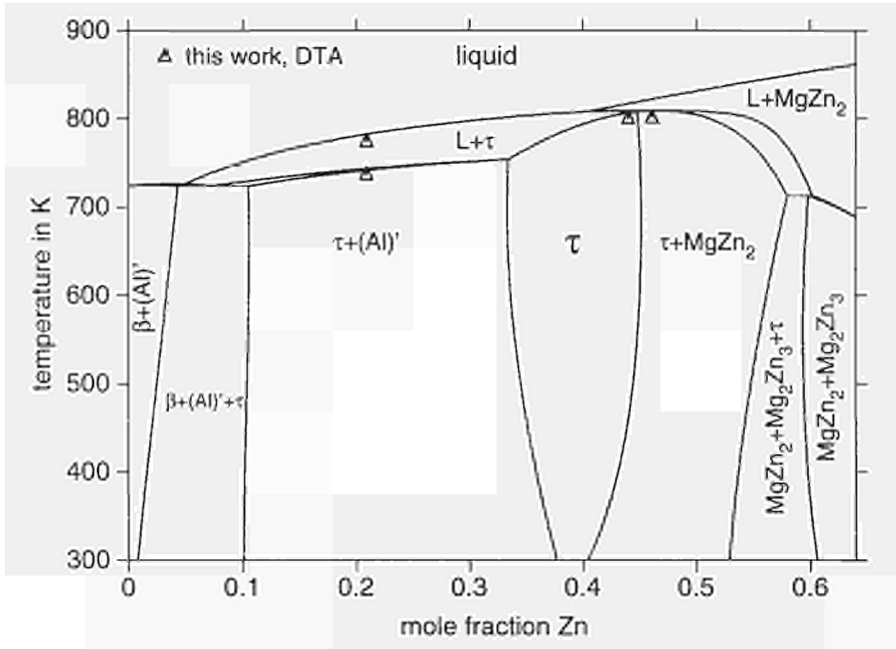

Fig. 11. Vertical section of the Al-Mg-Zn ternary system at 36 mol% Mg.

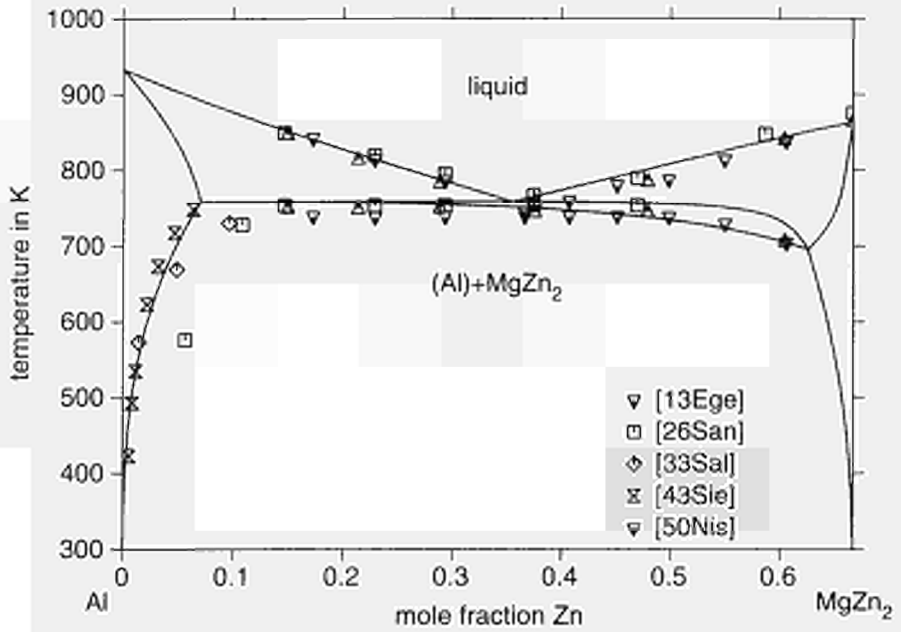

Fig. 12. Vertical section of the Al-Mg-Zn ternary system from Al to $MgZn_2$.

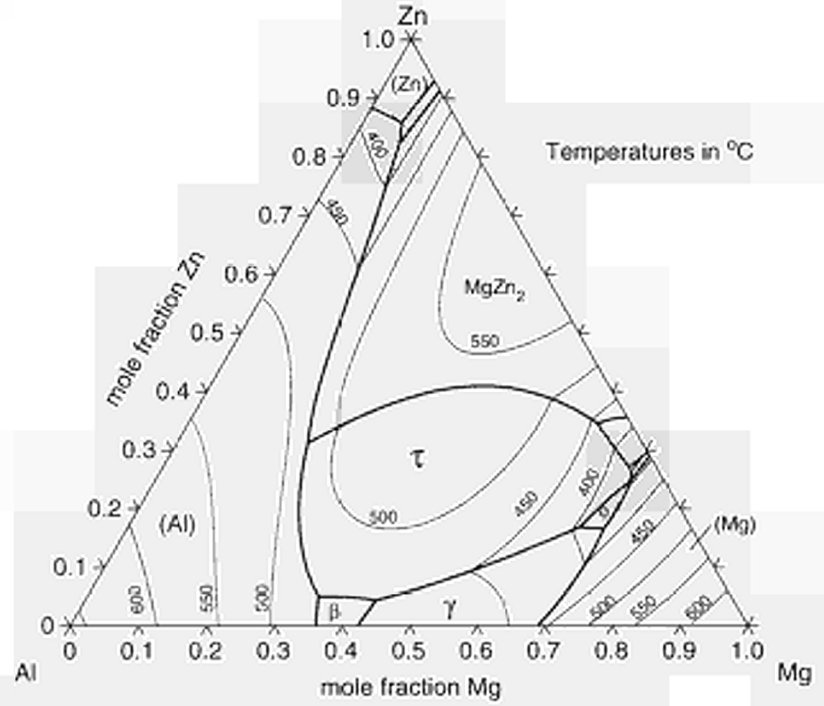

Fig. 13. Liquidus surface of the Al-Mg-Zn ternary system.

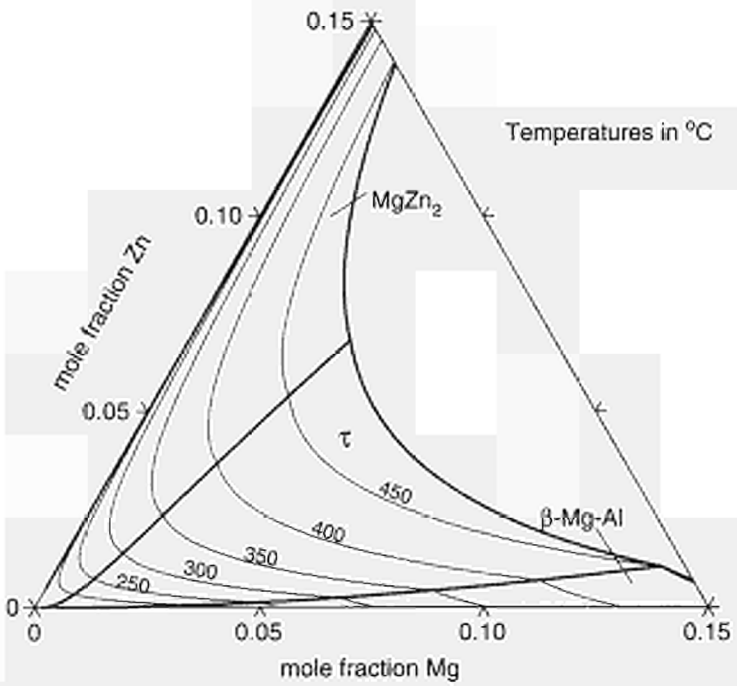

Fig. 14. Solvus of the (Al) solid solution of the Al-Mg-Zn system.

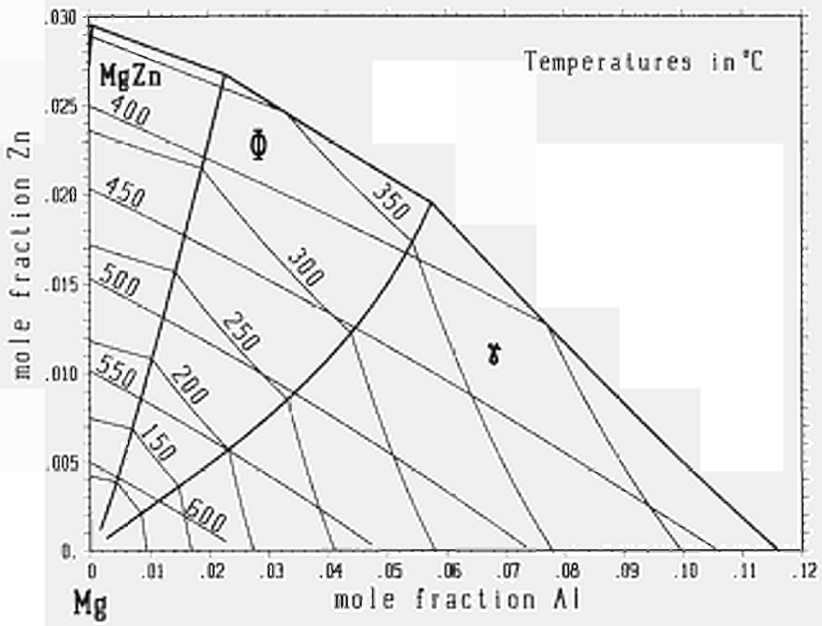

Fig. 15. Solvus and solidus of the (Mg) solid solution of the Al-Mg-Zn system.

Heat Capacity Data on some Al-based Alloys

C.Y.Zahra and A.-M. Zahra

Centre de Thermodynamique et de Microcalorimétrie, C.N.R.S.
26, rue du 141e R.I.A., F-13331 MARSEILLE CEDEX 3

Abstract

Specific heat capacities were determined on 2 industrial Al-Si based alloys and on 11 ternary Al-Si-Zn alloys. The data were obtained with the help of a heat flux DSC apparatus and have a reproducibility of ± 1.5 %. In the case of the industrial alloys, the c_p-values may be interpolated linearly between 50 and 250 °C. The values for the ternary alloys lie in general below those derived from the application of the additivity rule.

1 Introduction

The present study covers c_p-measurements on Al-based alloys made available from COST 507/II partners D9 (Dr. G. Neuer) and destined for the databank THERSYST. Two groups of alloys were studied :
- industrial ones already examined by partners D9. In this way, results of independent measurements may be compared;
- ternary alloys for which COST partners D3 (Dr. P.J. Spencer) calculated the thermodynamic properties starting from known data on the binary systems involved. The ultimate aim is to confront their predictions with experimental data.

2 Experimental

Two technical Al-Si based alloys prepared by Kolbenschmidt AG were selected for a comparative study; their chemical compositions (in mass%) and Brinell hardnesses before the c_p-measurements are given in table 1. The stability of their structural states was evaluated from DSC runs (fig. 1). Dissolution sets in above 280 °C.

Table 1 : Alloy compositions

KS-4	KS-5
8.44 % Si	13.46 % Si
3.09 % Cu	3.71 % Cu
0.49 % Mg	0.87 % Mg
0.05 % Ni	2.18 % Ni
0.60 % Fe	0.55 % Fe
0.39 % Mn	0.45 % Mn
0.46 % Zn	0.08 % Zn
0.09 % Ti	0.05 % Ti
0.08 % Pb	0.01 % Pb
0.02 % Sn	0.01 % Sn
HB : 99	HB : 152

The eleven ternary Al-Si-Zn alloys were cast by Vereinigte Aluminiumwerke Bonn. Their chemical compositions (in atom and mass %) are indicated in table 2 and also represented in fig. 2. From each alloy including the technical ones, 2 disks 5.9 mm in diameter and 1 mm thick were machined.

Table 2 : Alloy compositions

Alloy	atom%			mass%		
	Al	Si	Zn	Al	Si	Zn
1	76.46	4.40	19.14	60.01	3.59	36.40
2	72.73	9.08	18.19	57.61	7.49	34.90
3	60.82	18.69	20.49	46.81	14.98	38.21
6	39.13	1.02	59.85	21.13	0.57	78.30
7	84.83	5.04	10.13	74.02	4.58	21.40
8	79.89	9.97	10.14	69.57	9.04	21.39
9	11.73	0.05	88.22	5.20	0.02	94.78
10	90.19	4.71	5.10	83.93	4.56	11.51
11	58.51	1.00	40.49	37.11	0.66	62.23
12	55.84	4.66	39.50	35.70	3.10	61.20
13	53.28	10.64	36.08	35.10	7.30	57.60

Alloys 6 and 9 were kept at 360 °C for 7 h before oven cooling to room temperature; the other alloys were annealed for 5 h at 400 °C and maintained a week at 265 °C (1,2,3,11,12,13) or 240 °C (7,8) or 175 °C (10) before oven cooling. The hope of retaining stable structures at room temperature was vain, as successive DSC experiments at 5 °C/min still showed endothermal dissolution effects at low temperatures (fig. 3). As expected, the specimens 7, 8 and 10 with low Zn concentrations do not undergo a transformation around 277 °C. Due to complications arising from the existence of metastable phases and to the fact that c_p-measurements are very time consuming and tedious, it was decided to carry them out at selected temperatures only.

A Perkin-Elmer thermal analyser DSC 7 series 1020 was used in a constant temperature environment. The recommendations given by Höhne et al. in their book on differential scanning calorimetry [96Höh] were observed and the following procedure was adopted in order to obtain a high accuracy of the c_p-data :

- The discontinuous 3step technique which measures heats was employed, as it needs no correction for thermal lag after precise temperature calibration.
- Steps of 20 °C were chosen at a rate of 5 °C/min. In order to check reversibility, at least three heating and cooling cycles under argon atmosphere were performed after establishment of isothermal steady state conditions.
- Al was used as reference sample, as the alloy and calibrant should have similar heat capacities and similar thermal conductivities. c_p-data for Al were calculated according to a formula given in Dinsdale's paper "SGTE data for pure elements" [91Din]. A critical assessment of the thermodynamic properties of Al was also published by Desai [87Des]. Specific heat values of interest proposed by Dinsdale and Desai are confronted in table 3. They agree within 0,5 % except at 450 °C. Also are given some c_p-data on Si and Zn according to [91Din].

Table 3 : c_p in J/gK

	Al			Si	Zn
	SGTE	Desai	%	SGTE	SGTE
50 °C	0.91604	0.91367	0.25	0.73656	0.39156
100 °C	0.94297	0.94186	0.12		
150 °C	0.96649	0.96485	0.17		
250 °C	1.00954	1.00543	0.41		
350 °C	1.05180	1.04987	0.18	0.86572	0.44023
400 °C	1.07346	1.07546	0.08	0.87721	0.45037

3. Results

3.1. Industrial Al-Si based alloys

Table 4 summarises the results of c_p-determinations on alloys KS-4 and KS-5 as well as their repeatability (the maximum deviation is ± 0.2 %). Originally four temperatures were selected : 50, 150, 250 and 450 °C; at the latter, the alloy had been kept for an hour before the actual measurements, but results had to be discarded, as they did not give a unique value on heating and on cooling. Also indicated are the c_p-results of Jaroma-Weiland [96Jar] on the same alloys, with extrapolations to 50 °C. She used sapphire as reference material in conjunction with the normal continuous 3step procedure. The reproducibility of the two independent determinations, i.e. the deviation of the mean values of the results of an instrument from the total mean value [96 Höh] lies within ± 1.5 %. The agreement is very good, as Jaroma-Weiland et al. evaluate the inaccuracy (band) of their measurements to lie below 3 % [94Jar]. The present c_p-data may be connected linearly between 50 and 250 °C. The higher Si content of KS-5 is responsible for lower c_p-values.

Table 4 : c_p in J/gK

		50 °C	150 °C	250 °C
KS-4				
Present study		0.879	0.928	0.9715
repeatability	±	0.2 %	0.1 %	0.1 %
Jaroma-Weiland		0.889	0.928	0.985
reproducibility	±	1.1 %	~0 %	1.4 %
KS-5				
Present study		0.852	0.900	0.944
repeatability	±	0.1 %	0.2 %	0.2 %
Jaroma-Weiland		0.865	0.901	0.954
reproducibility	±	1.5 %	0.2 %	1 %

3.2 Al-Si-Zn alloys

Having gained confidence in the adopted measuring technique, the c_p-data on the ternary alloys were determined on heating each specimen three times over the temperature intervals 40 - 60 and 390 - 410 °C (340 - 360 °C in the case of alloys 6 and 9). The mean values ($c_p$exp in J/gK), often obtained on two different specimens, are given in table 5; their reproducibility is estimated to be the same as for the industrial alloys (± 1.5 %). The results are consistent with the compositions of the alloys : increasing Si and especially Zn concentrations decrease the c_p-values. For comparison, the $c_p$add-data derived according to the additivity rule are indicated; the values for the pure elements are taken from table 3 [91Din]. At 50 °C, the calculated values are more important than $c_p$exp. The alloys 7, 8 and 10 in the Al rich corner possess c_p-values at 400 °C which correspond to additivity within the experimental inaccuracy.

Table 5 : c_p in J/gK

Alloy	50 °C		350 °C		400 °C	
	$c_p$exp	$c_p$add	$c_p$exp	$c_p$add	$c_p$exp	$c_p$add
1	0.737	0.808			0.891	0.946
2	0.716	0.804			0.886	0.942
3	0.706	0.775			0.871	0.909
6	0.517	0.600	0.602	0.684		
7	0.814	0.845			1.003	1.000
8	0.797	0.845			0.982	0.991
9	0.428	0.453	0.530	0.512		
10	0.848	0.881			1.046	1.032
11	0.607	0.702			0.751	0.819
12	0.596	0.700			0.736	0.818
13	0.601	0.708			0.743	0.828

4 Conclusion

Specific heat capacities were measured with the help of a Perkin-Elmer thermal analyser DSC7 series 1020, applying the discontinuous 3step method. The repeatability of the data is of ± 0.2 %. Their reproducibility as derived from a comparison with independent determinations on some alloys is of ± 1.5 %.
The c_p-data obtained on two technical Al-Si based alloys may be connected linearly between 50 and 250 °C. Ternary Al-Si-Zn alloys possess c_p-values at 50 and 400 °C which lie in general below those corresponding to the Neumann-Kopp rule.

5 References

87Des P D Desai, Internat J Thermophys, 1987, **8**, 621-638.

91Din A T Dinsdale, Calphad, 1991, **15**, 317-425.

95Höh G Höhne, W Hemminger, H-J Flammersheim, *Differential Scanning Calorimetry*, Springer, 1995.

96Jar G Jaroma-Weiland, *Progress Report for Period July-December 1995*, COST 507 - Thermophysical Properties of Light Metal Alloys. University of Stuttgart.

94Jar G Jaroma-Weiland, R Brandt, G Neuer, *Final Report 1994*, COST 507 - Thermophysical Properties of Light Metal Alloys. University of Stuttgart.

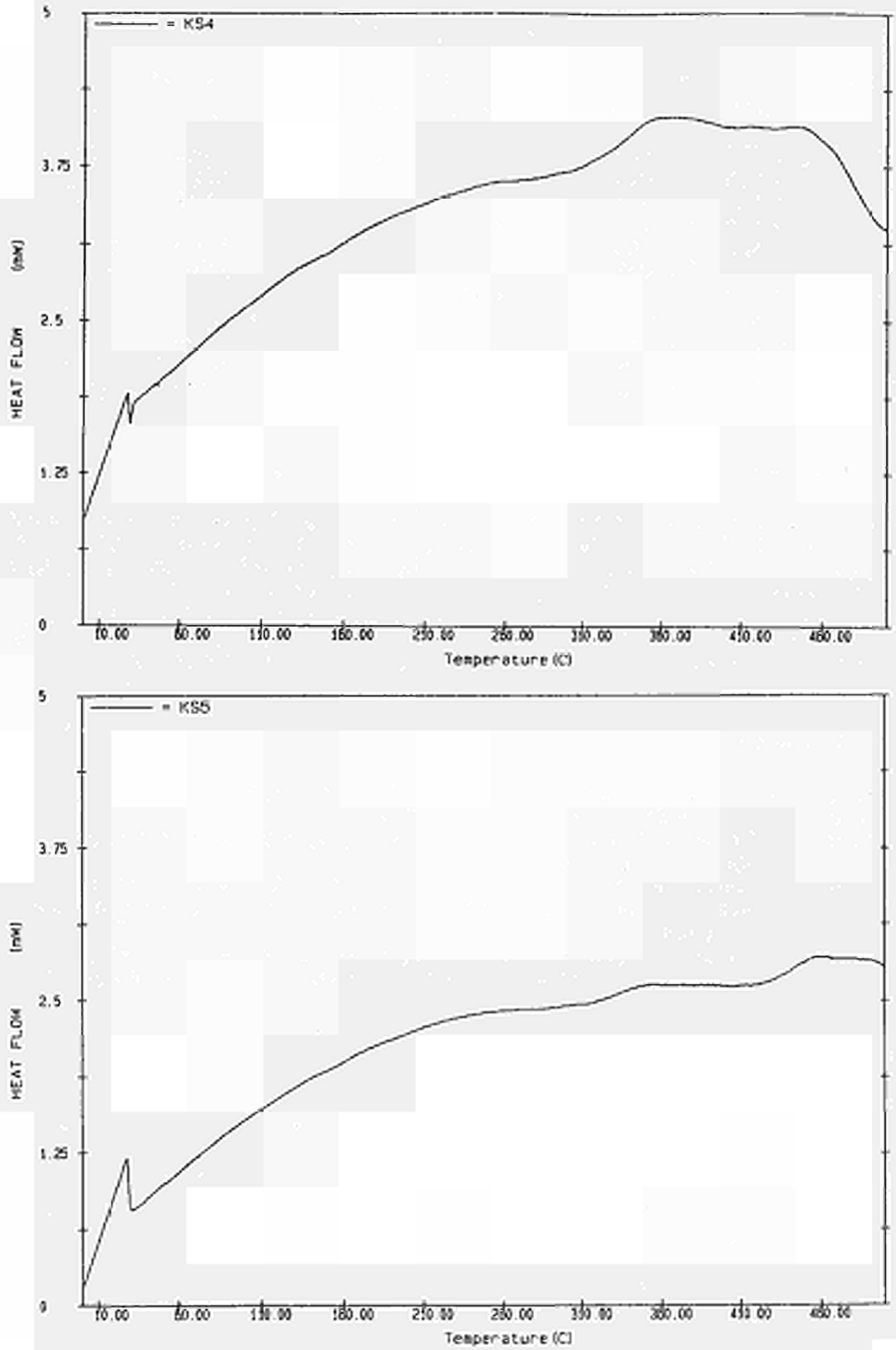

Fig. 1 : DSC curves, at 5 °C/min, on the industrial alloys KS-4 (upper curve) and KS-5 (lower curve)

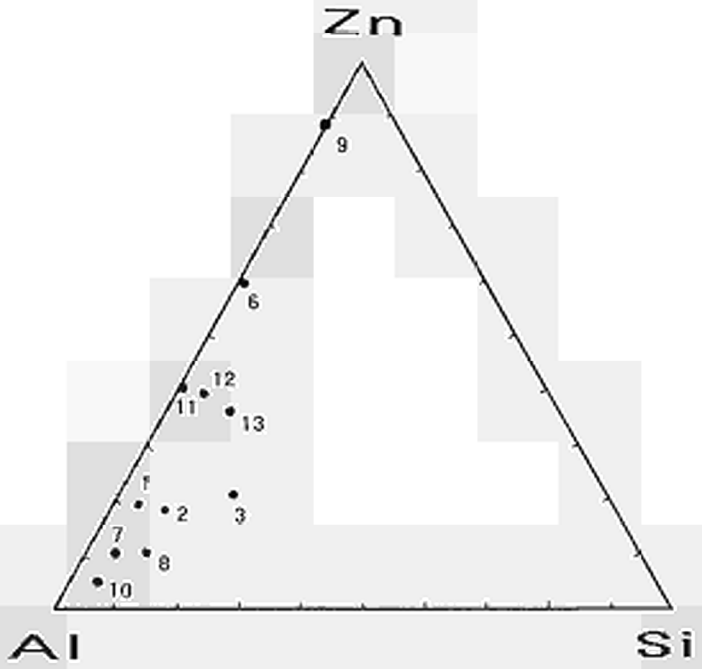

Fig. 2 : Position of the 11 alloys studied

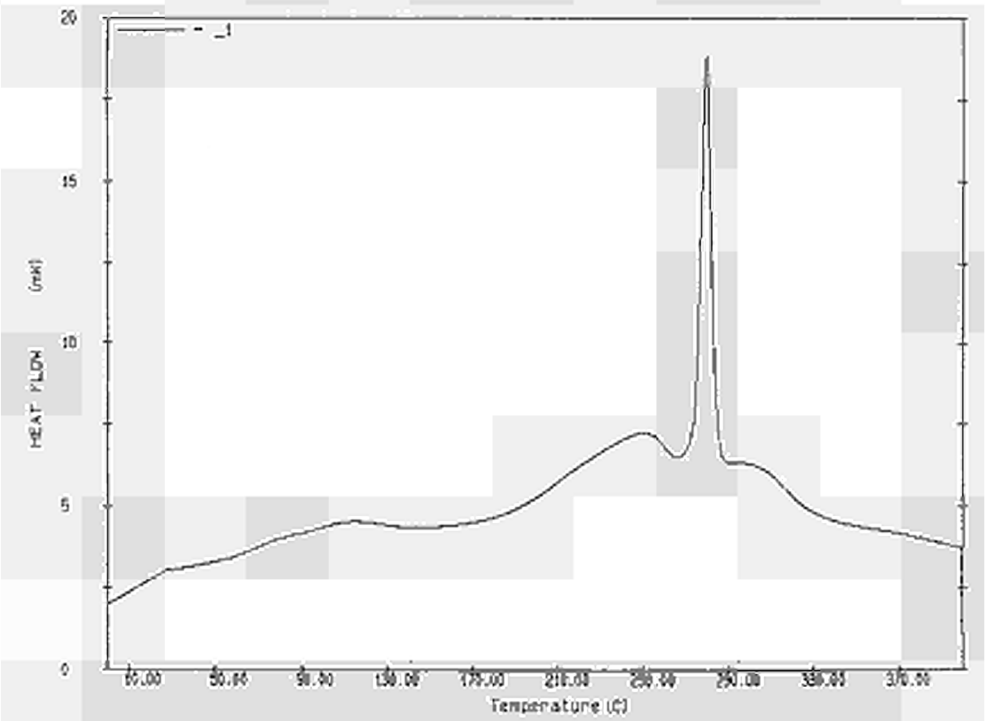

Fig. 3 : DSC curves, at 5 °C/min, of the Al-Zn-Si alloys 1 - 13 (n° indicated in upper left hand corner)

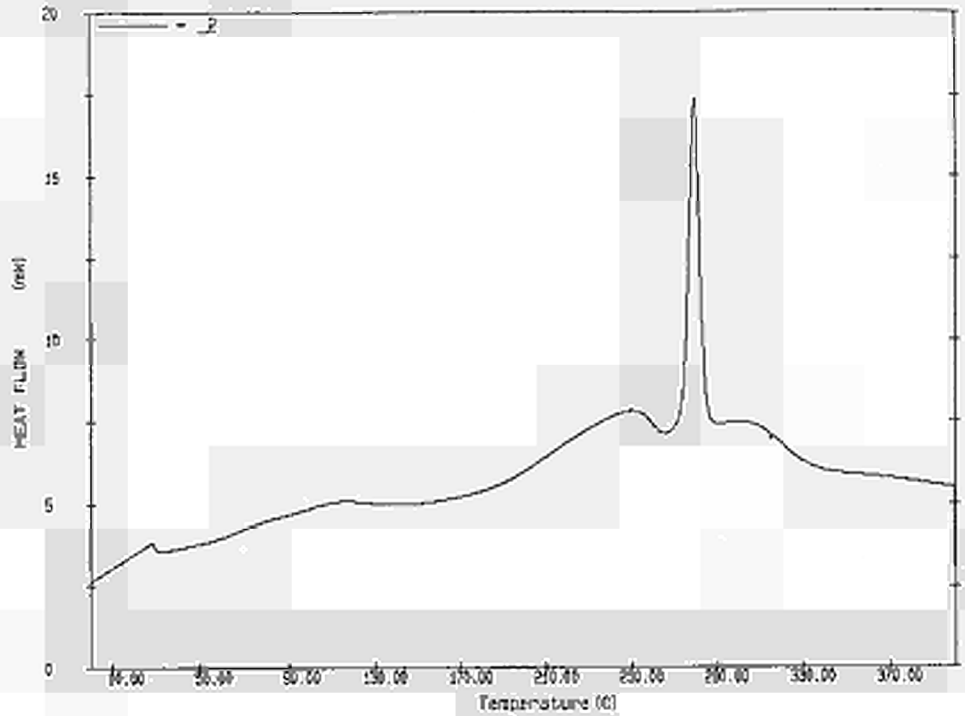
_2
20
15
10
5
0
HEAT FLOW (mW)
Temperature (C)

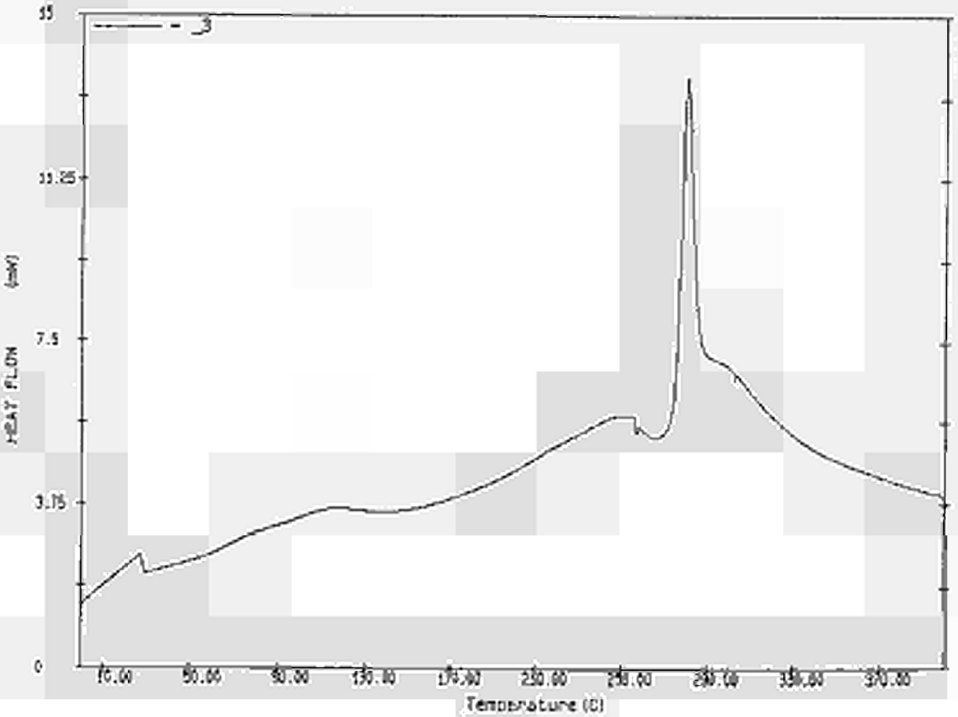
_3
11.25
7.5
3.75
0
HEAT FLOW (mW)
Temperature (C)

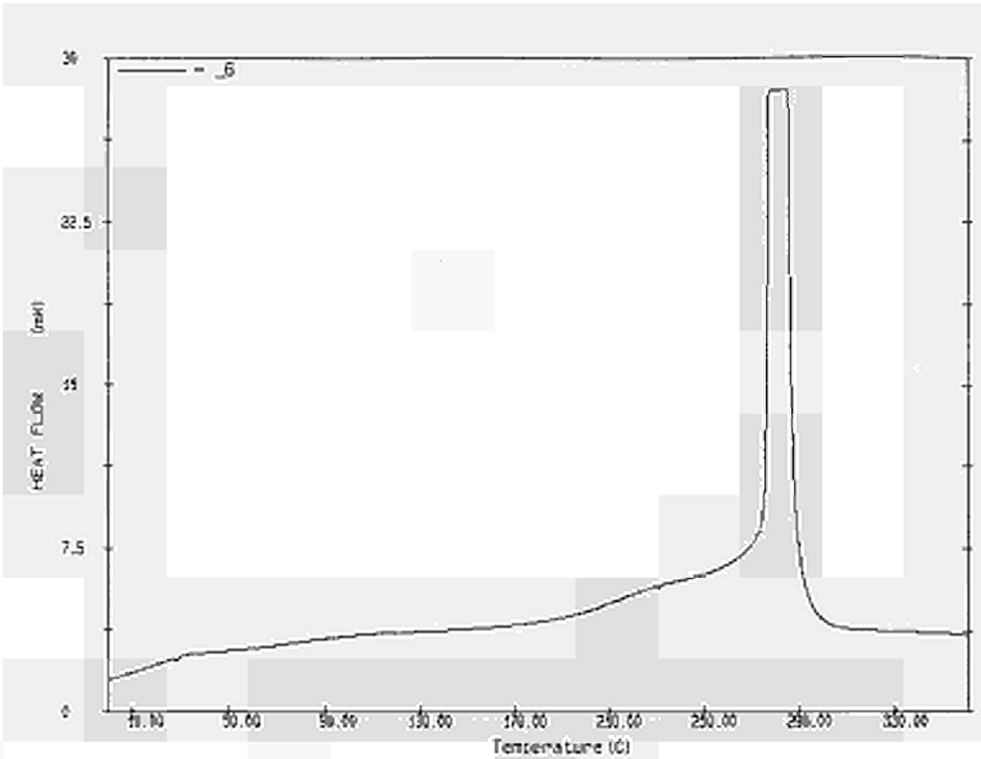
_6
30
22.5
15
7.5
0
HEAT FLOW (mW)
50.00
90.00
130.00
170.00
210.00
250.00
290.00
330.00
Temperature (C)

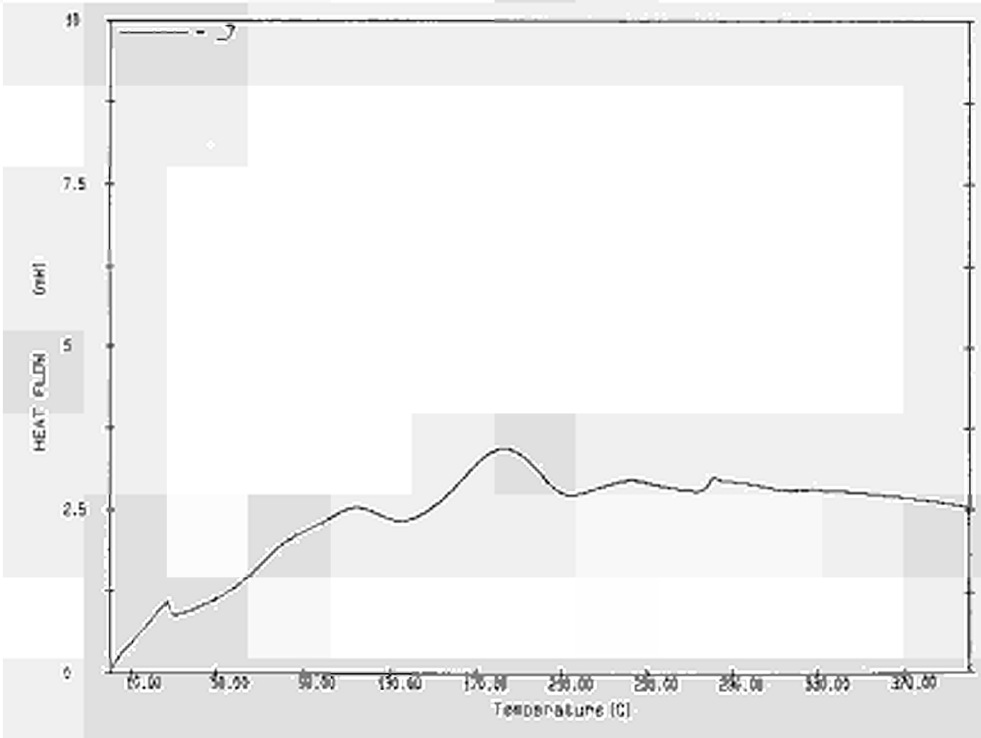
_7
10
7.5
5
2.5
0
HEAT FLOW (mW)
50.00
90.00
130.00
170.00
210.00
250.00
290.00
330.00
370.00
Temperature (C)

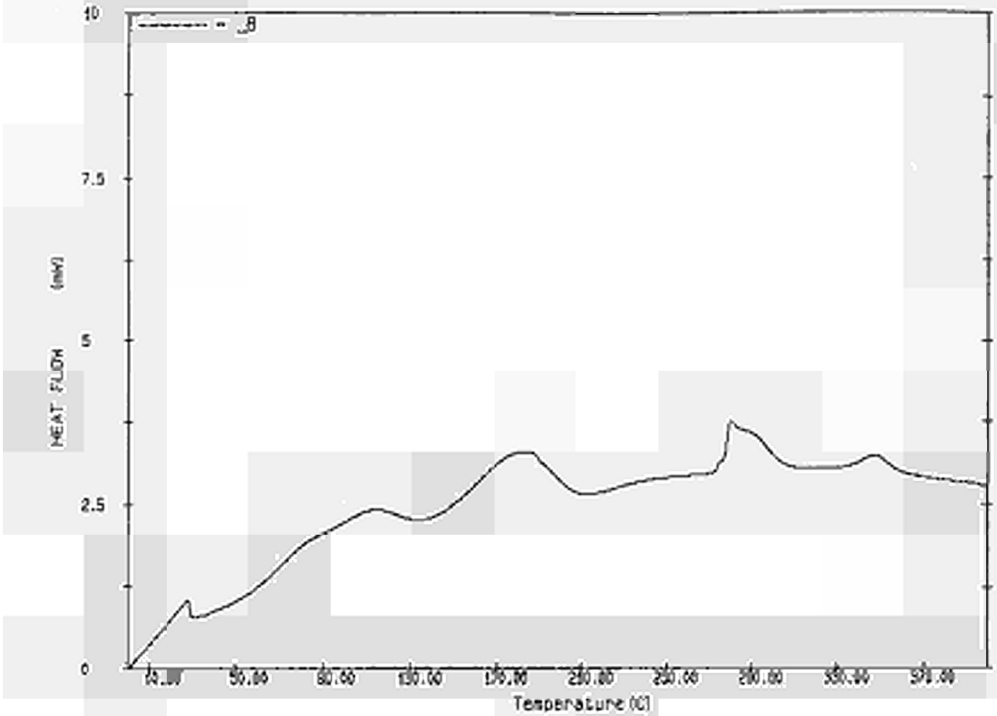
_8
10
7.5
5
2.5
0
HEAT FLOW (mW)
Temperature (C)

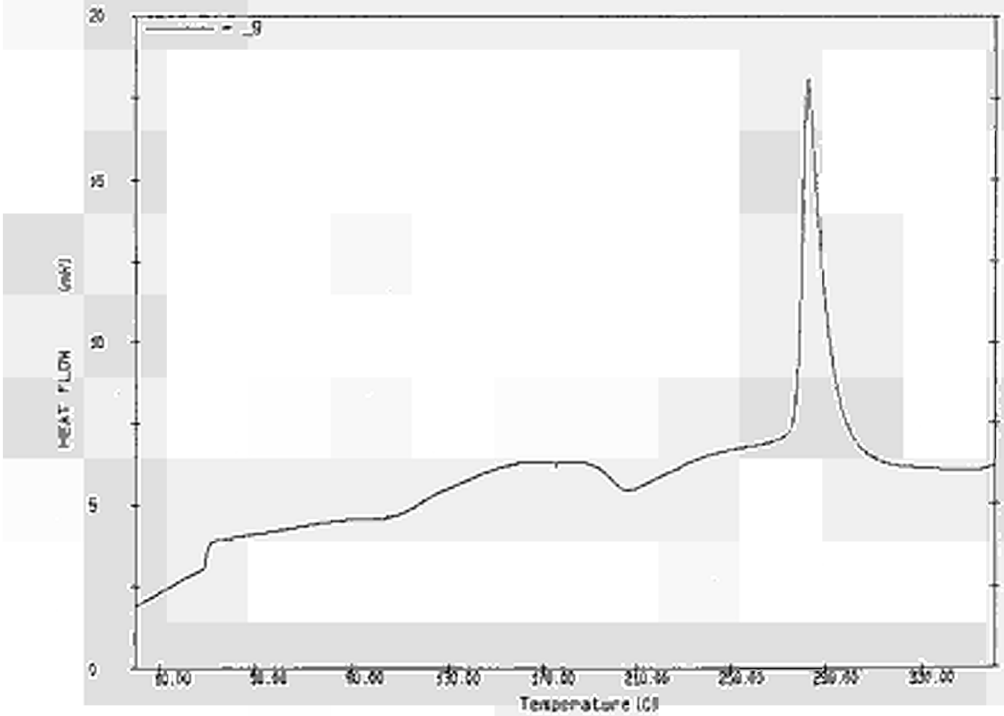
_9
20
15
10
5
0
HEAT FLOW (mW)
Temperature (C)

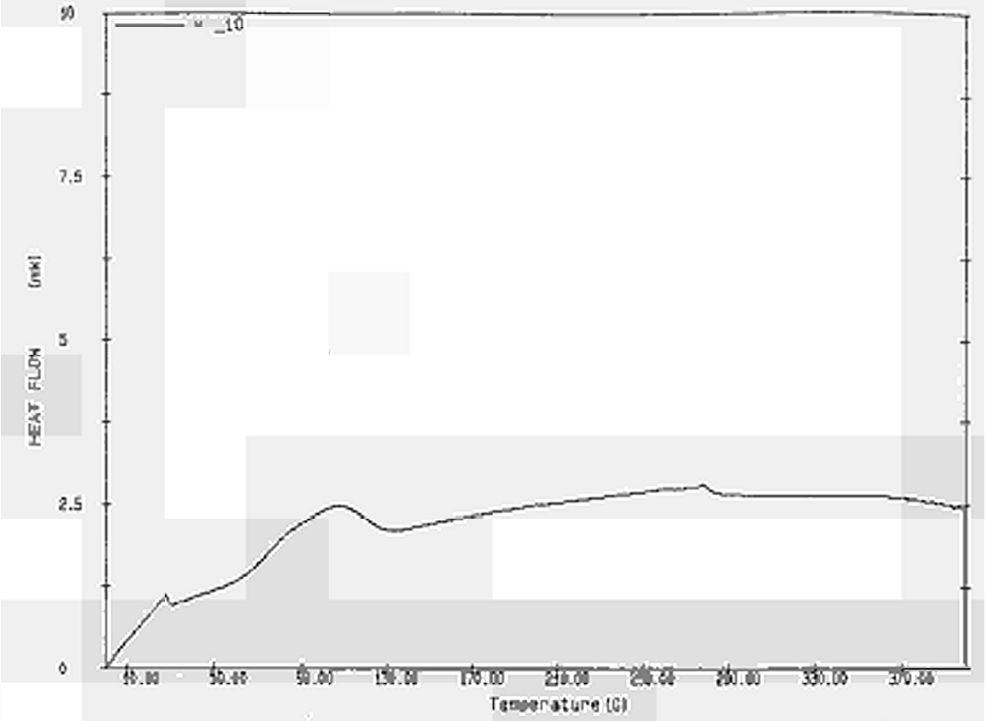
10
7.5
5
2.5
0
HEAT FLOW (mW)
Temperature (C)

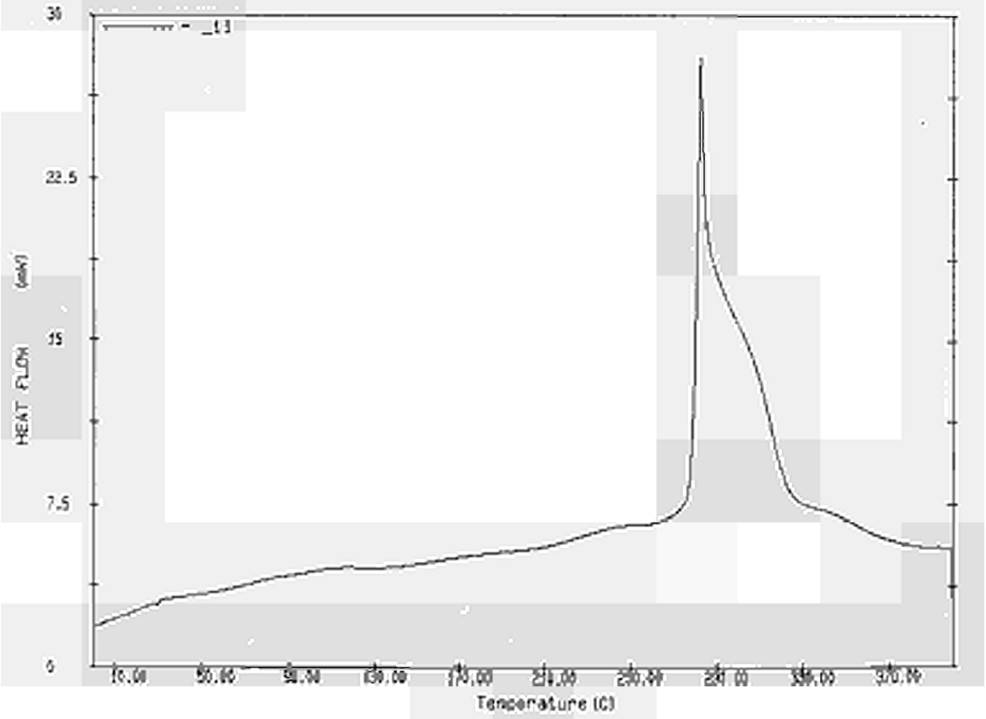
30
22.5
15
7.5
0
HEAT FLOW (mW)
Temperature (C)

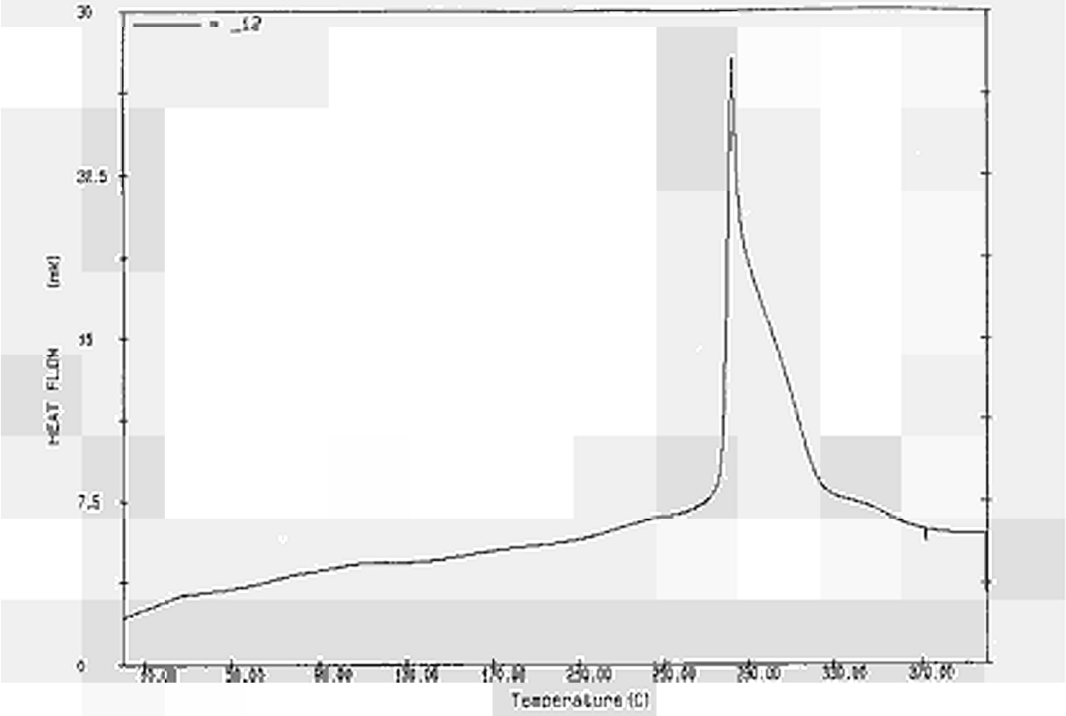
- _12
30
22.5
15
7.5
0
HEAT FLOW (mW)
Temperature (C)

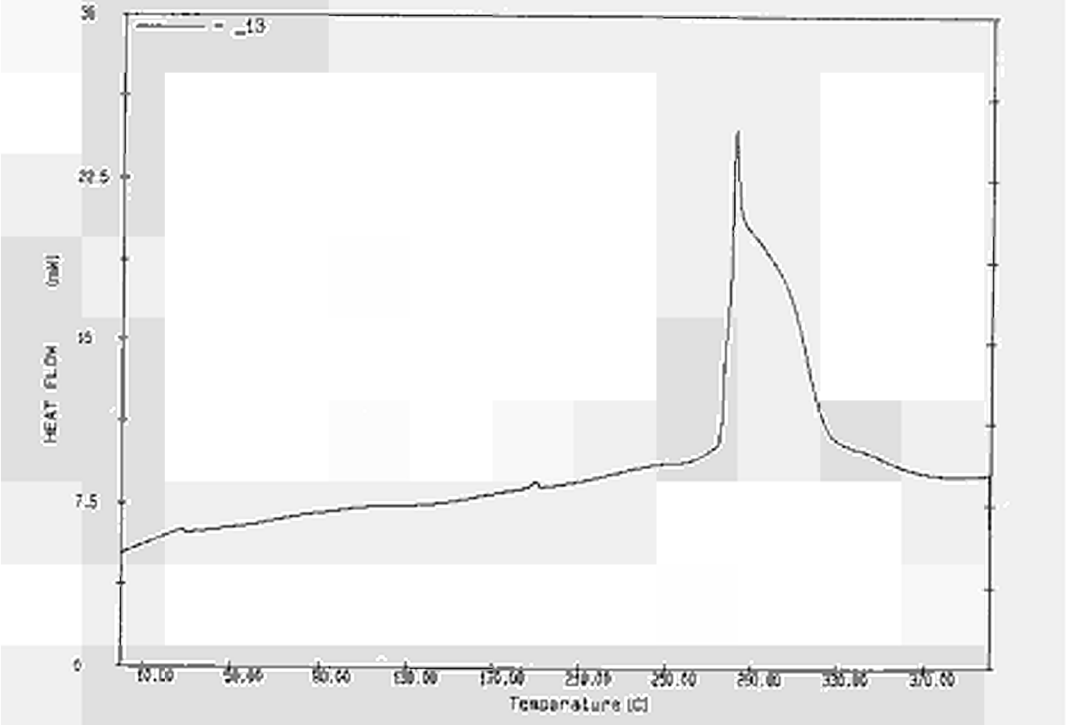
- _13
30
22.5
15
7.5
0
HEAT FLOW (mW)
Temperature (C)

Differential Scanning Calorimetry and Thermodynamic Calculations aimed at the Development of Al-Mg-Si Cast Alloys with Cu, Ag and Sm Additions

G. N. Haidemenopoulos and A. N. Vasilakos

Department of Mechanical and Industrial Engineering,
University of Thessaly, Volos, Greece

Abstract

This work has been performed within the framework of COST 507 Round II program on the Al-Mg-Si-Cu system (Leading system 2). DSC measurements have been performed on three alloys based on the conventional A357 composition with additions of Cu, Ag and Sm. For the three alloys, designated A357+Cu, A357+Cu+Ag, and A357+Cu+Sm, the solidification regimes as well as the transformation enthalpies for melting and solidification were determined. The results were compared with predictions of the thermochemical database and software system Thermo-Calc. Additional thermodynamic calculations included isopleth sections and Scheil solidification diagrams showing the development of microsegragation. Calculation of the precipitation driving forces for the strengthening phases Mg_2Si and Al_2Cu were conducted as a function of alloy composition and ageing temperature. These calculations established the recommended ageing temperatures of the alloys. Application of the modified ageing treatments (relative to the conventional A357 alloy) resulted in improved combinations of strength and ductility.

1. Introduction

Aluminum alloy A357, which is based on the Al-Mg-Si system, is widely used in precision casting applications. The effect of several alloying elements in A357 has been studied e.g. Be additions [89Bru, 83Nag, 84Gra], La additions [83Bac], as well as Na, Sr and Sb additions [88Oze, 86Mai, 89Ape]. It has been proposed [96Bri] that combined additions of Cu with Ag and Sm could lead to further enhancement in strength and ductility of precision cast alloy A357. The present work was conducted in the framework of COST 507 Round II program in order to investigate additions of Cu, Ag and Sm to the conventional alloy A357. Differential Scanning Calorimetry (DSC) was employed to determine the melting and solidification regimes as well as the enthalpies for melting and solidification. The results were then compared with the predictions of the thermochemical database and software program Thermo-Calc. Further calculations were targeted towards improving the ageing treatment of the alloys.

2. Experimental Procedures

Four alloys have been prepared for the present study. Alloy A357 used as reference, alloy A357 with Cu addition, designated as A357+Cu, alloy A357+Cu with Ag addition designated as A357+Cu+Ag and finally alloy A357+Cu with Sm addition designated as A357+Cu+Sm. The chemical compositions of the alloys are given in Table 1. Conventional precision casting of the four alloys was performed by ALPHA Spain in the form of bars with a length of 20 cm and with 2.3x2.3 cm^2 cross section. The bars received a solution heat treatment as follows :
A357 : 538° C/22h, water quench (<10° C),
A357+Cu, A357+Cu+Sm : 535° C/40h, water quench (<10° C),
A357+Cu+Ag : 525° C/40h, water quench (<10° C).

Table 1: *Chemical composition (in wt%) of the alloys used in the present study.*

Alloy	Si %	Fe %	Cu %	Mg %	Ni %	Zn %	Ti %	Ag %	Sm %	Al %
A357	6,42	0,036	0,021	0,60	0,007	0,008	0,160	-	-	92,74
A357+Cu	6,06	0,054	0,828	0,53	0,006	0,009	0,150	-	-	92,36
A357+Cu+Ag	6,40	0,070	1,142	0,77	0,009	0,018	0,145	0,7	-	91,44
A357+Cu+Sm	6,19	0,043	0,765	0,55	0,009	0,026	0,139	-	0,5	92,27

Artificial ageing has been performed in all four alloys. The temperature of artificial ageing was determined by computational thermodynamics (discussed below), while the time of artificial ageing was determined from hardness measurements (also discussed below).
Differential Scanning Calorimetry (DSC) was performed in the four alloys, in order to determine the melting and solidification regimes, as well as the enthalpies of fusion and solidification. These data were used to validate corresponding predictions of the computational thermodynamics program. The DSC used was a Rheometric Scientific. Specimens were pre-weighted (in the range of 3-4 mg) and heated from room temperature to 500° C with a rate of 20° C/min while from 500 to 700° C the heating rate was 1° C/min. After holding at 700° C for 5 min the specimens were cooled with rate 1° C/min.
Standard Brinell hardness measurements were performed as a function of time at the artificial ageing temperature. Tensile testing was performed on an INSTRON servo-hydraulic machine. Tensile specimens were prepared from the heat-treated bars according to DIN 50125.

3. Results and Discussion

3.1 DSC Results

Differential Scanning Calorimetry was carried out for the alloys. Characteristic DSC thermograms are shown in Fig.1 for alloy A357+Cu ,for alloy A357+Cu+Ag and for alloy A357+Cu+Sm with the characteristic temperatures shown in Fig.2. The DSC data are summarized in Table 2 and compared with the Thermo-Calc prediction for T_{start} and T_{end} temperatures. It can be seen that the agreement between experimental and calculated values is good for A357+Cu and becomes even better for A357+Cu+Ag and A357+Cu+Sm.

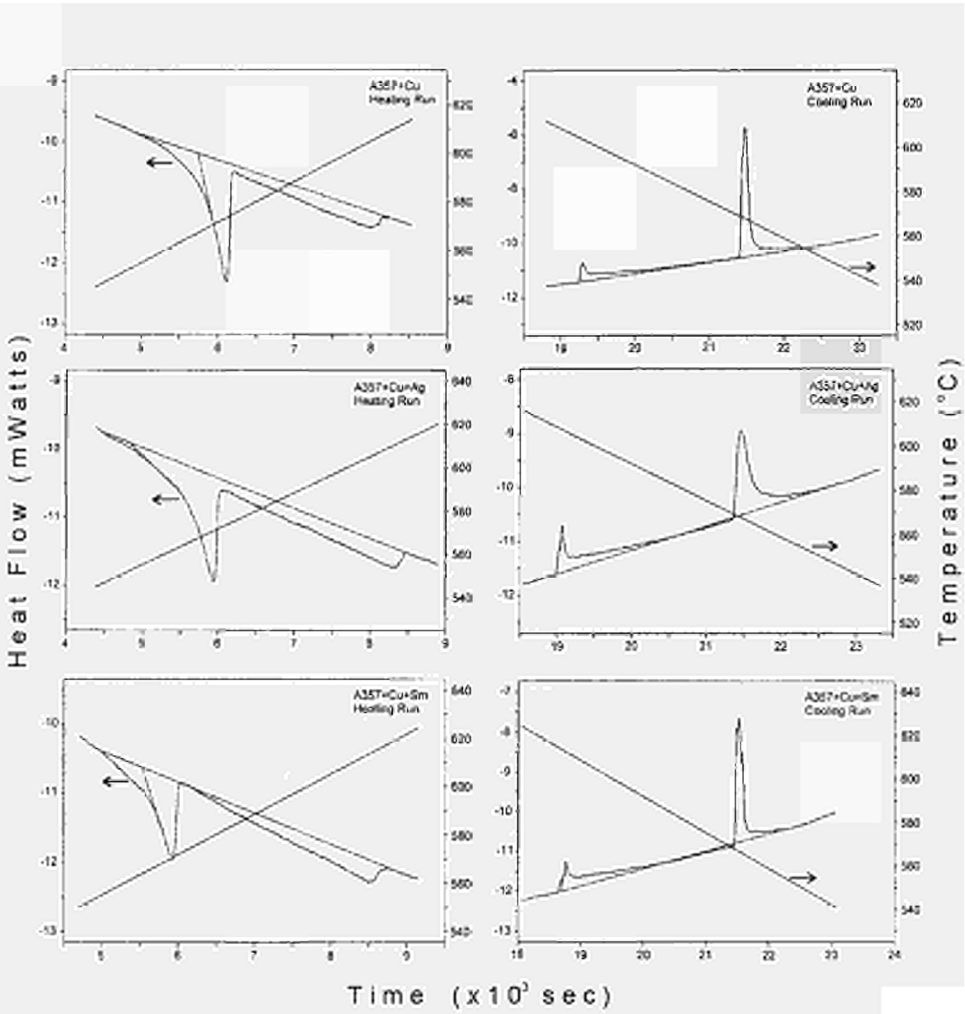

Fig. 1: *DSC Thermograms of alloys A357+Cu, A357+Cu+Ag, A357+Cu+Sm.*

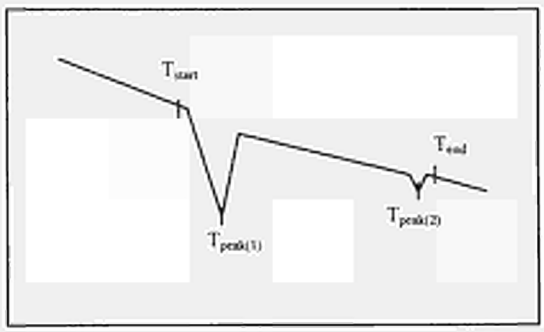

Fig. 2: *Schematic drawing of DSC run showing the determination of characteristic temperature of 'twin peak' during melting and solidification.*

Table 2: Results of the DSC measurements and comparison with corresponding Thermo-Calc (T.C.) predictions.

		A357 + Cu		A357 + Cu + Ag		A357 + Cu + Sm	
		DSC	T.C.	DSC	T.C.	DSC	T.C.
Heating run	T_{start} [°C]	562.83		557		558.42	
	$T_{peak(1)}$ [°C]	573.24		570.39		570.02	
	$T_{peak(2)}$ [°C]	605.52		610.88		614.03	
	T_{end} [°C]	609.06	619.2	613.2	616.4	615.93	619.9
	ΔH_f [mJ/mg]	277.67		294.21		218.35	
Cooling run	T_{start} [°C]	604.62	619.2	610.08	616.4	614.74	619.9
	$T_{peak(1)}$ [°C]	603.63		607.3		612.29	
	$T_{peak(2)}$ [°C]	567.52		567.44		566.39	
	T_{end} [°C]	561.83		557.63		558.94	
	ΔH_s [mJ/mg]	-224.19		-138.19		-164.96	

3.2 Thermodynamic Analysis

Computational thermodynamics was performed with the Thermo-Calc software package [85Sun] and the recently developed COST 507 database for light alloys [94Cos]. The isopleth section (with varying Si content) for alloy A357+Cu+Sm is shown in Fig.3. Sm precipitates as the rhombohedral phase below 250° C. An important feature of this diagram is that addition of Sm lowers the liquidus temperature to 420° C compared to 540-560° C in the alloys without Sm.

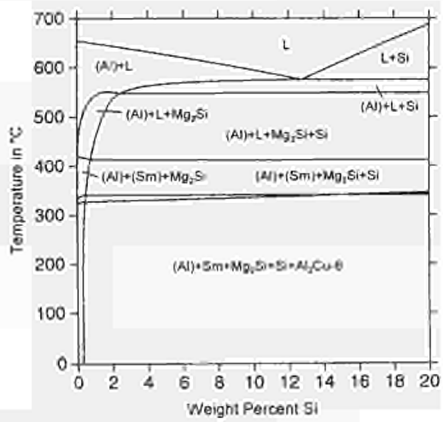

Fig. 3: Isopleth section for A357+Cu+Sm alloy.

Scheil solidification diagrams have been constructed, with the assumptions that no diffusion is taking place in the solid and that local equilibrium exists at the solid / liquid interface during solidification. Fig. 4 depicts the fraction of liquid phase as a function of temperature during solidification for the four alloys investigated. The kinks in the curves are due to the formation of solid phases ((Al), Si, Mg_2Si, θ) during solidification. From these diagrams, the temperature range for solidification can be determined. This range is of the order of 70° C for all alloys. Fig. 5 depicts the content of the remaining liquid phase during

solidification. It can be seen that Si content rises in the liquid as solidification proceeds. With the assumption of limited diffusion in the solid, this diagram then depicts the resulting microsegregation.

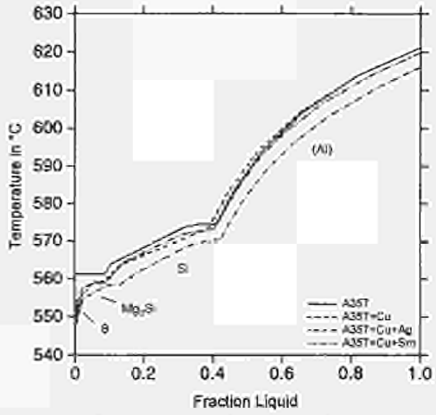

Fig. 4: Scheil solidification diagram depicting the fraction of liquid phase as a function of temperature during solidification.

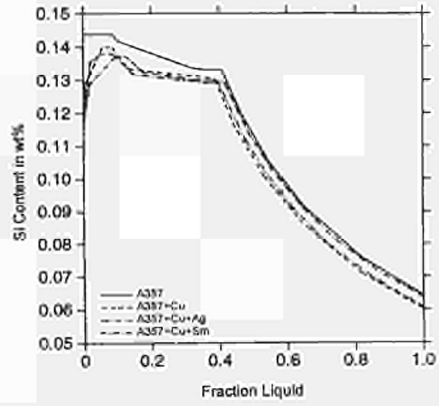

Fig. 5: Scheil solidification diagram depicting the Si content in the liquid phase as a function of fraction of liquid phase during solidification.

3.3 Determination of Ageing Temperature and Time

The temperature of artificial ageing was determined by considering the driving force for precipitation of the strengthening phases Mg_2Si and θ during ageing. The driving force ΔG (in J/mole) was calculated with Thermo-Calc. Results are shown in Fig. 6 for the precipitation driving force of Mg_2Si and θ as a function of Cu content in A357+Cu for two ageing temperatures 155 and 170° C. It can be seen that ΔG is higher for the lower ageing temperature and that increasing the Cu content has the effect of increasing the driving force for precipitation of θ-phase while decreasing the driving force for precipitation of Mg_2Si.

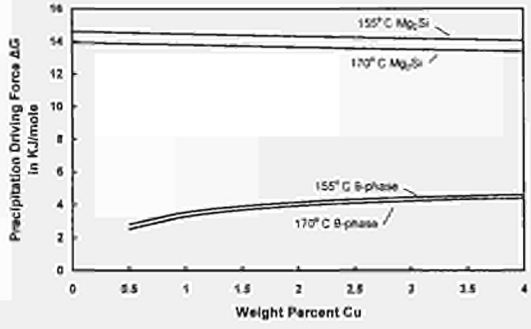

Fig. 6: Driving force for precipitation of Mg_2Si and θ (Al_2Cu) phases as a function of temperature and Cu content in A357+Cu alloy.

Thermodynamic calculations have also shown that the driving force ΔG is not affected by Ag or Sm. For supersaturated metastable solutions, the finer precipitate size scales with the initial nucleus size which in turn depends on the magnitude of ΔG. The higher the driving force for precipitation, the finer the dispersion and the higher the strength. For this purpose the ageing temperature was selected to be 155° C, in contrast to 170° C conventionally used in the A357 alloy.
The time of artificial ageing was determined from hardness measurements as a function of time at 155° C. Peak hardness is obtained at 25h for A357+Cu and A357+Cu+Ag, and at 20h for A357+Cu+Sm. Artificial ageing was then performed at 155° C for the times discussed just above.

3.4 Mechanical Properties

The results of the tensile testing of the heat-treated alloys are summarized in Fig. 7. The elongation values are lower than expected, however they are comparable since identical casting conditions were used in all alloys. The three alloys with Cu, Ag and Sm additions possess better combinations of strength and ductility than the reference conventional A357 alloy. Since all alloys have been casted in the same way it can be deduced that the improvement in mechanical properties is due to the alloying elements and the artificial ageing followed. In comparison to the reference A357 alloy, the alloys containing Cu posses higher strength and ductility due to the formation of fine dispersion of θ-phase. In addition the lower temperature ageing treatment (higher ΔG) produces also a finer dispersion of Mg_2Si precipitate.
Silver on the other hand enters the (Al) solid solution providing solid solution strengthening, while Sm forms fine particles of the rhombohedral phase.
Due to the fact that the strengthening dispersions are very fine, both strength and ductility in these alloys increase.

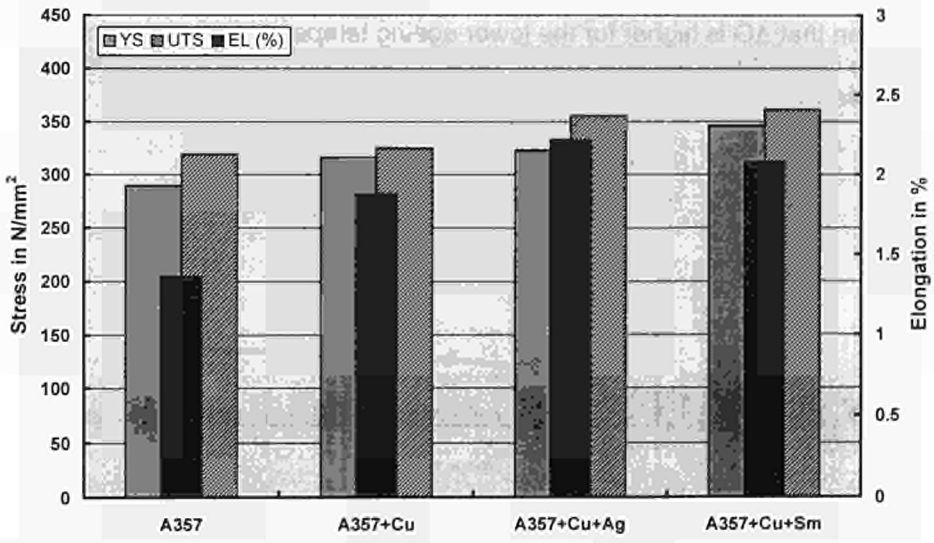

Fig. 7: Yield strength, ultimate tensile strength and elongation for alloys A357 (reference), A357+Cu, A357+Cu+Ag and A357+Cu+Sm.

4. Conclusions

Differential scanning calorimetry was conducted for alloys of the system Al-Mg-Si with additions of Cu, Ag and Sm in order to determine the melting and solidification regimes as well as melting and solidification enthalpies. The experimental results are in good agreement with Thermo-Calc predictions. Thermo-Calc was then used to calculate the precipitation driving forces for Al_2Cu and Mg_2Si as a function of temperature and composition. It was found that a lower ageing temperature provides a higher precipitation driving force. Mechanical testing of the alloys investigated really showed that the modified alloys exhibited enhanced strength/ductility combinations than the conventional A357 alloy.

5. References

83Bac Fr. -W. Bach, H. Haferkamp, B. Li, METTAL 37, (1983),Heft 12, p.1202.

83Nag G. E. Nagel, J. P. Mouret, J. Dubruelh: "A357 Type Alloy with Improved Properties", AFS Transactions Vol. 91 Rosemont, Illinois, USA, (1983).

84Gra D. A. Granger, R. R. Sawtell, M. M. Kersker: "Effect of Beryllium On the Properties of A357.0 Castings", AFS Transactions Vol. 92, St. Louis, Missouri, USA, (1984).

85Sun B. Sundman, B. Jansson, J-O. Anderson, CALPHAD, 9, (1985), p. 153.

86Mai E. Maier, G. Lang, ALUMINIUM, 62 (1986), Heft 3, p. 193.

88Oze M. W. Ozelten, G. R. Turk, P. G. Porter: "Relationships Between Mechanical Properties, Composition and Microstructure of the Aluminum Casting Alloy A357-T6", TMS Proc. on Technology for Premium Quality Castings, (1988), p. 81.

89Ape D. Apelian, S. Shivkumar, G. Sigworth, AFS Transactions Vol. 97, San Antonio, Texas, USA, (1989), p. 727.

89Bru Ernst Brunhuber, AFS Transactions Vol. 97, San Antonio, Texas, USA, (1989), p. 21.

96Bri Brite-Euram Project BE4084, "Advanced Aluminum Precision Casting for Integrally Stiffened Net Shape Components", Final Report, CEC, Brussels, 1996.

94Cos COST 507 Database for Light Alloys, Round I, COST 507 Program, CEC, Brussels, (1994).

Acknowledgment

This work has been performed within the framework of COST 507 program and was partially supported by the Research Committee of the University of Thessaly. This support is greatly appreciated.

COST 507 - II

Project group: Italy 1

Project title

Thermodynamic Optimization and Evaluation of Phase Equilibria in Rare Earth Alloys

R. Ferro, G. Borzone, A. Saccone, G. Cacciamani, S. Delfino, M. Giovannini, D. Macciò, N. Parodi

Dipartimento di Chimica e Chimica Industriale
Sezione di Chimica Inorganica e Metallurgia
via Dodecaneso, 31, I- 16146 Genova, Italy

The Italian team is involved in activity concerning both the coordination groups A and C, as summarised in the first and second part of the following text.

COST 507 - ROUND II

UNIT I1
SEZIONE DI CHIMICA GENERALE, INORGANICA E METALLURGIA
(former Istituto di Chimica Generale)
OF THE DIPARTIMENTO DI CHIMICA E CHIMICA INDUSTRIALE
UNIVERSITA' DI GENOVA, ITALY

1996 REPORT

1st PART: ACTIVITY CARRIED OUT WITHIN THE FRAMEWORK OF THE COORDINATION GROUP A

EXPERIMENTAL INVESTIGATIONS ON BINARY AND TERNARY RARE EARTH ALLOYS (WITH Mg or Al)

Summary

Experimental investigation of binary and ternary Aluminium (or Magnesium) alloys with the rare earth metals has been carried out. The investigation lines concerned:
Phase equilibria determination, Thermodynamic measurements (formation enthalpy and heat capacity) In cooperation, mainly with other units, structural and magnetic properties were also studied.
The different systems considered are the following:

-Aluminium Systems

Binary Systems:

Phase equilibria investigation in the rare earth-rich regions of R-Al systems.
Measurements of formation enthalpy of La-Al and Yb-Al alloys.
Measurements of molar heat capacity of R-Al alloys (R=La, Ce, Pr, Nd).

Ternary Systems:

Enthalpies of formation and phase equilibria in selected regions of Ce-Al-Ni and Y-Al-Ni systems.

-Magnesium Systems

Binary Systems:

Thermochemical investigation of selected Ce-Mg, Nd-Mg, Sm-Mg alloys.
Ternary Systems:
Structural, magnetic properties in the Ce-Mg-Y system.

Introduction

The project of our unit concerns the study of "Thermodynamics and phase equilibria in the system Al-Mg-Cu-Zn-R-(Ni, Mn) with R=rare earth. Effects of rare earth additions to Al-based or Mg-based alloys).

Within the coordination group A, work is being carried out on phase equilibria determination and thermochemical measurements of specific rare earth containing subsystems. On the same systems work is also in progress in the framework of coordination group C (see the corresponding report).

In the following a summary is reported of the results obtained in the investigation of Al and Mg alloys.

Aluminium Alloys

[96Bor1] The standard molar enthalpies of formation for the different solid La-Al and Yb-Al alloys have been measured by means of direct calorimetry. The composition and equilibrium state of samples were checked by micrographic and X-ray diffraction techniques. The following values have been obtained (kJ/mol of atoms): LaAl, $\Delta_{form}H°$= -46.0±2; $LaAl_2$, $\Delta_{form}H°$= -50.5.0±2; $LaAl_3$, $\Delta_{form}H°$= -44.0±2; La_3Al_{11}, $\Delta_{form}H°$= -41.0±2; $YbAl_2$, $\Delta_{form}H°$= -39.5.0±2; $YbAl_3$, $\Delta_{form}H°$= -32.5.0±2. Experimental results are discussed and compared with literature data.

[96Bor2] Several applications of selected R-Al-M (R=rare earth metals, M=transition metal) alloys for their typical characteristics such as magnetic properties have been discussed in order to gain information on stable and metastable phases of these systems. A systematic study on the reactivity of the R-Al and R-Al-Ni alloys has been started. To this end calorimetric techniques, X-ray diffraction and microscopy analyses are used. The results so far obtained for selected Ce-Ni and Ce-Al-Ni alloy compositions have been illustrated and discussed.

[96Bor3] The results obtained for Ce-Al-Ni system have been presented. The thermochemical investigation was performed with an isoperibol aneroid calorimeter. The ternary phases were synthetised directly in the calorimeter, starting from a mixture of the finely powdered components enclosed in a gas-tigth inox crucible sealed by electric welding. Metallographic analysis, electron probe microanalysis (EPMA), X-ray diffraction analysis (powder diffraction) were used to characterised all samples, to ascertain the absence of unreacted metals and to assess their equilibrium state. The data so far obtained for characteristics sections have been reported, discussed and compared with those relevant to the involved binary alloys.

[96Gam] The R-rich regions of the [Rare Earth + Al] systems (with R=La, Ce, Pr, Nd) have been recently reinvestigated by using the differential thermal analysis techniques and the melting behaviour of the (R+Al) alloys with a particular attention to the thermodynamic properties has been undertaken. In this paper the first results of the measurements of the molar heat capacity (Cp°) of some [La+Al], [Ce+Al], [Pr+Al] and [Nd+Al] alloys are presented and discussed.

[96Sac] The R-rich regions of the R-Al systems (R=La, Ce, Pr, Nd) have been studied by using thermal analysis (DTA), metallographic analysis, quantitative electron probe microanalysis (EPMA) and X-ray examinations (XRD). The coordinates of the R-rich eutectics, the lowering of the allotropic transformation temperatures of the rare earth metals by additions of Al and melting behaviours of the R-rich compounds have been particularly investigated. The terminal aluminium solubilities in the different rare earth metals and the relative stabilities of the catatectic and eutectoid equilibria have been discussed.

Magnesium Alloys

[96Cac] A systematic study of the enthalpy of formation of binary R-Mg alloy considering, to begin with, the systems formed with La, Ce, Pr, Nd, Sm and Yb, have been started. These systems were investigated by high temperature direct reaction drop calorimetry by using an instrument built in our laboratory and previously described. Other experimental methods employed in this research were X-ray diffractometry, optical and electron microscopy. Preliminary results concerning the enthalpy of formation of some alloys at the compositions RMg, RMg_2 and RMg_3 in the mentioned systems have been presented and discussed.

[96Fla] The structural and magnetic properties of a series of novel compounds in the ternary Ce-Mg-Y system have been studied by X-ray diffraction, SQUID magnetometry and XAS spectroscopy. The crystal structures of the compounds $Ce_{0.33}Y_{0.67}Mg_2$ and $Ce_{0.49}Y_{0.51}Mg_{4.7}$ have been refined by the Rietveld technique. Magnetic data are consistent with a tripositive ground state $^2F_{5/2}$ for the cerium atom. The XAS measurements confirm this result. Crystal field effects are apparent in the magnetic data at temperatures below about 50 K in the compounds with higher Ce concentration.

Publications of the 3rd year
(Coordination Group A)

[96Bor1] G.Borzone, A.M.Cardinale, N.Parodi, G.Cacciamani, "Aluminium Compounds of the Rare Earths: Enthalpies of Formation of Yb-Al and La-Al Alloys" J.Alloys and Compounds (1996), in press.

[96Bor2] G.Borzone, N.Parodi, R.Ferro "Recent Advance in the Thermochemical Investigation of Selected R-Al-Ni (R=rare Earth Metals) Alloys" Hume-Rothery Symposium of the Minerals, Metals and Materials Society (TSM) on "Thermodynamic of Alloy Formation", Feb. 9-13, (1997), Orlando (FLA), USA.

[96Fla] H.Flandorfer, A.Kostikas, P.Rogl, C.Godart, M.Giovannini, A.Saccone, R.Ferro, "On the Magnetic and Valence Properties of Ce-Mg-Y Compounds", J.Alloys and Compounds, 240 (1996) 116-123.

[96Sac] A.Saccone, A.M.Cardinale, S.Delfino R. Ferro, "Phase Equilibria in the Rare Earth (R) Rich Regions of the R-Al Systems (R = La, Ce, Pr, Nd)", Z. Metallkde, 87 (1996) 82-87.

[96Bor3] G.Borzone, N.Parodi, A.M.Cardinale, R.Ferro,"On Ternary Al-Ni-Ce Alloys Enthalpies of Formation",
Proc. Thermodynamics of Alloys, Marseille (France) Sept. 2-5 (1996).

[96Cac] G.Cacciamani, G.Borzone, R.Ferro
"Thermochemical Investigation of Rare Earth-Magnesium Alloy Systems"
Proc. Thermodynamics of Alloys, Marseille (France) Sept. 2-5 (1996).

[96Gam] M.Gambino, J.P.Bros, G.Borzone, N.Parodi, R.Ferro, "Contribution a l'Etude Thermodynamique des Systèmes Binaires [Terre Rare + Aluminium] Capacités Calorifiques Molaires dans la Region Riche en Terre Rare" Proc. XXIIèmes J.E.E.P., Journées d'Etude des Equilibres entre Phases, La Garde (France) Apr. 15-16 (1996), p.16.

List of publications in the framework of COST 507 Round I and II up to 1996

(Coordination Group A)

1-Articles in Scientific Journals

A.Saccone, S.Delfino, D.Macciò, R.Ferro
"A Contribution to the Magnesium Intermetallic Chemistry: Dysprosium-Magnesium System"
Z.Metallkde., 82 (1991) 568-573.

G.Borzone, G.Cacciamani, R.Ferro
"Heats of Formation of Aluminium-Cerium Intermetallic Compounds"
Met. Trans. 22A (1991) 2119-2123.

A.Saccone, S.Delfino, D.Macciò, R.Ferro
"Magnesium-Rare Earth Phase Diagrams: Experimental Investigation of the Ho-Mg System"
J.Phase Equilibria, 14 (1993) 280-287.

A.Saccone, A.M.Cardinale, S.Delfino, R.Ferro
"A Contribution to the Rare Earth Intermetallic Chemistry: Praseodymium-Magnesium Alloy System"
Intermetallics, 1 (1993) 151-158.

A.Saccone, S.Delfino, D.Macciò, R.Ferro
"Experimental Investigation of the Tb-Mg Phase Diagram"
J.Phase Equilibria, 14 (1993) 485-493.

G.Borzone, A.M.Cardinale, G.Cacciamani, R.Ferro
"On the Thermochemistry of the Nd-Al Alloys"
Z.Metallkde., 84 (1993) 635-640.

M.Giovannini, R.Marazza, A.Saccone, R.Ferro
"Isothermal Section from 50 to 75 at% Mg of the Ternary System Y-La-Mg",
J.Alloys Compounds, 201 (1994) 177-180

R.Ferro, G.Borzone, N.Parodi, G.Cacciamani
"On the Thermochemistry of the Rare earth compounds with the p-Block elements",
J.Phase Equilibria, 15 (1994) 317-329.

M.Giovannini, A.Saccone, R.Marazza, R.Ferro
"The Isothermal Section at 500°C of the Y-La-Mg Ternary System",
Met. Trans. A 26A (1995) 5-10

G.Borzone, A.M.Cardinale, A.Saccone, R.Ferro

"Enthalpies of Formation of Solid Sm-Al Alloys",
J.Alloys Compounds, 220 (1995) 122-125

A.Saccone, D.Macciò, S.Delfino, R.Ferro,
"The Interpolated Tm-Mg Phase Diagram",
J.Alloys Compounds, 220 (1995) 161-166.

M.Giovannini, A.Saccone , R.Ferro
"Phase Relationships at 500°C in the Y-Pr-Mg System",
J.Alloys and Compounds 220 (1995) 167-173.

M.Giovannini, A.Saccone, R.Ferro, P.Rogl, H.Flandorfer, G.Effenberg
"A Contribution to the Investigation of the Relationships in the Mg-Mn-Y System"
in "Syntheses and Methodologies in Inorganic Chemistry - New Compounds and Materials", Daolio, S. Tondello, E. and Vigato, P.A., Eds., La Photograph, Padova (Italy), Vol. 5, (1995) 538-542.

A.Saccone, A.M.Cardinale, S.Delfino R. Ferro,
"Phase Equilibria in the Rare Earth (R) Rich Regions of the R-Al Systems (R = La, Ce, Pr, Nd),
Z. Metallkde, 87 (1996) 82-87.

G.Borzone, A.M.Cardinale, N.Parodi, G.Cacciamani
"Aluminium Compounds of the Rare Earths: Enthalpies of Formation of Yb-Al and La-Al Alloys
J. Alloys and Compounds 247 (1997) 141-147.in press.

H.Flandorfer, A.Kostikas, P.Rogl, C.Godart, M.Giovannini, A.Saccone, R.Ferro
"On the Magnetic and Valence Properties of Ce-Mg-Y Compounds"
J.Alloys and Compounds, 240 (1996) 116-123.

G.Borzone, N.Parodi, R.Ferro
"Recent Advance in the Thermochemical Investigation of Selected R-Al-Ni (R=rare Earth Metals) Alloys"
Hume-Rothery Symposium of the Minerals, Metals and Materials Society (TSM) on "Thermodynamic of Alloy Formation", Feb. 9-13, (1997), Orlando (FLA), USA.

R.Marazza, G.Zanicchi, D.Mazzone, V.Contardi
"On Ternary Alloys R-R'-Al of Aluminium with Rare Earths"
Proc. CISCI 1990, S.Benedetto del Tronto (Italy) 30/9-5/10/1990, p.518.

A.Saccone, S.Delfino, D.Macciò
"Rare Earth-Rich Alloys in Rare Earth-Magnesium Systems"
Proc. CISCI 1991 Chianciano (Italy) 6-11/10/1991, p.112-113.

A.Saccone, J.J.Suñol, D.Macciò, R.Ferro
"Sm-Rich Alloys in the Sm-Al System"
Proc. JANUACHEM 92, 25-30/10/1992, p.1015.

G.Zanicchi, P.Riani, D.Mazzone, R.Marazza
"On Ternary Alloys $La_{1-x}Yb_xAl_x$ and $Y_{1-x}Yb_xAl_3$"
Proc. XXII Congr. Nazl. Chimica Inorganica, Villasimius (Italy) 26/9-1/10 (1993), p.443-444.

A.M.Cardinale, A.Saccone, S.Delfino
"Investigation of Rare Earth Rich Alloys in R-Al systems"
Proc. XXIII Congr. Nazl. Chimica Inorganica, Bressanone (Italy), 2-7/10/1994, p.228.

R.Raggio, G.Borzone , R.Ferro,
"On the Phase Equilibria in the Al-Rich Region of the Y-Ni-Al System",
Proc. 8th International Conference on High Temperature Materials Chemistry, April 4-9 1994, Vienna , Austria.

G.Borzone, A.M.Cardinale, N.Parodi, R.Ferro
"Thermodynamics Properties of Intermetallic Compounds of Binary R-Al and Ternary R-Al-Ni Alloys" (in italian)
Proc. "II Convegno Scientifico del Consorzio Interuniversitario Nazionale per la Chimica dei Materiali" Firenze (Italy) Feb. 13-15 (1995), B23.

M.Giovannini, A.Saccone, R.Ferro
"Phase Equilibria in the Y-Gd-Mg Ternary System",
Proc. G.Med CAT'95, XVII Conference AICAT-GICAT, VI Meeting GECAT, Chia Laguna-Domus de Maria (Cagliari) (Italy) Sept.12-16 (1995), p.153-154.

M.Giovannini, A.Saccone, R.Ferro
"Mg-Ternary Systems: Structural Variations in Compounds by Rare Earth Substitution" (in italian)
Proc. "II Convegno Scientifico del Consorzio Interuniversitario Nazionale per la Chimica dei Materiali" Firenze (Italy) Feb. 13-15 (1995), B34.

A.Saccone, A.M.Cardinale, D.Macciò, R.Ferro
"Aluminium-Rare earth Binary Systems: the Al-Dy System" (in italian)

Proc. "II Convegno Scientifico del Consorzio Interuniversitario Nazionale per la Chimica dei Materiali" Firenze (Italy) Feb.13-15 (1995), B33.

M.Gambino, J.P.Bros, G.Borzone, N.Parodi, R.Ferro
"Contribution a l'Etude Thermodynamique des Systèmes Binaires [Terre Rare + Aluminium] Capacités Calorifiques Molaires dans la Region Riche en Terre Rare"
Proc. XXIIèmes J.E.E.P., Journées d'Etude des Equilibres entre Phases, La Garde (France) Apr. 15-16 (1996), p.16.

G.Borzone, N.Parodi, A.M.Cardinale, R.Ferro
"On Ternary Al-Ni-Ce Alloys Enthalpies of Formation"
Proc. Thermodynamics of Alloys, Marseille (France) Sept. 2-5 (1996)

G.Cacciamani, G.Borzone, R.Ferro
"Thermochemical Investigation of Rare Earth-Magnesium Alloy Systems"
Proc. Thermodynamics of Alloys, Marseille (France) Sept. 2-5 (1996)

1996 REPORT

2st PART: ACTIVITY CARRIED OUT WITHIN THE FRAMEWORK OF THE COORDINATION GROUP C

THERMODYNAMIC OPTIMIZATION AND EVALUATION OF PHASE EQUILIBRIA IN RARE EARTH ALLOYS

Summary

Assessment and optimization have been carried out on some selected alloys of Magnesium and Aluminium with the rare earth metals (R). This work has been performed in close relationship with the experimental work (phase diagram study, thermodynamic measurements) being carried out at the same time and reported in a summary for group A.

-Aluminium Systems.

Revision of the phase equilibria and thermodynamic data has been carried out for the binary R-Al systems.

-Magnesium Systems

General properties of magnesium alloys with two different rare earth metals have been analysed, discussed and used to predict phase equilibria. The systems La-Y-Mg, Ce-Y-Mg, Pr-Y-Mg and Gd-Y-Mg have been especially considered and their isothermal sections described and assessed.

A contribution, moreover, has been given to the multi-unit work carried out on the thermodynamic calculation for the Mg-Mn-Y-Zr system.

Introduction

The project of our unit concerns the study of "Thermodynamic and phase equilibria in the system Al-Mg-Cu-Zn-R-(Ni, Mn) with R= rare earth. (Effect of rare earth additions to Al-based or Mg-based alloys)".

In connection with the experimental activity (thermochemistry and phase diagram determination) carried out and reported in group A, our unit is also involved in the calculation (and "prediction") of phase equilibria of selected rare earth alloy systems. Mg-based and Al-based alloys have been especially considered.

In the following a short summary is reported of the results obtained in a number of studies on Mg and Al alloys.

Magnesium Alloys

[96Fla] On the basis of the results of a critical assessment, selected regions of the Ce-Mg-Y system has been investigated employing X-ray diffractometry, optical microscopy and microprobe analyses. Phase relations have been determined in the complete isothermal section at 500°C revealing the existence of two novel ternary compounds: $Ce_xY_{1-x}Mg_{5-y}$ ($0.39 \leq x \leq 0.84$; $0 \leq y \leq 0.60$) with the $GdMg_5$ or the defect $Sm_{11}Cd_{45}$-type and the cubic Laves phase $Ce_xY_{1-x}Mg_2$ ($x \approx 0.67$). The binary Ce-Y has been reinvestigated and a constitutional diagram temperature versus concentration has been proposed. In contrast to earlier data, the so-called δ-phase with the αSm-type has been shown to be metastable. A final assessed description of the system has been presented.

[96Gio] General properties of magnesium alloys with one or two different rare earth metals are briefly summarised and discussed. The regular trends observed in the intermediate phase formation have been used to predict the characteristics of the room temperature isothermal section of the Gd-Y-Mg system. The partial experimental section at 500°C in the composition range ≈50 to 100 at% Mg, has then been determined and found to be in fair agreement with the predicted one. The determination has been carried out by using X-ray powder diffraction, optical and scanning electron microscopy and electron probe microanalysis. The following phases have been identified: the continuous solid solution cP2-CsCl type along the line $Gd_{1-x}Y_xMg$ and, along the line $Gd_{1-x}Y_xMg_2$, two Laves type solid solution fields (cF24-MgCu2 typr, GdMg2 based for about $0<x<0.18$ and hP12-$MgZn_2$ type, YMg_2 based for about $0.26<x<1$). The extension into the ternary field, moreover, has been determined for Mg and the $GdMg_3$, $GdMg_5$ and Y_5Mg_{24} based phases.

[96Sac1] The properties of a number of Mg-R-R' systems with two different rare earth metals (R and R') are presented and discussed, in particular those pertaining to the systems in which one of the rare earths is yttrium. A special procedure for predicting the characteristics of the ternary systems has been presented. The isothermal sections at 500°C of the systems La-Y-Mg, Ce-Y-Mg, Pr-Y-Mg and Gd-Y-Mg are reported and compared and a simulated section of a generalised R-Y-Mg system has been shown.

[96Sei] Excess Gibbs energy coefficients for the binary systems, Mn-Y, Mn-Zr and Y-Zr have been optimised using a least squares method applied to all of the experimental data in the literature plus additional data from new experiments. Combining these with the COST 507 data-sets for Mg-Mn and Mg-Zr plus the Mg-Y data-set from Kuang has enabled extrapolated phases diagrams to be computed for the ternary systems Mg-Mn-Y, Mg-Mn-Zr, Mg-Y-Zr and Mn-Y-Zr. Selected experiments carried out on three of these ternaries show good agreement with the calculated boundaries. On this basis a thermodynamic data-se for the Mg-Mn-Y-Zr system has been assembled which enables several different types of phase diagrams and sections to be computed for the quaternary system. As examples of the kind of diagrams of practical importance that can currently be obtained with modern thermodynamic software for multicomponent alloy systems, calculated phase fraction versus temperature diagrams have been presented for two quaternary alloy compositions, Mg-1wt% Mn-1wt% Zr with 5 and 10 wt% Y respectively. The data presented result from the cooperative network "MSIT Trainer Network on the Constitution of Engineering Materials", operating under EU Human capital and Mobility Programme, TMR.

Aluminum Alloys

[96Bor] To complete the investigation and the thermodynamic optimization of the Al alloys with trivalent R, the study of La-Al system is now in progress. The examination of the Yb-Al alloys has also been started. This system is different from those given by the trivalent Rs: only two compounds are formed. Even if in both cases the minimum in the trends of $\Delta_{form}H°$ versus composition corresponds to the RAl_2 stoichiometry, the different reactivity of Al with La and Yb is also reflected by the disparity between the values of the $\Delta_{form}H°$: -50.5±2 kJ/mol at. for $LaAl_2$ and -39.5±2 kJ/mol at. for $YbAl_2$. These results are discussed and compared with those of other similar R-Al compounds. An assessed version of different R-Al systems has been presented.

[96Sac2] As a contribution to the understanding of the R-Al diagrams, an assessed version of the Gd-Al system has been prepared and discussed. As a consequence the experimental investigation of the Gd-rich part of the Gd-Al diagram has been carried out. The coordinates of the Gd-rich eutectic, the lowering of the allotropic transformation temperature of the gadolinium by additions of Al and the melting behaviours of the Gd-rich compounds have been particularly discussed.

Publications of the 3rd year
(Coordination Group C)

[96Fla] H.Flandorfer, M.Giovannini, A.Saccone, P.Rogl, R.Ferro,"The Ce-Mg-Y System" Metall. Trans A (1997) in press.

[96Gio] M.Giovannini, A.Saccone, H.Flandorfer, P.Rogl, R.Ferro, "On the Systematics of Phase Equilibria in Complex Magnesium-Rare Earth Systems: Gd-Y-Mg System" Z. Metallkde., (1997) in press.

[96Bor] G.Borzone, A.M.Cardinale, N.Parodi, R.Ferro, "A Contribution to the Study of Rare Earth Reactivity with Aluminum",Proc.:7th Meeting on "Syntheses and Methodologies in Inorganic Chemistry" Bressanone (Bolzano) (Italy), Dec. 16-19 (1996).

[96Sac1] A.Saccone, M.Giovannini, P.Rogl, G.Effenberg, R.Ferro,"Regularities in Ternary Systems Formed by Magnesium with Two Different Rare Earth Metals",Proc. CALPHAD XXV, Erice (Italy), May 26-31 (1996)

[96Sac2] A.Saccone, A.M.Cardinale, D.Macciò, S.Delfino, "Contribution to the Phase Equilibria Investigation of the Binary Rare Earth-Aluminum Systems"Proc.: XXIV Congr. Nazl. Chimica Inorganica, Mondello (Palermo), (Italy), Jun. 25-29 (1996), D13.

[96Sei] H.J.Seifert, J.Gröbner, F.Aldinger, F.H.Hayes, G.Effenberg, C.Bätzner, H.Flandorfer, P.Rogl, A.Saccone, R.Ferro, "Thermodynamic Calculation and Experimental Studies of Phase Relations in the Mg-Mn-Y-Zr System", Proc. 8th International Magnesium Conference (UK), Apr. 1996, Institute Materials London Publ.

List of publications in the framework of COST 507 Round I and II up to 1996

(Coordination Group C)

1-Articles in Scientific Journals

G.Cacciamani, G.Borzone, R.Ferro
"Rare Earth-Aluminium Alloys: Optimization of Thermodynamic Properties and Phase Diagrams of the Ce-Al system"
Anales de Fisica 86B (1990) 160-162.

G.Cacciamani, A.Saccone, G.Borzone, S.Delfino, R.Ferro,
"Computer Coupling of Thermodynamics and Phase Diagrams: the Gd-Mg System as an Example"
Thermochimica Acta 199 (1992) 17-24.

M.Baricco, L.Battezzati, G.Borzone, G.Cacciamani
"Thermodynamic Investigation on Glass Forming Al-RE System"
J.Chim. Phys., 90 (1993) 261-268.

R.Ferro, S.Delfino, G.Borzone, A.Saccone, G.Cacciamani
"Contribution to the Evaluation of Rare Earth Alloy Systems"
J.Phase Equilibria, 14 (1993) 273-279

H.Flandorfer, M.Giovannini, A.Saccone, P.Rogl, R.Ferro
"The Ce-Mg-Y System"
Metall. Trans A (1997) in press.

M.Giovannini, A.Saccone, H.Flandorfer, P.Rogl, R.Ferro
"On the Systematics of Phase Equilibria in Complex Magnesium-Rare Earth Systems: Gd-Y-Mg System"
Z. Metallkde., (1997) in press.

G.Cacciamani, G.Borzone, R.Ferro
"Rare Earth-Aluminium Alloys: Optimization of Thermodynamic Properties and Phase diagrams of the La-Al and Ce-Al Systems"
Proc. Thermodynamics of Alloys, S.Feliu de Guixols (Spain) 23-26/5/1990 p.D5.

L.Battezzati, C.Antonione, M.Barricco, H.Fernandez, G.Riontino, G.Borzone, G.Cacciamani
"Thermodynamics of Metastable Phases: Application to Al-Rare Earth Metallic Glasses"
Proc. CISCI 91 Chianciano (Italy) 6-11/10/1991 p.109.

G.Cacciamani, R.Ferro
"On Some Al-Ba-R (R=Rare Earth) Systems"
Proc. CALPHAD XXI, Jerusalem (Israel) 14-19/6/1992, p.15

G.Cacciamani, A.Saccone, G.Borzone, P.Riani, R.Ferro,
"Rare earth-Magnesium Alloy Phase Diagrams: Assessment, Thermodynamics and Optimization",
Proc. CALPHAD XXIII, 12-17/6/1994, Madison (Wisconsin, USA), p.45.

G.Cacciamani, G.Borzone, L.Battezzati, M.Baricco, R.Ferro
"Thermodynamics of Al-Nd Alloys",
Proc. CALPHAD XXII, Catalonia (Spain) 16-21/5/1993, p.P5.

G.Cacciamani, A.Saccone, R.Ferro,
"Thermodynamic Optimization of the Ce-Mg System",
Proc. CALPHAD XXII, Catalonia (Spain) 16-21/5/1993, p.P6.

G.Cacciamani, G.Borzone, R.Ferro, L.Battezzati, M.Baricco
"Calculation of the Al-Ce-Nd Ternary System",
Proc. Thermodynamics of Alloys, S.Margherita Ligure (Italy) 25-28/4/1994, p. P10.

G.Borzone, G.Cacciamani, A.M.Cardinale, N.Parodi
"Rare Earth-Magnesium Systems: Thermochemical Investigation of Selected Solid Alloys"
Proc.: 7th Meeting on "Syntheses and Methodologies in Inorganic Chemistry" Bressanone (Bolzano) (Italy), Dec. 18-21 (1995).

A.Saccone, A.M.Cardinale, D.Macciò, S.Delfino
"Contribution to the Phase Equilibria Investigation of the Binary Rare Earth-Aluminum Systems"
Proc.: XXIV Congr. Nazl. Chimica Inorganica, Mondello (Palermo), (Italy), Jun. 25-29 (1996), D13.

G.Borzone, A.M.Cardinale, N.Parodi, R.Ferro
"A Contribution to the Study of Rare Earth Reactivity with Aluminum"

Proc.: 7th Meeting on "Syntheses and Methodologies in Inorganic Chemistry" Bressanone (Bolzano) (Italy), Dec. 16-19 (1996).

A.Saccone, M.Giovannini, P.Rogl, G.Effenberg, R.Ferro
"Regularities in Ternary Systems Formed by Magnesium with Two Different Rare Earth Metals"
Proc. CALPHAD XXV, Erice (Italy), May 26-31 (1996)

H.J.Seifert, J.Gröbner, F.Aldinger, F.H.Hayes, G.Effenberg, C.Bätzner, H.Flandorfer, P.Rogl, A.Saccone, R.Ferro
"Thermodynamic Calculation and Experimental Studies of Phase Relations in the Mg-Mn-Y-Zr System"
Proc. 8th International Magnesium Conference (UK), Apr. 1996, Institute Materials London Publ.

Evaluation of the Al-Mg-Mn-Fe-Si system

P. Kolby, C. J. Simensen and M. E. Seiersten.

SINTEF Materials Technology
P.O. Box 124 Blindern
N-0314 Oslo
Norway

Abstract

The Norwegian project, which consists of Elkem Aluminium ANS, Hydro Aluminium A/S, Raufoss ARC, and SINTEF Materials Technology has focused attention on evaluating the Al-Mg-Mn-Fe-Si. With respect to assessment we have had close links with Chart Associates, Wintershill Consultancy, the Royal Institute of Technology and the National Physical Laboratory, while experimental works have been coordinated with Alcan International Ltd, Katholicke Universiteit Leuven, Pechiney CRV, Universite Paris Sud, Universitat Wien and the University of Manchester/UMIST.

1 Introduction

The Al-Mg-Mn-Fe-Si system comprises some 90% of the total tonnage of aluminium produced, yet through the course of the COST507 action substantial inaccuracies in previously accepted literature has been revealed. In addition previously uninvestigated gaps in the phase diagrams have been studied. Through the COST507 efforts on the Al-Mg-Mn-Fe-Si system, it has become apparent that the only way to achieve the goal of evaluating higher order aluminium systems is through extensive collaboration. No single institution has the required expertise or resources to successfully master this task.

2 Experimental work

The Norwegian project has emphasised experimental efforts to fill the gaps in our knowledge on the Al-Mg-Mn-Fe-Si system. Mainly we have employed the SIBUT technique [80Sim, 84Sim] to dissolve the samples and subsequently used different techniques to measure the amount of elements in solid solution in the aluminium phase and the amount and composition of intermetallic particles in the alloy at the temperature. This enabled us to draw experimental tie lines with high accuracy which has been a valuable contribution to our understanding of the system.

Large particles of selected phases have also been grown for calorimetric measurements by Prof. Legendre at the Universite Paris Sud.

2.1 Solid solubility measurements

The COST507 effort on investigating the solid solubility of selected alloying elements in aluminium has been a collaborative project between Pechiney CRV and SINTEF Materials Technology. The systems targeted are Al-Mn, Al-Mn-Si, Al-Mn-Fe, and Al-Mn-Fe-Si. Pechiney CRV have been responsible for the casting and heat treatment of the alloys, as well as determining the Mn content by way of the Thermo Electric Power (TEP) technique [81Bou, 89Bor]. SINTEF has measured all the elements in solid solution by using the SIBUT dissolution technique [80Sim, 84Sim] combined with pertinent analysis techniques. In this fashion the measurement of the Mn content has been duplicated using two fundamentally different techniques, which ensures reliable results. The results of these investigations have prompted a reevaluation of the reliability of the work of [43 Phi] in the solid state. Due to extremely slow reaction rates in the Mn containing systems, up to 6000 hrs homogenisation time was required to reach equilibrium. This is longer than can be explained by a small diffusivity of Mn in solid Al. It is therefore probable that nucleation is sluggish and that the driving forces for precipitation are small. This could in turn help to explain the discrepancy between the COST507 assessment and the commonly accepted diagrams in all systems containing Mn.

The experimental tie line determinations have been conducted on the same samples used in the solvus measurements. By measuring the composition, type and amount of particles left on the filter after dissolution we are able to combine this with the corresponding solid solution composition to form an experimental tie line. Amongst the results of this work on the Al-Mn-Fe system, it was discovered that the $Al_{12}Mn$ phase is stable at 550°C in the pure Al-Mn system. However, an Fe content as low as 20ppm was sufficient to stabilise the $Al_6(Mn,Fe)$ phase, and bring the sample into the 3 phase field Al + $Al_{12}Mn$ + $Al_6(Mn,Fe)$. It is believed that as little as 100 ppm will be sufficient to completely surpress the formation of $Al_{12}Mn$. These results are in contradiction to previous beliefs based on the work of Schaefer et al [86Sch] which suggests that this phase decomposes at temperatures above 512°C, but in agreement with unpublished work conducted at the CNRS Vitry [96Har].

2.2 Determination of invariant points in Al-Mn-Si

Due to problems in fitting all the invariant points on the liquidus surface simultaneously, we have experimentally redetermined the eutectic point [93Sim]. Our coordinate for the eutectic is lower in Mn than that of Phillips, which already belongs to the lower spectrum of values quoted in the literature. We do, however, feel confident that this measurement is correct since the optimiser in Thermo-Calc seems to draw this point to lower Mn values. Our values have been obtained by performing area analysis in the microprobe in regions of the sample occupied by the eutectic structure. In this way the Mn content should be overestimated if regions which have solidified preeutectically formed part of the analysing volume.

The delta-AlMnSi phase has also been investigated from the point of view of determining the position of the invariant point comprising alpha, silicon and delta in addition to the melt. Our results contradict those reported by [76Mon], who claims the

appearance of this phase at 13.5 wt% Si. Our measurements indicate that this phase is not precipitated in equilibrium at Si contents below 20wt%, however the phase may be readily nucleated at lower Si contents under non equilibrium solidification conditions [93Sim].

2.3 Growth of Large Crystal

In order to establish the enthalpy of the two important ternary phases, alpha and beta, in the Al-Mn-Si system, a program was initiated at SINTEF to grow large crystals of these phases. Since these are peritectic phases, they could not be made simply by mixing appropriate amounts of Al, Mn and Si and having them react at high temperature in the liquid state. On the other hand the reaction kinetics in the solid state forms a serious barrier to achieving single phase samples with a homogenous composition on a practical time scale, at lower temperatures. The only possible approach was therefore to grow the alpha and beta crystals in the two phase liquid + alpha (or beta) region. Subsequently the samples were quenched to room temperature to minimise the problem of nucleation of other phases on the existing crystals during solidification. After dissolution of the aluminium matrix we were left with millimetre sized crystals of the desired phases [96Sim]. Attempts to measure the heat of formation of these phases are underway at the Universite Paris Sud.

A spin-off result of this investigation has been to question the results reported by Pratt and Raynor [51Pra]. In the round I assessment of the Al-Mn-Si system, heavy emphasis was placed on the results of Pratt and Raynor, with regard to the stability of the beta-AlMnSi phase. The present experimental investigation has, however, not succeeded in reproducing this earlier work. An attempt to grow the beta phase according to the same procedure as was employed by Pratt and Raynor [51Pra] was unsuccessful. Unfortunately this experiment resulted in a beta core surrounded by an alpha shell, indicating that the beta phase was the primary phase but that the holding temperature was in the liquid + alpha phase region [96Sim]. This observation has lead to some doubt as to the reliability of [51Pra], which is currently being incorporated in the reassessment of Al-Mn-Si [97Ran].

3 Calculations

Even though most of the work involved was completed in round I of the COST507 action the completion of our evaluation of the Al-Fe-Si [93Sei] and Al-Mn-Si [93Kol] systems took place during round II. The Al-Mn-Si system has been subject to extensive experimental and computational reevaluation during the course of round II as reported by Rand et al [97Ran]. No detail will therefore be given in this report.

In the case of the Al-Fe-Si system, the assessment by Seiersten [93Sei] remains as the accepted COST507 evaluation. The work is therefore detailed here.

3.1 The Al-Fe-Si Assessment

The central part of the assessment is based on experiments by Takeda and Mutuzaki [40Tak]. This is the only complete determination of the phase diagram, and later

reviews by Rivlin and Raynor [81Riv] and by Ghosh [92Gho] are based on these experiments. Takeda and Mutuzaki state that the evidence for some of the reactions is circumstantial, and they also found it difficult to distinguish some of the phases by etching. Their phase analysis are also inaccurate and do not agree with later work for the more known phases. In this assessment emphasis has thus been placed on the temperatures measured by Takeda and Mutuzaki as opposed to their reported compositions. More data exists in the aluminium rich part of the diagram, and experiments by Phillips [59Phi], Phragmen [50Phr], Munson [67Mun], Dons [84Don], Gringer [87Gri], Stefaniay [87Ste], Oscarsson [88Osc] and others have been used for this part of the diagram.

The calculated liquidus diagram is shown in Fig 1.. Takeda and Mutuzaki's diagram is generally reproduced, but there are differences. The primary precipitation field for Fe_2Si is more narrow and the Fe_2Si phase is also found to precipitate from the ternary liquid. This is mainly caused by differences in the binary Fe-Si diagrams. Moving into the central part of the diagram, the main differences are caused by the phases denominated τ_1 and τ_3. The primary field of the τ_1 phase is smaller compared to the experimental diagram, but it is peritectic and the reactions around it are in agreement with the determinations of Takeda and Mutuzaki. Since this part of the diagram is rather inaccurate, the fit is regarded as satisfactory.

In the calculated diagram t_3 melts congruently, while Takeda and Mutuzaki have determined the phase to be peritectic. Their results in one of the invariant points surrounding its primary field is a eutectic as opposed to a peritectic. The calculations are probably wrong on this point since the reaction involves the FeSi phase and the Fe-Si system is due to be revised. Therefore little effort was put into forcing the phase to become peritectic in the calculations at this stage. In any case further experimental studies are necessary to establish the composition and types of reactions involved in the invariant points in this region. The ordered bcc_b2 phase has been used in the assessment.

The aluminium rich region of the diagram agrees well with the present knowledge of the phase diagram. The liquidus surface does not reproduce Takeda and Mutuzaki, but agree with later results, especially Munson [67Mun] and Stefaniay [87Ste]. Several earlier sources have not distinguished between the hexagonal alpha-AlFeSi and the cubic alpha-AlMnFeSi phases. For this reason only results that clearly state the presence of the hexagonal phase have been used in this assessment. The primary field for alpha-AlFeSi precipitation has therefore been greatly reduced as compared to earlier diagrams of Phillips [59Phi] and Takeda and Mutuzaki [40Tak].

For the hexagonal alpha phase, data given by Mondolfo [76Mon] has been used in the assessment combined with isothermal data at 600°C [87Ste]. Mondolfo states that the alpha phase contains 7.0wt% Si regardless of which equilibrium it is involved in. This cannot be correct if the phase has a homogeneity range with respect to Si. The calculated values range form 6.2 to 7.2 wt% Si are thus well within the experimental error. In a later study it was found that the Si content in the alpha phase after rapid cooling is 6-11 wt% while it lays in the range 6-9.5 wt% at 600°C [87Ste]. Armand [54Arm] and Black [55Bla] have determined the Si content in the hexagonal alpha

phase to be 11.2 and 11 wt% respectively. These measurements were however conducted on samples where the cubic alpha-AlMnFeSi phase was also present which means that the hexagonal phase would have to contain an unnaturally high amount of Si compared to what is standard for the pure Al-Fe-Si system (without Mn). Corby [77Cor] found that the hexagonal phase contained 8.7 wt% Si. A complete review of the ternary phases included in the assessment is given in Table 1.

The calculated enthalpy of formation at 298.15K for the alpha and beta phase is 23.4 and 18.2 kJ/mol, while the experimental values determined by Moquet [71Moq] are 23.23 and 20.04 kJ/mol respectively.

The calculated diagrams generally reproduce the available experimental data well. However, emphasis has been placed on achieving a good fit in the aluminium rich corner, since this is where the bulk of the reliable data and the industrial interest is focused. It must be pointed out that even here there are still important points which have not been satisfactorily investigated such as the phase boundaries for $Al_{13}Fe_4$ and the alpha-AlFeSi phase at higher Si contents, and the solubility range for the delta-AlFeSi phase. A redetermination of the invariant points and the enthalpy of formation of at least one of the ternary phases would also improve the assessment. A comparison between the calculated and experimental positions of the invariant points is shown in Table 2.

As for the central part of the system, there is very little interest and thereby also little data in this region of the phase diagram. Two ternary compounds τ_1 and τ_3 are included in the diagram but their compositions and appearance in the diagram is uncertain. Later work has revealed the probable existence of several other phases [81Zar], but they can not be included in the diagram before more information, such as melting points, enthalpies and equilibria with other phases have been investigated.

4 References

[40Tak] H. P. Takeda and K. Mutuzaki, Tetso to Hagane, 1940, 26, 335.

[50Phr G. Phragmen, J. Inst. Met., 1950, 77, 489.

[51Pra] J. N. Pratt and G. V. Raynor, J. Inst. Metals, 1951, 79, 211.

[54Arm] M. Armand, Congres International de l'Aluminium, 1954.

[55Bla] P. J. Black, Philos. Mag., 1955, 46, 401.

[59Phi] H. W. L. Phillips, Annotated Equilibrium Diagrams of some Aluminium Alloy Systems, Inst. Met., London, 1959.

[67Mun] D. Munson, J. Inst. Met., 1967, 95, 217.

[71Moq] J. L. Moq, Contribution a l'estimasjon des grandeurs thermodynamiques des composes intermetalliques et des entropies de fusion des eutectiques

binaires. Thesis, Universite Scientifique et Medicale de Grenoble, 1971.

[76Mon] L. F. Mondolfo, Aluminum Alloys: Structure and Properties Butterworths, London, 1976

[77Cor] R. N. Corby and P. J. Black, Acta. Crystallogr., 1977, 33B, 3468.

[80Sim] C. J. Simensen, A. I. Spjelkavik, Fresenius Z. Analytische Chemie, 1980, 300, 177.

[81Bou] F. R. Boutin, S. Dermarkar and B. Meyer, Proc. 7th Light Metals Congress, Leoben 1981, 212.

[81Riv] V. G. Rivlin and G. V. Raynor, Int. Met. Rev., 1981, 26, 133.

[81Zar] O. S. Zarechnyuk, N. V. German, T. I. Yanson, R.M. Rykhal and A. A. Muravera, Some Phase Diagrams of Aluminium with Transition Metals, Rare Earth Elements and Silicon, Splav. Izd. Nauka, Moscow, 1981, 69.

[84Don] A. L. Dons, Z. Metallkd., 1984, 75, 170.

[84Sim] C. J. Simensen, P. Fartum and A. Andersen, Fresenius Z. Analytische Chemie, 1984, 319, 286-292.

[86Sch] R. J. Schaefer, F. S. Biancaniello and J. W. Cahn, Scripta Met., 1986, 20, 1439.

[87Gri] A. Griger, A. Lendvai, V. Stefaniay and T. Turmezey,J. Mater. Sci. Forum, 1987, 13/14, 331.

[87Ste] V. Stefaniay, A. Griger and T. Turmezey, J. Mater. Sci., 1987,22, 539.

[88Osc] A. Oscarsson et al., Z. Metallkd., 1988, 79, 600.

[89Bor] R. Borrely, P. Merle and D. Adenis, Light Metals 1989, Editor:P. G. Campbell, 703.

[92Gho] G. Ghosh, Ternary Alloys: Editors G. Petzow and G. Effenberg,VCH Verlagsgesellschaft, Weinheim, 1992.

[93Sei] M. E. Seiersten, ``An assessment of the Al-Fe and Al-Fe-Si systems", SINTEF report nr. STF28 F93051 June 1993.

[93Kol] P. Kolby, ``The aluminium rich corner of the ternary Al-Mn-Si alloy system", SINTEF report nr. STF28 F93022 March 1993.

[93Sim] C. J. Simensen, ``Eutectic solidification of Aluminium-Silicon-Manganese alloys", SINTEF report nr. STF28 F93039 June 1993.

[96Sim] C. J. Simensen, ``Production and analysis of intermetallic phases", SINTEF report nr. STF24 F96026 June 1996.

[96Har] M. Harmelin, Private Comunications based on experiments performed in 1986 on the same samples used by [86Sch].

[97Ran] M. Rand, P. Kolby and T. Chart: ``A Thermochemical Assessment of the Al-rich Corner of the Al-Mn-Si System", in these proceedings 1997.

Table 1. Review of the ternary phases included in the assessment. The experimental composition used in the assessment is indicated by an asterix (*)

Phase	Composition, Wt%		Composition, Atom%		Reference	Structure
	Fe	Si	Fe	Si		
α (τ_5)	38.1	15.9	23.1	19.2	40Tak	
	29.2	11.2			54Arm	Hexagonal
	32.5	8.7	18.9	10.1	77Cor	Hexagonal
	29.7	9.6	17.0	10.9	74Mur. 81Zar	
*	33.5	7.0–9.5	19.7	8.2-11.1	87Gri	Hexagonal (P63/mmc)
	31.0	8.0	17.9	9.2	75Bar	Hexagonal (P63/mmc)
	32.5	8.7	18.9	10.1	53Rob	Hexagonal (P63/mmc)
	30.0-33.0	7.4-11.0	17.2-19.3	8.4-12.8	67Sun	Hexagonal
(*)	28.0-36.0	6.0-13.0	15.9-21.5	6.8-15.4	87Ste	
	32.0	8.0	18.6	9.2	85Suz	
β (τ_6)	29.1	14.6	16.7	16.6	40Tak	
	27.2-27.8	13.5-14.0	15.4-15.8	15.2-15.8	50Phr	Monoclinic
*	26.6	13.4	15.0	15.0	74Mur. 81Zar	
	23.4-25.8	115.7-9.0	13.0-14.5	20.9-17.5	55Obi	Monoclinic
	25.0	13.0	14.0	14.4	75Bar	Monoclinic
	27.2	13.7	15.4	15.4	55Bla	Tetragonal (4/m)
	26.7-27.3	13.8-14.9	15.1-15.5	15.5-16.8	51Pra	
	27.2	13.7	15.4	15.4	51Now	
	25.5-26.5	12.1-14.6	14.3-14.9	13.5-16.4	67Sun	
	25.9-26.6	12.8-13.3	14.5-15.0	14.3-14.9	88Zak	Monoclinic
	25.0-28.0	13.0-16.0	14.0-15.9	14.4-18.1	87Ste	
	27.0	14.0	15.3	15.7	85Suz	
	25.0-30.0	12.0-15.0	13.9-17.3	13.3-17.2	79Mor	
γ (τ_2)	41.9	18.4	26.1	22.8	40Tak	
	35.3	12.8	21.0	15.1	52Arm. 55Arm	Cubic
	33.0-38.0	13.0-18.5	19.3-23.1	15.2-22.3	67Mun	Monoclinic
	36.7	12.6-21.7	22.0	15.0-26.0	74Mur. 81Zar	Monoclinic
*	34.0-35.2	15.6-17.1	20.1-21.0	18.3-20.2	67Sun	
(*)	31.0-37.0	9.0-18.0	17.9-22.3	10.3-21.6	87Ste	
δ (τ_4)	28.9	29.2	16.6	33.4	40Tak	
	28.9	29.2	16.6	33.4	69Pan	Tetragonal
	27.2	25.2	15.5	28.5	36Jae	Tetragonal
	28.9	29.2	16.6	33.4	51Now	Tetragonal
	26.5-27.5	24.9-33.5	15.7-15.1	28.2-37.9	74Mur.81Zar	Hexagonal
*	25.9-27.8	25.3-26.4	14.6-15.9	28.4-30.0	88Zak	
(*)	25.0-26.0	26.0-27.0	14.0-14.7	29.0-30.3	67Sun	
	29.0	29.6	16.7	33.9	84Sim	
τ_1	55.0	18.4	37.5	24.9	40Tak	
*	57.7	14.5	40.0	20.0	74Mur.81Zar	
τ_3	42.2	21.1	26.4	26.2	40Tak	
*	40.5	20.4	25.0	25.0	74Mur.81Zar	

Table 2. A comparison between calculated and experimental positions of the invariant points on the liquidus surface.

Reaction	Tempe-rature °C	Liquid wt% Fe	Liquid wt% Si	Solid phases wt% Fe	Solid phases wt% Si	Solid phases phase	Ref
A) Liq+$Al_{13}Fe_4$=fcc+α	632	1,9	3,8	39,1	0,27	Al_{13}	Calc
				0,0037	0,45	fcc	
				32,6	6,2	α	
	620	2,0	3,0				81Riv
	629	2,5	4,0	36,0	0,1	Al_{13}	76Mon
				0,05	0,6	fcc	
				33,0	7,0	α	
	629						55Arm
	630	2,0	4,0	0,052	0,64	fcc	59Phi
	632	2,0	4,2	39,2	0,8	Al_{13}	92Gho
				0,05	0,64	fcc	
				38,1	15,9	α	
B) Liq+β=fcc+α	621	1,6	5,8	0,026	0,7	fcc	Calc
				32,6	7,2	α	
	615	2,0	5,0				81Riv
	612	1,7	6,5	0,04	1,1	fcc	76Mon
				33,0	7,0	α	
	611	1,5	7,5	0,04	1,0	fcc	59Phi
	613	1,8	6,3	0,04	1,0	fcc	92Gho
				38,1	15,9	α	
C) Liq=β+fcc+Si_F4	578	0,57	12,6	$4,6 \cdot 10^{-3}$	1,8	fcc	Calc
	577						55Arm
	577		11,6				81Riv
	576	0,7	12,0	0,01	1,6	fcc	76Mon
	578	0,75	11,6	0,01	1,65	fcc	59Phi
	573	0,5	14,3	0,01	1,7	fcc	92Gho
D) Liq+δ=β+Si_F4	608	1,08	14,6				Calc
	595						55Arm
	600	1,0	14,0				81Riv
	596	1,5	14,0				76Mon
	597	0,95	13,5				59Phi
	600						92Gho
E) Liq+$Al_{13}Fe_4$+γ=α	749	7,6	12,0	39,3	1,6	Al_{13}	Calc
				32,6	7,9	α	
	ca. 710						55Arm
	855	25,0	17,0				81Riv
	710	7,5	12,5	36,0	0,2	Al_{13}	Mon
				33,0	7,0	α	
	855	25,0	17,0	39,2	0,8	Al_{13}	92Gho
F) Liq+γ+α=β	715	5,6	12,2	32,5	8,3	α	Calc
	675	6,0	13,0	34,0	7,0	α	76Mon
G) Liq+γ=δ+β	703	4,8	14,3				Calc
	700						55Arm
	700	7,0	14,0				76Mon
	700	8,0	14,0				81Riv[1]
H) Liq+Al_5Fe_4=bcc+Al_2Fe	1125	53,3	3,0	62,8	1,8	bcc	Calc
	1120	51,0	3,0				81Riv[2]
				58,0	14,0	bcc	92Gho
I) Liq+Al_2Fe=Al_5Fe_2+bcc	1067	52,0	7,6	62,5	5,3	bcc	Calc
J) L+Al_5Fe_2=$Al_{13}Fe_4$+τ_1	1041	48,2	10,5	40,3	2,1	Al_{13}	Calc
	1020	48,0	14,0				81Riv
	1020			39,2	0,8	Al_{13}	92Gho
K) Liq+τ_1=$Al_{13}Fe_4$+τ_3	976	41,2	17,4	39,8	4,1	Al_{13}	Calc

[1] For the reaction Liq+δ = α + β

[2] For the reaction Liq+Al_5Fe_4=bcc+Al_5Fe_2

	940	41,0	19,0				40Tak[3]
L) Liq+bcc=FeSi+τ_1	1064	58,6	20,5	66,9	16,5	bcc	Calc
	1050	50,0	19,0				81Riv[4]
	1050	50,0	19,0	63,0	11,0	bcc	92Gho
M) Liq+t_1=FeSi+τ_3	957	44,9	25,9				Calc
N) Liq=FeSi+τ_3+Si	884	36,5	36,6				Calc
	880 (885)	36,0	36,0				81Riv[5]
		(38,0)	(36,0)				
O) Liq+τ_3=Si_F4+δ	868	23,8	33,7				Calc
	865	23,0	32,0				81Riv
P) Liq+τ_3=γ+δ	871	20,3	24,4				Calc
	835	22,0	22,0				81Riv
Q) Liq+$Al_{13}Fe_4$+τ_3=γ	901	23,6	18,9				Calc
	940 (855)	40 (25)	19 (17)				81Riv[6]
R) Liq+bcc=Al_5Fe_2+τ_1	1048	49,9	9,7	61,2	8,3	bcc	Calc
	1020	48,0	14,0				81Riv
				58,0	14,0	bcc	92Gho
S) Liq+$FeSi_2$=FeSi+Si	935						Calc

[3] For the reaction Liq+τ-1=$Al_{13}Fe_4$+γ

[4] For the corresponding peritectic reaction

[5] For the reaction Liq+τ_1=$FeSi_2$+τ_3 or (numbers in parenthesis) Liq+$FeSi_2$=Si+τ_3

[6] For the reaction Liq+τ_1+$Al_{13}Fe_4$=γ or (numbers in parenthesis) Liq+$Al_{13}Fe_4$+γ=α

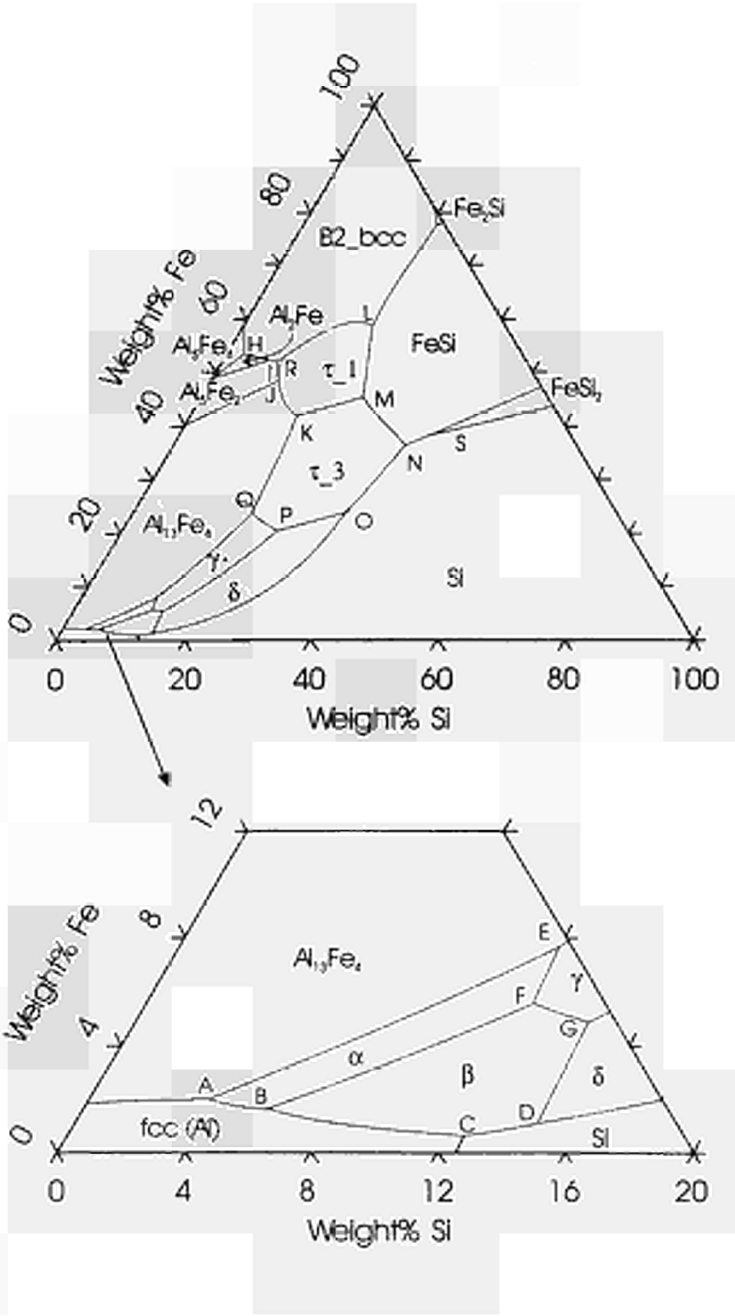

Fig 1. The calculated Al-Fe-Si liquidus surface.

Extrapolations based on Ti-C-N

Bo Sundman and Lucia F.S. Dumitrescu

Division of Computational Termodynamics
Department of Materials Science and Engineering
Royal Institute of Technology
Sweden

Abstract

The binary systems Ti-C and Ti-N are important in many metallic ternary systems. There have been difficulties during the COST project to reconcile many experimental observations in ternary systems involving Ti-C and Ti-N. Due to low solubilities it has not been possible to resolve the difficulties by using ternary parameters. This means that one has to reassess binary systems using ternary information.

There is a great risk that different groups in COST make different adjustments to the same binary system to fit their ternary. It is difficult to judge the importance of the different data and each group has the wish to present as good description of its systems as possible.

This presentation attempts to show how the Ti-C and Ti-N systems behave in some ternary systems and suggests a modification of the current Ti-C and a new Fe-Ti assessment. Different Al-Ti assessments are compared also. The ternary systems considered are Al-Ti-C, Al-Ti-N, Fe-Ti-N, Fe-Ti-C, Ni-Ti-C and Ti-C-N. Among other important systems still not checked are Co-Ti-C and W-Ti-C.

1. Introduction

Titanium carbonitride has a strong technical importance, e.g. in hard materials [92Cla] and in microalloyed steels [92Zou]. It should thus be interesting to assess its thermodynamic properties. The problem is that one should like to account for its equilibria in several systems. When such information shows inconsistencies it may be justified to include even more systems in order to choose between different alternatives. Thus, the main part of the present discussion will concern TiC and TiN in equilibrium with other phases in the Ti-C-N-Al-Ni-Fe system.

Jonsson has published an impressive group of assessments resulting in a self-consistent set of descriptions of the systems W-Ti-C-N [96dJon] and Fe-Ti-C-N [97Jon] and their subsystems. Some objections have been raised to his description of the Ti-N [96aJon] and Ti-C [96bJon] systems and have resulted in a different termodynamical description of the Ti-N system, Zeng et al. [96Zen], and of the Ti-C system , Dumitrescu [97Dum]. But there are also independent assessments of the Ti-N system by Ohtani et al. [90Oht] and of the Ti-C system by Albertsen et al. [95Alb]

and Seifert et al.[96Sei], which will also be considered in this paper. Some modifications will be recommended.

The consequences for the other systems due to the recommended modifications of the Ti-N and Ti-C systems will be examined, in particular Ti-C-N, Ni-Ti-C, Al-Ti-C, Al-Ti-N and Fe-Ti-C-N. The various descriptions of the Fe-Ti system will also be examined.

2. TiN and the binary Ti-N system

All the assessments of the Ti-N system, [96aJon], [96Zen] and [90Oht], begin with an assessment of the stoichiometric TiN and therefore we will first consider C_P and H-H_{298}, which is closely related to C_P.

2.1 TiN

JANAF[85JAN] gives an excellent description of C_P data up to about 1200 K but then their curve starts to bend upwards in a way not indicated by data. Ohtani et al. [90Oht] used a simple power series G_m - HSER = $a + bT + cTlnT + dT^2$, representing H - HSER rather well between 298 and 1000 K but not at higher temperatures. Jonsson [96aJon] added more terms, $G_m - H^{SER} = a + bT + cTlnT + dT^2 + eT^{-1} + fT^{-3}$, and obtained an excellent fit for all data above 200 K, except for a small deviation for the highest experimental point (1750 K). The melting point of TiN is about 3600 K and it is unfortunate that there is no experimental information above 1750 K. The description given by Jonsson [96aJon] yields only a modest increase of C_P above 1750 K, which may be preferable to the rapid increase according to JANAF [85JAN], see Fig.1 . Zeng et al. [96Zen] criticised Jonsson's [96aJon] assessment because it cannot be used below 200 K. They claimed that this problem disappears if the T^{-3} term is omitted. Instead, they introduced a T^{+3} term but did not describe how they evaluated its value. Anyway, the value they gave is rather small and even at 3600 K it yields a contribution to H by only about - 1 kJ/mol. It does not seem justified to introduce a new term for such a small effect in a region far above the experimental range. On the other hand, the T^{-3} term used by Jonsson [96aJon] is important inside the experimental range. By omitting that term but accepting his value of the other coefficients, Zeng et al. [96Zen] got a serious disagreement at low temperatures which starts already at about 500 K. Evidently, they failed to realize that Jonsson [96aJon] used the T^{-3} term to get agreement with data all the way down to 200 K. That term would not be needed if one was satisfied to describe data down to 298 K but then one would have to reevaluate the other coefficients. Fig.1 shows a comparison between the three different assessments for the C_P curve. It seems that one should use Jonsson's [96aJon] expression.

S_{298} and C_P are thus established and the stability (i.e. G_m) of TiN will then be fixed by choosing a value for ΔfH^{298}_{TiN}. It was measured by Humphrey [51Hum] and G_m would thus be fixed. In addition it was measured by Morozova et al. [66Mor] who studied not only TiN but also TiN_{1-x}. Their values extrapolate well to Humphrey's [51Hum] values but could also support a value 10 kJ/mol of TiN higher or lower. Humphrey's

value has been accepted in all three assessments discussed here.

2.2 Binary system Ti-N

So far we have only considered stoichiometric TiN. We may also like to make recommendations on the whole of the binary system. Fig.2 shows a comparison between the three existing descriptions of the Ti-N system [96aJon], [96Zen] and [90Oht].

2.3 δ-TiN_{1-x} solution

This is an interstitial solution of N in fcc Ti. The end-member, TiN, has just been discussed. The other end-member is identical to pure fcc Ti. Today it seems that one should use the SGTE descriptions for pure elements published by Dinsdale [91Din]. However, it should be realized that they contain an extrapolation of solid phases above the melting point which was invented in order to avoid making them stable at very high temperatures. It usually underestimates C_P of overheated solid phases. This is not a serious problem close to the melting point but Jonsson [96aJon] wanted to avoid this in the case of Ti-N where the fcc phase extends far above the melting point, about 3600 K compared to 1941 K. Thus, he used the solid Ti descriptions for 1150-1941 K at higher temperatures, as well. As a consequence, he found that the bcc phase is predicted to become stable above 5133 K but that is no practical problem. On the other hand, if one would insist on using Dinsdale's original description and combine it with Jonsson's set of parameter values for the Ti-N system, the differences would be relatively small and only occur in a high temperature region where there in no reliable experimental information. The congruent melting point of TiN_{1-x} would probably be about 20 K lower, which is within the experimental uncertainity.

There is much information on the partial pressures P_{Ti} and P_{N2} over the δ phase but the accuracy is probably not very high. Jonsson concluded that it may be "necessary to reproduce only the general information such as temperature and composition dependence...". Zeng et al. accepted this view. In spite of this, they made a new assessment but their results are very similar to Jonsson's.

Eron'yan et al. [76Ero] have published a series of measurements of P_{N2} at the melting of δ-TiN_{1-x} of different initial compositions which deserves special mention . When plotting their data they found it necessary to use a line with a sharp break. Ohtani et al. [90Oht] explained this by calculating a line with a very strong curvature but were not able to get a very good fit. Another explanation was given by Jonsson [96aJon] who proposed that the points in the lower temperature region concern the single-phase δ below the melting range. Those points were found to fall close to a line calculated for $TiN_{0.82}$. Zeng et al. did not accept this explanation but were not able to fit those data to the δ/liquid equilibrium better than Ohtani et al. Thus, their assessment did not differ much from Jonsson's in this respect.

2.4 Terminal Ti-N phases

Pure Ti exists as α(hcp) and β(bcc). For the α phase Jonsson chose the model

$Ti_2(Va,N)_1$ which yields Ti_2N_1 as a realistic end-member. This was accepted by Zeng et al. The β phase was modelled as $Ti_1(Va,N)_3$ in all assessments and that is the usual choice for a bcc phase. The experimental information on α+β close to the transition point for pure Ti seems to be well established by Palty [54Pal] but the peritectic equilibria for L+δ→α and L+α→β are more uncertain.

The main difficulty in the high Ti region seems to be the α/δ equilibrium where Jonsson chose to rely on data from Wolff et al. [85Wol], Etchessahar et al. [84Etc] and Lengauer et al. [88Len], whereas Zeng et al. trusted Palty [54Pal] and two tie-lines from a more recent unpublished work by Lengauer [91Len]. They also claim to have used the information from another study by Lengauer et al. but that is not indicated by the result of their assessment. Both assessments yield fairly straight and parallel phase boundaries. Jonsson's two-phase field is narrow and falls inside the wider two-phase field by Zeng et al. In their discussion they seem to agree with Jonsson on what the maximum N content of α should be at temperatures around 1300 K, where intermediary phases appear, but they would need a temperature dependent interaction parameter in the α phase in order to reconcile such high N contents with the lower N contents according to the two tie-lines by Lengauer [91Len] which fall at about 1600 and 1900 K. However, they did not try to do this. Instead, they claim that their description is supported by information on two intermediary phases, ζ and η, and unpublished information on the Ti-Ni-N system , Friec et al. [95Fri].

2.5 Intermediary Ti-N phases

An ε phase of an approximate composition Ti_2N is stable below about 1338 K. It is usually proposed to form by a peritectoid reaction but Wriedt et al. [87Wri] emphasised that the probable position of the (α+δ)/δ phase boundary would result in a congruent transition ε→δ if the composition of ε is Ti_2N. Evidently, the phase diagram could be modified in three ways to yield a peritectoid reaction, (1) by assuming that ε at its highest temperature has less N than according to TiN_2, (2) by moving the (α+δ)/δ phase boundary to higher N contents, (3) by introducing another intermediary phase above the ε phase. Zeng et al. considered it a very important conclusion that ε does not form congruently from δ and they wanted the phase diagram to show this. Indeed, they were able to predict a peritectoid transformation by accepting the higher N contents of the (α+δ)/δ boundary, indicated by Lengauer's [91Len] two tie-lines, and the existence of a new intermediary phase, η. On the other hand, from a practical point of view, it does not seem very important to reproduce the correct reaction for ε. It may be more important to establish the composition of ε by new experiments. In particular, it does not seem justified to accept the higher N content of the (α+δ)/δ phase boundary from Lengauer's [91Len] two tie-lines just because it contributes to the suppression of the congruent transformation point of ε under the assumption that ε is Ti_2N.

Lengauer and Ettmayer [88Len] first found the two new intermediary phases, ζ-Ti_4N_{3-x} and η-Ti_3N_{2-x} , existing close to the maximum temperature of ε and reacting with ε in two ways each. Zeng et al. reproduced the reported reaction temperatures

with high precision whereas Jonsson chose not to include them in his assessment.
It should also be mentioned that an ordered δ phase, denoted by δ', has been reported. It is natural to expect that δ should order at low temperatures, primarily with Ti_2N_1 as the ideal composition. However, the information on δ' is not quite clear and Zeng et al. proposed that δ' only occurs as a metastable phase. They did not include it in their assessment, nor did Jonsson.

When comparing the assessments of the Ti-N system by Jonsson and by Zeng et al., the inclusion of the ζ and η phases in the latter one may look as a major difference. However, they can probably be easily added to Jonsson's description without changing the parameters of the other phases if the experimental temperatures and compositions are accepted. On the other hand, it is puzzling that two phases should occur so close to each other and in such a narrow range of temperature. An independent check of the range of existence of all three, δ, ε and η, is needed before their role in the Ti-N phase diagram can be assessed with any certainity. It may be added that more information is also needed for the ordered δ' phase. Jonsson's assessment of the whole Ti-N system is thus preferred in the present work.

3. Application of the descriptions of TiN and Ti-N to higher order systems

G_m of TiN and the description of the Ti-N system should then be tested against information on higher-order systems of direct interest. In this case one should examine the Fe-Ti-N and Al-Ti-N systems.

3.1 The Fe-Ti-N system

Due to its technical importance the solubility of TiN in fcc-Fe has been examined many times and several equations for its variation with temperature have been proposed, [60Gur], [62Ada], [75Nar], [78Mat], [85Wad], [89Tur] and [82Kun]. See Table 1. These data can be compared with values calculated termodynamically by Jonsson [97Jon]. His value agrees well with Kunze [82Kun] and falls below Wada and Pehlke [85Wad] by a factor of about 2. However, it must be remembered that the termodynamic calculation depends on the descriptions of N in fcc-Fe and of Ti in fcc-Fe. The Fe-N system is probably well established, Frisk [91Fri], but not the Fe-Ti system.

Jonsson made similar calculations for L-Fe and δ-bcc-Fe finding a deviation of about 3 on the higher side, see Figs.3 and 4. To improve this requires a modification of the Fe-Ti system. A recent assessment, made by Saunders [97Sau], gave a good fit of the solubilities in L, see Fig.4, and bcc but lowered the solubility product in fcc by a factor of about 6. That would be closer to old measurements. See also the last value in Table I.

TiN may be non-stoichiometric and that should increase its stability. However, that effect was already taken into account in Figs.3 and 4.
In summary, it may be stated that Saunders has shown that the experimental

information on the Fe-Ti system can be well accounted for with a description that will also give reasonable agreement for the solubilities of TiN in liquid Fe and bcc-Fe using Jonsson's [96aJon] description of TiN. On the other hand, it will predict a solubility of TiN in fcc-Fe which is lower than recent experimental values, but in the direction of older values.

3.2 The Al-Ti-N system

It is interesting to examine the Al-Ti-N system because Al-Ti-C will also be involved in this paper and the Al-Ti is common to them. Zeng et al. [97Zen] discussed four-phase equilibria in Al-Ti-N and found agreement when he used an Al-Ti description according to Zhang et al. [96Zha] but not according to Al-Ti by Saunders [94Sau]. Saunders thinks he can make his Al-Ti work here after a very slight adjustment of the intermetallic phases.

Chen [97Che] has tested, for the assessment of the Al-Ti-N system, both descriptions of Al-Ti, [96Zha] and [94Sau], together with Jonsson's [96aJon] assessment of the Ti-N. Jonsson's assessment of the Ti-N system and Saunders assessment of the Al-Ti system work very well together and allow to describe the ternary experimental information easily.

4. TiC and the Ti-C system

All the assessments of the Ti-C system, [96bJon], [97Dum], [95Alb] and [96Sei], begin with an assessment of the stoichiometric TiC and therefore we will first consider C_P and $H-H_{298}$, which is closely related to C_P.

4.1 TiC

We will consider assessments of the Ti-C systems by Jonsson [96bJon], Dumitrescu [97Dum] , Albertsen et al. [95Alb] and Seifert et al. [96Sei]. For the stoichiometric TiC Jonsson used an expression $C_P = -c - 2dT - 2eT^{-2} - 12fT^{-4}$. The first two terms describe a rectilinear asymptot at high temperatures. The third term is necessary for describing the strong increase in C_P from room temperature and up to the high-temperature asymptot. The fourth term made it possible for Jonsson to fit C_P data down to 200 K.

In Fig.5 Jonsson's description for C_P is compared with experimental data and the description given by JANAF [85JAN]. The experimental data from different studies do not agree well with each other and Jonsson's description is a reasonable compromise. It may be objected that JANAF with its larger slope at high temperatures is a better description. However, it should be remembered that these data points have been derived from measurements of $H-H_{298}$. Fig.6 is a better test and it shows an excellent agreement of Jonsson's assessment with the primary H data, except for the highest point. At low temperatures Jonsson's C_P description is satisfactory down to 200 K.

Albertsen et al. used an expression $C_p = C_p^{fccTi} + C_p^{graphite} - c - 2dT$. Thus, they could

only fit the high-temperature asymptot and obtained a reasonably good description of data for $H-H_{298}$ at high temperatures, very close to Jonsson's. However, in the low-temperature region they had to accept the deviation from a straight line that $C_p^{fccTi} + C_p^{graphite}$ gave. This situation is almost the same for Seifert et al. who used an expression for $C_p = C_p^{hcpTi} + C_p^{graphite} - c - 2dT$.

The assessments by Albertsen et al. and by Seifert et al. are related because they both did not fit the C_P data down to room temperature. In this respect the assessments by Albertsen et al. and by Seifert et al. are not very satisfactory. It should also be mentioned that Seifert et al. predict decreasing values of C_P for TiC at high temperatures. That is an unfortunate artifact caused by their strategy of primarily considering the difference in C_P between TiC and a mixture of graphite and hcp Ti and also accepting a gradual decrease of C_P for hcp Ti above the melting point of Ti, according to the description given by Dinsdale [91Din].

The complete expression for the Gibbs energy of TiC used by Jonsson was $^oG_{TiC} - H^{SER} = a + bT + cTlnT + dT^2 + eT^{-1} + fT^{-3}$. He determined the b parameter by fitting the value of S_{298} evaluated by Kelley and King [61Kel] by integration of C_P from 0 K. Finally, the a parameter could be evaluated from the heat of formation at 298 K. It was measured to -183.47 kJ/mol TiC by Humphrey [51Hum] but was also measured by others, [61Low], [91Lih], [78Mas], [89Ber], [92Kor] and [61Fuj]. De Boer's [88DeB] value is about 30 kJ/mol TiC higher and such a high value is supported by other studies. This difference would decrease the solubility product of TiC in various solvents by a factor of about exp(30000/8.3145·1473)=12 at 1473 K. It is unfortunate that this information shows such a strong scatter. See Fig.7. Jonsson first tried to use Humphrey's value after a small correction, $\Delta_f {}^oH_m(298) = -184.4$ kJ/mole TiC, but was not able to fit all the information on the δ-TiC_{1-x} solution phase very well. The a parameter was then used as an adjustable parameter in the subsequent assessment of the whole Ti-C system.
However, Jonsson realised that information can also be obtained from ternary systems showing equilibria with TiC. He thus combined his assessment with information on the δ-Ti(C,N)+graphite +gas equilibrium in the Ti-C-N system. His final value was $\Delta_f {}^oH_m(298) = -188.0$ kJ/mole TiC, which differs by only 4.5 from the experimental value by Humphrey. The experimental uncertainty was given as ± 11.6. Jonsson then found that the same value worked well in the Ti-W-C [96dJon] and Ti-C-N [96cJon] systems. When determining the a and b parameters, Albertsen et al. did not use the value of S_{298} which would not have been logical because their C_P values are not accurate down to that temperature. Instead, they combined information on $\Delta_f {}^oH_m(298)$ with information on the δ-TiC_{1-x} solution phase to evaluate both a and b. Unfortunately, they used information on activities of Ti presented by themselves in a recent paper and that information differs significantly from the results of other studies. Albertsen et al. did not check on the consequences for the Ti-C-N or W-Ti-C, nor for Fe-Ti-C for which Jonsson's, [96dJon] and [97Jon], assessments were not yet available. The situation was similar for Seifert et al. and they used the same strategy and determined the a and b parameters from an assessment of the whole Ti-C system. Their main objection to Jonsson's assessment of the Ti-C system is his choice of value for $\Delta_f {}^oH_{TiC}^{\delta}$ at 298 K. Seifert et al. found that a less negative value, in

approximate agreement with de Boer, would be needed in order to describe the $L+Al_3Ti+Al_3C_3+TiC$ equilibrium in the Al-Ti-C system [96cJon]. To get a heat of formation of TiC they considered reasonable they found it necessary to use five independent parameters for the description of the liquid phase. Jonsson and Albertsen et al. used only two. In a recent assessment Dumitrescu accepted Jonsson description of C_P and S_{298} but for $\Delta_f {}^oH_{TiC}^{298}$ she chose a value as high as possible (i.e. less negative) with respect to measurements, having the same arguments as Seifert.

4.2 Binary system Ti-C

So far we have only considered stoichiometric TiC. We may also like to present the whole of the binary Ti-C system. Fig.8 shows a comparison between three of the existing descriptions of the Ti-C system [96bJon], [97Dum] and [96Sei].

The solution properties of δ-TiC_{1-x} according to Jonsson, Dumitrescu and Seifert et al. are fairly similar but Albertsen et al. have a different description because they wanted to fit their own data in preference to several other studies. For the liquid phase Seifert et al. used five parameters in order to fit information primarily concerning other phases. That may be a dangerous strategy. For example, their liquidus line shows two inflexion points close to the Ti side. Jonsson and Dumitrescu used only two parameters for the liquid. Albertsen et al. and Seifert et al. also differ from Jonsson and Dumitrescu on the solubility of C in the β phase. Admittedly, the information on the solubility of C in α and β may not be very well established experimentally but it does not seem as a natural choice to trust the information from Cadoff et al.[53Cad] on the α phase, Fig.9, but not on the β phase, Fg.10.

All the assessments show a very strong temperature dependence of the solubility of C in the α phase, in agreement with information from Cadoff et al. By using only one adjustable parameter Jonsson and Dumitrescu reproduced a similar temperature dependence for the β phase, in agreement with information from Cadoff et al. Albertsen et al. used two independent parameters and calculated a solubility almost independent of temperature. Seifert et al. did the same but then they had to use a very large third Redlich-Kister parameter in the liquid in order to adjust the eutectic composition. Dumitrescu has now reassessed the Ti-C system using her higher value of $\Delta_f {}^oH_m(298)$ for TiC and got a reasonable result showing a variation of the solubility in α with temperature.

It is recommended that one should use the assessment by Dumitrescu, which is very close to Jonsson's, except for the choice of a different value of $\Delta_f {}^oH_m(298)$.

5. Application of the descriptions of TiC and Ti-C to higher order systems

G_m of TiC and the description of the Ti-C system should then be tested, as it was done for TiN, against information on higher-order systems of direct interest.

5.1 Ti-C-N

Jonsson combined his descriptions of the Ti-C and Ti-N systems to describe the Ti-C-N [96cJon] system but had to introduce strong ternary interactions, in particular in the TiC-TiN section. Before a similar attempt was made, using the new assessment of the Ti-C system by Dumitrescu, an analysis was made of the information on the equilibrium between titanium carbonitrides of various compositions and liquid Fe [90Ozt]. It indicated that the interaction energy in the TiC-TiN section may be around -18000 J/mol which is about one third of Jonsson's [96cJon] value. This new value was then used by Dumitrescu in an assessment of the Ti-C-N system, in combination with the new description of Ti-C. Jonsson's [96aJon] description of the Ti-N system was used. The result was rather satisfactory as demonstrated in Figs.11, 12, 13 and 14.

5.2 The Al-Ti-C system

It was pointed out by Seifert et al. [96Sei] that the experimental four-phase temperature for L + TiC + Al_4C_3 + Al_3Ti in the Ti-Al-C system strongly favours the higher values of $\Delta_f {}^0H_{TiC}^{298}$. It should be noticed that the use of this information depends on choices for Al_4C_3 and Al_3Ti. Several alternatives should thus be examined.

The equilibrium temperature has been reported to be 1085 K which is not far from the melting point of Al. Thus, G_m of pure liquid Al at this temperature is well established. The effect of Ti and C on G_m of L is not very large because of the low contents of Ti and C. One can thus use any descriptions of the liquid phase in the Al-Ti and Al-C systems in a calculation of the four-phase equilibrium. G_m of Al_3Ti is obtained from assessing the Al-Ti system. There are two such assessments, by Saunders [94Sau] and by Zhang [96Zha]. We should thus use two values in our test. For Al_4C_3 an older value was used by Gröbner et al. [95Grö] but recently Meschel [95Mes] gave a different value and Lukas [96Luk] modified the Al-C system description. For TiC Jonsson's [96bJon] description gave very low values and the experimental temperature thus gives strong preference for less negative value. Dumitrescu's value gave the following values

[94Sau] + [96Luk]	908 K
[94Sau] + [95Grö]	1061 K
[96Zha] + [96Luk]	854 K
[96Zha] + [95Grö]	1033 K

These results give strong preference for the old value of Al_4C_3 and some preference for Saunders' [94Sau] description of Al-Ti.

5.3 The Ti-Ni-C system

Schuster et al. [97Sch] have studied the solubility of TiC in fcc Ni at equilibrium with graphite and compared with calculations and previous experiments. Experiments fell between calculated results based on Jonsson's , Fig.15, and Dumitrescu's values for TiC, Fig.16. However, Schuster et al. used an assessment of Ni-Ti by Bellen [96Bel].

With Saunders [95Sau] assessment of the Ni-Ti binary there is better agreement for Dumitrescu's value for TiC, Fig.17.

5.4 The Fe-Ti-C system

For Fe-Ti-C Jonsson [97Jon] obtained excellent agreement but we wanted to use the new description of TiC from Dumitrescu's assessment of Ti-C. It will now be demonstrated that introduction of the reassessment of the Fe-Ti system by Saunders [97Sau] compensates for the less negative value of $\Delta_f {}^{\circ}H^{298}_{TiC}$ and the agreement is still excellent .

There is an isoactivity line for Ti in L and also information on the point L/graphite + TiC. Fig.18 and Fig.19 show that the same good fit can be obtained with Saunders' Fe-Ti and Dumitrescu's Ti-C if the ternary interaction for the L phase is reassessed. Recent reports on the solubility in fcc-Fe [92Bal] are also well described with Dumitrescu's choice, see Fig. 20. Here the ternary parameter is of some but less importance.

There are also several expressions for the solubility product of TiC in fcc-Fe, [75Nar], [85Oht], [67Irv], [65Chi] and [74Wil], see Table II. When interpreting them, one should realize that the solubility curve is not quite hyperbolic in this case because the solubility of TiC is much higher than of TiN. However, below x_C=0.01 (m%C=0.2) it is fairly hyperbolic, see Fig. 20, and the expressions probably refer to such low C contents. A comparison is given in Table II. These expressions agree reasonably well with Ohtani's [85Oth] values which were considered in Fig. 20 and the assessments by Jonsson [96bJon] and by Dumitrescu [97Dum] are in close agreement with Ohtami's values.

Table I. Solubility product of TiN in fcc-Fe

The solubilities are low and the product should thus be reasonably constant at each temperature. With log(m%Ti·m%N)=A-B/T one has reported

A	B	A-B/1473	Ref.
6.75	19740	-6.65	[60Gur]
2.0	20790	-12.11	[62Ada]
3.82	15020	-6.38	[75Nar]
0.322	8000	-5.11	[78Mat]
4.94	14400	-4.84	[85Wad]
5.4	15790	-5.32	[89Tur]
5.19	15490	-5.33	[82Kun]
calculated		-5.17	[97Jon]
calculated		-5.87	present

Table II. Solubility product of TiC in fcc-Fe

A	B	A-B/1473	Ref.
2.75	-7000	-2.00	[67Irv]
5.33	-10475	-1.78	[75Nar]
5.54	-11300	-2.13	[75Nar]
4.37	-10580	-2.81	[65Chi]
2.97	-6780	-1.63	[74Wil]
		-1.95	[85Oht]
calculated		-1.95	[97Jon]
calculated		-1.95	present

6. Conclusion

It seems that Jonsson's assessment of the whole Ti-N system can be retained for the time being. It could be argued that one should now reassess the Ti-N system using Jonsson's description of the TiN but with due account of the two new intermediate phases. However, it is recommended that this should be postponed until their range of existence in composition and temperature has been confirmed by independent measurements.

Dumitrescu's assessment of the Ti-C system is recommended because it seems to be base on the best description of TiC. Jonsson tested his description of the Ti-C system on an assessment of Ti-C-N and got an excellent result. However, it seems that with Dumitrescu's assessment of the Ti-C system it is also possible to get a reasonable assessment not only for Ti-C-N but also for other Me-Ti-C (where

Me=Al, Ni, Fe) systems.

Compared to Fe-Ti-C there is less information on the corresponding systems with the W or Co instead of Fe but they should be examined in this connection.
It remains to try to reassess the W-Ti-C and Co-Ti-C systems with the new description of TiC and Ti-C.

7. References

51Hum Humphrey G.L., J.Am.Chem.Soc.73 (1951) 2261-2263
53Cad Cadoff I., Nielsen J.P., J.Metals 5 (1953) 248-252
54Pal Palty A.E., Margolin H., Nielsen J.P., Trans ASM, 46 (1954) 312-328
60Gur Gurevic J.G., Gernaya Metallurgija, No.6 (1960) 59
61Kel Kelley K.K., King E.G., Bull. US Bur.Mines 592 (1961)
61Low Lowell C.E., Williams W.S, Rev.Sci.Instrum.,32 (1961) 1120-1123
62Ada Adachi A. Mizukawa K., Kanda K., Tetzu to Hagane, 48 (1962) 1436
65Chi Chino H., Wada H., Jawata Techn.Rep. 251 (1965) 5817-5842
66Mor Morozova, M.P.,and Khernburg M.M., Russ.J.Phys.Chem. 40 (1966) 604-606
67Irv Irvine K.J., Pickering F.B., Gladman T., J.Iron Steel Inst., 205 (1967) 161-182
74Wil Williams , Harries , The Metals Soc. (1974) 152

75Nar Narita K., Trans. ISI, 15 (1975) 145-151

76Ero Eron'yan M.A., Avarbe R.G., Danisina T.N., High Temperature 14 (1976) 359-360

78Mas Maslov V.M., Neganov A.V., Borovinskaya I.P., Merzhanov A.G., Fiz.Goreniya Vzryva, 14(6) (1978) 73-82

78Mat Matsuda S., Okumura N., Trans. ISIJ, 18 (1978) 77

82Kun Kunze J., Metal Science, 16 (1982) 217-218

84Etc Etchessahar E., Bars J.P., Debuigne J., Less Comm.Metals, 134 (1984) 123-139

85JAN JANAF Thermochemical Tables, 3rd ed.,J.Phys.Chem.Ref.Data 14 (1985) Suplement No.1

85Oth Ohtani H., Tanaka T., Hasebe M., Nishizawa T., Solubility of NaCl-Type Carbides (NbC, VC and TiC) in Austenite. Japan-Canada seminar on Secondary Steelmaking, Dec.3-4 (Tokyo, Japan) (1985) J-7 -12

85Wad Wada H. and Pehlke R.D., Metall Trans.B, 16B (1985) 815-822

85Wol Wolff L., Bastin G., Heijligers H., Soid State Ionics, 16 (1985) 105-112

87Wri Wriedt H.A., Murray J.L., Bull.Alloy Phase Diagrams, 8 (1987) 378-388

88DeB De Boer F.R, Boom R., Mattens W.C.M., Miedema, Niessen A.K., Cohesion in Metals, Cohesion and Structure, vol.1 1st ed., (1988)

88Len Lengauer W., Ettmayer P., Mater. Sci.Eng. A, 105/106 (1988) 257-263

89Ber Berkane R., thesis, Universite de Nancy I (1989)

89Tur Turkdogan E.T., Trans Iron Steel Inst. (1989) 61-75

90Oht Ohtani H. and Hillert M. CALPHAD 14 (1990) 289-306

90Ozt Ozturk B., Frerehan R.J., Metall.Trans., 21 B (1990) 879-884

90Via Viala J.C., Vincent C., Vincent H., Bouix J., *Thermodynamic Approach to the Interaction Chemistry Between Aluminium and Titanium Carbide*, Mater.Res.Bull.,25 (1990) 457-464

91Din Dinsdale A. CALPHAD 15 (1991) 317-425

91Fri Frisk K., CALPHAD, 15 (1991) 79-106

91Len Lengauer W., Acta Metall.Mater.39 (1991) 2985-2996

91Lih Lihrmann J.M., Herve P., Petitet J.P., 2 nd European Ceramic Society Conference, Augsburg (Germany) (1991)

92Bal Balasubramanian K., Kroupta A., Kirkaldy S.J., Met.Trans.A, vol.23 A (1992) 709-727

92Cla Clark E.B. and Roebuck B., *Extending the Application Areas for Titanium Carbonitride Cermets, Refractory Metals & Hard Materials* 11 (1992) 23-33

92Ko Kornilov A.N., Chevlovskaya N.V., Shveikin G.P., Khim.Fak.,Mosk. Gos. Univ.,Moscow, Deposited Doc., VINITI (1982) 987-992

92Lee Lee B.J., CALPHAD, 16(2) (1992) 121-149

92 Zou Zou H. and Kirkaldy J.S., *Thermodynamic Calculation and Experimental Verification of the Carbonitride-Austenite Equilibrium in Ti-Nb Microalloyed Steels*, Metall.Trans. A, 23A (1992) 2, 651-657

93Jon Jonsson S., Ph. D.Thesis*: Phase Relations in Quaternary Hard Materials*, KTH Stockholm, 1993

94Sau Saunders N., COST 507, *Concerted Action on Materials Sciences, Thermochemical Database for Light Metal Alloys*, I.Ansara ed., ECSC-EEC-EAEC, Brussels, (1994) 52

95Alb Albertsen K. and Schaller H-J. *Constitution and Thermodynamic of the*

Ti-C, Z.Metallkd. 86 (1995) 5 319-325

95Grö Gröbner J., Lukas H-L., Aldinger F., *Thermodynamic calculations in the Y- Al-C system*, J.Alloys and Comp. 227 (1995) 93-96

95Fri Friec Y.L., Bauer J., Rogl P., unpublished work, University of Vienna (1995)

95Mes Meschel S.V., Kleppa O.J., *Standard enthalpies of formation of AlB_{12} and Al_4C_3 by high temperature direct synthesis calorimetry*, J.Alloys and Comp. 227 (1995) 93-96

95Sau Saunders N., Ni-Ti , unpublished work

96Bel Bellen P., Hari Kumar K.C., Wollants P., Z.Metallkde, 87(12) (1996) 972-78

96aJon Jonsson S., *Assessment of the Ti-N System*, Z.Metallkd. 87 (1996) 9, 691- 702

96bJon Jonsson S., *Assessment of the Ti-C System*, Z.Metallkd. 87 (1996) 9, 703-712

96cJon Jonsson S., *Calculation of the Ti-C-N System*, Z.Metallkd. 87 (1996) 9 713-720

96dJon Jonsson S., *Assessment of the Ti-W-C System and Calculations in the Ti-W-C-N System*, Z.Metallkd. 87 (1996) 10, 788-795

96Luk Lukas H-L., unpublished work for Al-C modified using Meschel 's calorimetric enthalpy of Al_4C_3

96Sei Seifert H-J., Lukas H.L., Petzow G., *Thermodynamic Optimization of the Ti-C System*, J. of Phase Equilibria, 17 (1996) 1, 24-35

96Zha Zhang F. and Chang Y.A., private comunication (1996)

96Zen Zeng K. and Schmid-Fetzer R. , *Critical Assessment and Thermodynamic Modeling of the Ti-N System*, Z.Metallkd. 87 (1996) 7 540-554

97Che Chen Q., *Thermodynamic Assessment of The Ti-Al-N System*, unpublish work, (1997)

97Dum Dumitrescu L.F.S., Sundman B., *A Thermodynamic reassessment of the Ti-C and Ti-C-N systems*, unpublished work , (1997)

97Jon Jonsson S. *Assessment of the Fe-Ti-C System, Calculation of the Fe-Ti-N System and Prediction of the Solubility Limit of Ti(C,N) in liquid Fe*, unpublished work , (1997)

97Sau Saunders N., *Reassessment of the Fe-Ti*, unpublished work, 1997

97Sch Schuster J.C., Du Y., unpublished work (1997)

97Zen Zeng K. and Schuster J.C., *Thermodynamic Modeling and Applications of the Ti-Al-N Phase Diagram*, presented at Orlando, Florida, Feb.1997

Figure captions

Fig1. Heat capacity of TiN from experiments and calculations.

Fig.2 The Ti-N phase diagram according to the different assessments.

Fig.3 Solubility product of TiN in liquid, bcc and fcc Fe.

Fig.4 Solubility of TiN in liquid Fe at 1873 K.

Fig.5 Heat capacity of TiC from experiments and calculations.

Fig.6 Enthalpy of TiC from experiments and calculations.

Fig.7 Enthalpy of formation of δ-TiC_{1-x} from experiments and assessments.

Fig.8 The Ti-C phase diagram.

Fig.9 Equilibria with α(hcp) in the Ti-C system.

Fig.10 Equilibria with β(bcc) in the Ti-C system.

Fig.11 The TiN-TiC quasibinary section calculated from the new description [97Dum]. The open symbols represent experimental information on the δ/graphite +gas(1bar N_2) corner.

Fig.12 Isothermal section of Ti-C-N at 773 K.

Fig.13 Isothermal section of Ti-C-N at 1423 K.

Fig.14 Isothermal section of Ti-C-N at 1923 K.

Fig.15 Experimental information on the solubility of graphite in the Ni-rich fcc phase in the Ni-Ti-C system at various temperatures. Comparison is made with calculations of the fcc+graphite, fcc+TiC and fcc+graphite+TiC equilibria, using Ni-C from Lee [92Lee], Ni-Ti from Bellen [96Bel] and Ti-C from Jonsson [96bJon].

Fig.16 Same as fig.15 but using Ti-C from Dumitrescu [97Dum].

Fig.17 Same as fig.15 but using Ti-C from Dumitrescu [97Dum] and Ni-Ti by Saunders [95Sau].

Fig.18 The Fe rich corner of an isothermal section of Fe-Ti-C at 1873 K.

Fig.19 Section at a_c=1 through the Fe-Ti-C diagram.

Fig.20 The Fe rich corner of an isothermal section of Fe-Ti-C at 1473 K.

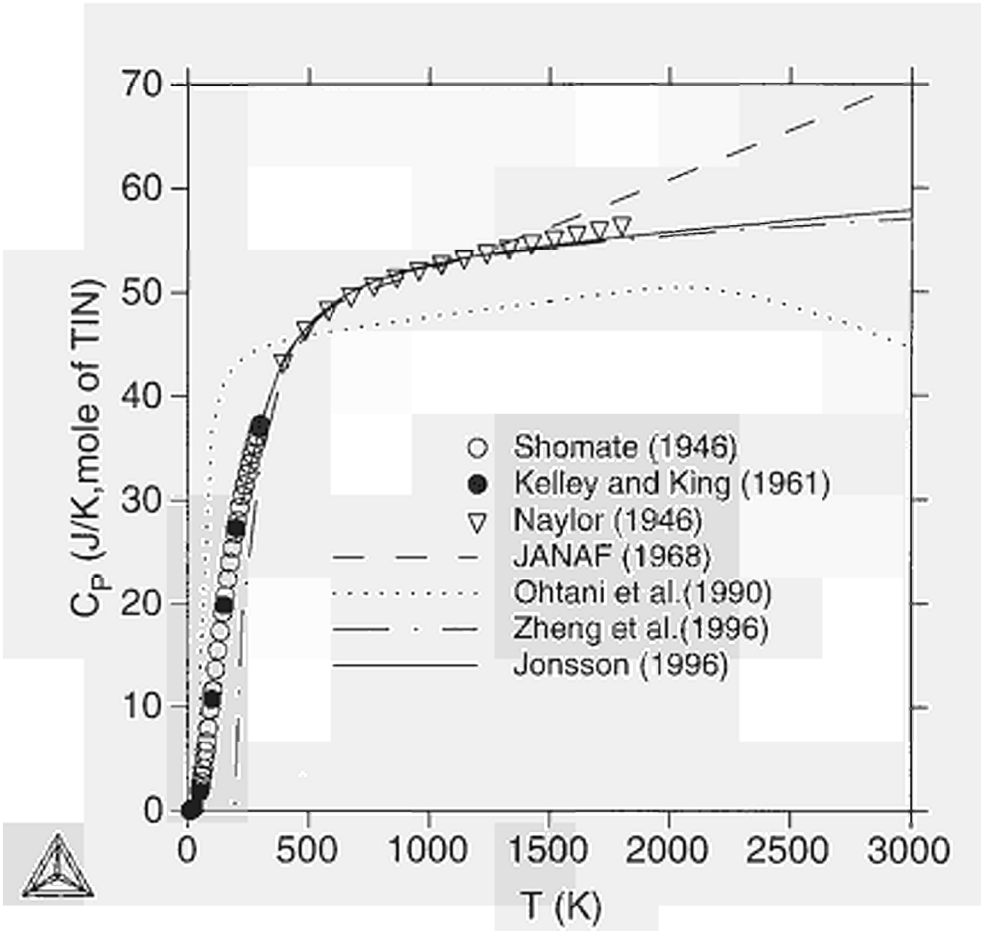

Fig.1 Heat capacity of TiN from experiments and calculations.

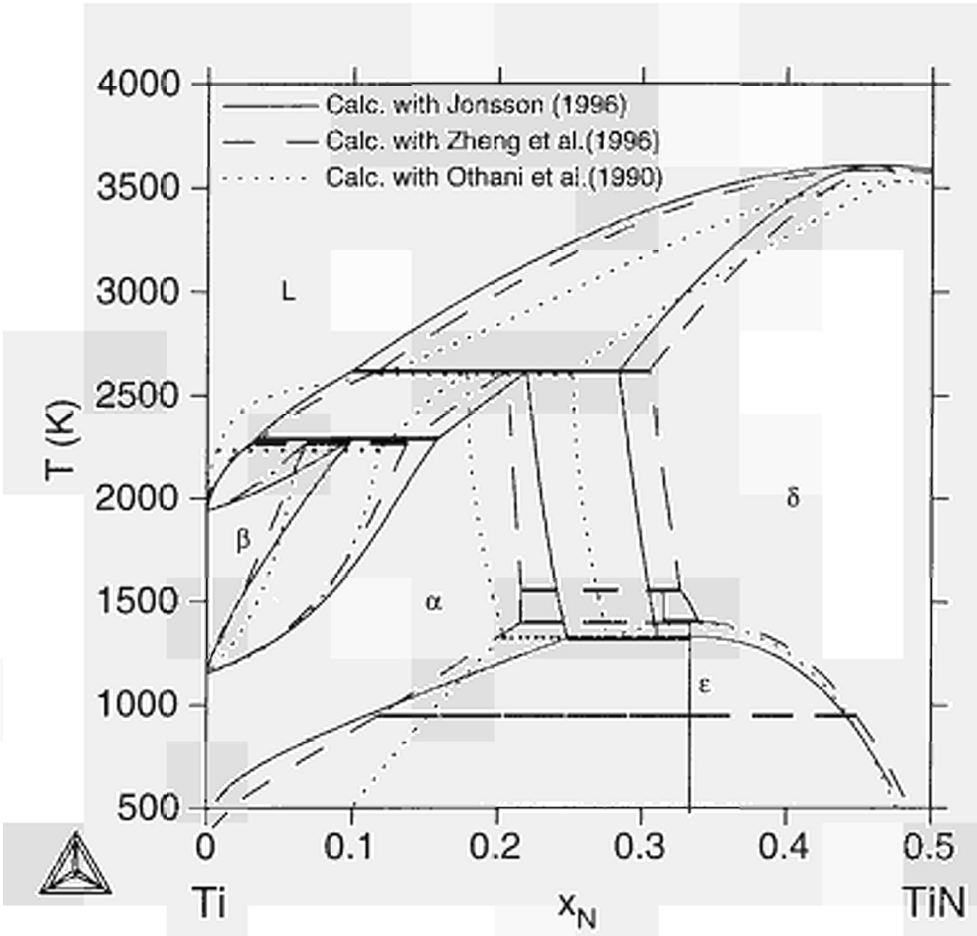

Fig.2 The Ti-N phase diagram according to the different assessments.

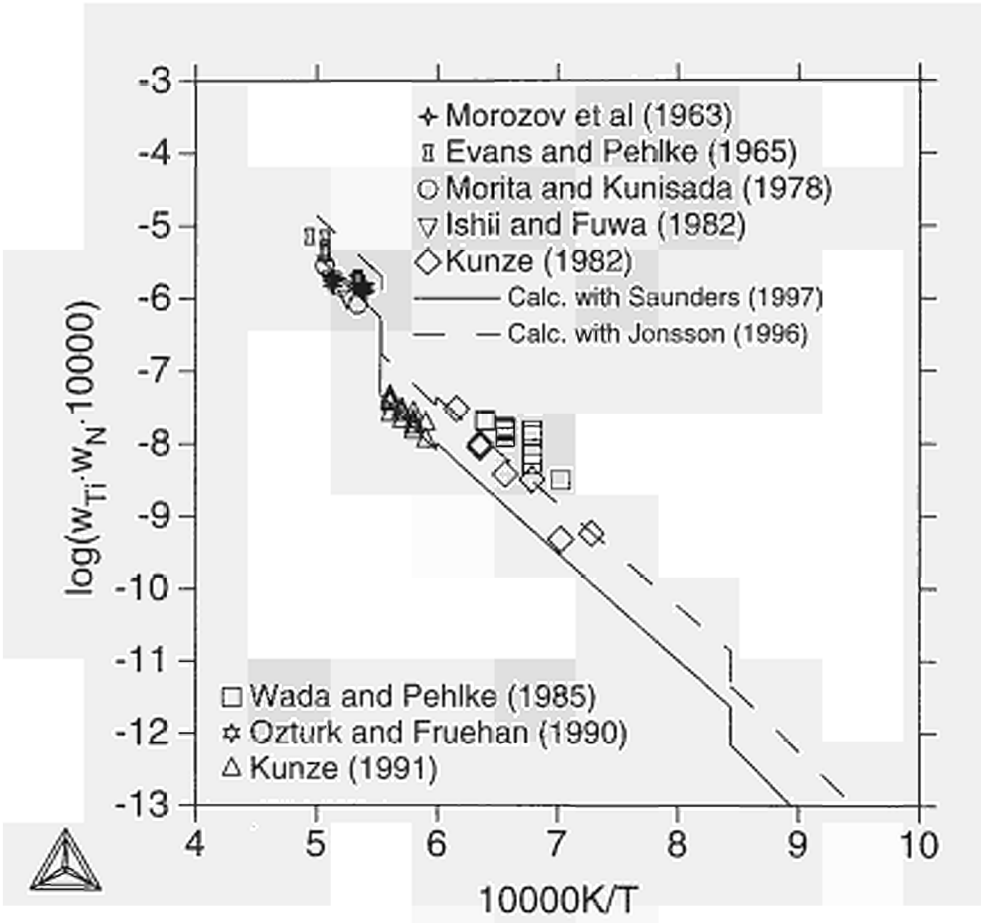

Fig.3 Solubility product of TiN in liquid, bcc and fcc Fe.

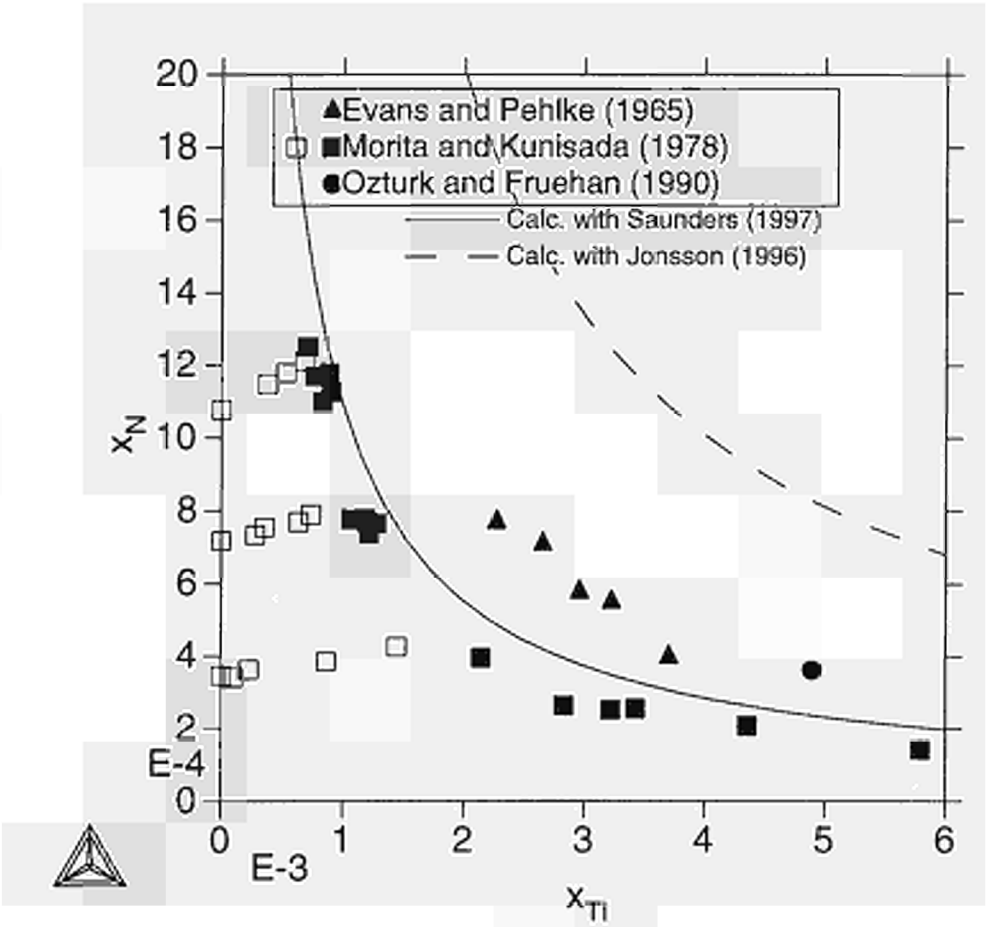

Fig.4 Solubility of TiN in liquid Fe at 1873 K.

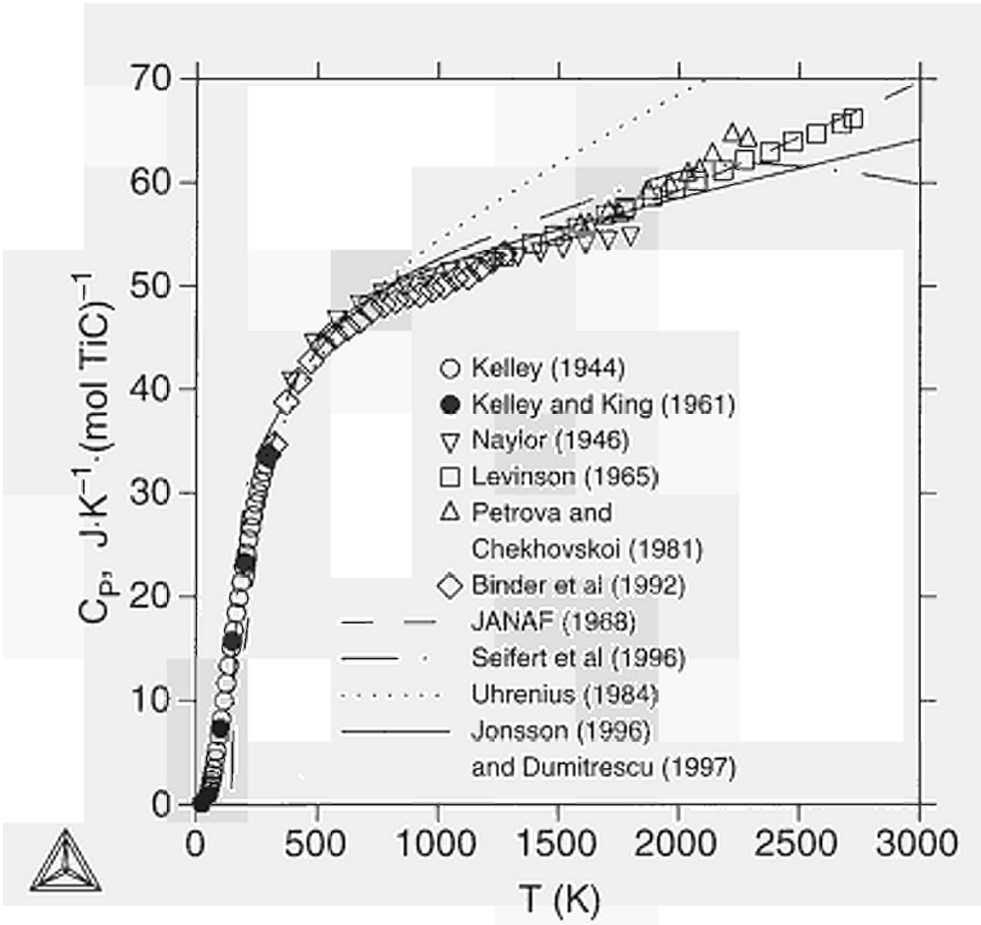

Fig.5 Heat capacity of TiC from experiments and calculations.

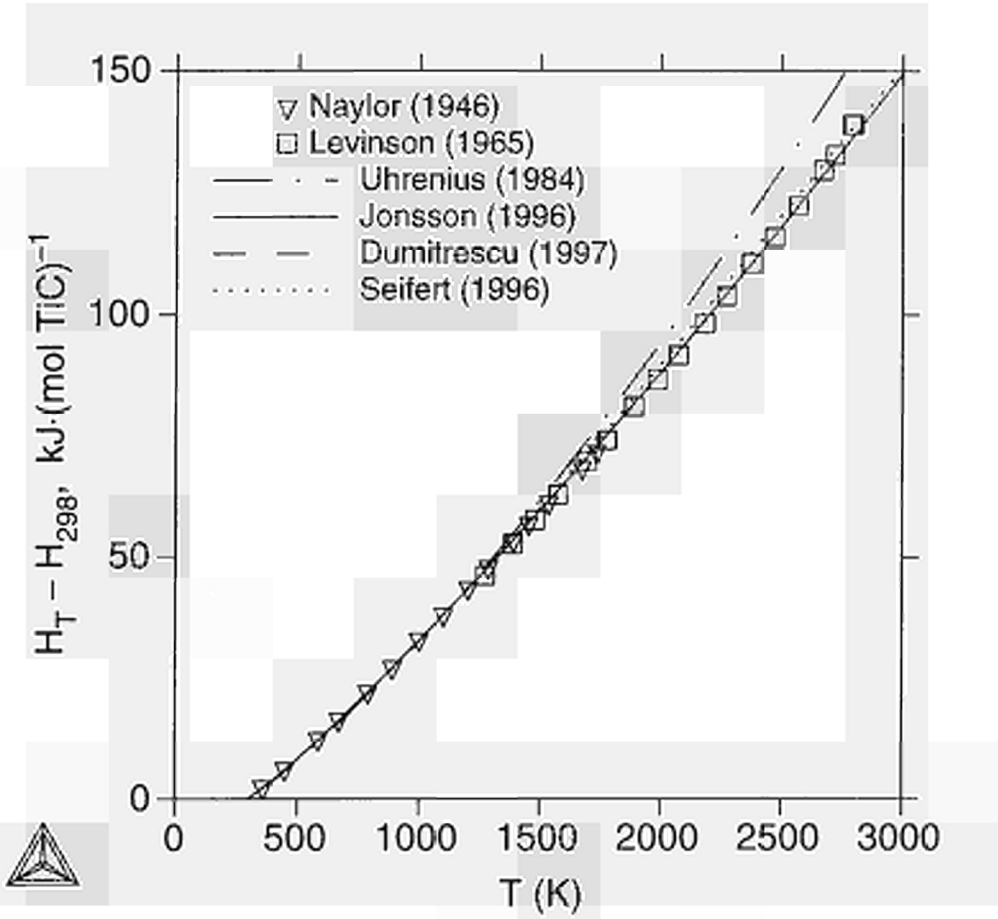

Fig.6 Enthalpy of TiC from experiments and calculations.

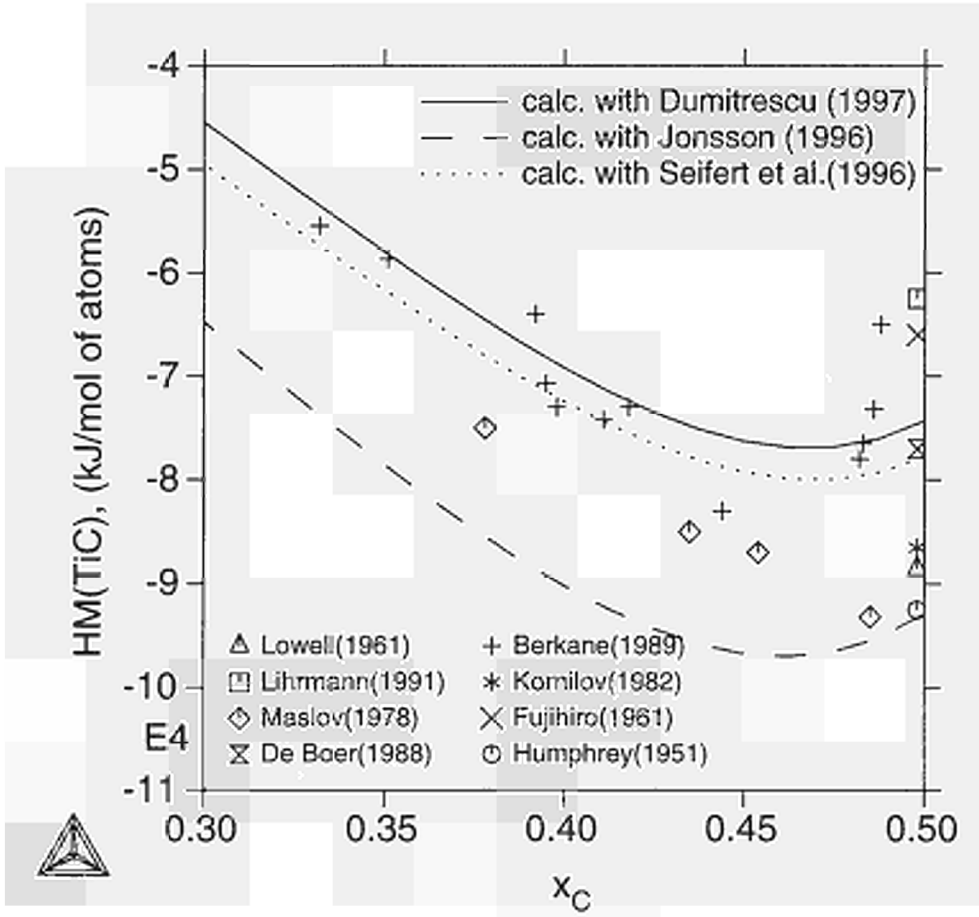

Fig.7 Enthalpy of formation of δ-TiC_{1-x} from experiments and assessments.

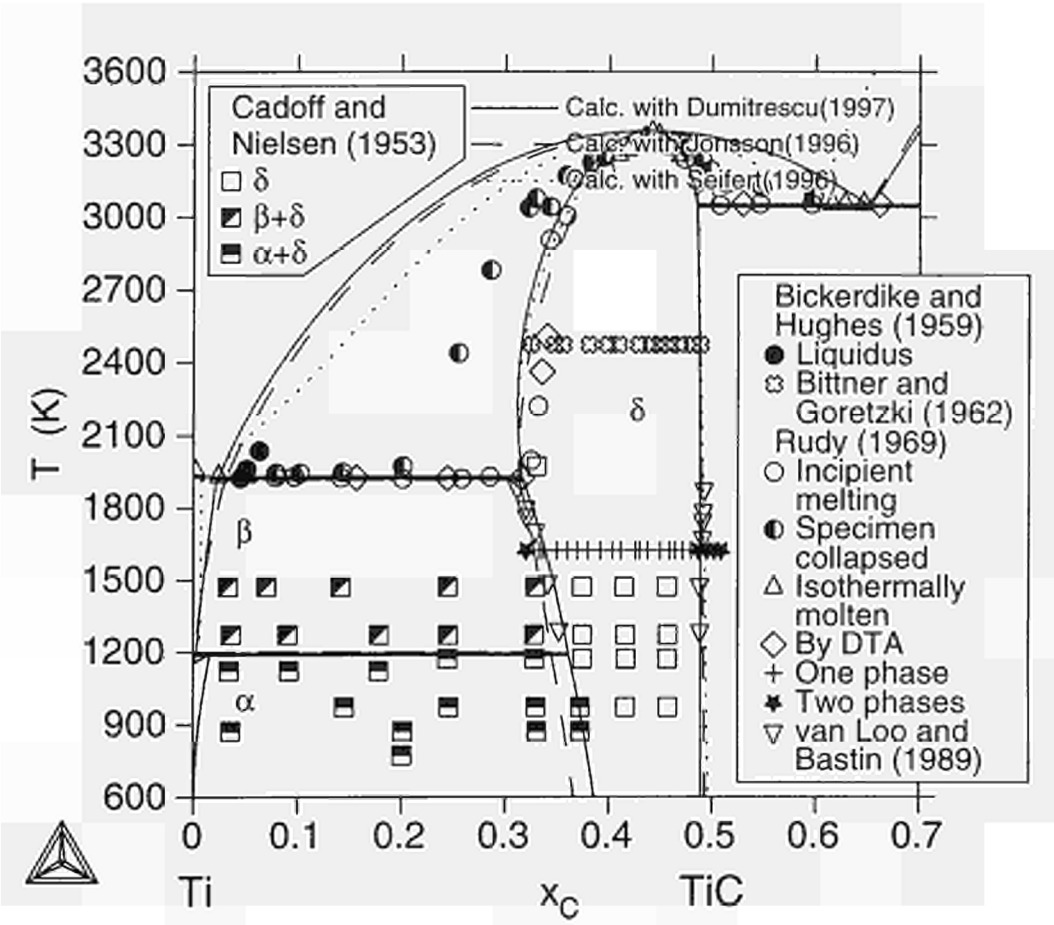

Fig.8 The Ti-C phase diagram.

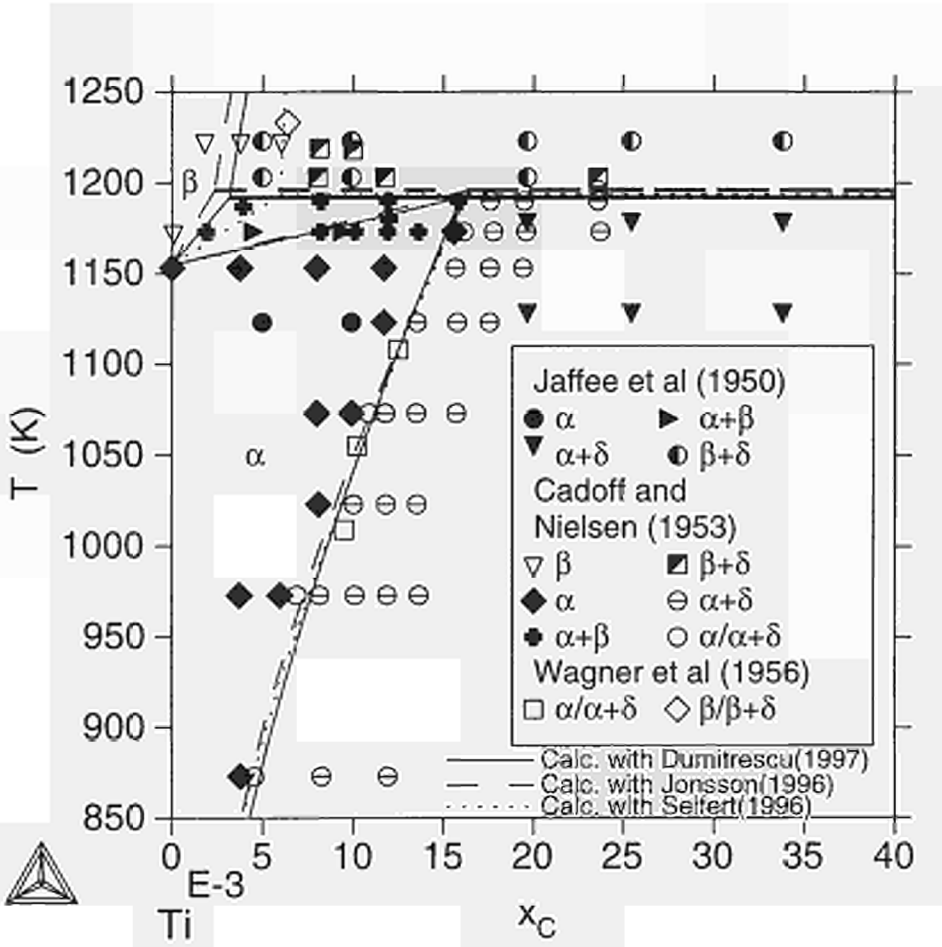

Fig.9 Equilibria with α(hcp) in the Ti-C system.

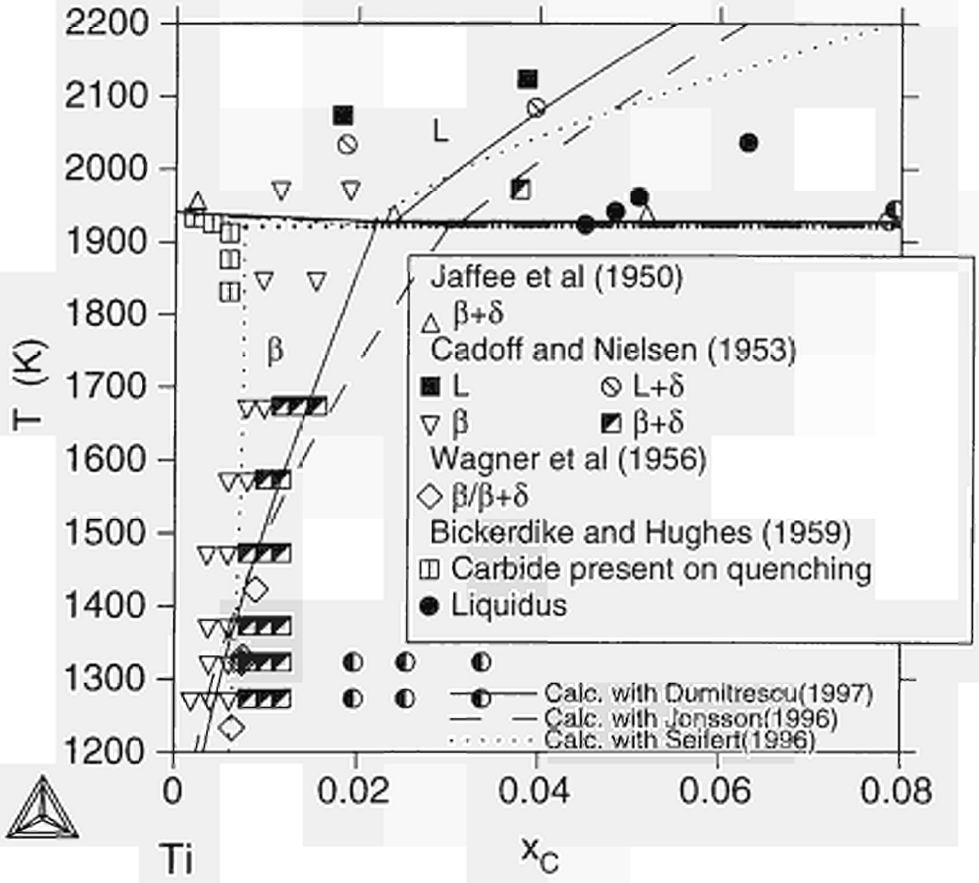

Fig.10 Equilibria with β(bcc) in the Ti-C system.

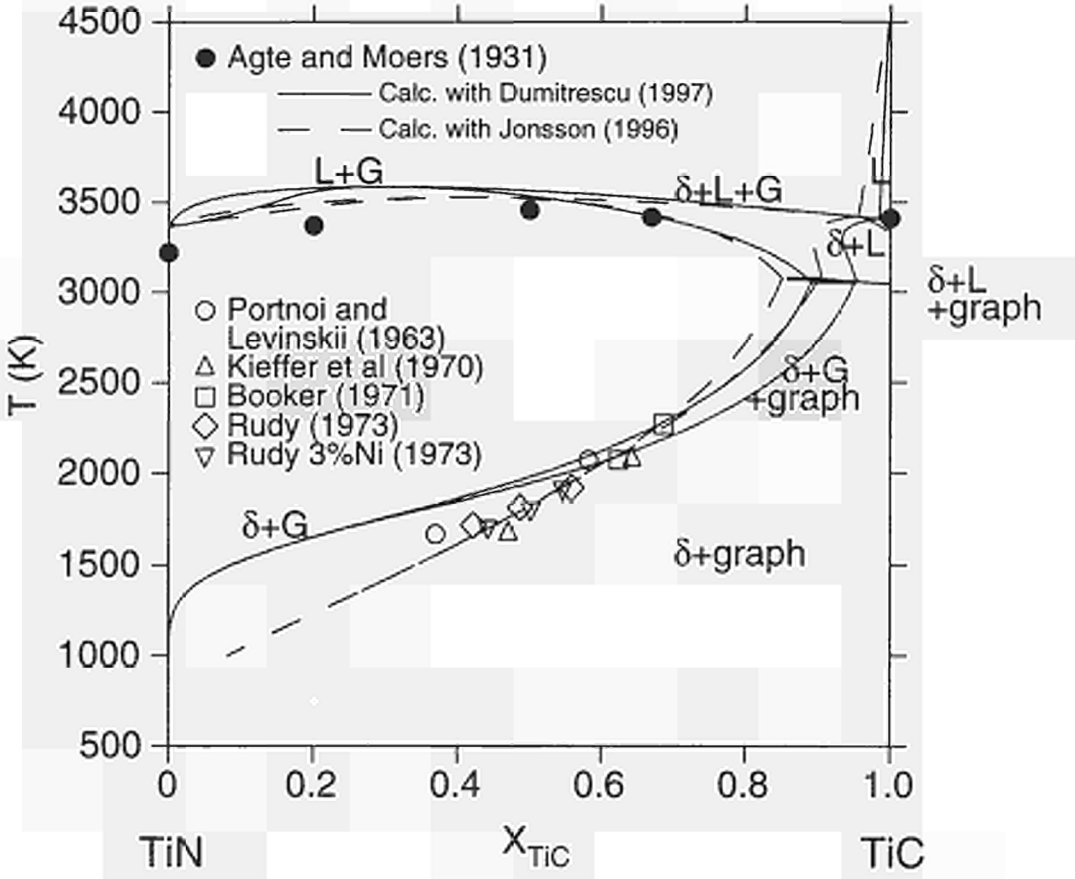

Fig.11 The TiN-TiC quasibinary section calculated from the new description [97Dum]. The open symbols represent experimental information on the δ/graphite+gas (1bar N_2) corner.

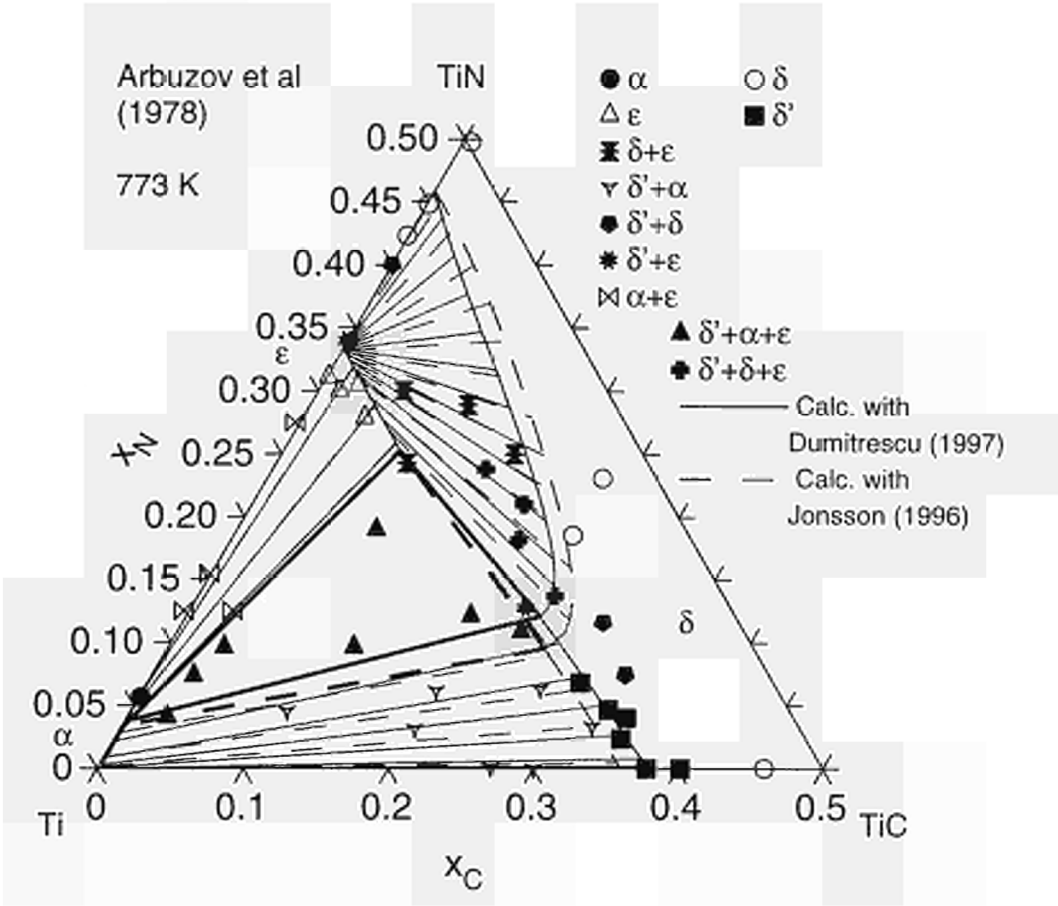

Fig.12 Isothermal section of Ti-C-N at 773 K.

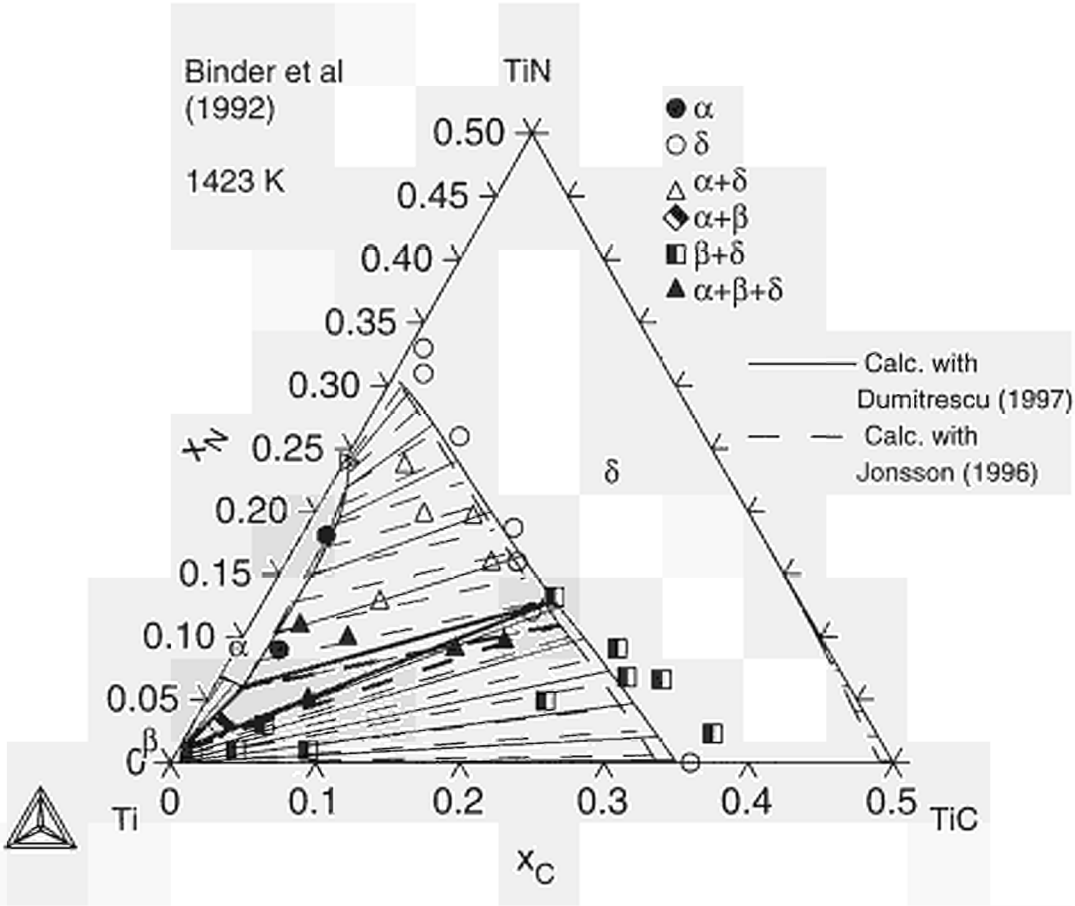

Fig.13 Isothermal section of Ti-C-N at 1423 K.

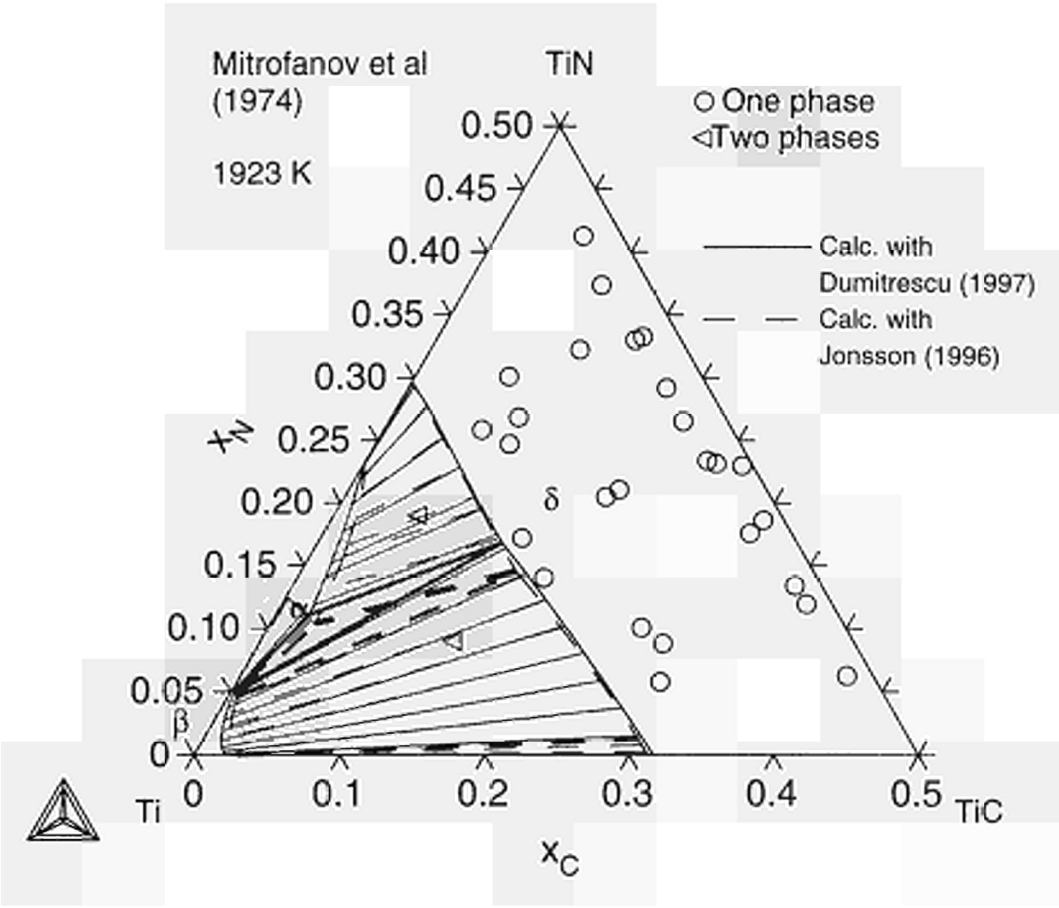

Fig.14 Isothermal section of Ti-C-N at 1923 K.

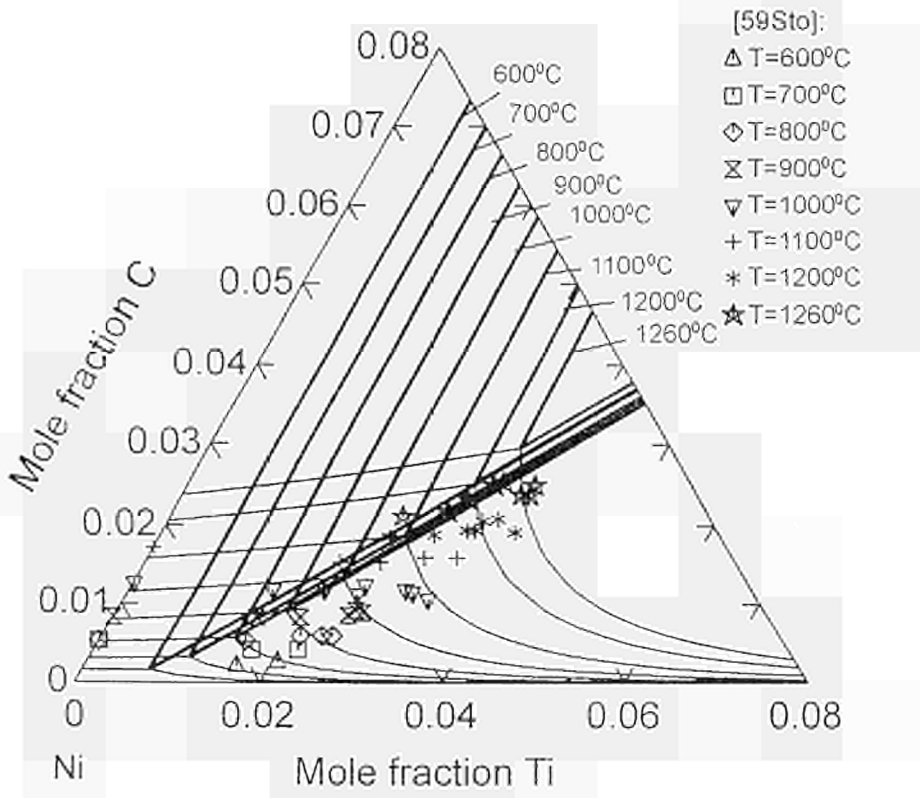

Fig.15 Experimental information on the solubility of graphite in the Ni-rich fcc phase in the Ni-Ti-C system at various temperatures. Comparison is made with calculations of the fcc + graphite and fcc + graphite + TiC equilibria, using Ni-C from Lee [92Lee], Ni-Ti from Bellen [96Bel] and Ti-C from Jonsson [96bJon].

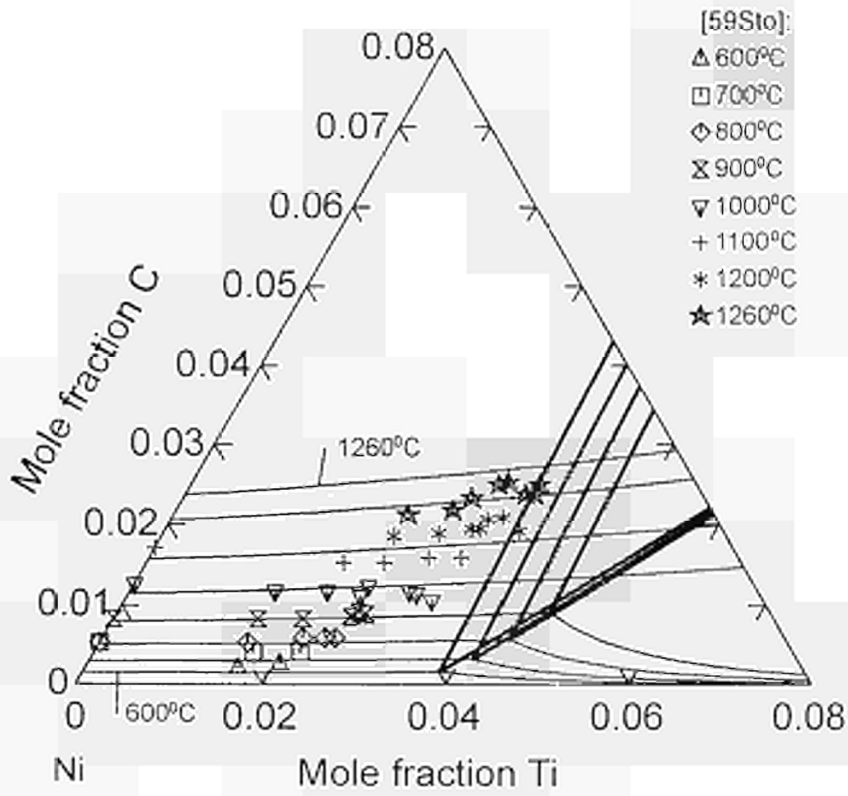

Fig.16 Same as fig.15 but using Ti-C from Dumitrescu [97Dum].

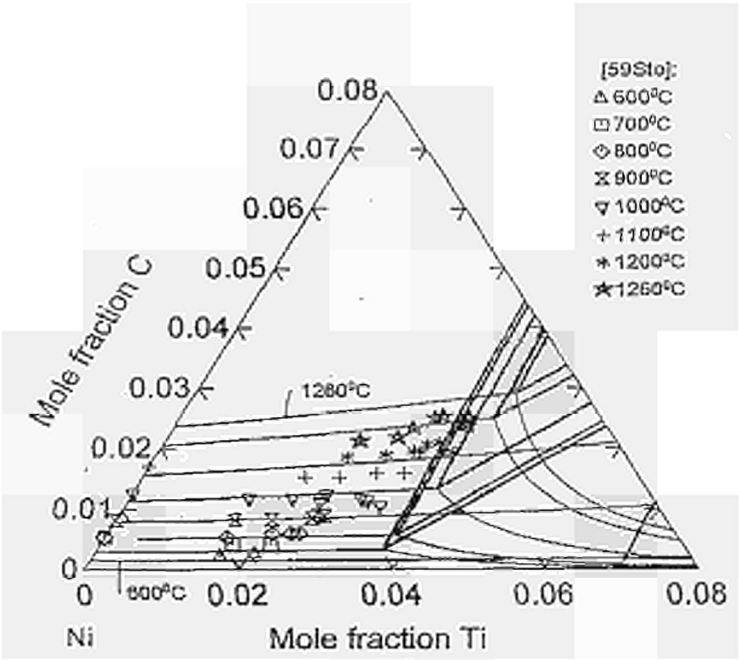

Fig.17 Same as fig.15 but using Ti-C from Dumitrescu [97Dum] and Ni-Ti by Saunders [95Sau].

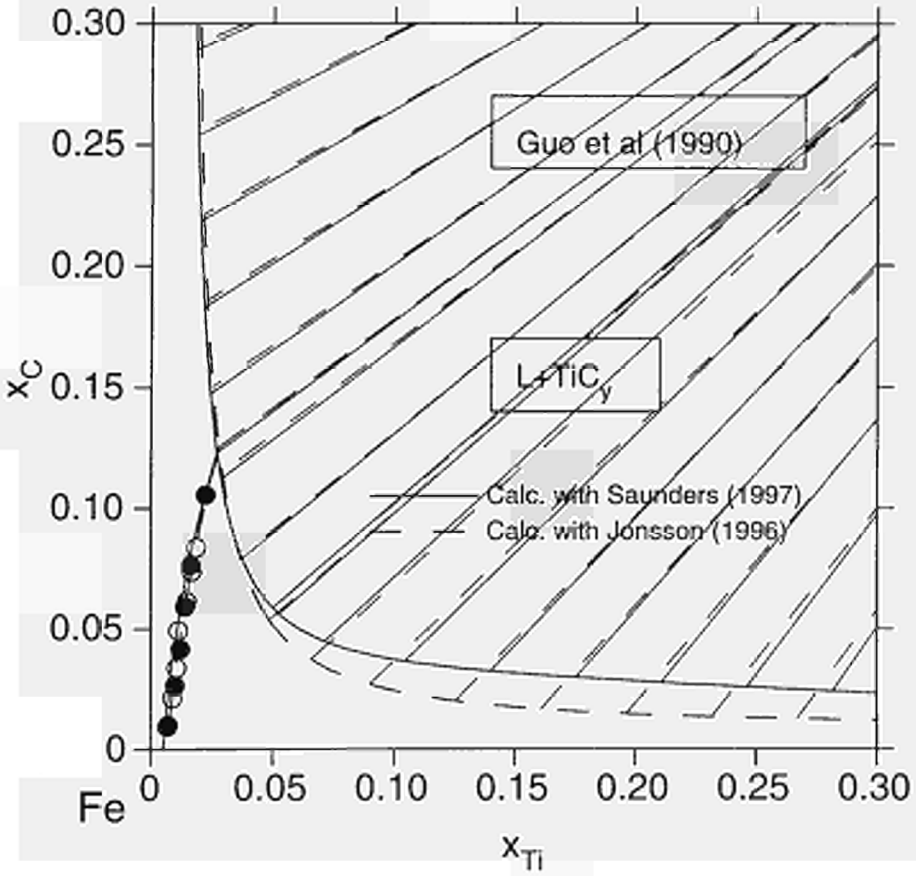

Fig.18 The Fe rich corner of an isothermal section of Fe-Ti-C at 1873 K.

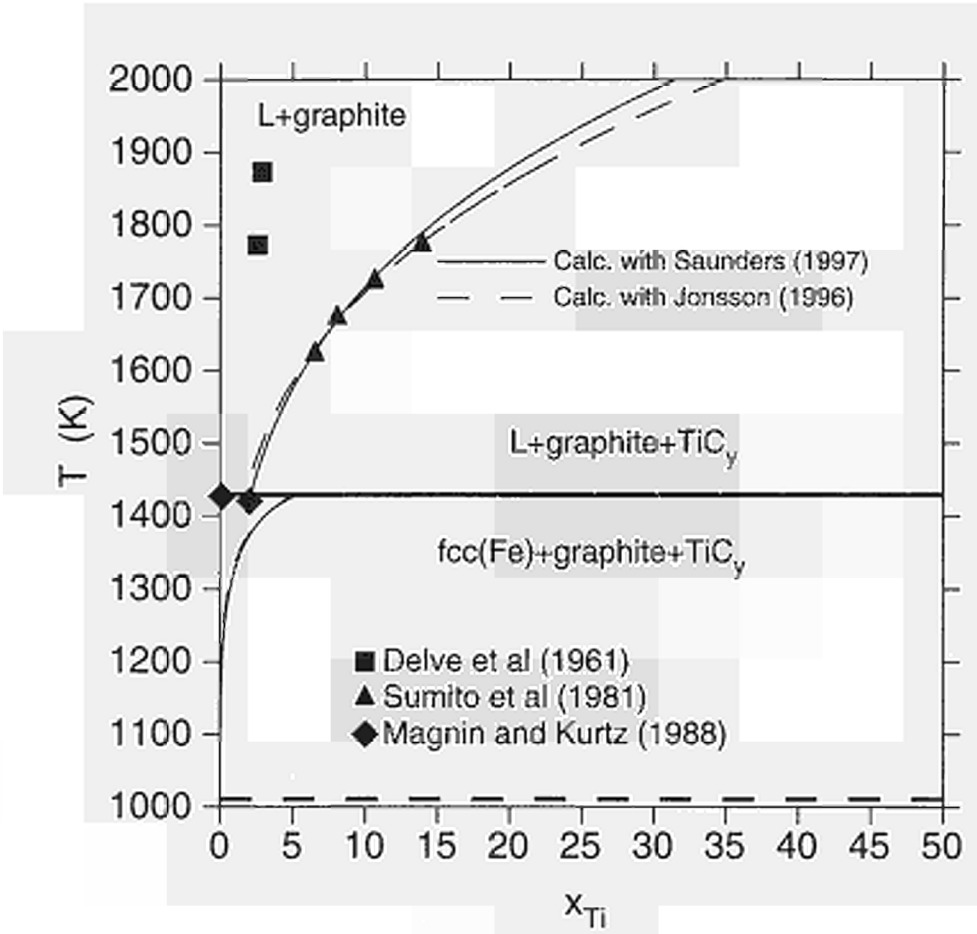

Fig.19 Section at a_c=1 through the Fe-Ti-C diagram.

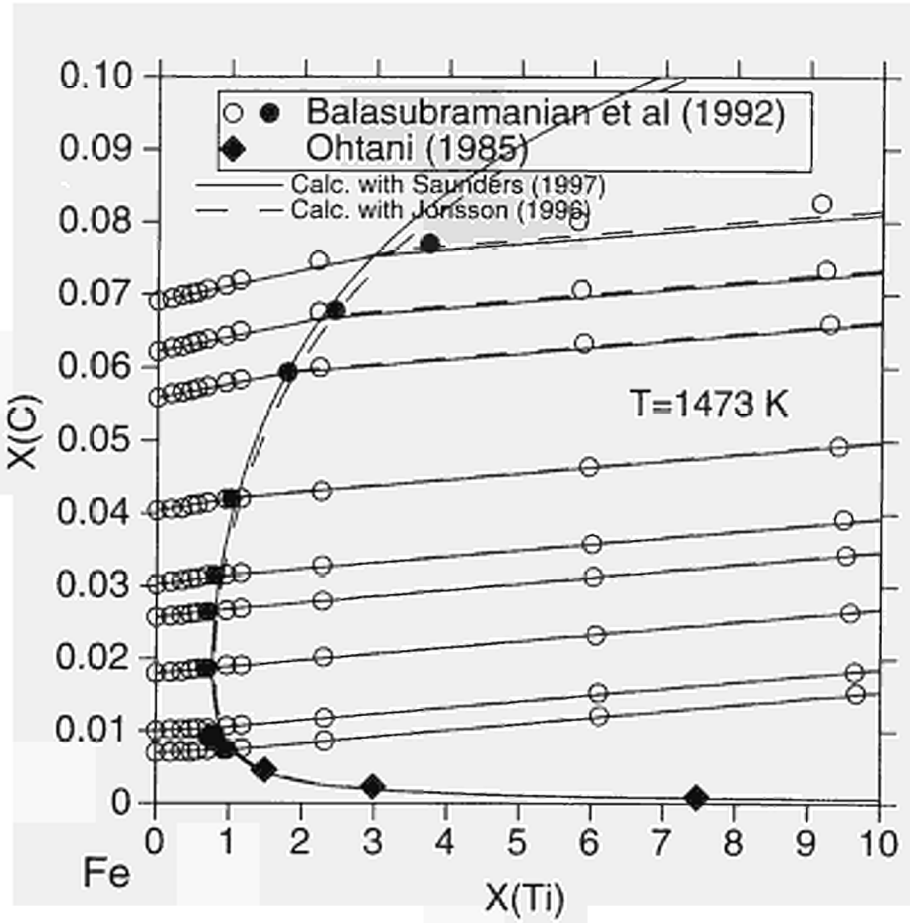

Fig.20 The Fe rich corner of an isothermal section of Fe-Ti-C at 1473 K.

An Experimental Investigation of the Cu-Li-Mg Phase Diagram

Lazar Rokhlin*, Marko Hamalainen#, and Tatyana Dobatkina*

*Baikov Institute of Metallurgy, Moscow, Russia
#Helsinki University of Technology, Helsinki, Finland

Abstract

This research forms a part of the COST 507 program on the Cu-Al-Mg-Zr-Li system. The research included the investigation of the part of the Cu-Li-Mg ternary sub-system aiming mainly to check and construct the phase diagram in the area near a proposed compound of the $Li_8Mg_{60}Cu_{32}$ composition [76Mel]. The investigation did not confirm formation of this ternary compound. As result of the investigation, one polythermal section of the phase diagram was constructed. One invariant four-phase equilibrium at 430 °C in the system was discovered. The phase relationships in the Mg corner of the system in solid state were determined.

1 Introduction

The overall system under study is the Cu-Al-Mg-Zr-Li system. This system is quite complicated and its constitution may be understand from the knowledge of its sub-system constitutions. The ternary Cu-Li-Mg system is one of these sub-system. Some years ago one ternary compound of the $Li_8Mg_{60}Cu_{32}$ composition was proposed in the system [76Mel]. Nevertheless, its existence was not confirmed reliably. The present work was directed mainly to study the Cu-Li-Mg phase diagram in the concentration area near to this composition and to check this compound formation.

2 Experimental Techniques

The phase diagram was investigated by study the alloys along the polythermal section for 64 at.% Mg which ran near the proposed ternary compound consisting of 32 at.%Cu, 8 at.%Li, and 60 at.%Mg. Besides, some alloys close the proposed ternary compound were study, as well. The starting materials were Cu 99.996 wt.%, Li 99.8 wt.%, and Mg 99.96 wt.% purity. The alloys for the investigation were prepared by melting in alumina crucibles under flux consisting of 75%LiCl + 25%LiF or 50%KCl + 50%LiCl. The heating was performed in the electrical resistivity furnace. Chemical analysis showed that Mg and Li losses during melting were insignificant. The alloys were poured into ingots of 15 mm in diameter. The pieces of the ingots were used for differential thermal analysis and the structure studies by microscopy and X-ray methods. The structure was studied in the as cast condition and after annealing at 370 °C for 96 hours followed by quenching into cold water. Differential thermal analysis was performed using the apparatus TAG-24 of the "Setaram" firm under He atmosphere or the own equipment under above mentioned fluxes. X-ray investigations were performed from the plane samples using the Russian X-ray register DRON-3M with Fe and Cu radiation.

3. Results of the Investigation

The polythermal section for 64 at.% Mg constructed is shown in Fig. 1. It shows

absence of the proposed ternary compound. This result was confirmed also by the studies of the additional alloys close the composition of the proposed ternary compound. In the system there is at least one invariant four-phase reaction. This reaction is of transition type: L + Mg_2Cu = (Li) + $MgCu_2$ and run at 430 °C. According to the microstructure investigations magnesium solid solution is in equilibrium only with lithium solid solution (Li), and the Mg_2Cu, $MgCu_2$ compounds of the Mg-Cu binary system.

4. References

76Mel E.V.Melnik, M.F.Mitrofanova, P.I.Kripyakevich, M.Yu.Teslyuk, A.N.Malinkovich, Izv. AN SSSR Metally, 1976, (3), 200-204 (In Russian).

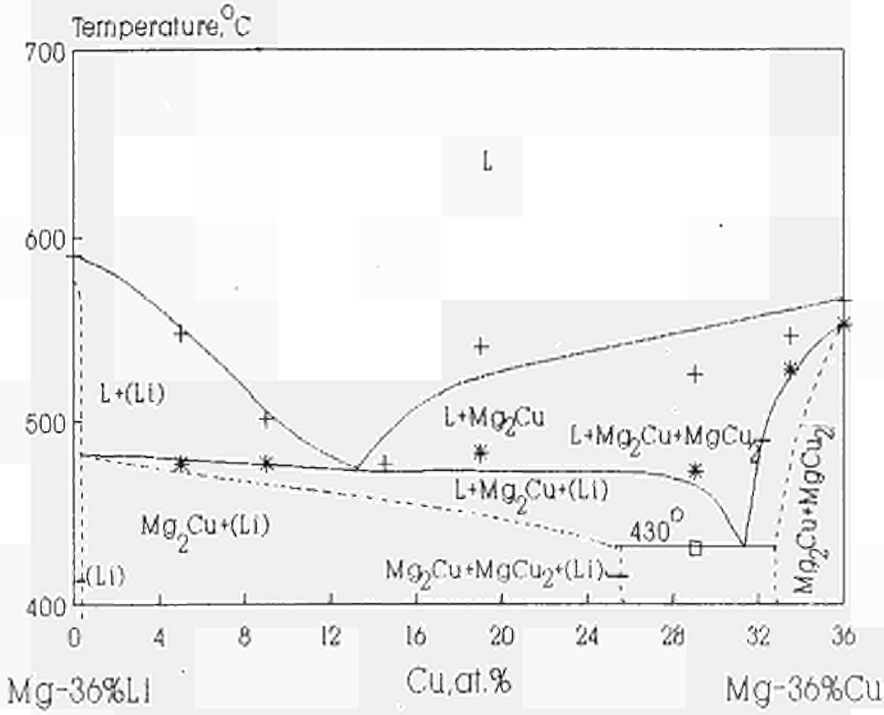

Fig. 1: Polythermal section of the Cu-Li-Mg phase diagram for 64 at.% Mg.

An Experimental Investigation of the Cu-Mg-Zr Phase Diagram

Nataliya Bochvar*, Marko Hamalainen**,
Lazar Rokhlin*, Evgeniya Lysova*

*Baikov Institute of Metallurgy Academy of Science of Russia,
Moscow, Russia
**Helsinki University of Technology, Institute of Materials
Science and Technology, Espoo, Finland

Abstract

This research forms part of COST 507 project "Thermodynamic assessment of the system Cu-Al-Mg-Zr-Li". The work included the experimental investigation of Cu-Mg-Zr phase diagram as the subsystems of general system Cu-Al-Mg-Zr-Li. A number of the alloys of Cu-Mg-Zr system were prepared by melting. The differential thermal analysis of the alloys was conducted and the structure of them were studied by different methods. The results of the experiments enabled to construct isothermal and polythermal sections of the phase diagram. The experimental investigations carried out in Baikov Institute of Metallurgy and the optimization of theses data with use by the thermodymic calculations carried out in Helsinki University of Technology.

1 Introduction

The experimental data on Cu-Mg-Zr system are very limited. [82Kuz] constructed the polythtemal section in Cu-corner for constant Mg concentration 1 at.% and from 0 up to 15 at.% Zr using differential thermal analysis, X-ray phase analysis and microscopic method. No ternary compounds have been found in the alloys. The phases Cu_9Zr_2 and Cu_7Zr_2 (or $Cu_{51}Zr_{14}$) of the Cu-Zr system are existed. [59Ish, 68Bab] studied the solubility of Zr in molten Mg at 700 °C with copper additions up to about 0.4 at.% Cu [59Ich] and at 780-800 °C with copper additions up to 0.6 at.% Cu [68Bab]. According X-ray investigations [59Ich] (Zr), Mg_2Cu and $CuZr_2$ are in equilibrium with Mg phase. This work was undertaken to enlarge the knowledge about the Cu-Mg-Zr phase diagram in the Cu corner up to 40 wt.% (64 at.%) Mg and 40 wt.% (32 at.%) Zr.

2 Experimental Procedure

Cu-Mg-Zr alloys (120 compositions) were prepared by arc melting under He atmosphere (for alloys with up to 10 wt.% Mg) and by induction melting under Ar atmosphere (for alloys with 10-50 wt.% Mg). The starting materials were Cu of 99.996 wt.%, Mg of 99.96 wt.%, and Zr of 99.9 wt.% purity. The alloys were rolled for the height reduction of 50%, annealed at 500 °C for 100 h and then quenched into cold water. The alloys were studied by microstructure analysis,

DTA, microhardness measurements, X-ray analysis and microprobe X-ray spectral analysis.

Data of the microprobe X-ray spectral analysis showed that:

1) A ternary compound called τ exists in the system. Its composition is about 54 wt.% Cu, 10 wt.% Mg, 36 wt.% Zr (50 at.% Cu, 25 at.% Mg, 25 at.% Zr). So, its formulae may be presented as Cu_2MgZr. The ternary compound is in the equilibrium with $Cu_{51}Zr_{14}$, Cu_2Mg and $CuMg_2$;

2) The binary compounds Cu_5Zr and $Cu_{51}Zr_{14}$ solve up to 1 wt.% (3at.%) Mg;

3) The binary compound Cu_2Mg solve up to 4 wt. (2.5 at.%) Zr.

Data of the X-ray diffraction analysis confirm the presence of the ternary compound.

Microstructure analysis after annealing at 500 ^{0}C and after DTA showed the phases formed in the studied area of concentration. The phases may be distinguished according to their shape and color.

The isothermal section of the phase diagram at 500 °C was constructed (Fig.1).

DTA was carried out for all prepared alloys. One of the polythermal section between Cu-10 wt.% Zr and Cu-7 wt.% Mg was constructed (Fig.2).

3 References

59Ich R.Ishikawa, *On favorable alloying elements for Mg-Zr system alloys*, (in Japanese), Nippon Kinzoku Gakkai-Si, 1959, **23**, N 10, 612-616.

68Bab V.M. Babkin, *Solubility of zirconium in molten magnesium and magnesium alloy ML5*, (in Russian), Metalloved. i Term. Obrabotka Metal., 1968, N 3, 61-64.

82Kuz G.M. Kuznetsov, V.N. Fedorov, I.N. Tokarchuk, O.P. Zhizhchenko, V.V. Kozlov, *Phase equilibria in the copper-chromium-zirconiu m-magnesium system,* (in Russian), Izv. Vyssh. Uchebn. Zaved., Tzveth. Metall., 1982, N 6, 90-93.

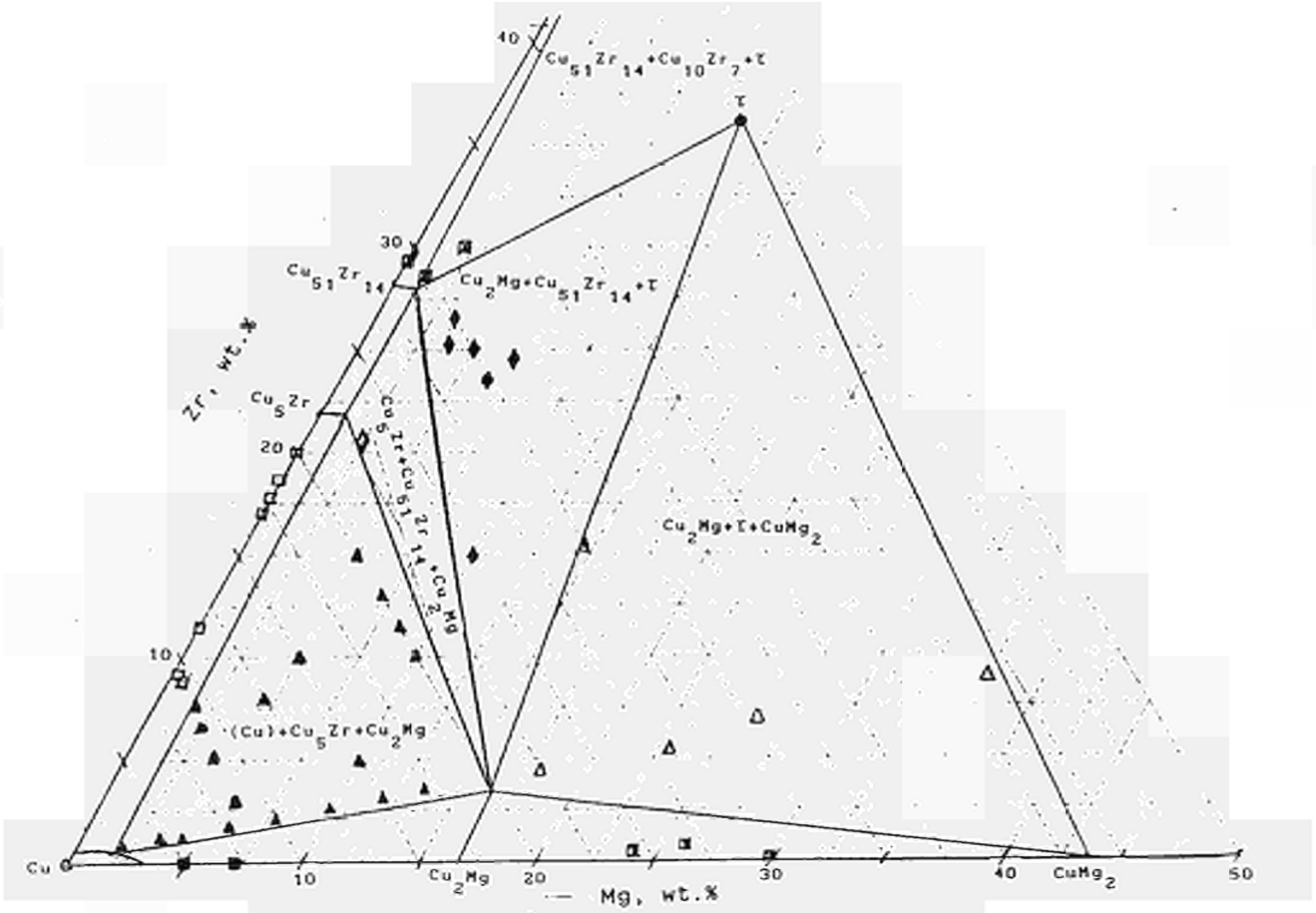

Fig.1 Isothermal section of Cu-Mg-Zr phase diagram at 500 °C

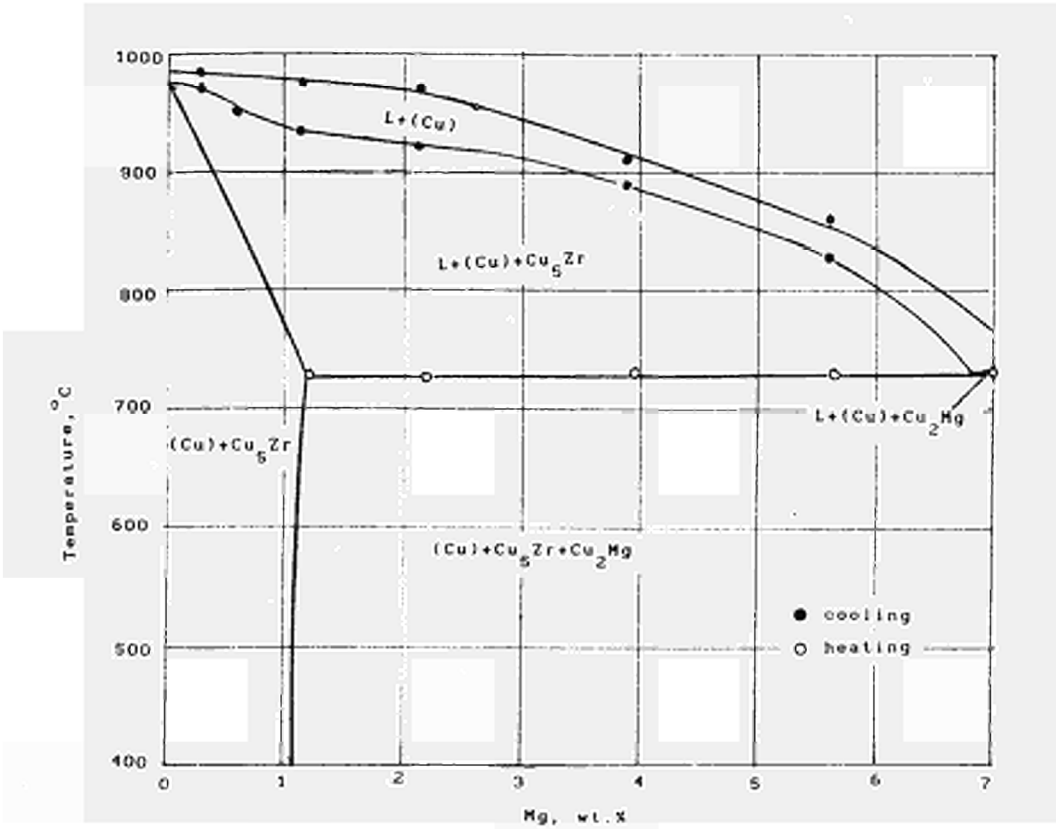

Fig.2 Polythermal section of Cu-Mg-Zr phase diagram between compositions 90 wt.% Cu, 10 wt.% Zr to 93 wt.% Cu, 7 wt.% Mg

EXPERIMENTAL INVESTIGATION OF THE CU-MG-ZR SYSTEM.

Baikov Institute of Metallurgy, Moscow, Russia
Helsinki University of Technology, Espoo, Finland

Cu-Mg-Zr alloys (50 alloys) were prepared by arc melting under He atmosphere (for alloys with up 10 wt.% Mg) and by induction melting under Ar atmosphere (for alloys with 10-50 wt.% Mg). The alloys were rolled by the height reduction of 50%, annealed at 500°C for 100 h, quenched and studied by microcopy analysis, DTA, microhardness measurements, X-ray analysis and microprobe X-ray spectral analysis.

Data of the microprobe X-ray spectral analysis showed that:
- there is a ternary compound called τ with composition of 54wt.%Cu, 10wt.% Mg, 36wt% Zr (50at.% Cu, ~25at.% Mg, ~25at% Zr) and formulae ~Cu_2MgZr; this compound is in equilibrium with binary compounds $Cu_{51}Zr_{14}$, Cu_2Mg and $CuMg_2$ (see tabl.1, Fig.1);
- the binary compounds Cu_5Zr and $Cu_{51}Zr_{14}$ dissolve up to 1 wt.% (3at.%) Mg.
- the binary compound Cu_2Mg dissolve up to 4 wt.% (2.5at.%) Zr.

Data of the X-ray diffraction analysis (the diffraction patterns are shown in Fig.2) confirm the presence of the ternary compound. So, there are some unidentified peaks besides those of $Cu_{51}Zr_{14}$ and Cu_2Mg, and these peaks can not be recognized as the peaks of the other possible in this system binary compounds. Therefore, it is naturally to suppose that this peaks belong to the unknown ternary compound τ.

The data of the microstructure analysis (see Fig.3-after annealing at 500°C and Fig.5-after DTA) showed the phases formed in the studied area of concentration. The phases differ according to their shape and color. After etching of the metallographic specimens with the 30% solution of $(NH_4)_2S_2O_8$ the phase Cu_5Zr is seen as the thin plates having blue color, and Cu_2Mg has black color. The phase $Cu_{51}Zr_{14}$ forms crystals of regular shape and white color. The phase τ rounds the $Cu_{51}Zr_{14}$ crystals. It is of grey or light brown color. The isothermal section at 500°C was constructed (Fig.4).

DTA was carried out for all prepared alloys. One polythermal section (between Cu-10wt.% Zr and Cu-7wt.% Mg) was constructed (Fig.6), as well.

Table 1. Data of microbrobe X-ray spectral analysis (annealing of 500°C)

Composition of alloys (wt.%, Cu, balance)		Phases	Composition of each phase					
			Cu		Mg		Zr	
Mg	Zr		wt.%	at.%	wt.%	at.%	wt.%	at.%
3.5	16.5	Cu_5Zr (white)	75.6	80.9	0.9	2.4	22.3	16.6
		(Cu) (black)	99.0	95.2	1.8	4.5	0.4	0.3
10.0	10.0	Cu_5Zr (white)	75.8	80.6	1.0	2.9	22.2	16.5
		Cu_2Mg (black)	86.6	67.5	15.6	31.8	1.2	0.7
		(Cu) (grey)	96.6	92.1	3.1	7.7	-	-
5.0	20.0	$Cu_{51}Zr_{14}$ (white)	72.0	76.7	1.2	3.4	29.2	20.0
		τ (grey)	54.0	50.3	10.7	26.1	36.2	23.5
		Cu_2Mg (black)	79.6	64.0	15.8	33.2	4.9	2.7
27.5	2.5	Cu_2Mg (white)	80.0	61.4	19.0	38.0	1.1	0.6
		$CuMg_2$ (black)	56.6	31.7	46.7	68.3	-	-

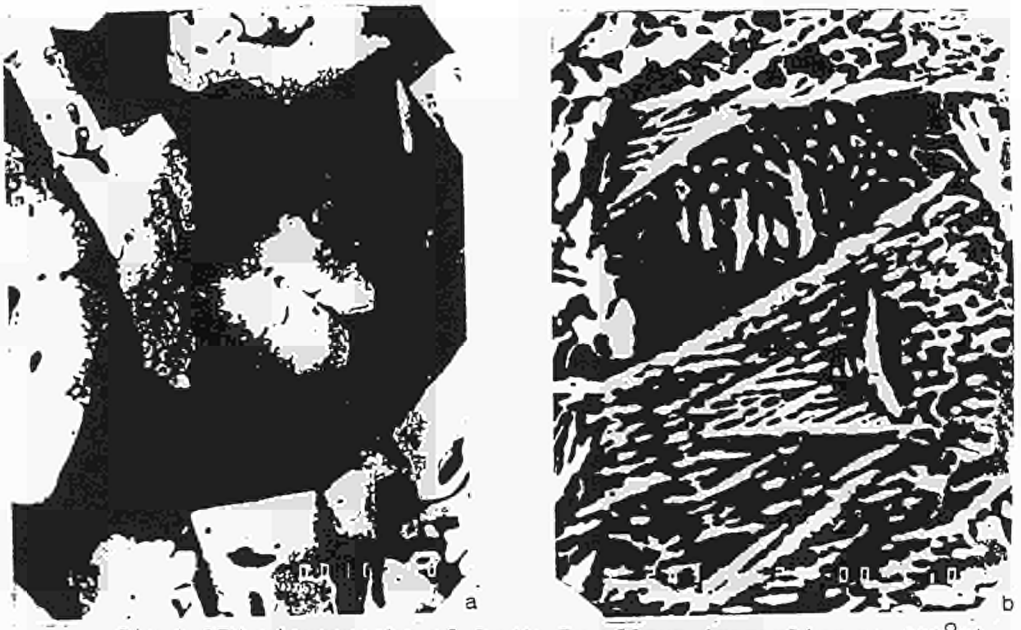

Fig.1 SEM micrographs of Cu-Mg-Zr alloys (annealing at 500°C)
(a, x600) 70wt.%Cu, 5wt.%Mg, 25wt.%Zr,
phases: $Cu_{51}Zr_{14}$, white; τ, grey; Cu_2Mg, black;
(b, x2000) 80wt.%Cu, 10wt.%Mg, 10wt.%Zr,
phases: Cu_5Zr, white; (Cu), grey; Cu_2Mg, black.

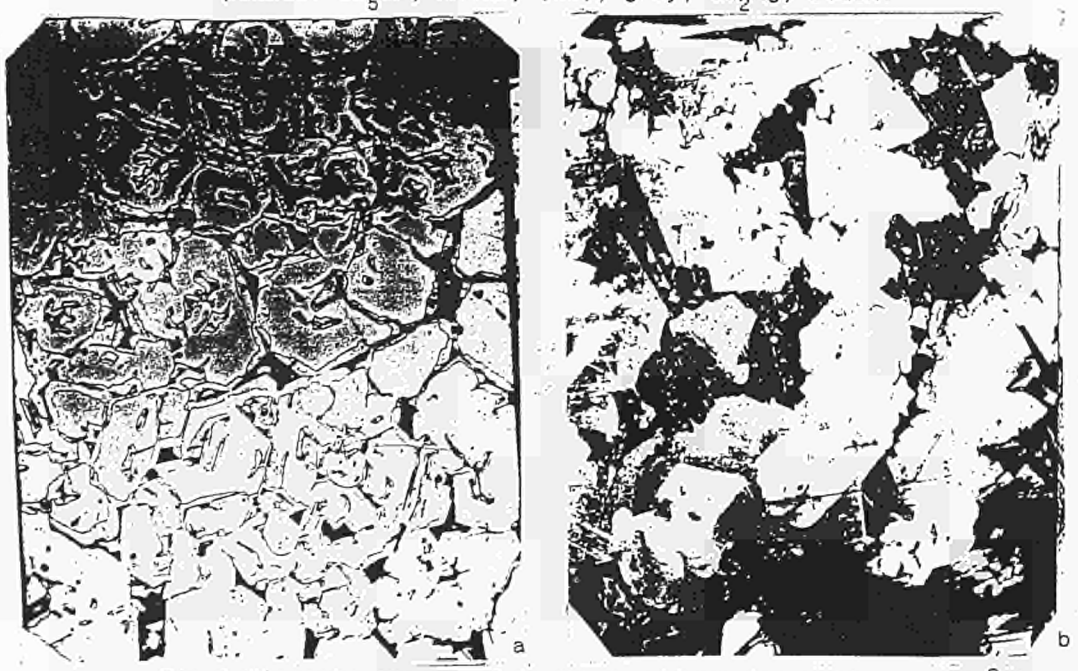

Fig.3 Microstructures of Cu-Mg-Zr alloys (annealing at 500°C)
(x340): (a) 70wt.%Cu, 3.5wt.%Mg, 26.5wt.%Zr;
(b) 70wt.%Cu, 15wt.%Mg, 15wt.%Zr;
phases: $Cu_{51}Zr_{14}$, light; τ, grey; Cu_2Mg, black.

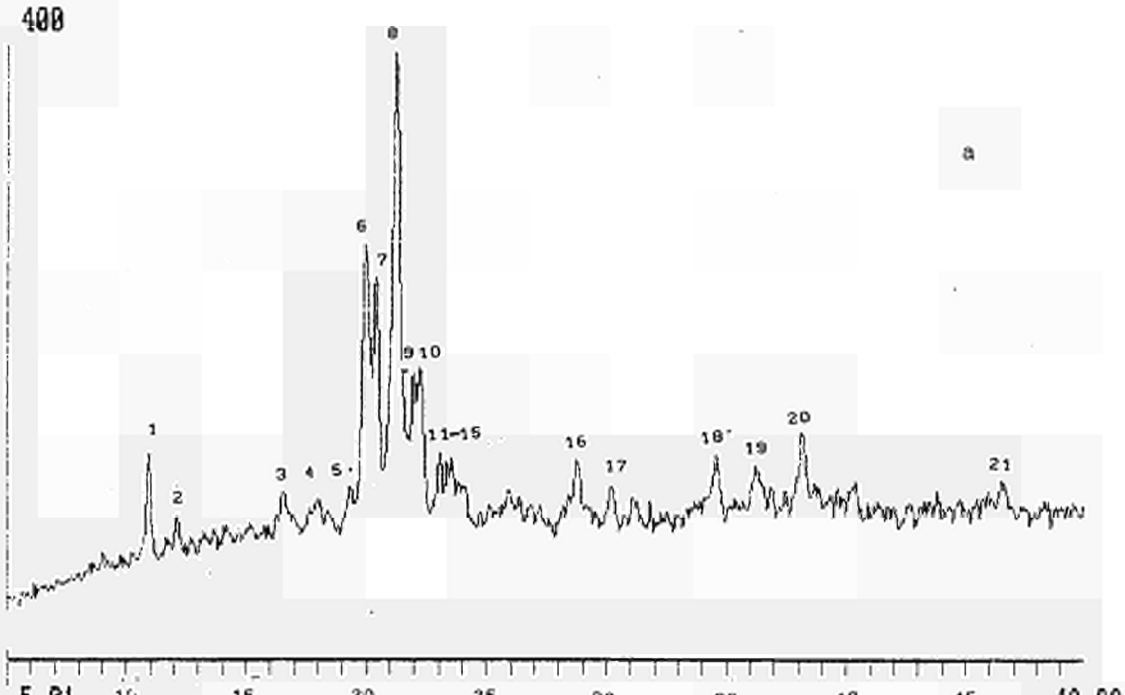

Smoosing No. - 2

N	Teta	d,A	Int.	a	Phase	hkl
1	10.885	4.0823	66	0	Cu_2Mg	111
2	12.093	3.6797	27	0	$Cu_{51}Zr_{14}$	310
3	16.522	2.7107	35	0	$Cu_{51}Zr_{14}$	401
4	17.962	2.4998	24	0	$Cu_{51}Zr_{14}$	132
5	19.245	2.3388	27	0	$Cu_{51}Zr_{14}$	213
6	19.907	2.2640	176	0	Cu_2Mg	311
7	20.345	2.2173	159	0	$Cu_{51}Zr_{14}$	004
8	21.204	2.1313	292	0	Cu_2Mg	222
9	21.909	2.0600	97	0	$Cu_{51}Zr_{14}$	232
10	22.179	2.0421	101	0	$Cu_{51}Zr_{14}$	600
11	23.018	1.9715	45	0	$Cu_{51}Zr_{14}$	313
12	23.315	1.9478	40	0	$Cu_{51}Zr_{14}$	204
13	23.520	1.9317	43	0	$Cu_{51}Zr_{14}$	142
14	23.791	1.9110	27	0	$Cu_{51}Zr_{14}$	340
15	24.075	1.8898	25	0	$Cu_{51}Zr_{14}$	423
16	28.720	1.6043	38	0	$Cu_{51}Zr_{14}$	523
17	30.167	1.5340	23	0	$Cu_{51}Zr_{14}$	415
18	34.516	1.3605	38	0	$Cu_{51}Zr_{14}$	440
19	36.191	1.3045	28	1	Cu_2Mg	622
20	38.105	1.2482	48	1		
21	46.486	1.0621	22	1		

Fig.2 Diffraction patterns of Cu-Mg-Zr alloys:
(a) 70wt.%Cu, 5wt.%Mg, 25wt.%Zr;
(b) 70wt.%Cu, 15wt.%Mg, 15wt.%Zr

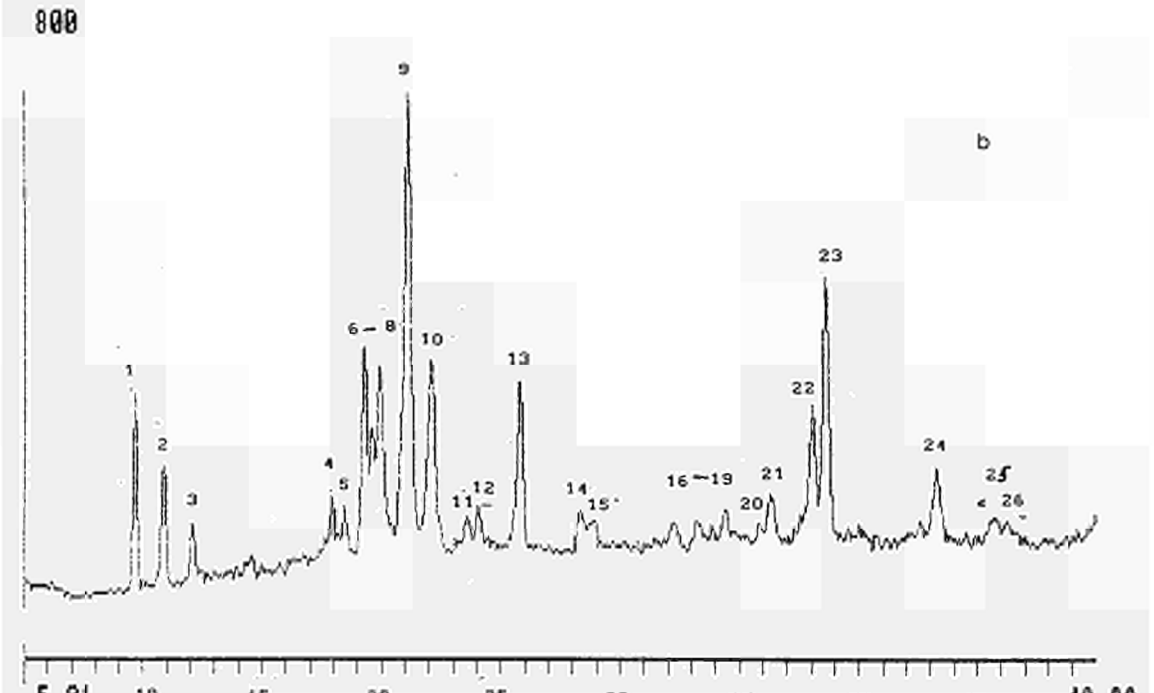

Smoosing No. - 2

N	Teta	d.A	Int.	a	Phase	hkl
1	9.623	4.6117	250	0		
2	10.818	4.1073	163	0	Cu_2Mg	111
3	12.041	3.6955	78	0		
4	17.916	2.5060	97	0		
5	18.418	2.4399	83	0	$Cu_{51}Zr_{14}$	400
6	19.282	2.3345	285	0	$Cu_{51}Zr_{14}$	401
7	19.585	2.2997	181	0		
8	19.933	2.2612	256	0	$Cu_{51}Zr_{14}$	132
9	21.132	2.1383	594	0	$Cu_{51}Zr_{14}$	140
10	22.096	2.0493	266	0	Cu_2Mg	222
11	23.583	1.9268	71	0	$Cu_{51}Zr_{14}$	313
12	24.041	1.8923	83	0	$Cu_{51}Zr_{14}$	142
13	25.798	1.7714	240	0	Cu_2Mg	400
14	28.332	1.6244	79	0	Cu_2Mg	331
15	28.876	1.5962	69	0		
16	32.235	1.4453	65	0		
17	33.154	1.4096	85	0	$Cu_{51}Zr_{14}$	433
18	33.817	1.3852	63	0		
19	34.413	1.3640	82	0		
20	35.825	1.3160	63	1		
21	36.257	1.3024	102	1	$Cu_{51}Zr_{14}$	415
22	38.041	1.2499	211	1		
23	36.598	1.2347	372	1		
24	43.245	1.1243	133	1		
25	45.638	1.0774	70	1	Cu_2Mg	533
26	46.236	1.0666	68	1	Cu_2Mg	622

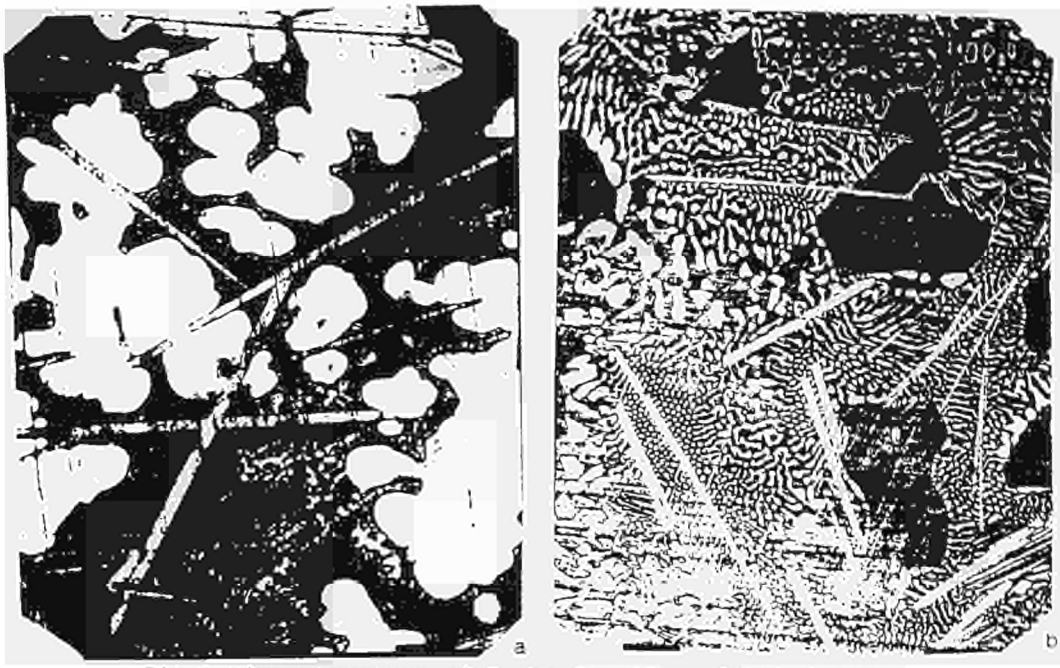

Fig.5 Microstructure of Cu-Mg-Zr alloys (DTA) (x340):
(a) 92.2wt.%Cu, 6.23wt.%Mg, 1.57wt.%Zr;
(b) 87.7wt.%Cu, 9.82wt.%Mg, 2.48wt.%Zr;
phases: (Cu), white; Cu_5Zr, grey plates; Cu_2Mg, black.

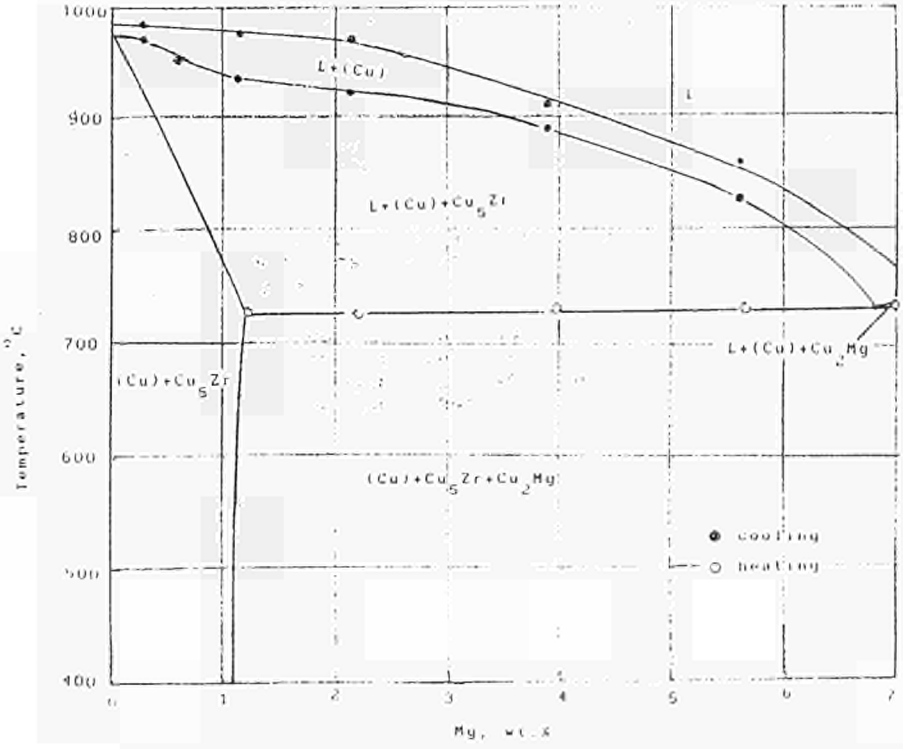

Fig.6 Polythermal section of Cu-Mg-Zr phase diagram between compositions 90wt.%Cu, 10wt.%Zr to 93wt.%Cu, 7wt.%Mg

Thermodynamic Evaluations of the Al-Li-Cu-Mg-Zr Systems

Marko Hämäläinen,* Helena Braga,**
N. Bochvar, T. Dobatkina, E. Lyssova, L.L. Rokhlin***

*Helsinki University of Technology, Espoo, Finland
**University of Porto, O'Porto, Portugal
***Baikov Institute of Metallurgy, Moscow, Russia

Abstract

The investigation of the Al-Li-Cu-Mg-Zr system is accomplished in this report. The evaluations of the Cu-Mg-Zr and Cu-Li-Mg systems and the experimental study of the Al-Li-Cu-Mg system were carried out during the COST 507 second round.

The evaluation of the Cu-Li-Mg system was based on the DSC experiments at the large range of composition. The parameters of the excess Gibbs energy obtained agreed quite well with the temperatures of the phase transformations but the fit was not so good using the experimental enthalpies. The decomposition temperature of the τ phase was fixed at 702.7 K and was not defined earlier in the literature.

The optimisation of the Cu-Mg-Zr system was based on the experimental data from the literature and on one set of the DTA experiments measured. The calculated phase diagram was in good agreement with the data used. The existence of the new τ phase as well as the parameters of formation of the excess Gibbs energy contributed well the system studied.

The phase relations near to Al-rich corner containing up to 7 wt.% Li, 7 wt.% Mg and 10 wt.% Cu were investigated using microscopy analysis, quality local X-ray spectral analysis and X-ray phase analysis in the experimental study of the Al-Li-Cu-Mg system done by Baikov Institute of Metallurgy.

1 The Cu-Li-Mg system

1.1 Introduction

The Cu-Li-Mg system is not well defined in the literature. Melnik [76Mel] carried out annealing experiments in the Cu-Li-Mg system at 370 °C and detected a new phase called X phase with the composition of 32 at.% copper, 8 at.% lithium and 60 at.% magnesium. The stoichiometry of the X phase was estimated as $Cu_{32}Li_8Mg_{60}$. Kripyakevich [71Kri] ascribed the X phase as the τ phase and defined its theoretical stoichiometry as $(Li_{0.08}Mg_{0.92})_{12}LiCu_5$. The phase region close to the pure lithium corner is not well known.

Two sets of experiments using the differential scanning calorimeter (DSC) were measured in the Cu-Li-Mg system. The first set of experiments for the samples N11 to N43 (13 samples) was carried out using the apparatus provided by Perkin-Elmer model 7 Series at the Helsinki University of Technology (HUT). The second set of experiments for the samples N11 to N40 (11 samples) was measured using the apparatus provided by Shimatsu-50 at the University of Porto (Porto). The samples N11 to N43 were studied using sealed aluminium and stainless steel crucibles under argon (purity 99.99 vol.%) atmosphere. The samples N11 to N43 were studied using stainless steel crucibles under helium (99.9999 vol.%) atmosphere.

1.2 Assessment

The evaluation of the Cu-Li-Mg system was based on the DSC experiments. The experimental datafile was created using the onset or peak values from the temperatures of the phase transformations and the enthalpy values which were calculated from the surface area of the peaks obtained. The reference states used in the optimisation for the enthalpy values were Bcc_A2 (Li), Fcc_A1 (Cu), Hcp_A3 (Mg). The estimated experimental errors were ±5 K for the temperatures and ±10 at.% for the enthalpy measurements. **Figure 1** shows the calculated phase diagram with 8 at.% Li and the decomposition of the τ ($Cu_{32}Li_8Mg_{60}$) phase at 702.7 K.

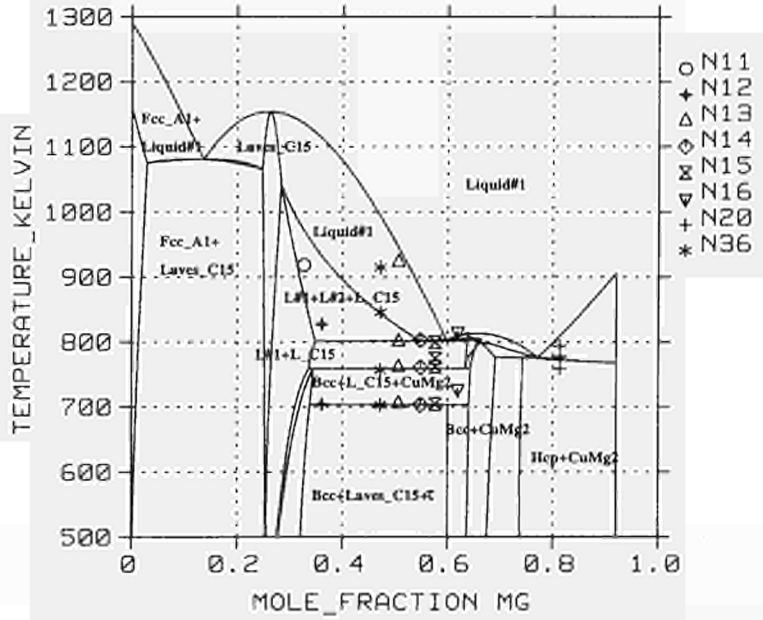

Figure 1. The assessed Cu-Li-Mg phase diagram with 8 at.% Li.

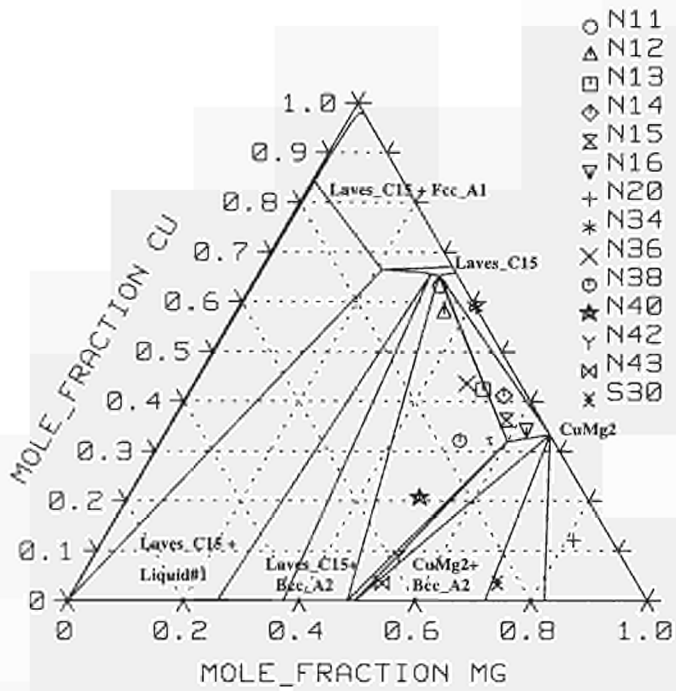

Figure 2. The isothermal section of the Cu-Li-Mg system at 370 °C.

Figure 2 shows the isothermal cut at 370 °C with the experimental data used. The phase boundaries in the system were in good agreement with the experimental values obtained. However, there were some differences concerning the phase boundaries compared with the phase diagram by Melnik [76Mel]. According to the results from the X - ray analysis at 643 K the sample N15 had the same phase composition as calculated one in **Figure 2**. Sample N16 was close to the two phase boundary between the τ and $CuMg_2$ phases. The sample N38 had the same phase composition as calculated one but the samples N36, N42, N43 had different compositions. **Table 1** shows the calculated and the experimental values obtained in the four phase equilibria in **Figure 1** using the assessed excess Gibbs energy parameters. The estimated error of the invariant temperatures was ±1 K. The calculated values in the four phase equilibria are close to the experimental values.

Table 1. The experimental and calculated temperatures in the invariant four phase equilibria.

PHASES	T(EXP)/K	T(CALC)/K
Bcc_A2, CuMg2, Laves_C15, Cu32Li8Mg60	703.7	702.7
Bcc_A2, CuMg2, Laves_C15, Liquid#1	761.2	762.8
Bcc_A2, CuMg2, Hcp_A3, Liquid#1	-	776.7
CuMg2, Laves_C15, Liquid#1, Liquid#2	800.7	799.2

The assessed excess Gibbs energy parameters in the liquid phase showed the existence of the miscibility gap. The excess Gibbs energy parameters in the Fcc_A1 phase were not optimised. **Table 2** shows the assessed parameters in the Cu-Li-Mg system.

Table 2. The assessed excess Gibbs energy parameters in the Cu-Li-Mg system

PHASE	L	A	B * T
Liquid	L_0	14191.577	-
Liquid	L_1	14191.577	-
Liquid	L_2	14191.577	-
Bcc_A2	L_0	1764.073	-
$Cu_{32}Li_8Mg_{60}$ (τ)	$\Delta_f G$	-9005.163	-
G(Laves_C15,Cu:Li;0)	G	25000.000	-
G(Laves_C15,Mg:Li;0)	G	30000.000	-
L(Laves_C15,Cu:Li,Mg;0)	L_0	-55000.000	-

The values in **Table 2** were assessed using the temperatures of the phase transformations and verified with the enthalpy values obtained. The assessed parameter of the Bcc_A2 phase was probably too low because there was no significant solid solubility of copper both in the copper-lithium and the copper-magnesium systems. For the same reason the Hcp_A3 phase was considered as a binary phase. The optimisation of the Laves_C15 phase was carried out manually and yielded one interaction parameter as *L(Laves_C15,Cu:Li,Mg;0)* = -55000.

2 The Cu-Mg-Zr system

2.1 Introduction

Baikov Institute of Metallurgy investigated the Cu-Mg-Zr system up to the amount of 50 wt.% Mg and 50 wt.% Zr using methods as light microscopy, X-ray phase analysis, local X-ray spectral analysis, and differential thermal analysis. One ternary phase was found in the system. According to local spectral analysis, the composition of the ternary phase was estimated as 50 at.% Cu, 25 at.% Mg, and 25 at.% Zr. Moreover, the phases from the binary systems as Cu-Mg and Cu-Zr could be distinguished in the studied alloys. The substantial homogeneity ranges of some other phases were also established. The binary compounds Cu_5Zr and $Cu_{51}Zr_{14}$ exist in the solution up to the amount of 3 at.% Mg. The phase Cu_2Mg exists in the solution up to the amount of 2.5 at.% Zr. The phase equilibria in the solid state between ternary phase, binary phases, and Cu solid solution were determined. Two invariant phase reactions near Cu-rich corner were discovered, as well. Using the experimental results, the isothermal section of the phase diagram at 500 °C and the polythermal section in the composition of 90 wt.% Cu were constructed in this study [96Boc].

2.2 Assessment

The optimisation of the Cu-Mg-Zr system was carried out using the data introduced in this work and from Kuznetsov [82Kuz]. The experimental data was stored in the file which was read to the optimisation module. The optimisation was carried out using the enthalpy parameters for the liquid and Fcc_A1 phases. The entropy terms were excluded because there was no thermodynamic data available. **Figure 3** shows the assessed phase diagram with the fixed amount of 93 wt.% copper including the experimental points N2 to N9.

The assessed phase diagram agrees reasonably well with the experimental data except the sample N5 which showed minor solubility in the Fcc_A1 + Cu_5Zr phase region. The calculated invariant temperature was 995.0 K which was lower than the experimental value of 1003 K. **Table 3** shows the assessed parameters of the excess Gibbs energy in the system. The Laves_C15 was predicted as a binary phase due to the reason that there was no information available on the solubility of zirconium in this phase.

Table 3. The assessed ternary excess Gibbs energy parameters in the Cu-Mg-Zr system

PHASE	L	A	B * T
Liquid	L^0	+18168.2502	
Liquid	L^1	+18168.2502	
Liquid	L^2	+18168.2502	-
Fcc_A1 (Cu)	L^0	+ 35752.6281	-

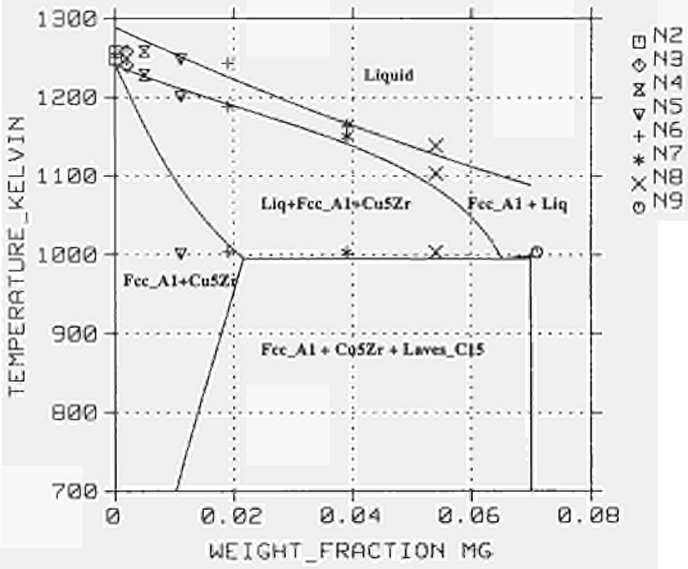

Figure 3. The assessed Cu-Mg-Zr phase diagram with 93 wt.% Cu.

Figure 4 shows the assessed phase diagram with the fixed amount of 1 at.% magnesium using data from Kuznetsov [82Kuz].

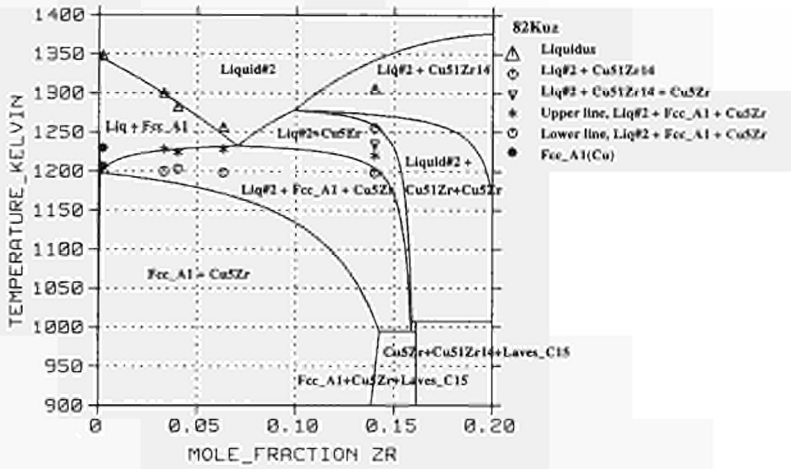

Figure 4. The assessed Cu-Mg-Zr phase diagram with 1 at.% Mg.

The assessed phase diagram agreed well with the liquidus data but not with the lower boundary of the Liquid#2 + Fcc_A1 + Cu_5Zr phases. The invariant temperatures were 995.0 K and 1007 K. The large positive value of the excess Gibbs energy parameter in the Fcc_A1 phase did not have a great influence on the lower limit of the phase region liquid#2 + Fcc_A1 + Cu_5Zr mainly perhaps because the invariant phase boundary at 995.0 K was fixed.

Figure 5 shows the isothermal cut at 500 °C with the new τ phase (Cu_2MgZr). In **Figure 5** the τ phase was in the equilibrium with the Laves_C15 phase with the negligible solubility of zirconium. The τ phase was also in the equilibrium with the phases $Cu_{51}Zr_{14}$, Cu_8Zr_3 and $Cu_{10}Zr_7$. **Table 4** shows the optimized parameter of the Gibbs energy of formation in the τ phase.

Table 4. The calculated Gibbs energy of formation in the τ phase at 298.15 K.

PHASE	G	A	B * T
Cu_2MgZr (τ)	$\Delta_f G$	-72654.140	-

The τ phase was optimized without any exact knowledge of the melting point. The calculated melting point was 1044.78 K in the equilibrium with the τ, Laves_C15 and liquid#2 phases. The solubility of zirconium in the Laves_C15 phase was taken negligible because there were no experimental data available concerning the zirconium solubility in the Laves_C15 phase.

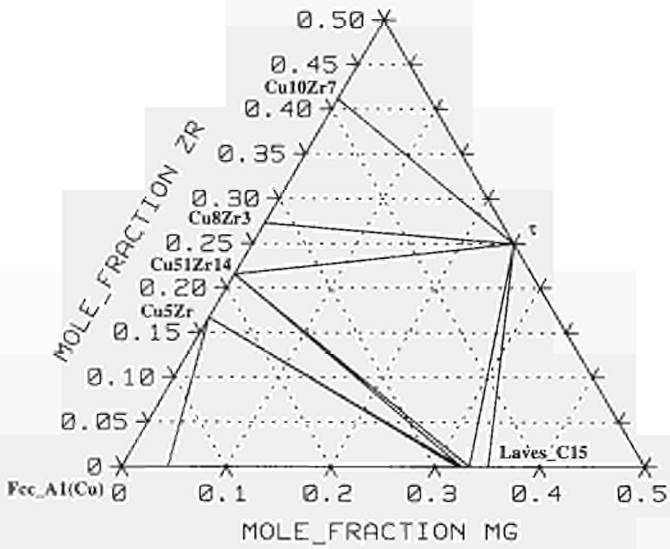

Figure 5. The assessed Cu-Mg-Zr phase diagram at 500 °C with the τ phase.

3 The Al-Li-Cu-Mg system

3.1 Introduction

The experimental study of the Al-Li-Cu-Mg system was carried out by the Baikov Institute of Metallurgy [94Rok].

3.2 Experimental part

The phase relations in the Al-rich alloys containing up to 7 wt.% Li, 7 wt.% Mg, and 10 wt.% Cu were investigated. Microscopy analysis, quality local X-ray spectral analysis, and X-ray phase analysis were applied. The alloys were prepared by melting in alumina crucibles in electrical resistivity furnace under flux containing 80 wt.% LiCl + 20 wt.% LiF preserving from Li burning out. The alloys were poured into copper mould with round cavity of 15 mm in diameter. The ingots were squeezed by 50% reduction of their height and cut into pieces. One part the pieces was placed into silica ampoules which were evacuated and then filled by Ar up to 0.5 bar. The ampoules were annealed at 500 °C for 50 hours or at 400 °C for 100 hours followed by quenching into cold water. These samples were used for construction of the isothermal sections. The other part of pieces were used for differential thermal analysis needed for construction of the polythermal sections [96Rok].

3.3 Results

The investigation showed that in the system studied, only few phases belonged to the binary and ternary Al subsystems. These phase were Al_2Cu, AlLi, $Al_{7.5}Cu_4Li(T_B)$, $Al_2CuLi(T_1)$, $Al_6CuLi_3(T_2)$, Al_2LiMg, $Al_2CuMg(S)$. Using the results from the experiments three isothermal sections of the phase diagram were constructed:

1. At 400 °C with the amount of 1.5 wt.% Cu
2. At 400 °C with the amount of 2.8 wt.% Cu
3. At 500 °C with the amount of 1.5 wt.% Cu
4. At 500 °C with the amount of 2.8 wt.% Cu.

Figure 6 shows the phase boundaries measured at 400 °C.

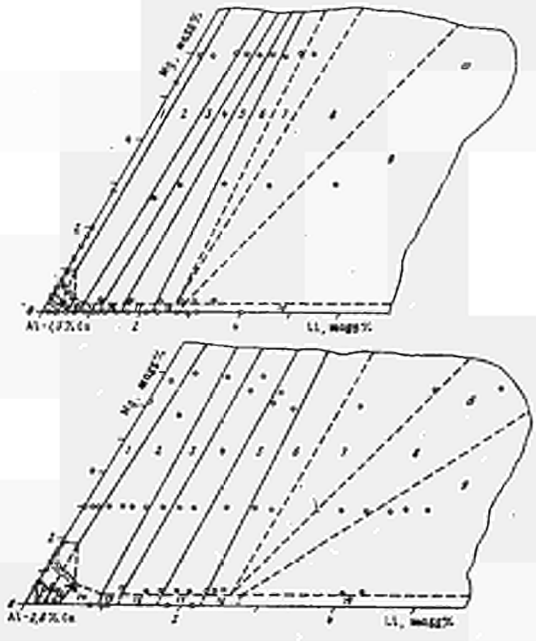

1. (Al) + S
2. (Al) + S + T_B
3. (Al) + S + T_B + T_1
4. (Al) + S + T_1
5. (Al) + S + T_1 + T_2
6. (Al) + S + T_2
7. (Al) + S + T_2 + Al_2LiMg
8. (Al) + T_2 + Al_2LiMg
9. (Al) + T_2 + Al_2LiMg + AlLi
10. (Al) + S + Θ
11. (Al) + T_B + S + Θ
12. (Al) + Θ
13. (Al) + T_B + Θ
14. (Al) + T_B
15. (Al) + T_1 + T_B
16. (Al) + T_1
17. (Al) + T_2 + T_1
18. (Al) + T_2
19. (Al) + AlLi + T_2

Figure 6. The isothermal sections of the Al-Li-Cu-Mg tetrahedron with the constant Cu content of 1.5 wt.% (a) and 2.8 wt.% (b) at 400 °C.

References

[71Kri]
Kripyakevich, P.I., Mel'nik, E.V., Structure of a Mg-Li-Cu Compound: Twelve-Layer Analogue of the Al_2Cu, Mg_2Ni and Mg_2Cu Structures (in Russian), *All-Union Conf. Chem. Intermetallic Compounds*, Lvov 19-21 Oct, (1971), 28

[76Mel]
Melnik, E.V., et.al., X - ray Diffraction Study of Some Ternary systems Containing Mg and Li, *Russ. Metall.*, **3** (1976), 152-156

[82Kuz]
Kuznetsov, G.M., et.al, Phase equilibria in the Cu-Cr-Zr-Mg system, *Izv. Vyss, Uchebn. Zaved. Tsvetn. Metall.*, **6** (1982), 90-93

[94Rok]
Rokhlin, L.L., et.al., Aluminium alloys Containing Lithium, Copper, Magnesium, Izv. *Rus. Acad. Nauk. Met.* (1) (1994), 113-118

[96Boc]
Bochvar, N., Lysova, E., Dobatkina, T., Rokhlin, L.L., Short Report of COST 507, Internal Report, Baikov Institute of Metallurgy, June,1996, 1-15

[96Rok]
Rokhlin, L.L., et.al., *Tekhnologiya Legkikh Splavov*, (5), (1996), 13-19.

The Cu-Cr-Zr Phase Diagram and Its Applications

K .Zeng* and M. Hämäläinen**

*Institute of Materials Research, GKSS-Research Center, Germany
**Helsinki University of Technology, Espoo, Finland

Abstract

The phase diagrams of the Cu-Cr-Zr ternary and its sub-binary systems were optimised and calculated by using the CALPHAD method. An experiment was also carried out to check the reliability of the optimised thermodynamic parameters and clear up the confusion concerning the phase relationships in the Cu-rich corner of the Cu-Cr-Zr phase diagram. All the experimental data from the literature, phase diagram data and thermodynamic data, were evaluated carefully before being used in optimisation. The adjustable parameters of a thermodynamic model for each phase were selected by considering what thermodynamic quantities are connected with the measured values and how these quantities are connected with the parameters. When the entropy term is necessary in the case where Gibbs energies or phase diagram data are measured within a narrow temperature range, the Tanaka-Gokcen-Morita relationship was used to keep the ratio of enthalpy of mixing to the excess entropy of mixing constant.

A complete thermodynamic description of the Cu-Cr-Zr system was obtained and used to calculate various phase diagram sections which are of theoretical and practical importance. Some experimental results from the literature were discussed on the basis of the calculated phase diagrams. The existence of the pseudobinary Cu-Cr_2Zr system proposed in the literature has been ruled out. The results of the present study can be used not only as references for the experimental investigations on optimisation of the composition of Cu-Cr-Zr alloys and their production techniques, but also be combined with other evaluations based on the same type of thermodynamic models to provide a thermodynamic basis for alloy design.

Publications

1. Kejun Zeng, Marko Hämäläinen, and Kaj Lilius, "Thermodynamic Modeling of theLaves Phases in the Cr-Zr System", **CALPHAD** 1993, 17 (1), 101-107.
2. Kejun Zeng and Marko Hämäläinen, "A Thermodynamic Assessment of the Cr-Zr System", **Z. Metallkde.** 1993, 84 (1), 23-28.
3. Kejun Zeng and Marko Hämäläinen, "Thermodynamic Analysis of Stable and Metastable Equilibria in the Cu-Cr System", **CALPHAD** 1995, 19 (1), 93-104.
4. Kejun Zeng, Marko Hämäläinen, and Hans Leo Lukas, "A New Thermodynamic Description of the Cu-Zr System", **J. Phase Equilibria** 1994, 15 (6), 577-586.

5. Kejun Zeng and Marko Hämäläinen, "A Theoretical Study of the Phase Equilibria in the Cu-Cr-Zr System", **J. Alloys and Compounds** 1995, 220, 53-61.
6. Kejun Zeng, Marko Hämäläinen, and Kaj Lilius, "Phase Relationships in Cu-rich Corner of the Cu-Cr-Zr Phase Diagram", **Scr. Metall. Mater.** 1995, 32 (12), 2009-2014.
7. K .Zeng and M. Hämäläinen, "The Cu-Cr-Zr Phase Diagram and Its Applications", in "European Concerted Action: Database for the Development of New Light Alloys (COST-507)", Proc. Conf. (ed. P. Spencer), March 9-12, 1997, Vaals, Netherland

Publications in COST 507 Action

1. Zeng, K., Hämäläinen M., Luoma, R., A thermodynamic assessment of the Cr-Zr system, Report TKK-V-B66 (1991)
2. Coughanowr, C.A., Ansara, I., Luoma, R., Hämäläinen, M., Lukas, L., Assessment of the Cu-Mg system, *Z. Metallkunde*, 1991, 82, (7), pp. 574-581
3. Zeng, K., Hämäläinen, M., Lilius, K., Thermodynamic modeling of the Laves phases in the Cr-Zr system, *CALPHAD*, 17 (1993), p. 101-107.
4. Zeng, K., Hämäläinen, M., Luoma, R., A thermodynamic assessment of the Cr-Zr system, *Z. Metallkunde*, 84, (1993), p. 23-28.
5. Zeng, K., Hämäläinen, M., Thermodynamic analysis of the stable and metastable equilibrium diagrams of the Cu-Cr system, Report TKK-V-B87 (1993)
6. Zeng, K., Hämäläinen, M., A new thermodynamic description of the Cu-Zr system, Report TKK-V-B87 (1993)
7. Zeng, K., Hämäläinen, M., Lukas, H.-L., A New Thermodynamic Description of the Cu-Zr System, *J. of Phase Equilibria*, vol. 15, No. 6, 1994, pp. 577-586
8. Zeng, K., Hämäläinen, M., A Theoretical Study of the Phase Equilibria in the Cu-Cr-Zr System, Proceedings of the 5th Inter. Conf. on Thermodynamics of Alloys, April 25-28, 1994, Genova, Italy, *J. Alloys & Compounds*, vol 220 (1995), pp. 53-61
9. Isopiestic determination of the coefficients of activity of magnesium in Al-Cu-Mg liquid alloys, Soares, D., Malheiros, L.F., Hämäläinen, M., Castro, F., Proceedings of the 5th Inter. Conf. on Thermodynamics of Alloys, April 25-28, 1994, Genova, Italy, *J. Alloys & Compounds*, vol 220 (1995), pp. 179-181
10. Phase relationships in Cu-rich corner of the Cu-Cr-Zr phase diagram, Zeng, K., Hämäläinen, M., Lilius, K., *Scripta metall. et mater.* vol 32, No. 12, 1995, pp. 2009-2014

Smith Thermal Analysis Studies of Al-rich regions of the Al-Mn, Al-Mn-Fe and Al-Mn-Si Systems

J.A.J.Robinson*, F.H.Hayes, A.Serneels** F.Weitzer*** and P.Rogl***

Manchester Materials Science Centre, University of Manchester & UMIST, UK
*present address: National Physical Laboratory, Teddington, Middlesex, UK.
**Dept. Metaalkunde en Toegepaste Materiaalkunde, KUL, Leuven, Belgium.
*** Institut für Physikalische Chemie der Universität Wien, Vienna, Austria.

Abstract

Smith thermal analysis measurements carried out in Manchester during COST 507-II (Round 2) on selected Al-rich alloys in the Al-Mn, Al-Mn-Si and Al-Fe-Mn systems are reported. Phase boundary and invariant reaction temperatures are given for Al-Mn-Si alloys containing 4wt% Si, 0-6 wt% Mn, for Al-Fe-Mn alloys containing 2 wt% Mn, 0-3 wt% Fe, carried out in collaboration with Group B1 (KUL,Leuven), and for selected Al-Mn binary and Al-Fe-Mn ternary alloys, carried out in collaboration with Group A1 (University of Vienna). Liquidus temperatures for the Al-Mn-Si and Al-Fe-Mn alloys are found to be higher than reported by Philips [43Phi]. Results for the Al-Mn binary system agree well with the data presented by McAlister and Murray [87McA] although not all of these are for stable equilibria.

1 Introduction

During the COST 507-II Action it became evident that new and additional phase diagram measurements were needed to resolve questions arising from Al-Fe-Mg-Mn-Si assessment programme. The Smith method of thermal analysis [40Smi], successfully used previously in Manchester to study phase boundaries and invariant reactions for a variety of low melting Au, Ag, In and Al-alloy systems [92Hor, 94Hay1&2].

2 Smith Thermal Analysis

Smith thermal analysis, originally proposed mainly as a calorimertric method for determining heat capacities and latent heats [40Smi], differs from conventional differential thermal analysis, DTA, in a number of ways. In the Smith method, the temperature *difference* between the sample and the furnace wall is maintained at a pre-selected value. Thus in the Smith method the heating or cooling rate is not controlled directly. Maintaining a constant temperature difference between the sample and the heat source/sink creates a condition of constant rate of heat transfer to/from the sample. Over temperature ranges where the sample lies in a single phase region or in a two-or three-phase region where the phase fractions and compositions remain constant, the effective heat capacity of the sample also remains constant, resulting in a constant rate of change of temperature with time, i.e dT/dt = constant. When the sample reaches a phase boundary or invariant reaction temperature on heating or cooling there is an abrupt change in the effective heat capacity which gives a corresponding immediate change in dT/dt. This effect is very sensitive and forms the basis of the Smith method

for determining phase boundary and invariant reaction temperatures. Furthermore, once the sample starts to undergo an invariant reaction, such as a eutectic reaction etc, the temperature remains constant as heat is being absorbed/evolved until the reaction is complete, i.e.dT/dt = zero during the reaction. This results in the sample being in a condition close to equilibrium throughout and minimises non-equilibrium effects such as supercooling etc. Also, reactions that lie within as few degrees can be studied (see for example [92Hor]). A schematic diagram of the Smith rig is given in Figure 1.

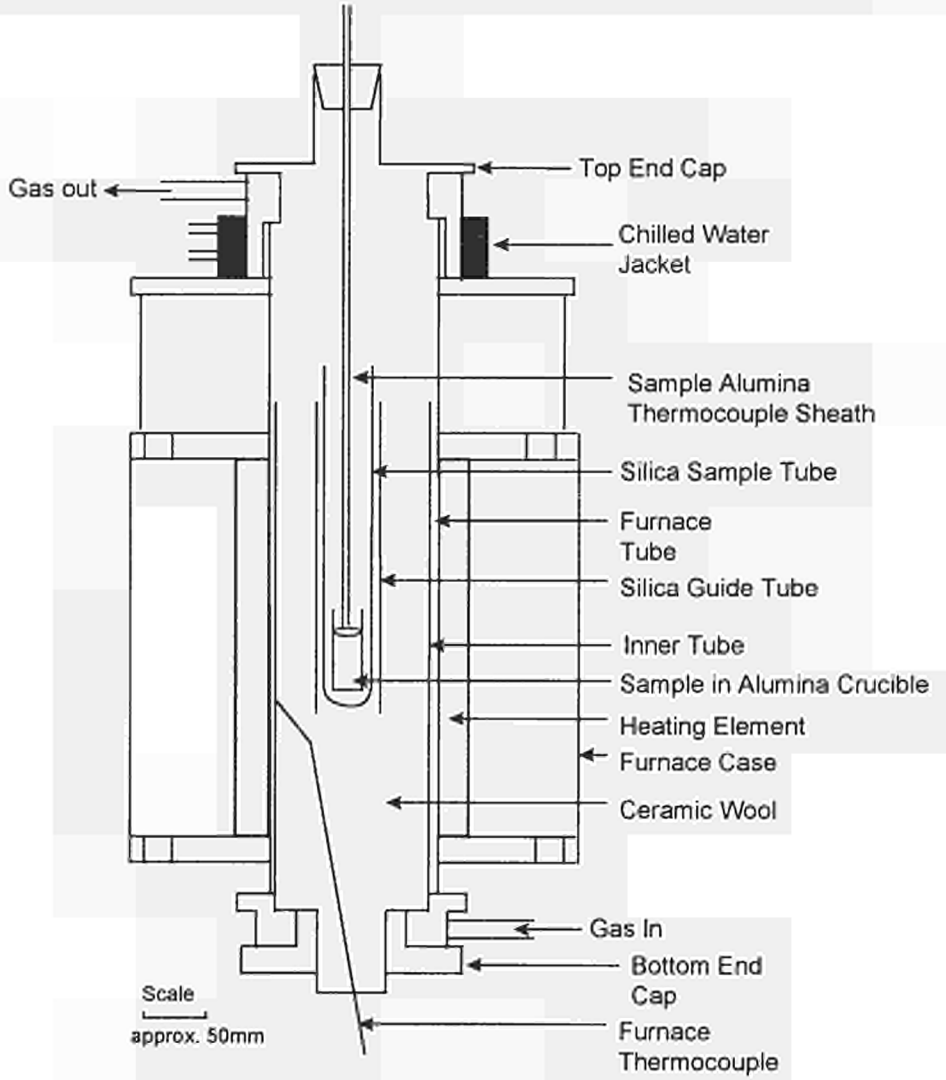

Figure 1 Schematic Diagram of the Smith thermal analysis rig.

3. Al-Mn-Si measurements (James Robinson)

Smith thermal analysis experiments have been carried out by Robinson and Hayes on the Al-Mn-Si system, across the 4wt% Si vertical section in the Al-rich corner of the

system. Alloys at compositions of 1, 2 and 3 - prepared in Vienna - and at 6 wt% Mn - prepared by Alcan - have been studied to determine liquidus, phase boundary and invariant reaction temperatures,. The thermal arrests found so far are summarised in the Table 1 below and shown in Figure 2.

Table 1 - Al-Mn-Si results

Alloy Comp wt% Mn	Eutectic Reaction Temperature (°C)		Other Thermal Arrests (°C)				Liquidus Temp (°C)
	Heating	Cooling	Heating	Cooling	Heating	Cooling	
1	576.9	575.8	635.6	633.0	-	-	667.9
2	577.0	576.7	636.7	634.1	-	-	-
3	576.1	576.4	639.1	637.0	-	-	702.9
6	578.0	576.0	614.8	640.5	715.6	694.3	759.3

4. Al-Fe-Mn measurements(Anja Serneels)

Smith thermal analysis studies were carried out by Serneels and Hayes on four Al-Fe-Mn alloys with 2wt% Mn, with 0.5, 1, 2 and 3wt% Fe respectively. Sample were prepared in Leuven by melting and casting master alloys with Al under an Ar atmosphere. Experiments were carried out determine liquidus, secondary separation and invariant reaction temperatures. Following Smith thermal analysis, the phases present in the samples were identified using optical metallography, XRD and SEM/EDX. DSC measurements were also carried out on the same samples. The thermal arrests found so far are given in the Table 2 below and are shown in the Figure 3. It is seen that the Smith results for the Al_6Mn liquidus temperatures are consistently higher than those given by [43Phi]; other temperatures agree well.

5. Al-Mn and Al-Fe-Mn measurements (Franz Weitzer)

Seven selected Al-Mn alloys were studied by the Smith method. In addition to equilibrium phase boundary and reaction temperatures, metastable reactions were also studied on cooling. The results are summarised in Figure 4 superimposed on the phase diagram published in [90Mas] after [87McA]. The present results agree well with the data presented by [87McA]. Eight further alloys, $Al_{12}Mn$, $Al_{81.3}Fe_{2.2}Mn_{16.5}$, $Al_{81.3}Fe_{5.7}Mn_{13}$, $Al_{79}Fe_6Mn_{15}$, $Al_{73.7}Fe_{10.5}Mn_{15.8}$, $Al_{76}Fe_8Mn_{16}$, $Al_{72.5}Fe_{18.5}Mn_{9.5}$, $Al_{72.5}Fe_{18.5}Mn_{9.5}$ and $Al_{69}Fe_{11.5}Mn_{19.5}$ were also studied. Samples were prepared in Vienna. Results have already been presented [96Wei].

6 References

40Smi C S Smith, Trans. American Inst. Met. Eng., 1940, **137**, 236-245.

43Phi H W L Phillips, J.Institute of Metals, 1943, **69**, 275-316.

87McA A J McAllister, J M Murray, Bull.Alloy Phase Diag, 1987, 8, 438-447.

90Mas T B Massalski et al, *Binary Alloy Phase Diagrams*, 2nd edition, 1990.

92Hor P J Horrocks, F H Hayes and N D Moulson, Thermochimica Acta, 1992, **204**, 25-33.

Table 2 Al-Fe-Mn results

wt% Fe	Liquidus Temperatures (°C)		Secondary Separation Temps. (°C)	Solidus/Eutectic Temperatures (°C)	
	heating	cooling		heating	cooling
0.5	674.3	666.4		655.2	655.7
	674.5	669.7		653.1 (651)	655.4
	671.4	663.5		652.8(646)	655.2
	667.1	663.3		653.1(650)	654.8
	668.0	691.1		654.5	655.2
		668.8		654.7	655.1
		669.8			656.0
1		682.7		653.3	653.5
		680.0		650.9	653.1
		680.0			651.9
		679.3			652.0
					651.4
2	695.5	700.9		652.4	654.7
	695.8	699.5		652.5	654.3
	697.9	699.0		652..1	654.6
		703.5		652.4	
		701.2			
		700.5			
3		729.3	691.6	651.1	651.2
		732.5	691.2	650.2	652.6
		734.7	691.4	650.2	
		734.6	(694.3)		
		733.6	691.8		
		731.5			
		728.4			
		740.2			
		741.9			
		739.9			

94Hay1 F H Hayes, W T Chao and J A J Robinson, *'Experimental Methods of Phase Diagram Determination,* ed J.E.Morral , R.S.Schiffman and S.M.Merchant, TMS, Warrendale, Penn.,USA, 101-111, 1994.

94Hay2 F H Hayes, W T Chao and J A J Robinson, Journal of Thermal Analysis, 1994, **42**, 745-758.

96Wei F Weitzer, P Rogl, F H Hayes, and J A J Robinson, *"Phase Relations in the Aluminium-rich Part of the System: Aluminium -Iron-Manganese"*, presented at the Hauptversammlung der Deutschen Gesellschaft für Materialkunde, May 1996, Stuttgart; in press Keramische Berichte, 1997" Deutsche Keramische Gesellschaft.

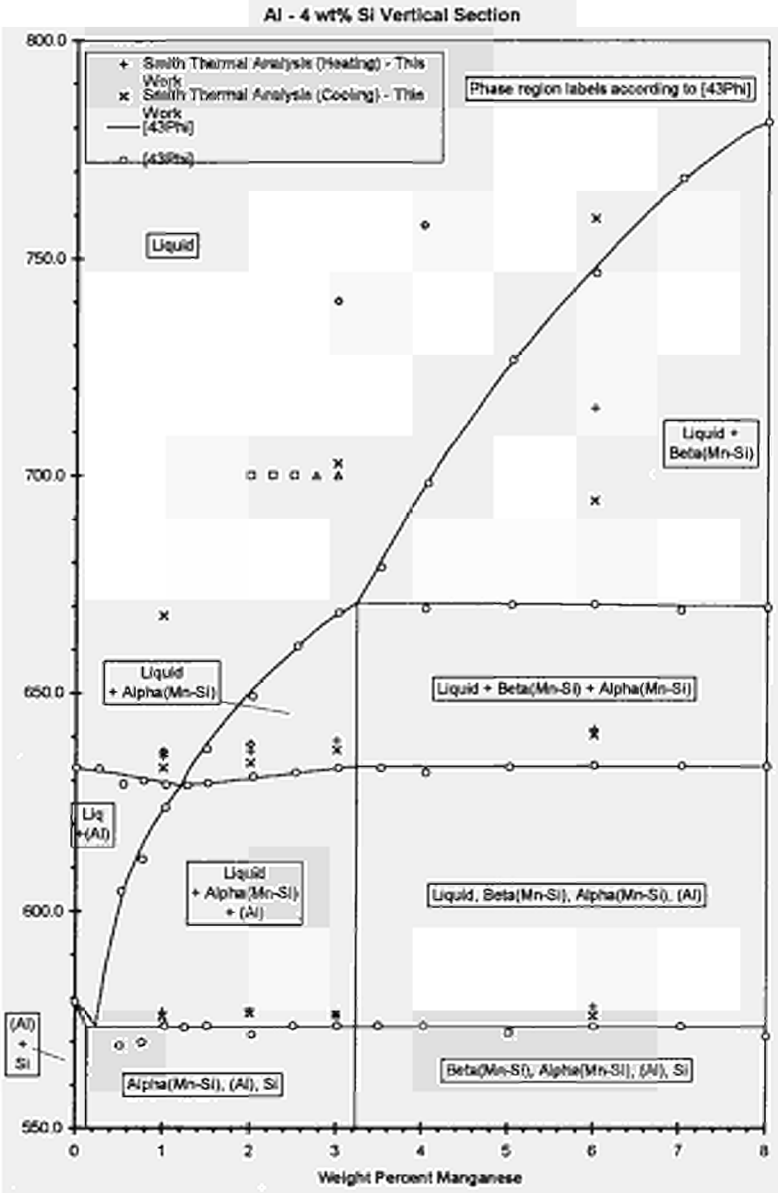

Figure 2. Present results for Al-Mn-Si superimposed on [43Phi] boundaries

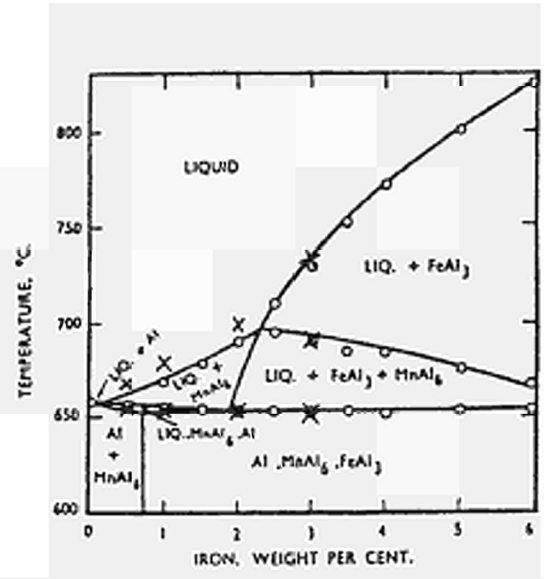

Figure 3 Present results for Al-Fe-Mn, crosses, superimposed on [43Phi] boundaries

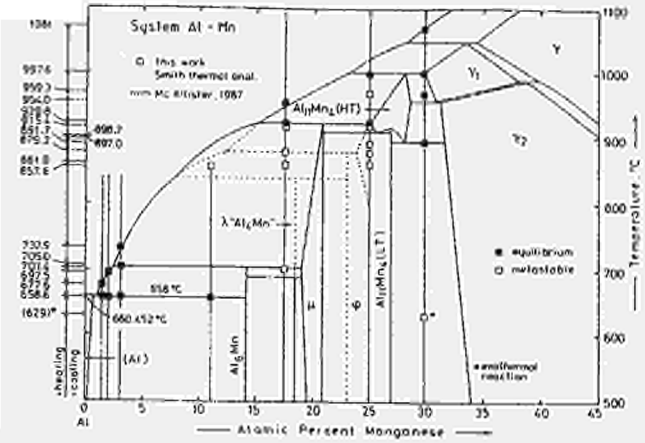

Figure 4 Partial Al-Mn phase diagram after [87McA] with present Smith thermal analysis results for seven alloys (squares) superimposed

A Themodynamic Assessment of the Ti-Al-V System

F. H. Hayes and J. A. J. Robinson*

Manchester Materials Science Centre, University of Manchester & UMIST, UK
*present address: National Physical Laboratory, Teddington, Middlesex, UK

Abstract

As part of the COST 507 programme on the leading system Ti-Al-Me-X a thermodynamic dataset for the Ti-Al-V system has been derived by applying the Thermo-Calc Parrot module to the available experimental data. Published data consist of tie-line and tie-triangle data, calorimetric enthalpies of formation of solid alloys, thermal analysis results for invariant reactions, a partial liquidus surface and partial reaction scheme. Since the Ti-Al-V literature review by Hayes [93, 95Hay] new experimental studies have been reported which include partial isothermal sections with some information on A2-B2 ordering from Ahmed and Flower [94Ahm1], a partial liquidus surface and possible reaction scheme by Ahmed, Rack and Flower [94Ahm2], and solidification and thermal analysis studies by Paruchuri and Massalski [91Par]. The present dataset is based mainly on the models and binary assessments of the Al-Ti, Al-V and Ti-V systems by Saunders [95Sau] with some changes to the Al_3M $D0_{22}$ phase description and addition of B2 ordering. This paper compares the thermodynamically calculated Ti-Al-V results from the present assessment with the original experimental data points for tie-lines, tie-triangles and enthalpies of formation. Calculated A2-B2 boundaries from 1573K to 873K and a calculated liquidus projection are also given.

1 Introduction

The aim has been to produce a dataset able to reproduce by calculation:
(i) the experimental Ti-Al-V tie-line and tie-triangle data [68Tsu, 85Has, 88Mae, 91Par, 93Nak, 94Ahm1] (ii) the calorimetric enthalpies of formation of the solid alloys [60Kub] (iii) the known features of the liquidus surface and (iv) the observed invariant reactions and probable reaction scheme [68Kor, 91Par, 94Ahm2]. Since publication of the Ti-Al-V literature review carried out by Hayes [93, 95Hay] and the COST 507(I) dataset [94Hay], important new experimental data have been published by Ahmed and Flower for several partial isothermal sections including information on A2-B2 ordering [94Ahm1] and on the liquidus surface and reaction scheme by Ahmed, Rack and Flower [94Ahm2] and by Paruchuri and Massalski [91Par]. The present dataset is based on the models and binary assessments of the Al-Ti, Al-V and Ti-V systems given by Saunders [95Sau]. It was necessary to modify the description of the Al_3M $D0_{22}$ phase to account for the experimentally observed single phase region reported by [94Ahm1] and others. Also the bcc phase description has been changed to account for

the observed A2-B2 ordering. This paper compares thermodynamically calculated Ti-Al-V results from the present assessment with the original experimental data points.

2 Data Assessment

2.1 Isothermal Sections

Figures 1 and 2 compare the calculated boundaries at 1573K and 1473K with the data points given by Kikuchi and co-workers [93Nak]. Figures 3-6 and 8 show the experimental tie-line and tie-triangle data points reported by Ahmed and Flower [94Ahm1] superimposed on the calculated isothermal sections at 1473K, 1173K, 1073K, 973K and 873K respectively. Figure 7 compares the calculated boundaries with those from Paruchuri and Massalski for 900K [91Par]. Figure 9 gives the calculated Ti-Rich corner at 873K with the experimental data from [88Mae].

2.2 Enthalpies of Formation of Solid Alloys

Kubaschewski and co-workers [60Kub] used direct reaction calorimetry, optical metallography and X-ray diffraction to study 50 Ti-Al-V alloy compositions. Measured enthalpies for solid alloy formation were reported for ten constant vanadium sections. All of these data were used in the assessment. Figures 10-13 compare the calculated enthalpy curves with the experimental data for constant vanadium contents of 5, 10, 15 and 20 at%.

2.3 A2-B2 Boundaries

Figure 14 shows the A2-B2 boundaries from 1573K to 873 calculated with the present dataset. The B2 boundaries are in good agreement with the experimental data given by Ahmed and Flower [94Ahm1].

2.4 Liquidus Projection

Figure 15 gives the calculated liquidus projection. The sequence and positions of the invariant reactions are in broad agreement with the available experimental results [94Ahm2, 91Par].

3 Conclusions

The present dataset give calculated phase equilibria which show good agreement with the experimental data over a wide range of temperature ie from 1573K to 873K. The dataset is consistent with the calorimetric values for the enthalpies of formation of the solid alloys for alloys containing > 50 at% Ti. Towards the Al-rich corner however the agreement with the experimental data points is poor. For all of the sections studied the Al-rich phases have lower heats than given by the dataset.

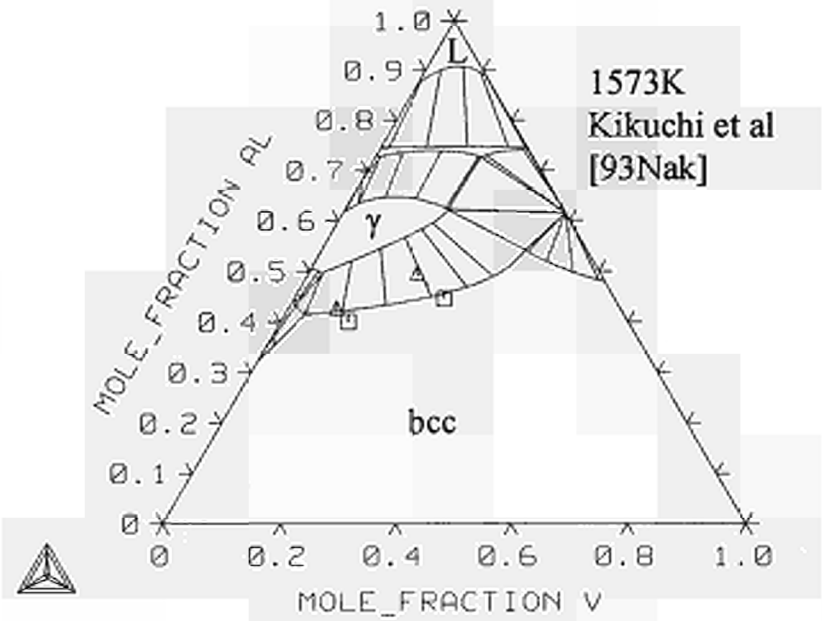

Figure 1

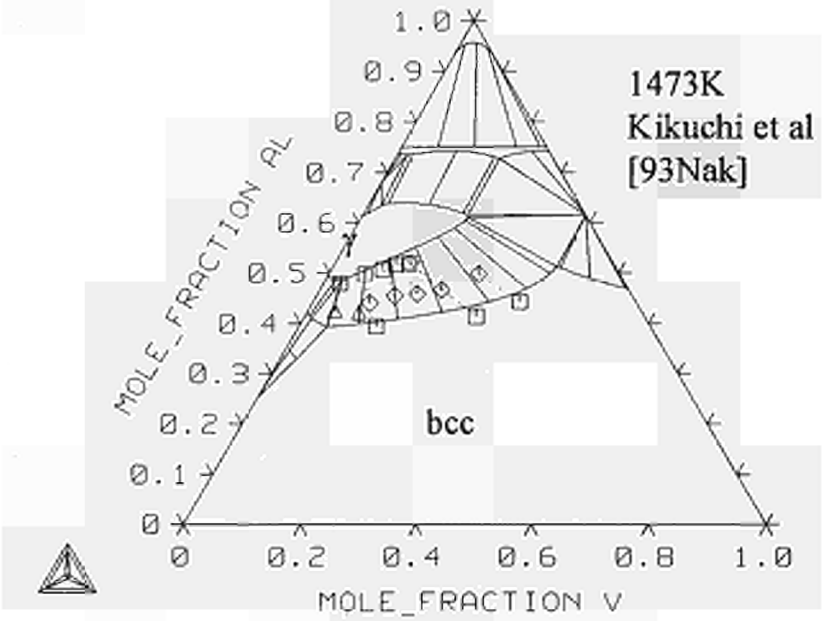

Figure 2

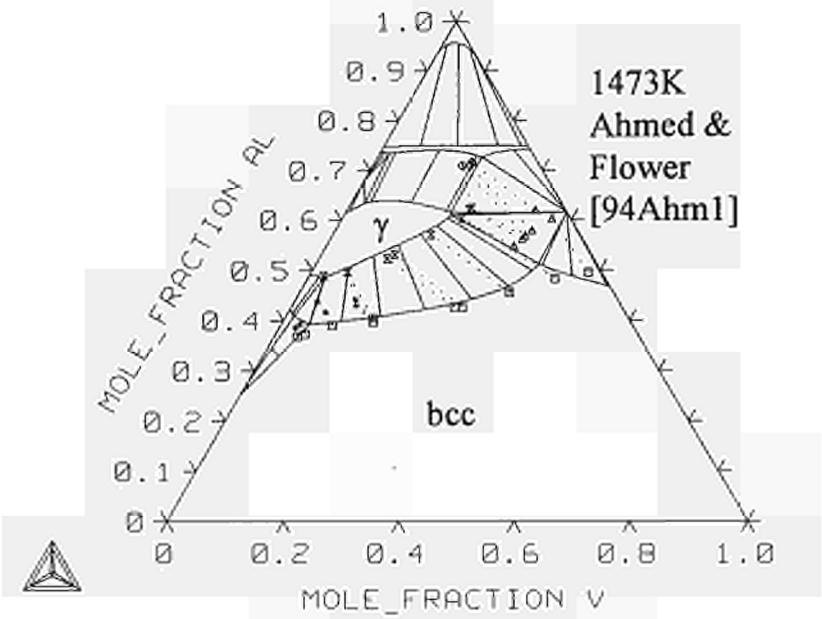

Figure 3

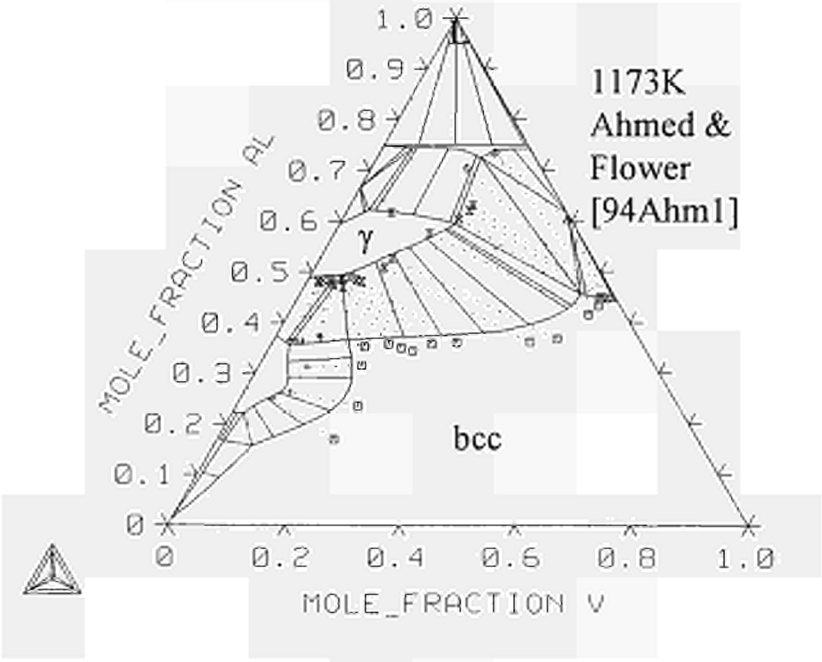

Figure 4

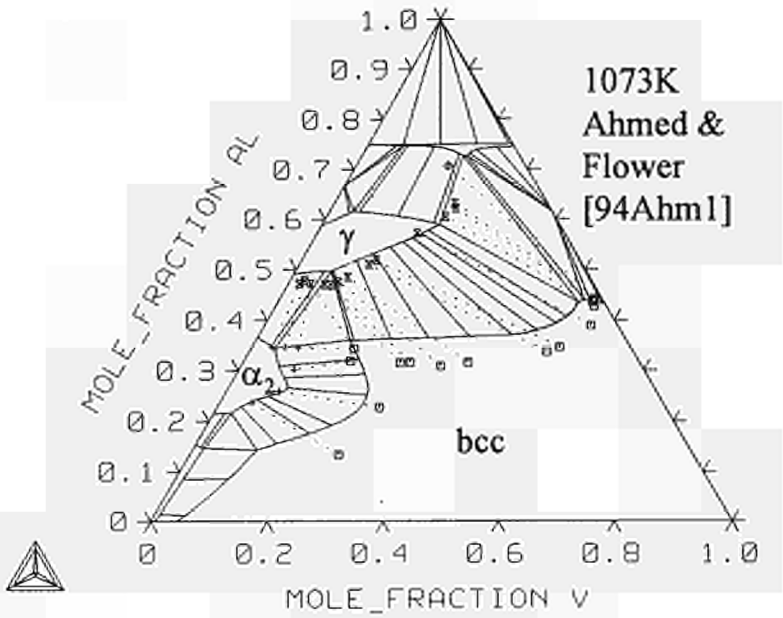

Figure 5

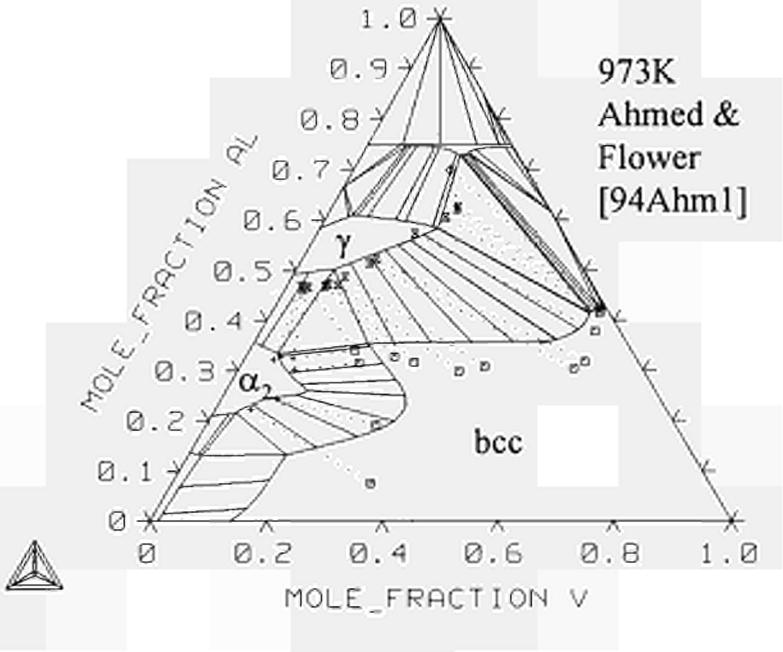

Figure 6

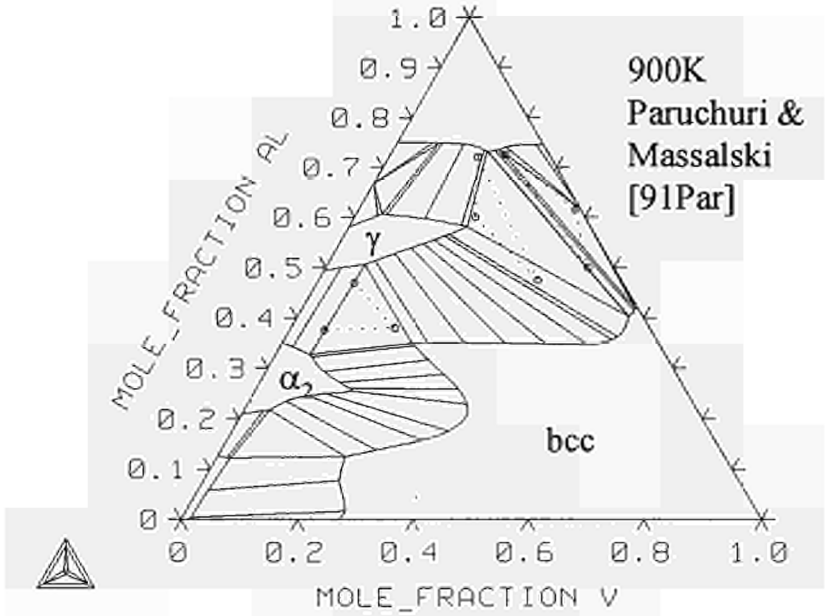

Figure 7

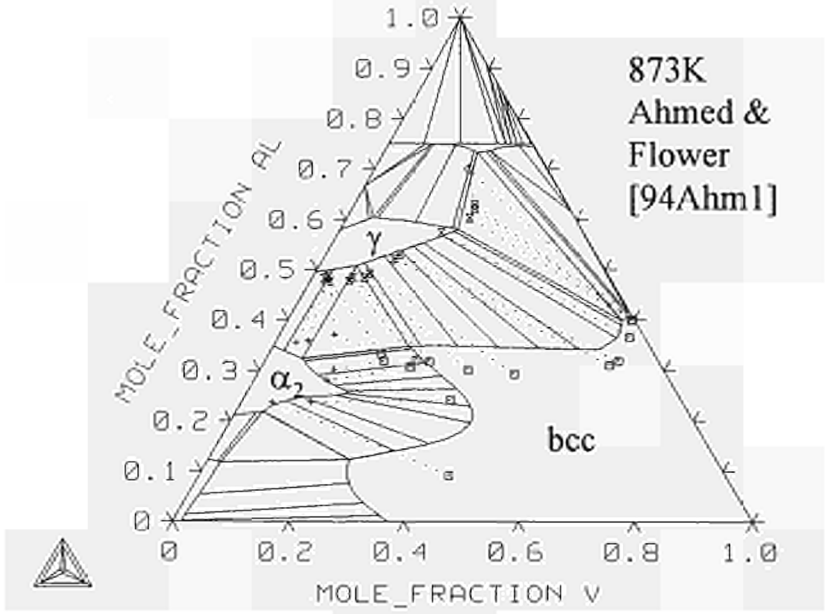

Figure 8

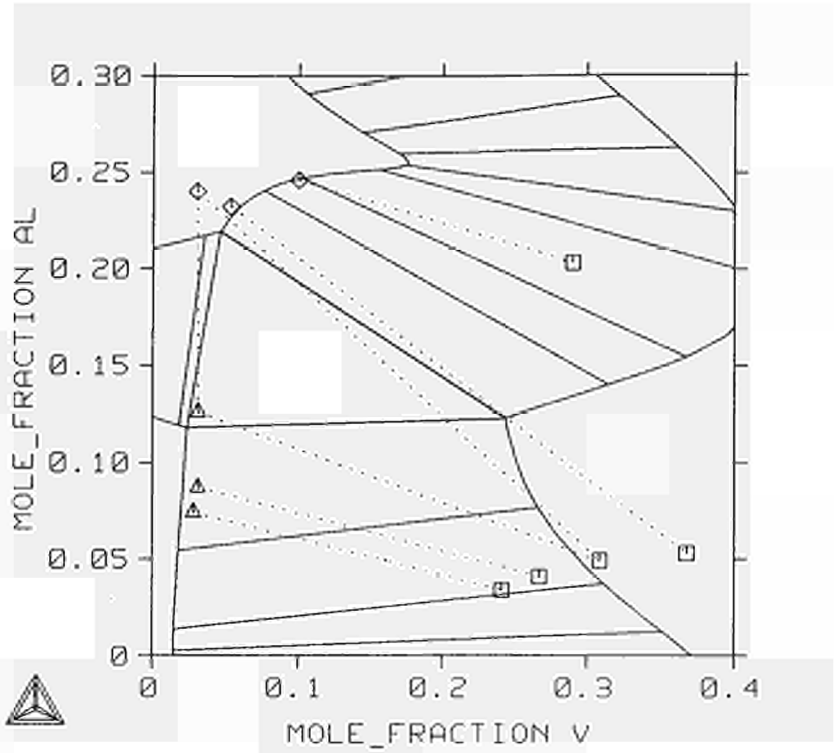

Figure 9

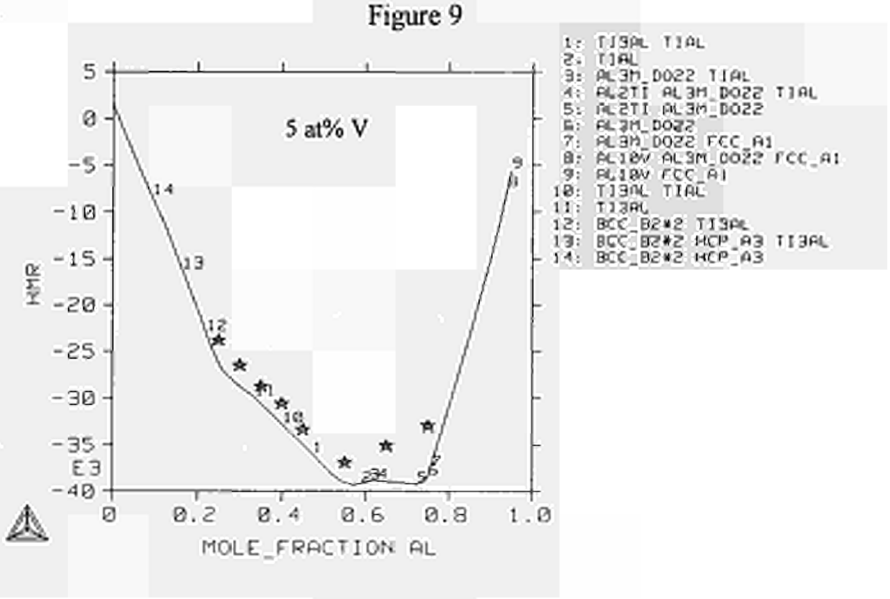

Figure 10

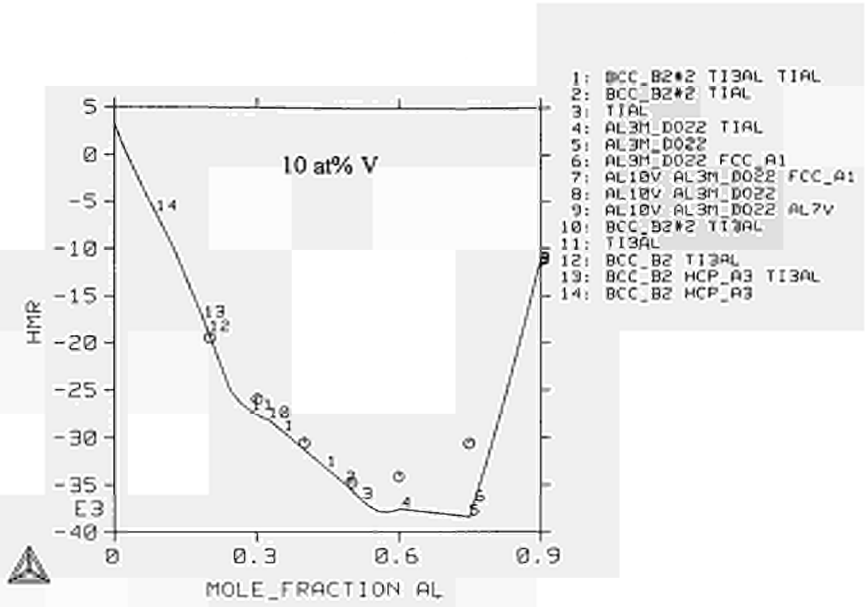

Figure 11

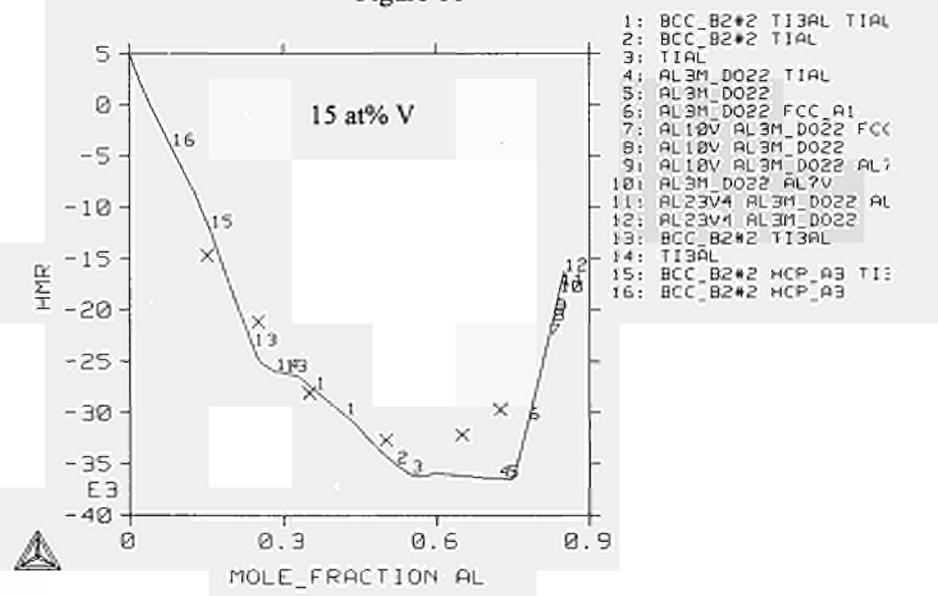

Figure 12

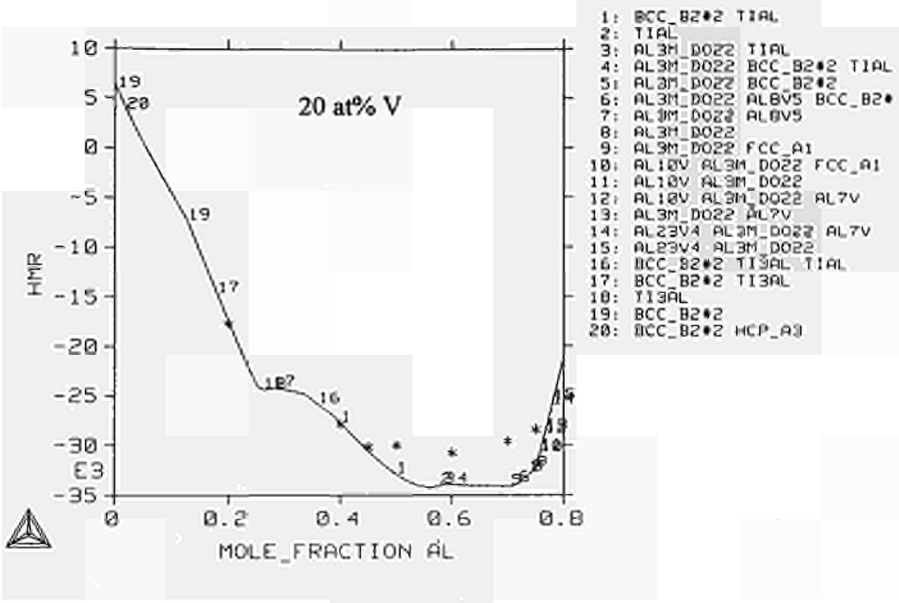

Figure 13

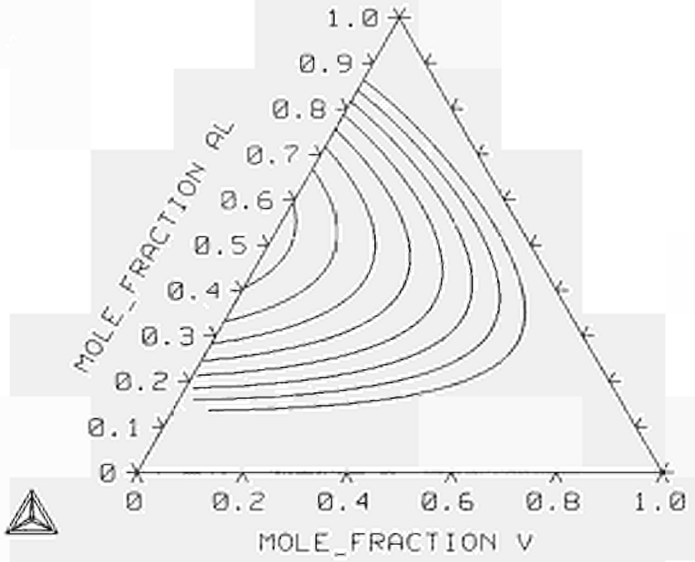

Figure 14: Calculated A2-B2 boundary 1573K-873K

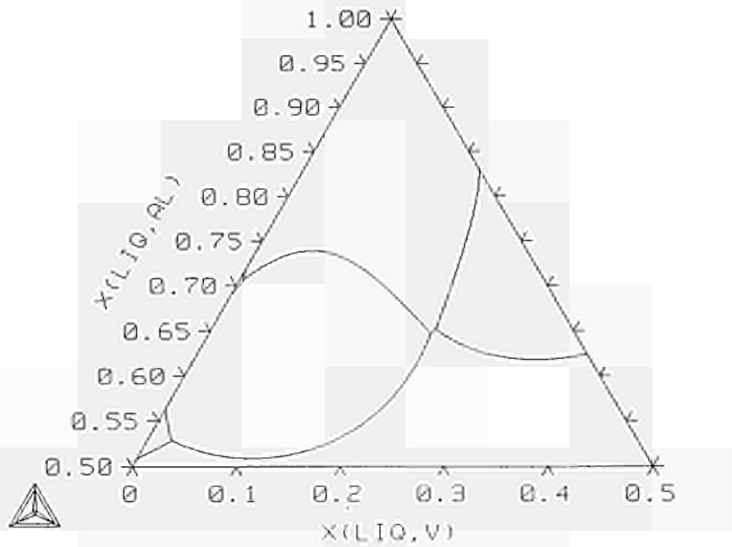

Figure 15 Calculated liquidus surface

4 References

[60Kub] O Kubaschewski, C Wainwright, F J Kirby, J.Inst. Metals,1960, **89,** .139-144.

[68Kor] I I Kornilov, M A Volkova, Izvestia Akad. Nuak, S.S.S.R., 1968, **Met (1),** 176-180.

[68Tsu] T Tsuijimoto, Trans. Japanese Institute of Metals, 1969, **10,** 281-286, translated from Journal of the Japanese Institute of Metals 1968, **32**(10), 970-975.

[85Has] K Hashimoto, H Doi, T Tsuijimoto, Trans. Japanese Institute of Metals, 1986, **27**(10), 741-749, translated from Journal of the Japanese Institute of Metals, 1985, **49**(6), 410-416.

[88Mae] T.Maeda, Ph.D. Thesis, Imperial College, University of London (1988).

[91Par] M Paruchuri, T B Massalski, *Materials Research Society Symposium Proceedings* 1991, **213,** 143-149.

[93Hay] F H Hayes, *'Ternary Alloys'*, Volume 8, ed. G Petzow and G Effenberg , pub VCH Verlagsgesellschaft, Weinheim, Germany, 426-455, 1993.

[93Nak] H Nakamura, M Takeyama, L Wei, Y Yamabe, M Kikuchi, *Symposium on Intermetallic Compounds for High Temperature Structural Applications,* 3rd Japanese Int. SAMPE Symposium, December 1993, *Scripta Met. & Mat.*, 1993, **28**, 997-1002.

[94Ahm1] T Ahmed, H M Flower, Materials Science and Technology, 1994, **10,** 272-288.

[94Ahm2] T Ahmed, H.J.Rack, H.M.Flower, Materials Science and Technology, 1994,**10,** 681-690.

[94Hay] F H Hayes, COST 507 I Project Final Report, *Thermodynamic Assessment of the Ti-Al-V system,* June 1994.

[95Sau] N.Saunders, *Thermodynamic Database for Light Metal Alloys,* ed. I Ansara COST 507, Concerted Action on Materials Sciences, European Commission, DG XII, Luxembourg, 1995.

[95Hay] F H Hayes, J.Phase Equilibria, 1995, **16** (2), 163-176.

A Thermochemical Assessment of Data for the Al-rich Corner of the of the Al-Mn-Si System

Malcolm H Rand,[■] Per Kolby[♦] and Tim G Chart[★]

[■]WintersHill Consultancy, Abingdon, Oxfordshire, UK
[♦]SINTEF, Oslo, Norway
[★]Chart Associates, Ashford, Middlesex, UK

Abstract

This research forms part of the COST 507 programme on the Al-Fe-Mg-Mn-Si system (Leading System 1). It provides an optimisation of data for the Al-rich corner of the Al-Mn-Si ternary system, which in addition to the available published data, incorporates the results of experimental measurements carried out during the Action by Alcan International Ltd (Banbury Laboratory), Pechiney Centre de Recherches de Vorrepe, SINTEF and University of Manchester/UMIST, and incorporates a revision of data for the binary Al-Mn system, based upon the original COST 507 assessment for this system [92Jan, 94Ans].

The results of the assessment are summarised. The experimental phase equilibrium studies carried out in combination by the above groups have proven to be essential to the project. It is clear, however, that some further information is required, particularly to define unambiguously the relative stabilities of the cubic alpha, hexagonal beta and liquid phases. The solid phases are not easy to nucleate, and the associated thermal effects are small, so quite detailed and careful experimentation is required to produce reliable results.

1 Introduction and Overview of the System

The Al-Mn-Si system is of crucial importance in the evaluation of the Al-Fe-Mg-Mn-Si quinary system, since one of the important phases in commercial alloys, eg for canning and recycling, is based on the ternary cubic alpha phase in this system.

The most recent assessment of the Al-Mn-Si system is by Prince [93Pri]. This necessarily relied heavily on the pioneering work by Phillips [43Phi], (revised slightly in the later publications [59Phi, 61Phi]), since this is still the only substantial study of the Al-rich corner of the system. Although the overall picture of the Al-Mn-Si system from this work is undoubtedly correct, particularly at low Mn levels, some doubt was thrown on some of Phillips' transition temperatures by the work of Chadwick *et al* in COST 507 Round I. It is clear that the difference in stability of the phases in many Al-Mn binary and higher systems is quite small, so that effects such as difficulties of nucleation and the presence of small amounts of impurities, eg Fe, can have noticeable effects on the experimental phase diagrams for this system. These effects appear to be particularly relevant to Phillips' study, bearing in mind the likely levels of impurities in Al alloys of the 1940s, and the techniques employed.

Recent experimental work on this system initiated as a result of the current project, particulary on the section containing 4 wt% Si, by a combination of Alcan International Ltd (Banbury Laboratory) and University of Manchester/UMIST, have confirmed that some of the liquidus temperatures measured by Phillips are indeed substantially (at least 20 K) too low. In addition, new solvus data which differ appreciably from those of Phillips have been produced by SINTEF and Pechiney as part of the project [94Kol/Sig]. These data have been incorporated into a new thermodynamic description of this system. This new description reproduces well the data for the 4 wt% Si section, but raises doubts as to the accuracy of the previously available experimental information available in many parts of the system.

The phases in this ternary system which are in equilibrium with aluminium are Al_6Mn, Al_4Mn and two ternary phases, usually called alpha and beta. These are different in both composition and structure from the similarly-named phases in the Al-Fe-Si system.

2 Phase diagram

As noted above, the only systematic study of the system was carried out by Phillips more than fifty years ago, with some more recent work at silicon levels close to the binary Al-Si eutectic (c. 12 wt% Si) [88Zak/Gul] and data for equilibria between liquid, beta and cubic-alpha at 1027 K by Redford *et al* [90Red/Tib]. Axon and Hume-Rothery [48Axo/Hum] also gave partial sections at 460 °C, but they may not correspond to true equilibrium.

The liquidus projection suggested by Prince [93Pri] is very similar to that proposed by Phillips [59Phi, 61Phi] in his revision of his earlier work. However, thermal analysis work during COST 507 Round I suggested that some of the liquidus temperatures on this diagram were appreciably too low - particularly those for the separation of the complex cubic-alpha and beta phases.

An experimental program was thus initiated during COST 507 Round II, in order to clarify this situation. Attention has been focused mainly on the isopleth containing 4 wt% Si. The results of the annealing experiments by Thornton at Alcan International [96Tho] and the Smith calorimetric work of Hayes and Robinson at UMIST [96Hay/Rob] are summarised in Fig 1. A few studies have also been made on the 4 wt % Mn isopleth, as shown in Fig 2. These two figures also show the calculated phase boundaries resulting from the present assessment. The more complete study on the 4 wt% Si section does indeed indicate that the liquidus temperatures measured by Phillips for the separation of the cubic-alpha and beta phases are too low by some 20 - 30 K.

There is also fairly convincing evidence that the manganese level in the ternary eutectic involving fcc, cubic-alpha and silicon is somewhat lower than the value of c. 0.8 wt% suggested by Phillips. Mn levels in the liquid near this eutectic measured by Zakhorov *et al* [88Zak/Gul] and Simensen [96Sim] suggest that the Mn content in the liquid is between 0.5 and 0.7 wt%.

The position of the line for the co-existence of cubic-alpha, beta and liquid is also not well-defined. Pratt and Raynor [51Pra/Ray] extracted relatively large crystals of the beta-phase by cooling alloys to 660 - 700 °C, annealing for 1 hour and quenching. However, Simensen [96Sim] has repeated this experiment with an alloy containing 6 wt% Mn, 4 wt% Si, using annealing times of 1 day, and found crystals of cubic-alpha containing a little beta, surrounded by alpha (see Fig 1). This indicates that although beta can be the phase first formed, as found by Pratt and Raynor (1 hr anneal), the equilibrium phase is cubic-alpha. Redford *et al* have suggested that the cubic-alpha phase is not in equilibrium with the liquid above c. 7.5 wt% Mn and 1023 K.

Phillips[43Phi, 59Phi, 61Phi] has given data for four invariant points in the system, detailed in Section 6 below. Clearly if the liquidus temperatures from which these are derived are somewhat in error, there will be some uncertainty in these values.

Recent data for the mutual solid solubility of Mn and Si in fcc Al are also available [94Kol/Sig].

We must therefore conclude that although the general form of the Al-Mn-Si ternary is well-established, the details of the system at Mn levels above 1 wt% are still subject to appreciable uncertainty and we are in the unhappy situation of not being able to rely with any certainty on the main corpus of experimental phase diagram information for this system [43Phi, 59Phi, 61Phi].

3 Phase Models

The cubic alpha phase, called here C alpha, has a variable composition around $Al_{17}Mn_4Si_2$ and is formed at relatively low Mn and Si contents. This has been modelled with a range of silicon content using the sublattice description

$$Al_{16}Mn_4Si \quad (Al,Si)_2$$

which corresponds to an essentially constant manganese content of 30.0 wt%, and a silicon content which could vary from 3.8 to 11.4 wt%. This is an important phase in the quaternary Al-Fe-Mn-Si system, since the Mn in this phase can be replaced up to

at least 95% by Fe, possibly 99%, although the pure Fe cubic analogue is (probably) not truly stable in the Al-Fe-Si system, at least at temperatures close to where the compound is formed from the melt. In the quaternary system, Fe will mix with Mn on the second sublattice.

The hexagonal beta phase, of approximate composition $Al_{10}Mn_3Si$, is formed at high Mn and low Si levels. This also exists with a range of Si composition, and we are currently modelling this phase with the sublattice description

$$Al_{15}Mn_6Si(Al,Si)_4$$

There is no evidence of any appreciable solubility of silicon in Al_6Mn or Al_4Mn and these phases have taken to be stoichiometric binary compounds in this ternary system.

4 Thermodynamic Data

The only thermodynamic data available during the period in which the assessment was carried out were some Cp measurements for the cubic-alpha phase and the enthalpy of transformation of a cubic-alpha phase to beta plus liquid, all derived from DTA measurements [90Red/Tib, 96Tib]. However, a preliminary value for the enthalpy of formation of a sample of the C alpha phase has just become available [97Leg], but has not yet been incorporated into the assessment, since further enthalpy data are likely to emerge from the same source.

5 Optimisation.

A considerable effort has been expended in the optimisation of the phase diagram information for this system, but with the uncertainty in the phase equilibria noted above, the current assessment can still only be regarded as preliminary. The revision of data for the Al-Mn binary system of Jansson and Chart [97Jan/Cha] has been incorporated.

In the current optimisation, the highest weighting has been placed on the latest results for the 4 wt% Si isopleth due primarily to Thornton [96Tho] (see Fig 1) and the primary phase crystallising from a liquid containing 6 wt% Mn, 4 wt% Si was taken to be cubic-alpha [96Sim] and not beta, as suggested by [51Pra/Ray]. The data of Zakharov *et al* [88Zak/Gul] have also been included, together with the information from Redford *et al* [90Red/Tib] and [94Kol/Sig].

6 Results

The calculated co-ordinates of the four invariant points are compared to the literature values (mostly based solely on those of [43Phi]) in Table 1.

Table 1 Invariant points in Al-Mn-Si

Phase assemblage	T °C	Liquid compositions wt %		Reference
		w(Mn)	w(Si)	
liq + beta AlMnSi + Al_6Mn + Al_4Mn	703.9	4.32	0.29	Calculated
	690	3.8	0.7	[76Mon]
	690	4.5	0.5	[61Phi]
	690	4.5	0.5	[93Pri]
liq + beta AlMnSi + Al_6Mn + C alpha	644.4	2.50	0.72	Calculated
	657	2.8	1.6	[76Mon]
	655	2.65	1.6	[61Phi]
	655	2.6	1.6	[93Pri]
liq + fcc + C alpha + Al_6Mn	653.9	2.09	0.69	Calculated
	648	2.5	1.5	[76Mon]
	649	2.0	1.28	[61Phi]
	649	2.0	1.2	[93Pri]
liq + fcc + C alpha + diamond	576.4	0.35	12.57	Calculated
	574	1.0	12.0	[76Mon]
	573	0.75	11.75	[61Phi]

The calculated isopleths for 4 wt% Si and 4 wt% Mn are given in Figs 1 and 2 and the calculated liquidus projection is shown in Fig 3. A calculated partial isothermal section for 600 °C is compared with experimental data from Thornton [95Tho] in Fig 4 and the calculated fcc solvus is compared with the experimental data of Kolby *et al* [94Kol/Sig] in Fig 5.

It will be seen that the current assessment gives a good representation of those data in which we have the highest confidence. A reassessment should be carried out when additional phase equilibria and thermodynamic information on the cubic-alpha and beta phases becomes available.

7 Acknowledgements

The authors gratefully acknowledge valuable discussions with Dr Paul V Evans and Martin C Thornton (Alcan International Ltd), Dr Christophe Sigli (Pechiney) Dr Christian Simensen (SINTEF) Dr J E Tibballs (University of Oslo) and Dr F H Hayes (University of Manchester/UMIST).

8 References

43Phi H W L Phillips, J Inst Metals, 1943, **69,** 275-316.

48Axo/Hum H J Axon, W Hume-Rothery, J Inst Metals, 1948, **74**, 315-329.

51Pra/Ray J N Pratt, G V Raynor, Proc Roy Soc 1951, **205A**, 103-118.

59Phi H W L Phillips, *Annotated Equilibrium Diagrams of Some Aluminium Alloys Systems,* The Institute of Metals, London, (1959), Monograph and Report Series, No 25, pp 77-83.

61Phi H W L Phillips, *Equilibrium Diagrams of Aluminium Alloys Systems,* The Aluminium Development Association, London, (1961), pp 109-112.

76Mon L F Mondolfo, *Al Alloys; Structure and Properties*, Butterworths, London & Boston, 1976.

88Zak/Gul A M Zakharov, I T Guldin, A A Arnold, Yu A Matsenko, Izv Vyss Uchebn Zaved Tsvetn Metall, 1988, (2), 90-94.

90Red/Tib K Redford, J E Tibballs, R McPherson, Thermochim Acta, 1990, **158**, 115-123.

92Jan A Jansson, Metall Trans A, 1992, **23A**, 2953-2962.

93Cha G A Chadwick, Progress Report to COST 507 Coordination Group C, March 1993.

93Pri A Prince, *Aluminium-Manganese-Silicon* in *Ternary Alloys,* Ed G Petzow and G Effenberg, VCH Weinheim & New York, **5,** 110 - 128 (1993).

94Ans I Ansara, *Thermochemical Database for Light Metal Alloys*, COST 507, Concerted Action on Materials Sciences, European Commission, DG XII, Luxembourg, 1995

94Kol/Sig Kolby P, Sigli, C, Simensen, C J, in *Aluminium Alloys; Their Physical and Mechanical Properties*, 4th International Conference on Aluminium Alloys, Ed T H Sanders Jr and E A Starke Jr (1994).

95Tho M C Thornton, Alcan International Ltd, Banbury Laboratory, Private Communication, July, 1995.

96Hay/Rob F H Hayes, J A J Robinson, Private communication, August 1996.

96Sim C J Simensen, SINTEF, Private communication May 1996.

96Tib J E Tibballs, Oslo University, Private communication, September 1996.

96Tho M C Thornton, Alcan International Ltd, Banbury Laboratory, Private Communication, May, July and August, 1996.

97Leg B. Legendre, Private Communication to Per Kolby, March 1997

97Jan/Cha A Jansson, T G Chart, *A Thermochemical Assessment of Data for the Al-rich corner of the Al-Fe-Mn System, and a Revision of Data for the Al-Mn System*, Proceedings of COST 507 Final Workshop, Vaals, The Netherlands, March 1997, European Commission, DG XII, Luxembourg.

97Rob/Hay J A J Robinson, F H Hayes, A Serneels, F Weitzer, P Rogl, *Smith Thermal Analysis Studies of the Al-rich Portion of the Al-Mn and Al-Mn-X (X = Fe, Si) Systems*, Proceedings of COST 507 Final Workshop, Vaals, The Netherlands, March 1997, European Commission, DG XII, Luxembourg.

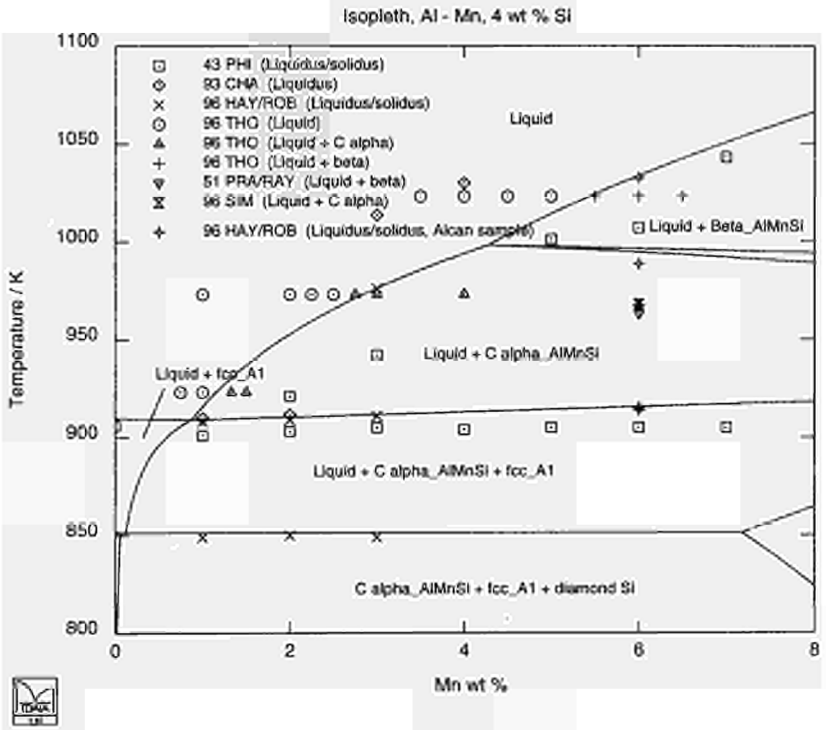

Fig 1 Calculated isopleth for the Al-Mn-Si system at 4 wt % Si. Experimental data from [43Phi], [51 Pra/Ray], [93Cha], [96Hay/Rob], [96Sim] and [96Tho] are superimposed.

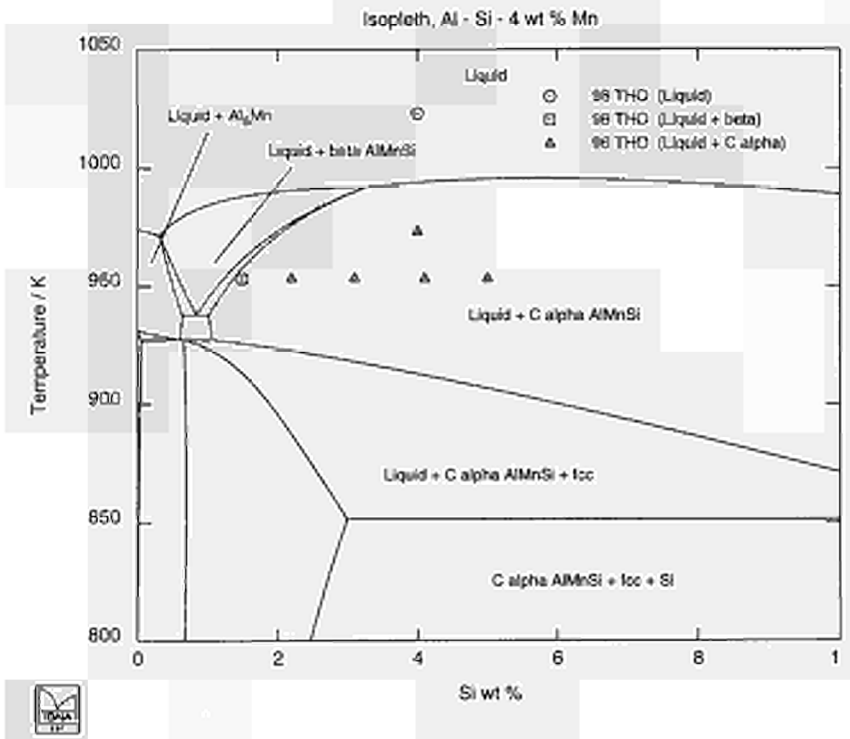

Fig 2 Calculated isopleth for the Al-Mn-Si system at 4 wt % Mn. Experimental data from [96Tho] are superimposed.

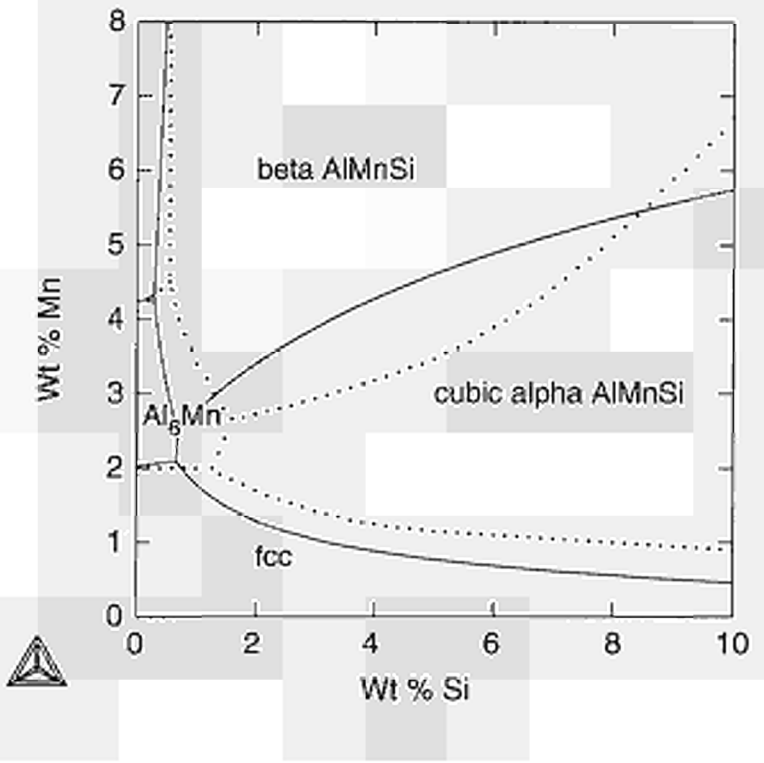

Fig 3 Calculated liquidus projection for the Al-rich corner of the Al-Mn-Si system (full line). The data of Phillips [43Phi] are superimposed (dotted line).

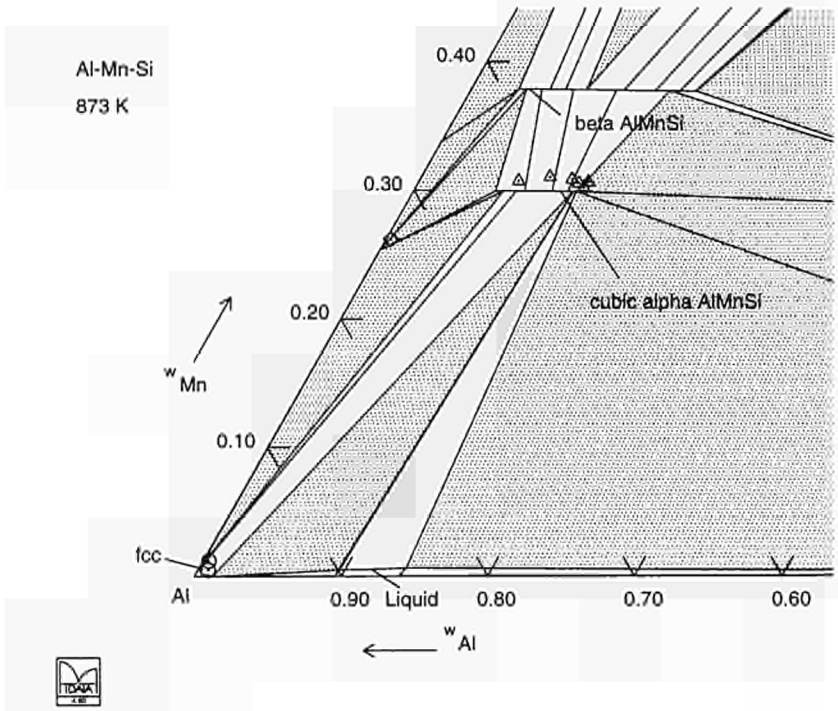

Fig 4 Calculated partial isothermal section for the Al-rich corner of the Al-Mn-Si system at 873 K. Experimental data of Thornton et al [95Tho] are superimposed.

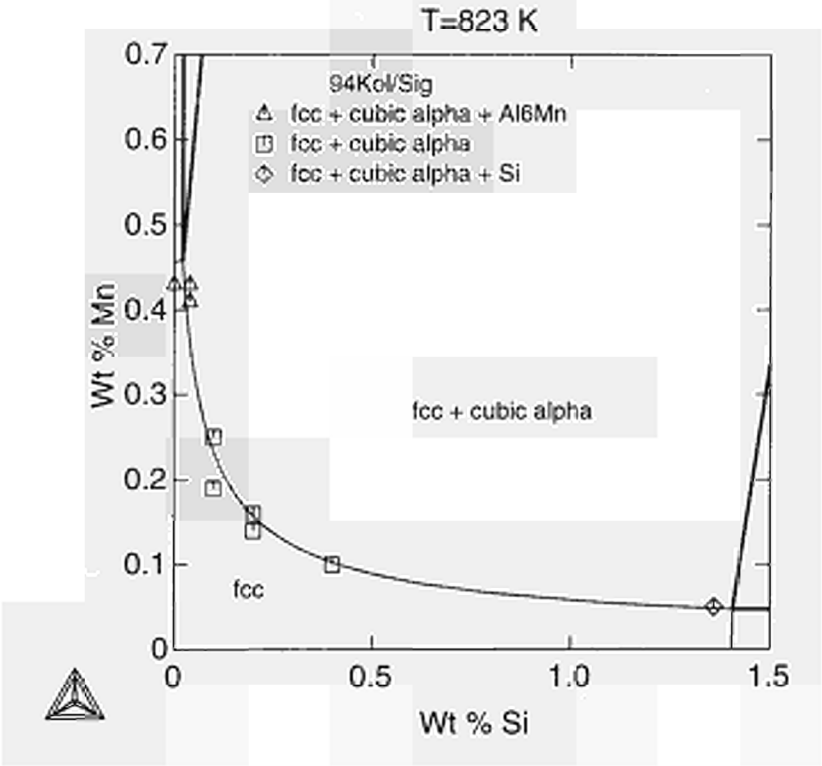

Fig 5 Calculated partial isothermal section for the Al-rich corner of the Al-Fe-Mn system at 823 K, showing the fcc solvus. Experimental data of Kolby *et al* [94Kol/Sig] are superimposed.

A Thermochemical Assessment of Data for the Al-rich Corner of the Al-Fe-Mn System, and a Revision of Data for the Al-Mn System

Åke Jansson[▪] and Tim G Chart[★]

[▪]Royal Institute of Technology, Stockholm, Sweden
[★]Chart Associates, Ashford, Middlesex, UK

Abstract

This research forms part of the COST 507 programme on the Al-Fe-Mg-Mn-Si system (Leading System 1). It includes a revision of data for the binary Al-Mn system, based upon the original COST 507 assessment for this system [92Jan, 94Ans] and an optimisation of data for the Al-rich corner of the Al-Fe-Mn ternary system, which in addition to the available published data, incorporates the results of experimental measurements carried out during the Action by a combination of Alcan International Ltd (Banbury Laboratory), Katholieke Universiteit Leuven, Pechiney, SINTEF, Universität Wien and University of Manchester/UMIST; these experiments specifically performed to provide missing data, as described in other papers of the proceedings of the COST 507 Final Workshop, *eg* [97Rob/Hay].

The overall system currently under study is the Al-Fe-Mg-Mn-Si system. The phase relationships in the base Al-Fe-Mn-Si system itself are very complex and not well-established. In particular, during Leading System 1 meetings held on the quinary system and its constituent sub-systems, it became clear that the phase diagram data for some of these key sub-systems, largely based on the early work of Phillips [43Phi] may be subject to considerable experimental uncertainty, especially data for the Al-Mn binary system and the Al-Fe-Mn and Al-Mn-Si ternary systems, due, *eg*, to difficulties of nucleation, the presence of metastable phases and the effects of impurities.

The results of the assessments are summarised. The experimental phase equilibrium studies carried out in combination by the above groups have proven to be essential to the project. It is clear, however, that some further careful experimentation is required.

1 Introduction

During the last two years new experimental measurements on the Al-Mn and Al-Fe-Mn systems have been carried out at Alcan International Ltd (Banbury Laboratory) by Thornton and Evans, and at University of Manchester/UMIST by Hayes et al, specifically to elucidate the problems, following recommendations made COST 507 progress meetings. Work carried out as part of the COST 507 Action and under the present project, together with supplementary work has incorporated these new data, and (a) has provided a revised and improved dataset for the Al-Mn binary system which is consistent with our current understanding of experimental data for this system, and (b) has provided an updated dataset for the Al-Fe-Mn ternary system which is considered very satisfactory for present purposes.

The effort has been considerable, and the problems, now largely resolved, have understandably delayed the development of the Al-Fe-Mg-Mn-Si database, also the addition of Cu. Although further work is required on the Al-Mn-Si system, which suffers related experimental uncertainties, especially the data of [43Phi], the current situation is good, very much improved compared with that of a year ago. The results of experimental measurements on the Al-Mn and Al-Fe-Mn systems carried out at Alcan International during the course of the project, have proven essential to our understanding of the experimental uncertainties and to the development of the database.

2 Data Assessment

2.1 Al-Mn system

The calculated phase diagram for this system is shown in Fig 1. The phase diagram data for this binary system, crucial to the present project, has caused great concern due to experimental inadequacies. Much painstaking work and careful analyses of the available information has been carried out both in the present work and by others in the field. The experimental data, particularly for equilibria involving Al_4Mn, are fraught with problems due to the appearance of metastable phases, rather than the stable phase, see eg, [87Mur/McA, 87 McA/Mur, 92Jan, 96Wei/Rog]. This leads to low, non-equilibrium liquidus temperatures, which, however, are consistently reproduced by different experimental studies. For the present project the most important part of the system is the range 0 to 4 or 6 wt % Mn, although for multicomponent calculations it is important to have a good overall representation of the system. For the Al-rich region the prime data source is due to Phillips [43Phi], coupled with recent data from University of Manchester/UMIST [95Hay/Rob], now more generally available [96Wei/Rog], carried out using a sophisticated calorimetric technique, and data of Thornton [96Tho4]. In addition Sigli [95Sig] has redetermined the solid solubilities of Mn in fcc Al.

The current analysis takes into account a revision of the original [43Phi] thermal analysis data by Phillips himself, reported obscurely in an evaluation of the Al-Mn-Si system [59Phi] (see also [61Phi]), and includes information obtained on heating, rather than cooling, by [33Dix/Fin, 87McA/Mur], which avoids the problem of undercooling. The data of [96Wei/Rog] and [96Tho4] have been incorporated. Figs 2-4 show calculated phase equilibria for the Al-rich part of the system. Fig 2 shows the undercooling effects observed over the composition range 10 - 30 wt % Mn, almost

certainly due to the appearance of metastable phases, and Fig 3 shows the corrected [59Phi] information together with a single value of [33Dix/Fin] at ≈ 10 % Mn, and the recent data of [96Tho4]. The fcc solvus is shown in Fig 4. The current re-assessment, which is a modified and improved version of that in the COST 507 database [92Jan], represents a very satisfactory outcome.

2.2 Al-Fe-Mn System

During the course of the current project new experimental information concerning the solid-state equilibria has been determined by Thornton [95Tho1, 95Tho2] at 570 and 600 °C, and liquidus data have been determined at University of Manchester/ UMIST [95Hay/Ser] to corroborate the 2 wt % Mn isopleth due to [43Phi]. In addition solid-state equilibria at 550 °C by Rogl, Universität Wien [95Wei/Rog], [95Rog], have been made available to the project. These latter data are now more generally available [96Wei/Rog].

An optimisation has been carried out whereby substantial consistency between the low-temperature (570 and 600 °C) solid-state data of [95Tho1, 95Tho2], the solid-state data of Rogl (550 °C) [96Wei/Rog], and the liquidus data of Phillips [43Phi] (allowing for expected undercooling, see Section 2.1), and Hayes [95Hay/Ser], has been achieved. The revised data for the Al-Mn system have been incorporated. Figs 5 and 6 show calculated partial isothermal sections for 873 and 843 K, with the results of [95Tho1, 95Tho2] superimposed. Fig 7 shows a calculated partial isothermal section for 823 K, with the results of [96Wei/Rog] superimposed. Fig 8 shows the calculated isopleth for a constant 2 wt % Mn. Experimental data of [43Phi], [95Hay/Ser] and [96Tho1, 96Tho2, 96Tho3] are superimposed. Figs 9 and 10 show the calculated fcc solvus at 823 and 873 K respectively, with experimental data made available by SINTEF [95Sim/Kol] and due to Hamerton [96Ham] superimposed.

Figs 5 - 10 show that substantial agreement between the experimental data and the current assessment has been achieved. Fig 8 indicates the undercooling experienced by [43Phi] (these experimental values were not corrected by Phillips), and probably reflects the true situation. It has not yet been possible to obtain agreement with all of the data due to Thornton without unreasonable stabilisation of the $Al_6(Mn,Fe)$ phase and an accompanying unreasonable raising of the liquidus curve. The data for 3, 3.25 and 3.5 wt % Fe are currently under review by Thornton; with respect to Fig 8 it may be that very small amounts of $Al_{13}(Fe,Mn)_4$ were present, but extremely difficult to detect.

3 Conclusions and Recommendations for Further Work

The current thermodynamic data assessments for the binary system Al-Mn and the ternary system Al-Fe-Mn represents a significant milestone for the overall project, and a considerable advancement in our knowledge of phase diagram information for these two systems. Subject to further limited confirmatory experimental studies, the assessment of data for these two systems can now be regarded as substantially complete.

Completion of the above paves the way for completion of data for the Al-Mn-Si system, both experimental studies (in progress at Alcan International Ltd, Banbury

Laboratory, as part of this COST Action) and the subsequent assessment of data. Furthermore, major emphasis can now be placed on the assessment of data for Cu-containing systems, very important to the overall project.

The results of experimental measurements on the Al-Mn and Al-Fe-Mn systems carried out by the combination of Alcan International Ltd, Katholieke Universiteit Leuven, Pechiney, SINTEF, Universität Wien and University of Manchester/UMIST, during the course of the project have proven essential to our understanding of the experimental problems associated with these systems, and to the development of the database.

4 Acknowledgements

The authors gratefully acknowledge support from NUTEK, Swedish National Board for Industrial and Technical Development (Åke Jansson), National Physical Laboratory, UK (Tim G Chart) and the COST Secretariat, DGXII. Valuable discussions with Dr Paul V Evans, Martin C Thornton and Dr Richard Hamerton (Alcan International Ltd), Dr Christophe Sigli (Pechiney) and Prof Peter Rogl (Universität Wien) are gratefully acknowledged.

5 References

33Dix/Fin E H Dix, W L Fink, L A Willey, Trans AIME, 1933, **104**, 335-352.

40Fah/Hof E Fahrenhorst, W Hofmann, Metallwirtschaft, 1940, **19**, 891-893.

43Phi H W L Phillips, J Inst Metals, 1943, **69**, 275-350.

45But/Hum E Butchers, W Hume-Rothery, J Inst Metals, 1945, **71**, 78-91.

53Obi/Hat I Obinata, E Hata, K Yamaji, Jpn J Inst Met, 1953, **17**, 496-501.

58Liv/Voz V A Livanov, V M Vozdvizhenskii, Tr Mosk Aviats Tekhnol Inst, 1958, (31) 84-99.

59Phi H W L Phillips, *Annotated Equilibrium Diagrams of Some Aluminium Alloys Systems,* The Institute of Metals, London, (1959), Monograph and Report Series, No 25, pp 77-83.

61Phi H W L Phillips, *Equilibrium Diagrams of Aluminium Alloys Systems,* The Aluminium Development Association, London, (1961), pp 91-96.

64Dri/Kad M E Drits, E S Kadaner, E M Padezhnova, N R Bochvar, Russ J Inorg Chem, 1964, **9**, 759-762.

71God/Kos T Gödecke, W Köster, Z Metallkde, 1971, **62**, 727-732.

87Mur/McA J L Murray, A J McAlister, R J Schaefer, L A Bendersky, F S Biancaniello, D L Moffat, Metall Trans A, 1987, **18A**, 385-392.

87McA/Mur A J McAlister, J L Murray, Bull Alloy Phase Diag, 1987, **8**, 438-447.

91Min/Yam Y Minamino, T Yamane, H Araki, N Takeuchi, Y-S Kang, Y Miyamoto, T Okamoto, Met Trans A, 1991, **22A**, 783-786.

92Jan A Jansson, Metall Trans A, 1992, **23A**, 2953-2962.

94Ans I Ansara, *Thermochemical Database for Light Metal Alloys*, COST 507, Concerted Action on Materials Sciences, European Commission, DG XII, Luxembourg, 1995

95Hay/Rob F H Hayes, J A J Robinson, *COST 507 II Project, Report on Smith Thermal Analysis Studies of Al-Mn (-Fe) Alloys*, Manchester

Materials Science Centre, November 1994.

95Hay/Ser F H Hayes, A Serneels, J A J Robinson, *COST 507 II Project, Report on Smith Calorimeter Experiments in the Ternary Al-Fe-Mn System*, Manchester Materials Science Centre, April 1995.

95Rog P Rogl, Universität Wien, Private Communication, July 1995.

95Sig C Sigli, CALPHAD XXIV Conference, Kyoto, Japan, May 1995.

95Sim/Kol C J Simensen, P Kolby, A contribution to the ternary phase diagram of aluminium-manganese-iron, SINTEF Report, STF24 F95085, December 1995.

95Tho1 M C Thornton, Alcan International Ltd, Banbury Laboratory, Private Communication, March 1995.

95Tho2 M C Thornton, Alcan International Ltd, Banbury Laboratory, Private Communication, April 1995.

95Wei/Rog F Weitzer, P Rogl, Deutsche Gesellschaft für Materialkunde meeting, Bochum, June 1995.

96Ham R G Hamerton, Alcan International Ltd, Banbury Laboratory, Private Communication, June 1996.

96Tho1 M C Thornton, Alcan International Ltd, Banbury Laboratory, Private Communication, January 1996.

96Tho2 M C Thornton, Alcan International Ltd, Banbury Laboratory, Private Communication, April 1996.

96Tho3 M C Thornton, Alcan International Ltd, Banbury Laboratory, Private Communication, May 1996.

96Tho4 M C Thornton, Alcan International Ltd, Banbury Laboratory, Private Communication, September 1996.

96Wei/Rog F Weitzer, P Rogl, F H Hayes, J A J Robinson, *Phase Relations in the Aluminium-Rich Part of the System: Aluminium-Iron-Manganese*, in "Werkstoff Woche '96, Materialwissenschaftliche Grundlagen", ed. F Aldinger and H Mughrabi, 1997, Deutsche Gesellschaft für Materialkunde, pp 185-190.

97Rob/Hay J A J Robinson, F H Hayes, A Serneels, F Weitzer, P Rogl, *Smith Thermal Analysis Studies of the Al-rich Portion of the Al-Mn and Al-Mn-X (X = Fe, Si) Systems*, Proceedings of COST 507 Final Workshop, Vaals, The Netherlands, March 1997, European Commission, DG XII, Luxembourg.

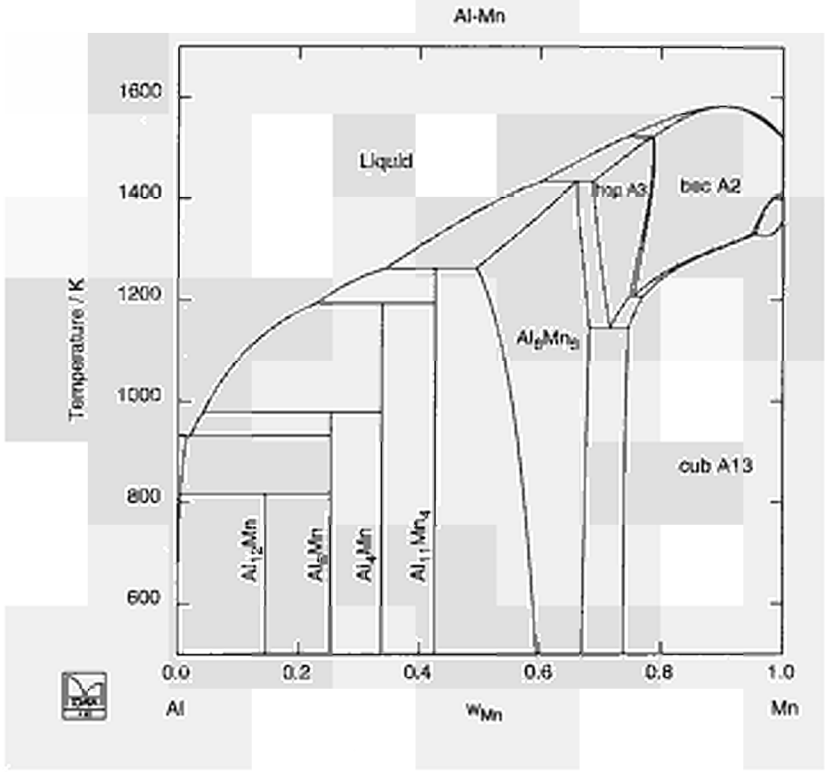

Fig 1 Calculated phase diagram for the Al-Mn system.

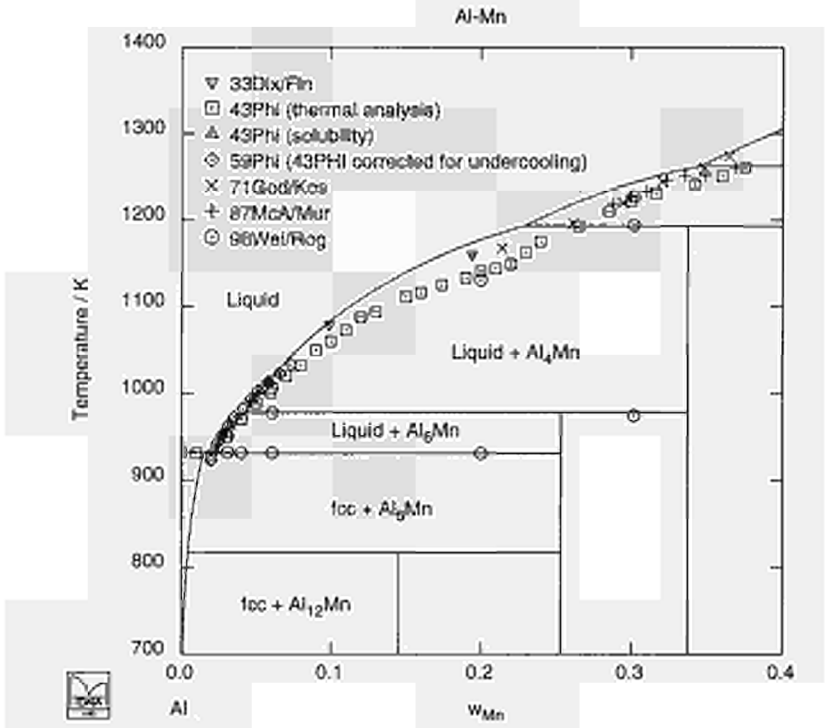

Fig 2 Calculated partial phase diagram for the Al-Mn system, showing experimental data.

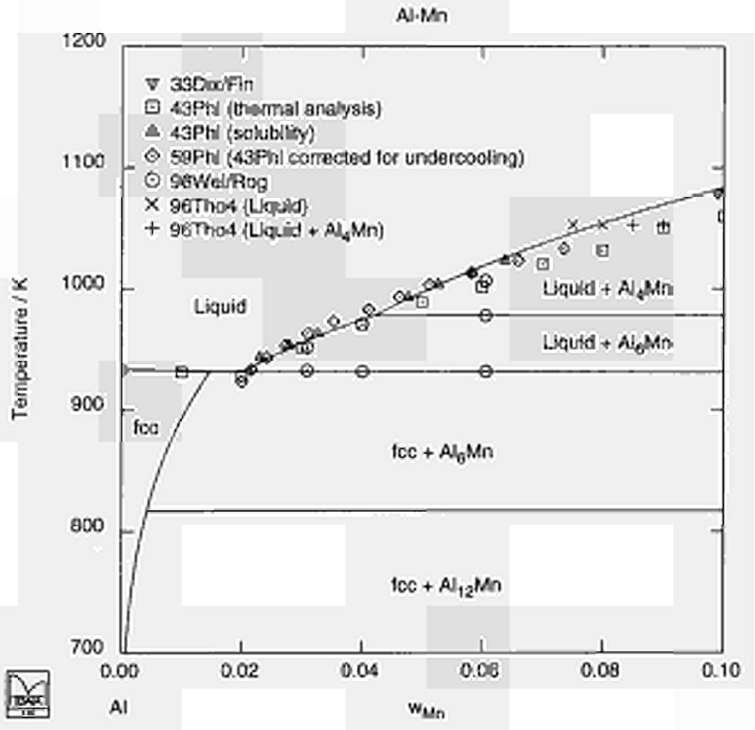

Fig 3 Calculated partial phase diagram for the Al-rich portion of the Al-Mn system, showing experimental data.

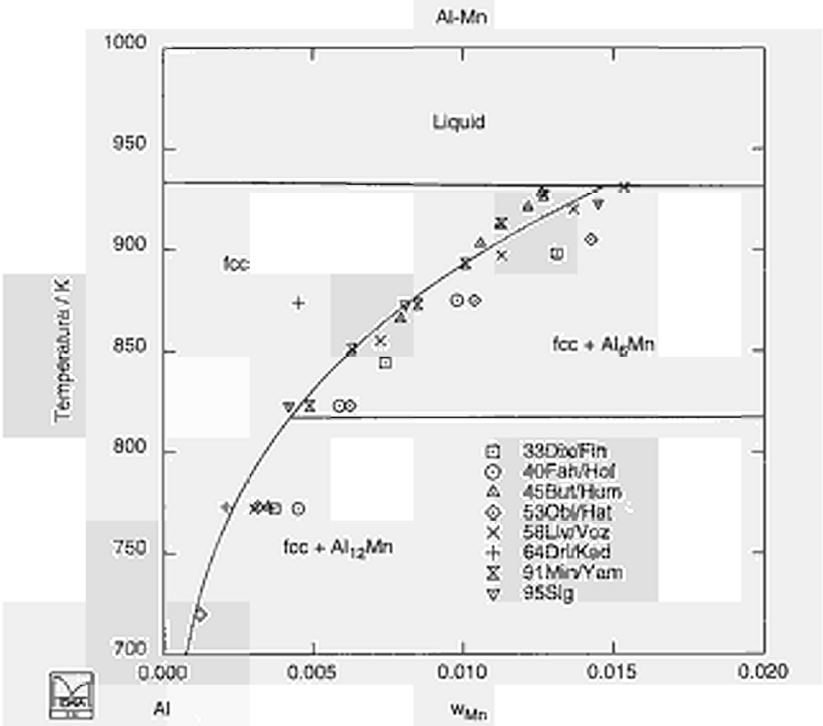

Fig 4 Calculated partial phase diagram for the Al-rich portion of the Al-Mn system, showing experimental data for the fcc solvus.

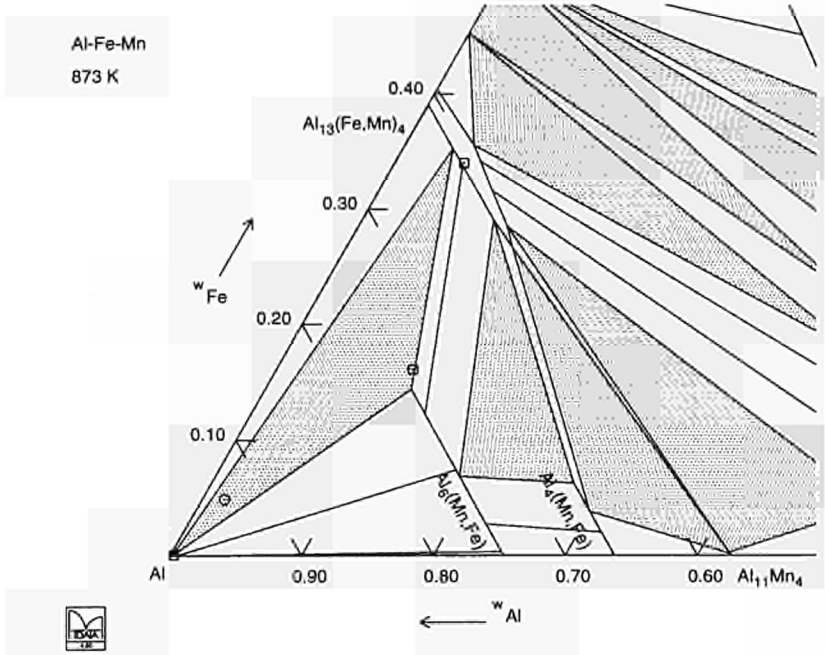

Fig 5 Calculated partial isothermal section for the Al-rich corner of the Al-Fe-Mn system at 873 K. Experimental data of Thornton et al [95Tho1,95Tho2] are superimposed.

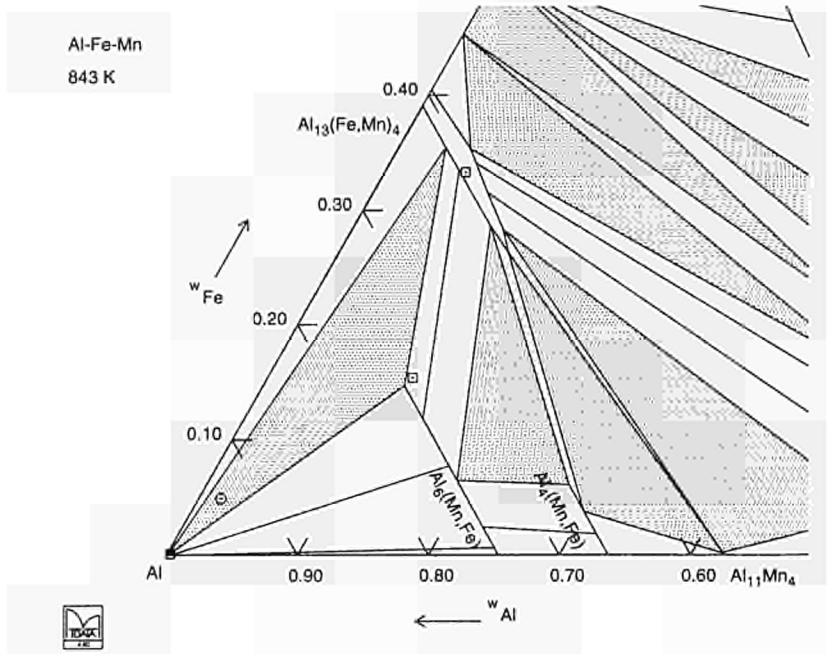

Fig 6 Calculated partial isothermal section for the Al-rich corner of the Al-Fe-Mn system at 843 K. Experimental data of Thornton et al [95Tho1,95Tho2] are superimposed.

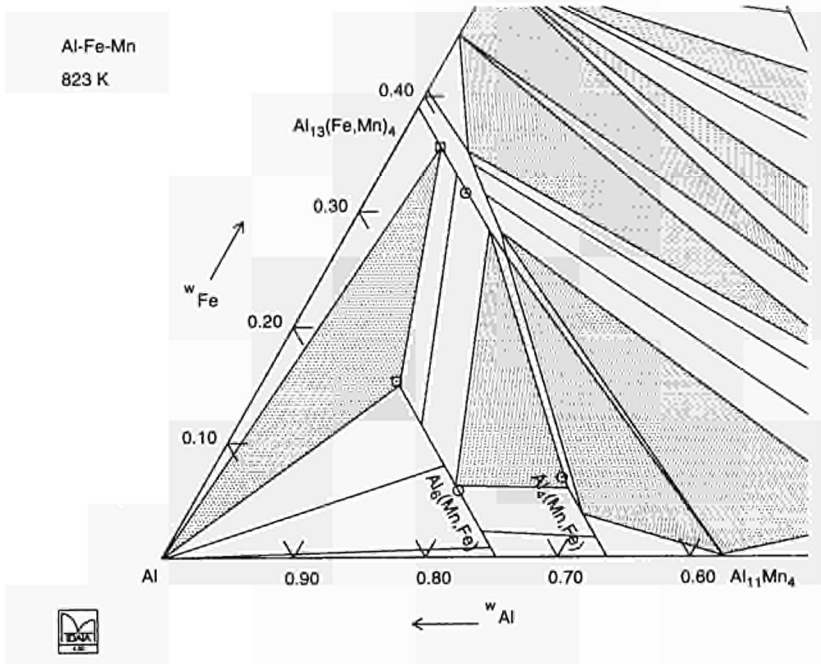

Fig 7 Calculated partial isothermal section for the Al-rich corner of the Al-Fe-Mn system at 823 K. Experimental data of Weitzer et al [96Wei/Rog] are superimposed.

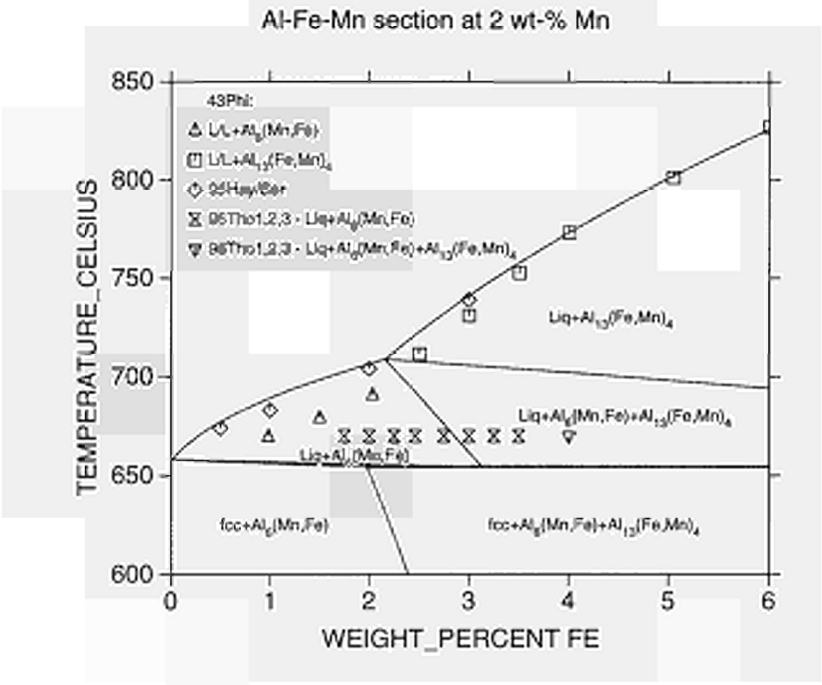

Fig 8 Calculated isopleth for the Al-Fe-Mn system at 2 wt % Mn. Experimental data from [43Phi], [95hay/Ser] and [96Tho1,96Tho2,96Tho3] are superimposed.

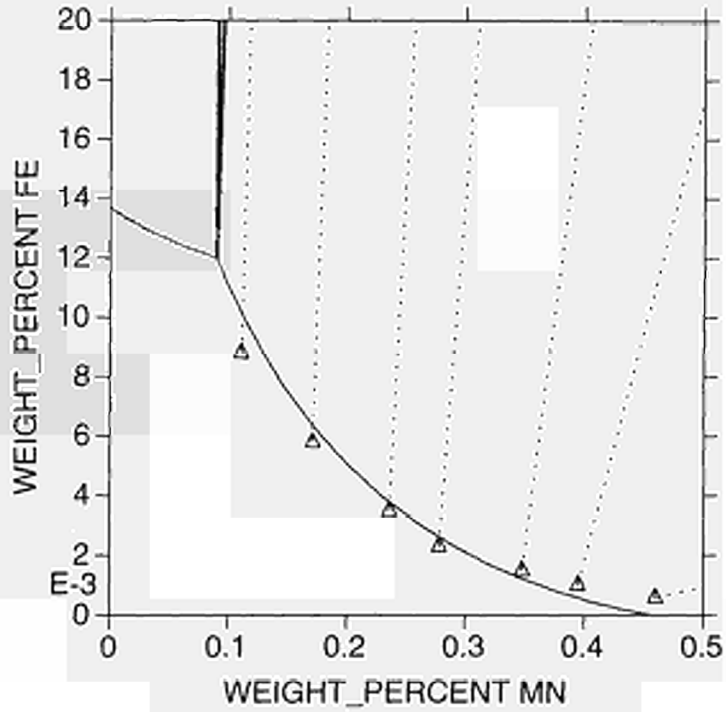

Fig 9 Calculated partial isothermal section for the Al-rich corner of the Al-Fe-Mn system at 823 K, showing the fcc solvus. Experimental data of Simensen and Kolby [95Sim/Kol] are superimposed.

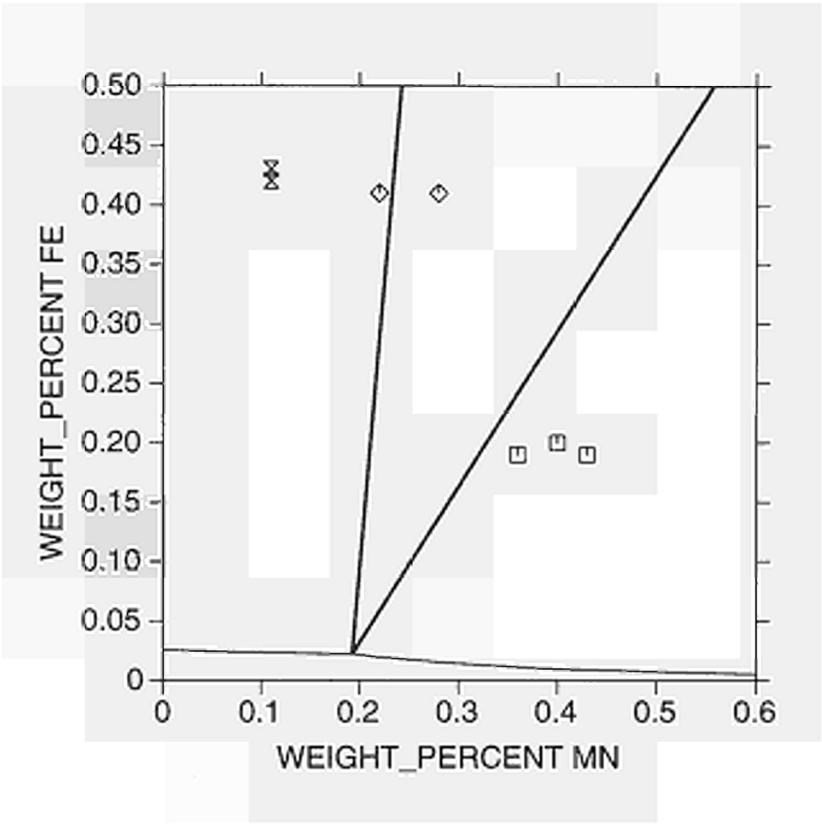

Fig 10 Calculated partial isothermal section for the Al-rich corner of the Al-Fe-Mn system at 873 K, showing the fcc solvus and three-phase region fcc + $Al_{12}(Fe,Mn)_4$ + $Al_6(Mn,Fe)$. Experimental data of Hamerton [96Ham] are super-imposed (diamond = three-phase).

CORDIS

The Community Research and Development Information Service

Your European R&D Information Source

CORDIS represents a central source of information crucial for any organisation - be it industry, small and medium-sized enterprises, research organisations or universities - wishing to participate in the exploitation of research results, participate in EU funded science and technology programmes and/or seek partnerships.

CORDIS makes information available to the public through a collection of databases. The databases cover research programmes and projects from their preparatory stages through to their execution and final publication of results. A daily news service provides up-to-date information on EU research activities including calls for proposals, events, publications and tenders as well as progress and results of research and development programmes. A partner search facility allows users to register their own details on the database as well as search for potential partners. Other databases cover Commission documents, contact information and relevant publications as well as acronyms and abbreviations.

By becoming a user of CORDIS you have the possibility to:

- Identify opportunities to manufacture and market new products
- Identify partnerships for research and development
- Identify major players in research projects
- Review research completed and in progress in areas of your interest

The databases - nine in total - are accessible on-line free of charge. As a user-friendly aid for on-line searching, Watch-CORDIS, a Windows-based interface, is available on request. The databases are also available on a CD-ROM. The current databases are:

News (English, German and French version) - Results -
Partners - Projects - Programmes - Publications -
Acronyms - Comdocuments - Contacts

CORDIS on World Wide Web

The CORDIS service was extended in September 1994 to include the CORDIS World Wide Web (WWW) server on Internet. This service provides information on CORDIS and the CORDIS databases, various software products, which can be downloaded (including the above mentioned Watch-CORDIS) and the possibility of downloading full text documents including the work programmes and information packages for all the research programmes in the Fourth Framework and calls for proposals.

The CORDIS WWW service can be accessed on the Internet using browser software (e.g. Netscape) and the address is: http://www.cordis.lu/

The CORDIS News database can be accessed through the WWW.

Contact details for further Information

If you would like further information on the CORDIS services, publications and products, please contact the CORDIS Help Desk :

CORDIS Customer Service
B.P. 2373
L-1023 Luxembourg

Telephone: +352-441012-2240
Fax: +352-441012-2248
E-mail: helpdesk@cordis.lu
WWW: http://www.cordis.lu/

European Commission

EUR 18171 — COST 507

Definition of thermochemical and thermophysical properties to provide a database for the development of new light alloys (Volume 1)

Luxembourg: Office for Official Publications of the European Communities

1998 — 273 pp. — 17.6 x 25 cm

Volume 1: ISBN 92-828-3901-X
Volumes 1 to 3: ISBN 92-828-3900-1

Venta • Salg • Verkauf • Πωλήσεις • Sales • Vente • Vendita • Verkoop • Venda • Myynti • Försäljning

BELGIQUE/BELGIË

Jean De Lannoy
Avenue du Roi 202/Koningslaan 202
B-1190 Bruxelles/Brussel
Tél. (32-2) 538 43 08
Fax (32-2) 538 08 41
E-mail: jean.de.lannoy@infoboard.be
URL: http://www.jean-de-lannoy.be

La librairie européenne/De Europese Boekhandel
Rue de la Loi 244/Wetstraat 244
B-1040 Bruxelles/Brussel
Tél. (32-2) 295 26 39
Fax (32-2) 735 08 60
E-mail: mail@libeurop.be
URL: http://www.libeurop.be

Moniteur belge/Belgisch Staatsblad
Rue de Louvain 40-42/Leuvensesteenweg 40-42
B-1000 Bruxelles/Brussel
Tél. (32-2) 552 22 11
Fax (32-2) 511 01 84

DANMARK

J. H. Schultz Information A/S
Herstedvang 10-12
DK-2620 Albertslund
Tlf. (45) 43 63 23 00
Fax (45) 43 63 19 69
E-mail: schultz@schultz.dk
URL: http://www.schultz.dk

DEUTSCHLAND

Bundesanzeiger Verlag GmbH
Vertriebsabteilung
Amsterdamer Straße 192
D-50735 Köln
Tel. (49-221) 97 66 80
Fax (49-221) 97 66 82 78
E-Mail: vertrieb@bundesanzeiger.de
URL: http://www.bundesanzeiger.de

ΕΛΛΑΔΑ/GREECE

G. C. Eleftheroudakis SA
International Bookstore
Panepistimiou 17
GR-10564 Athina
Tel. (30-1) 331 41 80/1/2/3/4/5
Fax (30-1) 323 98 21
E-mail: elebooks@netor.gr

ESPAÑA

Boletín Oficial del Estado
Trafalgar, 27
E-28071 Madrid
Tel. (34) 915 38 21 11 (Libros)/
913 84 17 15 (Suscripciones)
Fax (34) 915 38 21 21 (Libros)/
913 84 17 14 (Suscripciones)
E-mail: clientes@com.boe.es
URL: http://www.boe.es

Mundi Prensa Libros, SA
Castelló, 37
E-28001 Madrid
Tel. (34) 914 36 37 00
Fax (34) 915 75 39 98
E-mail: librena@mundiprensa.es
URL: http://www.mundiprensa.com

FRANCE

Journal officiel
Service des publications des CE
26, rue Desaix
F-75727 Paris Cedex 15
Tél. (33) 140 58 77 31
Fax (33) 140 58 77 00

IRELAND

Government Supplies Agency
Publications Section
4-5 Harcourt Road
Dublin 2
Tel. (353-1) 661 31 11
Fax (353-1) 475 27 60

ITALIA

Licosa SpA
Via Duca di Calabria, 1/1
Casella postale 552
I-50125 Firenze
Tel. (39-55) 64 54 15
Fax (39-55) 64 12 57
E-mail: licosa@ftbcc.it
URL: http://www.ftbcc.it/licosa

LUXEMBOURG

Messageries du livre SARL
5, rue Raiffeisen
L-2411 Luxembourg
Tél. (352) 40 10 20
Fax (352) 49 06 61
E-mail: mdl@pt.lu
URL: http://www.mdl.lu

Abonnements:

Messageries Paul Kraus
11, rue Christophe Plantin
L-2339 Luxembourg
Tél. (352) 49 98 88-8
Fax (352) 49 98 88-444
E-mail: mpk@pt.lu
URL: http://www.mpk.lu

NEDERLAND

SDU Servicecentrum Uitgevers
Christoffel Plantijnstraat 2
Postbus 20014
2500 EA Den Haag
Tel. (31-70) 378 98 80
Fax (31-70) 378 97 83
E-mail: sdu@sdu.nl
URL: http://www.sdu.nl

ÖSTERREICH

Manz'sche Verlags- und Universitätsbuchhandlung GmbH
Kohlmarkt 16
A-1014 Wien
Tel. (43-1) 53 16 11 00
Fax (43-1) 53 16 11 67
E-Mail: bestellen@manz.co.at
URL: http://www.austria.EU.net:81/manz

PORTUGAL

Distribuidora de Livros Bertrand Ld.ª
Grupo Bertrand, SA
Rua das Terras dos Vales, 4-A
Apartado 60037
P-2700 Amadora
Tel. (351-2) 495 90 50
Fax (351-2) 496 02 55

Imprensa Nacional-Casa da Moeda, EP
Rua Marquês Sá da Bandeira, 16-A
P-1050 Lisboa Codex
Tel. (351-1) 353 03 99
Fax (351-1) 353 02 94
E-mail: del.incm@mail.telepac.pt
URL: http://www.incm.pt

SUOMI/FINLAND

Akateeminen Kirjakauppa/Akademiska Bokhandeln
Keskuskatu 1/Centralgatan 1
PL/PB 128
FIN-00101 Helsinki/Helsingfors
P./tfn (358-9) 121 44 18
F./fax (358-9) 121 44 35
Sähköposti: akatilaus@stockmann.fi
URL: http://www.akateeminen.com

SVERIGE

BTJ AB
Traktorvägen 11
S-221 82 Lund
Tfn. (46-46) 18 00 00
Fax (46-46) 30 79 47
E-post: btjeu-pub@btj.se
URL: http://www.btj.se

UNITED KINGDOM

The Stationery Office Ltd
International Sales Agency
51 Nine Elms Lane
London SW8 5DR
Tel. (44-171) 873 90 90
Fax (44-171) 873 84 63
E-mail: ipaenquries@theso.co.uk
URL: http://www.the-stationery-office.co.uk

ÍSLAND

Bokabud Larusar Blöndal
Skólavördustig, 2
IS-101 Reykjavik
Tel. (354) 551 56 50
Fax (354) 552 55 60

NORGE

Swets Norge AS
Østenjoveien 18
Boks 6512 Etterstad
N-0606 Oslo
Tel. (47-22) 97 45 00
Fax (47-22) 97 45 45

SCHWEIZ/SUISSE/SVIZZERA

Euro Info Center Schweiz
c/o OSEC
Stampfenbachstraße 85
PF 492
CH-8035 Zürich
Tel. (41-1) 365 53 15
Fax (41-1) 365 54 11
E-mail: eics@osec.ch
URL: http://www.osec.ch/eics

BĂLGARIJA

Europress Euromedia Ltd
59, blvd Vitosha
BG-1000 Sofia
Tel. (359-2) 980 37 66
Fax (359-2) 980 42 30
E-mail: Milena@mbox.cit.bg

ČESKÁ REPUBLIKA

ÚSIS
NIS-prodejna
Havelkova 22
CZ-130 00 Praha 3
Tel. (420-2) 24 23 14 86
Fax (420-2) 24 23 11 14
E-mail: nkposp@dec.nis.cz
URL: http://www.nis.cz

CYPRUS

Cyprus Chamber of Commerce and Industry
PO Box 1455
CY-1509 Nicosia
Tel. (357-2) 66 95 00
Fax (357-2) 66 10 44
E-mail: info@ccci.org.cy

EESTI

Eesti Kaubandus-Tööstuskoda (Estonian Chamber of Commerce and Industry)
Toom-Kooli 17
EE-0001 Tallinn
Tel. (372) 646 02 44
Fax (372) 646 02 45
E-mail: einfo@koda.ee
URL: http://www.koda.ee

MAGYARORSZÁG

Euro Info Service
Európa Ház
Margitsziget
PO Box 475
H-1396 Budapest 62
Tel. (36-1) 350 80 25
Fax (36-1) 350 90 32
E-mail: euroinfo@mail.matav.hu
URL: http://www.euroinfo.hu/index.htm

MALTA

Miller Distributors Ltd
Malta International Airport
PO Box 25
Luqa LQA 05
Tel. (356) 66 44 88
Fax (356) 67 67 99
E-mail: gwirth@usa.net

POLSKA

Ars Polona
Krakowskie Przedmiescie 7
Skr. pocztowa 1001
PL-00-950 Warszawa
Tel. (48-22) 826 12 01
Fax (48-22) 826 62 40
E-mail: ars_pol@bevy.hsn.com.pl

ROMÂNIA

Euromedia
Str. G-ral Berthelot Nr 41
RO-70749 Bucuresti
Tel. (40-1) 315 44 03
Fax (40-1) 315 44 03

SLOVAKIA

Centrum VTI SR
Nám. Slobody, 19
SK-81223 Bratislava
Tel. (421-7) 531 83 64
Fax (421-7) 531 83 64
E-mail: europ@tbbl.sltk.stuba.sk
URL: http://www.sltk.stuba.sk

SLOVENIA

Gospodarski Vestnik
Dunajska cesta 5
SLO-1000 Ljubljana
Tel. (386) 611 33 03 54
Fax (386) 611 33 91 28
E-mail: repanseki@gvestnik.si
URL: http://www.gvestnik.si

TÜRKIYE

Dünya Infotel AS
100, Yil Mahallesi 34440
TR-80050 Bagcilar-Istanbul
Tel. (90-212) 629 46 89
Fax (90-212) 629 46 27

AUSTRALIA

Hunter Publications
PO Box 404
3067 Abbotsford, Victoria
Tel. (61-3) 94 17 53 61
Fax (61-3) 94 19 71 54
E-mail: jpdavies@ozemail.com.au

CANADA

Renouf Publishing Co. Ltd
5369 Chemin Canotek Road Unit 1
K1J 9J3 Ottawa, Ontario
Tel. (1-613) 745 26 65
Fax (1-613) 745 76 60
E-mail: order.dept@renoufbooks.com
URL: http://www.renoufbooks.com

EGYPT

The Middle East Observer
41 Sherif Street
Cairo
Tel. (20-2) 393 97 32
Fax (20-2) 393 97 32

HRVATSKA

Mediatrade Ltd
Pavla Hatza 1
HR-10000 Zagreb
Tel. (385-1) 43 03 92
Fax (385-1) 43 03 92

INDIA

EBIC India
3rd Floor, Y. B. Chavan Centre
Gen. J. Bhosale Marg.
400 021 Mumbai
Tel. (91-22) 282 60 64
Fax (91-22) 285 45 64
E-mail: ebic@giasbm01.vsnl.net.in
URL: http://www.ebicindia.com

ISRAËL

ROY International
PO Box 13056
61130 Tel Aviv
Tel. (972-3) 546 14 23
Fax (972-3) 546 14 42
E-mail: royil@netvision.net.il

Sub-agent for the Palestinian Authority:

Index Information Services
PO Box 19502
Jerusalem
Tel. (972-2) 627 16 34
Fax (972-2) 627 12 19

JAPAN

PSI-Japan
Asahi Sanbancho Plaza #206
7-1 Sanbancho, Chiyoda-ku
Tokyo 102
Tel. (81-3) 32 34 69 21
Fax (81-3) 32 34 69 15
E-mail: books@psi-japan.co.jp
URL: http://www.psi-japan.com

MALAYSIA

EBIC Malaysia
Level 7, Wisma Hong Leong
18 Jalan Perak
50450 Kuala Lumpur
Tel. (60-3) 262 62 98
Fax (60-3) 262 61 98
E-mail: ebic-kl@mol.net.my

PHILIPPINES

EBIC Philippines
19th Floor, PS Bank Tower
Sen. Gil J. Puyat Ave. cor. Tindalo St.
Makati City
Metro Manilla
Tel. (63-2) 759 66 80
Fax (63-2) 759 66 90
E-mail: eccpcom@globe.com.ph
URL: http://www.eccp.com

RUSSIA

CCEC
60-letiya Oktyabrya Av. 9
117312 Moscow
Tel. (70-95) 135 52 27
Fax (70-95) 135 52 27

SOUTH AFRICA

Safto
Safto House
NO 5 Esterhyzen Street
PO Box 782 706
2146 Sandton
Tel. (27-11) 883 37 37
Fax (27-11) 883 65 69
E-mail: emailstar@ide.co.za
URL: http://www.safto.co.za

SOUTH KOREA

Information Centre for Europe (ICE)
204 Woo Sol Parktel
395-185 Seogyo Dong, Mapo Ku
121-210 Seoul
Tel. (82-2) 322 53 03
Fax (82-2) 322 53 14
E-mail: euroinfo@shinbiro.com

THAILAND

EBIC Thailand
29 Vanissa Building, 8th Floor
Soi Chidlom
Ploenchit
10330 Bangkok
Tel. (66-2) 655 06 27
Fax (66-2) 655 06 28
E-mail: ebicbkk@ksc15.th.com
URL: http://www.ebicbkk.org

UNITED STATES OF AMERICA

Berman Associates
4611-F Assembly Drive
Lanham MD20706
Tel. (1-800) 274 44 47 (toll free telephone)
Fax (1-800) 865 34 50 (toll free fax)
E-mail: query@berman.com
URL: http://www.berman.com

ANDERE LÄNDER/OTHER COUNTRIES/ AUTRES PAYS

Bitte wenden Sie sich an ein Büro Ihrer Wahl / Please contact the sales office of your choice / Veuillez vous adresser au bureau de vente de votre choix

NOTICE TO THE READER

Information on European Commission publications in the areas of research and innovation can be obtained from:

- **CORDIS, the Community R & D Information Service**
  For more information, contact:
  CORDIS Customer Service, BP 2373, L-1023 Luxembourg
  Tel. (352) 44 10 12-2240; fax (352) 44 10 12-2248; e-mail: helpdesk@cordis.lu
  or visit the website at http://www.cordis.lu/

- **Euroabstracts**
  The European Commission's periodical on research publications, issued every two months.
  For more information, contact:
  RTD help desk, European Commission, DG XIII, L-2920 Luxembourg
  Fax (352) 43 01-32084; e-mail: rtd-helpdesk@lux.dg13.cec.be

15

CG-NA-18171-EN-C

OFFICE FOR OFFICIAL PUBLICATIONS
OF THE EUROPEAN COMMUNITIES

L-2985 Luxembourg

ISBN 92-828-3901-X